THE

LONDON EDINBURGH AND DUBLIN

PHILOSOPHICAL MAGAZINE

AND

JOURNAL OF SCIENCE.

[SEVENTH SERIES.]

FEBRUARY 1929.

XXVI. *The Heats of Solution of some Salts in Water and Ethyl Alcohol Solutions.* *By* Prof. J. R. PARTINGTON *and* Dr. W. E. SOPER *.

Introduction.

THE increasing interest which is now being shown in solutions of electrolytes in non-aqueous media led to the somewhat surprising discovery that there are practically no data for the heats of solution and dilution in such media. This work is a preliminary attempt to fill this gap to some degree, and, for this reason, it has been thought to be of more advantage to examine the salts chosen at each end of the concentration range, rather than to examine the whole concentration range, the middle portion of which is relatively unimportant from a theoretical standpoint. The heats of solution and dilution of the same salts in water do not appear to have been recorded completely at the points chosen, and have therefore been included for purposes of comparison. The heats of solution and dilution of potassium chloride in water have been included as a check on the experimental method.

One of the authors (W. E. S.) is indebted to the Chemical Society and to the Dixon Fund of the University of London for grants towards the purchase of apparatus and materials. The work is part of a thesis submitted by W. E. Soper for the degree of Ph.D. of the University of London.

* Communicated by the Authors.

Definition of the various Heats of Solution and Dilution.

The *integral heat of solution* for concentration c, denoted L_c, is the heat evolved by the solution of one mol of a substance in as much pure solvent as is required to make a solution of concentration c. In the special case when $c=0$, $L_c=L_0$, the *first heat of solution*, and when c corresponds with saturation, $c=s$, L_c is equal to the *total heat of solution*, L^s. The integral heat of a solution in which m mols of solute are dissolved in a mols of solvent is denoted by the symbol ${}_aL^m$, where $m/a=c$. The *intermediate heat of solution* is the heat evolved by the solution of solute in an already prepared solution. If we dissolve one mol of a solute in an infinitely large quantity of solution of concentration c, so that the concentration of the solution is practically unaltered, then we have the *true intermediate* or *differential heat of solution*, Λ_c. In the special case when $c=s$ we have the theoretically important *final heat of solution*, Λ_s. This is sometimes called the "theoretical" or "fictitious" heat of solution. In a practical case n mols of solute are dissolved in a solution already containing m mols of solute in a mols of solvent, so that a measurable change in concentration takes place. This quantity is denoted the *intermediate heat of solution* ${}^m_a\Lambda^n$. The heat of solution calculated from this is the *mean intermediate heat of solution*, Λ_c', which can be obtained from the mean concentration c of the concentrations before and after the addition of the solute. The differential heat of solution corresponds with the *differential heat of dilution*, ϕ_c, which is the quantity of heat evolved on addition of one mol of solvent to an infinite quantity of a solution of concentration c, so that practically no change in concentration takes place. In the case of a saturated solution, the magnitude here involved is given the name, *first heat of dilution*, ϕ_s. In a practical case one dilutes a solution containing m mols of solute in a mols of solvent with a large quantity of solvent, b mols. The heat of reaction involved is called the intermediate heat of dilution, ${}^m_a\phi_b$. From first principles it is seen that there exist certain simple relations between the various heats of solution and dilution, and from some of these relations we obtain results from indirect calorimetric determinations. We have first relations:—

$$ {}_aL^m + {}^m_a\Lambda^n = {}_aL^{m+n}. \quad . \quad . \quad . \quad . \quad . \quad (1) $$

$$ {}_aL^m + {}^m_a\phi_b = {}_{a+b}L^m. \quad . \quad . \quad . \quad . \quad . \quad (2) $$

If we start out with a solution containing m mols of solute

in a mols of solvent, and add n mols of solute, we have the intermediate heat of solution evolved, ${}^{m}_{a}\Lambda^{n}$. If, now, we dilute this solution with b mols of solvent, and in so doing we bring the solution back to the original concentration, *i. e.*, $m/a = n/b$, we obtain the intermediate heat of dilution, ${}^{m+n}_{a}\phi_{b}$, and the following relation holds :—

$$ {}^{m}_{a}\Lambda^{n} + {}^{m+n}_{a}\phi_{b} = {}_{b}\mathrm{L}^{n}. \quad . \quad . \quad . \quad . \quad . \quad (3) $$

If the concentration is given in molar fractions, then we may generalize from equation (3), and obtain

$$ \mathrm{L}_{c} = \Lambda_{c} + 1/c \,.\, \phi_{c}. \quad . \quad . \quad . \quad . \quad . \quad (4) $$

In the present work the following calorimetric determinations have been made in order to arrive at the various heats of solution and dilution. Single portions of solute have been introduced successively into a fixed quantity of solvent, and a series of mean intermediate heats of solution calculated for one mol of solute at the mean concentration of each interval. In this way the differential heat of solution is obtained, a correction for curvature being applied where necessary, on the basis of the mean value equation :—

$$ \Lambda'_{c} = \frac{{}^{m}_{a}\Lambda^{n}}{n} = \int_{m/a}^{(m+n)/a} \Lambda_{c}\, dn. $$

The remaining values were then obtained by use of the formulæ just given. In the neighbourhood of saturation, however, this method fails, because here the process of solution takes too long a time. In this region, especially for the determination of the total heat of solution and the final heat of solution, a different method was used. A concentrated initial solution was diluted one or more times with solvent, and the heats of dilution evolved were measured. With each of these was combined the known integral heat of solution by means of formula (2), and the other unknowns were thus calculated.

Previous Measurements.

The classic investigations of Julius Thomsen were begun in 1853. A large number of salts were investigated, but the measurements were as a rule limited to one concentration, and to water as a solvent.

Berthelot commenced his equally famous investigations in 1865, and investigated several salts. His measurements also were generally confined to one concentration.

In 1888, S. U. Pickering[1] published the results of a series of investigations of the heats of solution of certain salts in water and in anhydrous ethyl alcohol. He obtained the following results among others :—

TABLE I.

Salt.	Weight of salt used, grams.	Weight of solvent, grams.	Heat of solution, g. cals./mol salt.
Earlier determinations.			
$Ca(NO_3)_2$	1·006	214·39 (EtOH)	7548
$Ca(NO_3)_2 . 4H_2O$.....	2·855	214·39 (EtOH)	1835
Later determinations.			
$Ca(NO_3)_2$	2·3312	476·76 (EtOH)	8708
$Ca(NO_3)_2$	2·2419	476·76 (EtOH)	8711
$Ca(NO_3)_2$	14·687	400·00 (H_2O)	3940
$Ca(NO_3)_2$	14·842	400·00 (H_2O)	3945
$Ca(NO_3)_2 . 4H_2O$.....	20·803	400·00 (H_2O)	−8354
$Ca(NO_3)_2 . 4H_2O$.....	19·796	400·00 (H_2O)	−8354

In the earlier experiments an open calorimeter was used, but in the later experiments the calorimeter was made larger and fitted with a lid.

Von Steinwehr[2] in 1901 introduced the method of differential calorimetry to measure the heat of dilution of hydrochloric acid. He measured temperature differences by means of thermocouples.

In 1905, Richards, Henderson, and Forbes[3] first introduced the practice of adiabatic calorimetry. Hot water was first used to maintain the adiabatic condition of the outer bath, but this was afterwards replaced by the heat of neutralization of alkali by acid. This method was improved by Richards, Henderson, and Frevert[4] for use in the determination of heats of combustion. Richards and Rowe[5] in 1908 used the method for the determination of the specific heats of liquids, when heat was supplied to the liquid in the calorimeter by immersion of a platinum vessel in which acid and alkali were mixed. This was further elaborated by Richards and Rowe in 1920 and 1921[6] for the determination of heats of dilution.

Rümelin[7] in 1907 measured among others the heat of dilution of various solutions of calcium nitrate in water. He used a double calorimeter and measured the difference in temperature of the two vessels by means of thermocouples.

The temperature at which the experiments were performed, however, varied between 17° and 20° C.

In comparing the effects of various non-aqueous solvents, Walden [8] measured the heats of solution of potassium iodide, tetraethylammonium iodide, and tetrapropylammonium iodide in a variety of solvents. Some of his results will be tabulated for comparison purposes.

TABLE II.

Weight of salt, grams.	Weight of solvent, grams.	Molecular proportions.	Temp. rise.	Integral heat of solution, g. cals./mol salt.	
Potassium Iodide in Water at 18° C.					
5·145	111·60	1 : 200	−1·265	−5145	
5·270	114·17	1 : 200	−1·270	−5156	
Potassium Iodide in Methyl Alcohol at 18° C.					
2·105	81·26	1 : 200	−0·160	− 752	
Potassium Iodide in Ethyl Alcohol at 18° C.					
1·4452	80·22	1 : 200	−0·340	−2204	Mean.
1·147	86·9	1 : 273	−0·230	−2124	−2140
1·105	86·9	1 : 284	−0·225	−2156	
0·7206	79·98	1 : 400	−0·167	−1994	
0·533	86·78	1 : 586	−0·080	−1521	−1537
0·496	84·10	1 : 612	−0·075	−1552	
Potassium Iodide in Acetone at 18° C.					
1·400	87·70	1 : 179	0·580	4050	4079
1·391	86·60	1 : 178	0·590	4108	
1·076	75·34	1 : 200	0·553	4153	4188
1·132	79·23	1 · 200	0·568	4223	
0·600	86·95	1 : 411	0·275	4420	

De Kollosowski [9] has measured a series of heats of solution of various salts at various concentrations in aqueous ethyl alcohol as solvent.

Various designs of adiabatic calorimeters have since been described for the measurement of heats of solution, among which are those of Wust and Lange [10] and Lange and Schwartz [11]. Cohen, Moesveld, and Helderman [12] describe a calorimeter in which electrical energy is passed into a solution which is being cooled by a negative heat of solution,

and thus the temperature of the mixture remains practically constant. No further record of any measurements with anhydrous ethyl alcohol has been found.

References.

(1) S. U. Pickering, J. C. S. liii. p. 865 (1888).
(2) Von Steinwehr, *Zeit. physik. Chem.* xxxviii. p. 185 (1901).
(3) Richards, Henderson, and Forbes, *Zeit. physik. Chem.* lii. p. 551 (1905).
(4) Richards, Henderson, and Frevert, *Zeit. physik. Chem.* lxix. p. 532 (1907).
(5) Richards and Rowe, *Zeit. physik. Chem.* lxiv. p. 187 (1908).
(6) Richards and Rowe, J. A. C. S. xlii. p. 1621 (1920); xliii. p. 770 (1921).
(7) Rümelin, *Zeit. physik. Chem.* lviii. p. 449 (1907).
(8) Walden, *Zeits. physik. Chem.* lxix. p. 192 (1908).
(9) De Kollosowski, Bull. Acad. Roy. Belg. 1912, p. 591, 1913, pp. 36, 329; *Journ. Chim. Phys.* xxii. p. 97 (1925).
(10) Wust and Lange, *Zeit. physik. Chem.* cxvi. p. 161 (1925).
(11) Lange and Schwartz, *Zeit. physik. Chem.* cxxxiii. p. 129 (1928).
(12) Cohen, Moesveld, and Helderman, *Zeit. physik. Chem.* xcv. p. 317 (1920).

The Experimental Method.

The calorimeter employed (fig. 1) could be used either isothermally or adiabatically. The calorimeter vessel, made of spun copper and silver-plated, was enclosed in a submarine jacket made of sheet-copper. It was supported inside the jacket by cork wedges which served for thermal insulation. The calorimeter was fitted with a brass lid to prevent evaporation of the liquid into the air-space between it and the jacket. The liquid in the calorimeter was stirred by an ordinary propeller stirrer of copper heavily silver-plated. The propeller shaft ran in bearings which were attached to the submarine jacket, and it was at the same time supported by it. In this way the stirrer was free from contact with the calorimeter, and heating by friction was avoided. Evaporation from the calorimeter through the entrance of the stirrer was prevented by fitting an annular oil-seal to the top of the calorimeter lid and to the propeller shaft. Heat conduction along the propeller shaft, which was made from silver-plated copper inside the calorimeter and from brass from the annular seal upwards, was avoided by interposing a short shaft of ebonite at the junction between the silver-plated shaft and the oil-seal on the top of the calorimeter. The resistance heater was made to screw into an "Ivoride" cylinder which was clamped to the calorimeter lid. The heater was connected in series to a battery of accumulators

by heavy copper wires, and the current passing through the heater was measured by measuring the fall in potential across a standard 1-ohm resistance which was connected in series in the circuit. The temperatures of the calorimeter liquid and of the outer bath were measured by calibrated Beckmann thermometers.

Fig. 1.

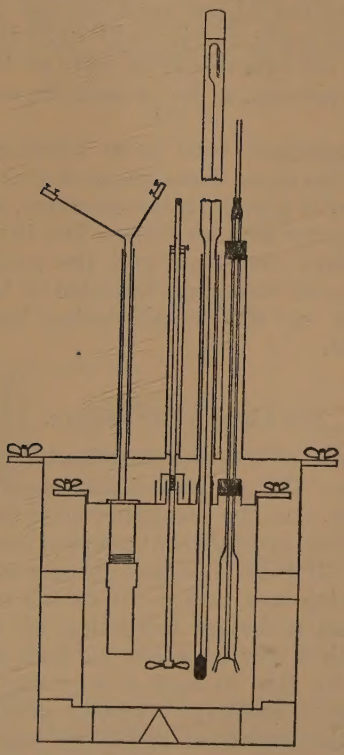

This is a brief outline of the experimental arrangement, several details of which will now be described more fully.

The Calorimeter and Lid.

The calorimeter consisted of a spun-copper beaker of 550 c.c. content, the rim of which was removed and replaced by a flange with five bolts projecting from it. The inside of the calorimeter was heavily silver-plated, and except in two cases, when the solution was a concentrated aqueous

solution of a halide ($CuCl_2$ and KCl), this was sufficient to protect the copper. In these other cases, provided that the concentrated solution was not left for too long a time in the vessel, it was found sufficient to cover the silver with a thin film of vaseline in order to protect it. The lid of the calorimeter fitted over the five bolts projecting from the flange and was fastened by means of wing nuts. An indiarubber washer was placed between the calorimeter flange and lid. The central part of the lid was sunk into the calorimeter for a short distance in order that it could be in thermal contact with the sides of the calorimeter in spite of the indiarubber washer, and thus prevent, as far as possible, condensation on the lid.

The lid was provided with holes fitted with chimney-like projecting tubes about three-quarters of an inch long for the introduction of a pipette, a thermometer, and the stirrer (this latter having an annular seal). The thermometer was steadied by a sleeve over itself and the projecting copper tube. The resistance heater was threaded on to a cylinder of "Ivoride," about one and a half inches long, which was clamped to the lid.

The Calorimeter Heater.

The development of a satisfactory heater was a somewhat difficult problem. The resistance wire must be insulated from the solution, and the insulation must be impervious to the latter. The final arrangement adopted was as follows :— About 4 feet of 30 S.W.G. nickel chrome wire was wound into a spiral which was pulled out to the required length and wound round a former consisting of a flat piece of "Micanite" with a saw edge cut on each side. The wire was supported by this in such a way that it was not in contact with the "Micanite" except at the saw edges. The lead from the bottom of the spiral was insulated with an asbestos sleeve and brought up through the middle of the spiral. The leads were pinched into two small brass terminals which were brought through the lid of a cylindrical copper case and insulated from it by two ebonite bushes. The heavy copper leads were soldered into the top caps of the terminals. The heating coil was then put into the cylindrical copper vessel, the spiral being allowed to press against the side, but insulated from it by a single sheet of "Micanite." The lid and vessel were then soldered together, the whole being copper-plated and then heavily silver-plated.

The Energy Measurement.

The electrical energy supplied to the calorimeter heater was determined by measuring the potential drop across the ends of the heater windings and the potential drop across a standard 1-ohm resistance which was in series in the circuit. The arrangement used is shown in the diagram (fig. 2).

H is the heater through which the current flowed from the battery B through one-half of the closed double-throw switch W. The regulating resistance W_1 consisted of

Fig. 2.

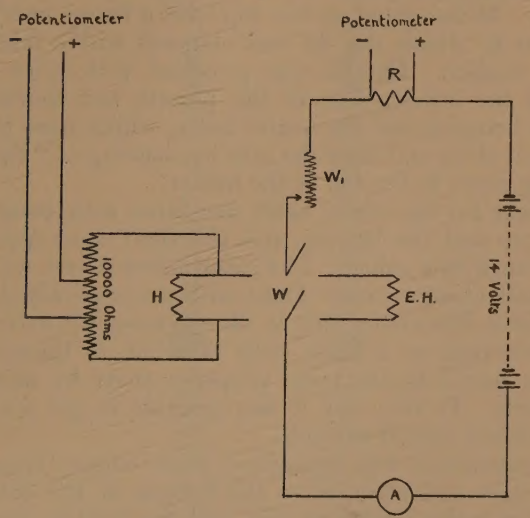

two slide rheostats. R was the standard 1-ohm resistance. In parallel with the heater windings was an accurately-known resistance of 10,000 ohms, and from this a resistance of 1000 ohms was tapped off to give 1/10 of the total fall of potential across the 10,000 ohms, and therefore across the heater windings. This fall in potential and also the fall in potential across the standard 1-ohm resistance was measured on a special Tinsley ionization potentiometer against a standard Weston cell. The current was not switched directly on to the heater in the course of an experiment, but was previously switched on through the resistance coil E.H., equal in resistance to the calorimeter heater, by means of the other half of the double-throw switch W. By this

means the accumulators were allowed to settle down to a more or less steady potential, and this was not upset on quickly switching over to the heater.

The measurement of the time of heating was made by a carefully-regulated stop-watch, which could be read accurately to one-twentieth of a second.

For the conversion of electrical energy into heat the value

$$1 \text{ joule} = 0{\cdot}2389 \text{ calorie}$$

was used.

The Submarine Jacket and the Outer Bath.

The submarine jacket of sheet copper provided a 1-inch air-gap. It was fitted at the top with a flange carrying six bolts, on to which the lid was clamped with a thick india-rubber washer. The lid was provided with tubes 7 inches long for the introduction of the pipette and thermometer, and for bringing out the heater leads, which were insulated from each other and from the case by sleeving of "Sistoflex" reaching down to the top of the heater.

The tube for the stirrer shaft was fitted with brass bushes at the top and the bottom, and the shaft was supported on the top bush by a collar. The calorimeter stirrer was driven by a small electric motor fitted with a worm-reducing gear and a chain drive from this to the stirrer-shaft drive, which ran in bearings on a brass strip attached to the outer bath and was joined to the main propeller shaft by means of a dog clutch. In this way it was possible to get a slow and very uniform rate of stirring.

The submarine was supported on a copper tripod with raised edges and clamped to the bottom of the bath. The submarine jacket rested on this, and was held in position by two rods from the cross-bar of the bath clamped down on top of the lid.

The outer bath was filled with light lubricating oil so that a wire-resistance heater could be used for raising the temperature of the bath quickly. This heater consisted of eleven yards of 22 S.W.G. nickel chrome wire wound over a frame made up from two "Syndano" strips of one-quarter of an inch thickness, spaced about 10 inches apart by means of half-inch brass bolts. The "Syndano" strips were made with V-nicks along one edge about one-quarter of an inch apart, and had holes drilled along their length along the middle to correspond with the V-nicks. The wire was then threaded through the nicks so that the heater then took the form of a double mat of parallel wires 10 inches long.

The bath also contained a 240-watt heating lamp and a toluene thermo-regulator, so that the temperature could be kept constant at any desired point within $\pm 0{\cdot}05°$ C. The oil was very vigorously stirred by means of a fast-running propeller stirrer driven by means of an electric motor.

The Introduction of Solid or Liquid into the Calorimeter.

Solid or liquid was introduced into the calorimeter when it was set up by means of glass pipettes with long stems

Fig. 3.

(fig. 3). The pipette for delivering liquid was similar to that described by Dürr and Lange (*Zeit. physik. Chem.* cxxi. p. 361, 1926). The pipette with a long stem was closed by a ground-glass rod sealed to a tube running inside the pipette stem and almost touching it. This tube had an opening communicating with the inside of the pipette. The long tube attached to the ground stopper and the stem of the pipette were joined at the top by means of an india-

rubber sleeve. By placing the nozzle of the pipette in a liquid and drawing up the glass tube the pipette could be filled by sucking at the top of the glass tube. This glass tube was now pushed down and the pipette closed. A cap was placed over the top of the glass tube, and the liquid remaining on the outer walls was carefully wiped off, so that the pipette could now be weighed full of liquid. After fitting in the calorimeter through a rubber bung, the pipette could be opened and the liquid delivered quickly and without splashing. A similar method was used for the introduction of solid, except that the pipette was replaced by an arrangement similar to an inverted weighing bottle, the ground stopper of which could be pushed out by means of the arrangement described.

The Thermometers.

The two Beckmann thermometers used were carefully compared over the whole length of their scale with a thermometer reading to 0·01°, calibrated by the German Reichsanstalt. The thermometers were compared in positions corresponding to those in which they were to be used. They were read by means of a hand-lens to $\pm 0{\cdot}001°$, but the probable accuracy is not more than $\pm 0{\cdot}005°$ on account of the sticking of the mercury. The thermometers were tapped by hand for some moments before a reading was taken.

Manipulation of the Apparatus.

A known weight of solvent was introduced into the calorimeter, and the weighed pipette containing a known weight of salt or solvent according to the experiment was then introduced. The apparatus was then left stirring for some hours until an equilibrium had been set up between the calorimeter and the outer bath, and the difference of temperature then prevailing was taken as that required to maintain the adiabatic condition for that experiment. As others have pointed out, the heating effect due to stirring is not constant over a series of experiments, and it varies among other things with the volume and concentration of the liquid stirred, and therefore the difference in temperature required to maintain the adiabatic condition between the inner and outer vessels necessarily alters over a series of readings.

A series of readings was now taken over some minutes of the temperatures of the inner and outer vessels, and at the proper moment the solid or liquid was allowed to

enter the liquid in the calorimeter. The temperature now either rose or fell. In the case of rising temperature, the heater in the outer bath was quickly switched on in order to maintain the adiabatic condition. With the quicker temperature changes the adiabatic condition could not be kept so accurately during the initial stages, and so the rate of leakage for a given thermal head was afterwards found for the solution, and by this means a correction was applied.

In cases of falling temperature the apparatus was used isothermally. The heater was switched on at a noted time in order to keep the temperature constant as far as possible. At the same time the fall of potential across the heater and that across the standard ohm were quickly measured. In some cases it was not possible to supply the large quantity of heat required quickly enough to prevent the temperature of the contents from falling. In these cases the correction obtained as described from the rate of thermal leakage was applied. The largest correction applied in this way was about 4 per cent. of the total heat absorbed.

At this stage another series of measurements of temperature was taken over some minutes to see that the temperature has actually become constant. At the end of this time the pipette was quickly and carefully withdrawn and made ready for another observation.

The method of calculation will be illustrated by an experiment requiring a large correction for failure to hold the adiabatic condition and the overshooting of the isothermal.

In an experiment 8·9318 grams of potassium chloride were dissolved in a solution containing 66·5862 grams of potassium chloride in 391·42 grams of water.

The initial temperature as read on the Beckmann thermometer was 2·837° C., the final temperature was 2·871° C. The isothermal correction is thus +0·034° C. In addition the adiabatic condition was not accurately kept at the beginning of the experiment. The temperature of the calorimeter contents and the temperature were plotted against time on the same diagram. The deviations from the adiabatic conditions may now be summed in the form of a mean value for a constant thermal head for a given time, in this case 0·400° C. for seven minutes. The fundamental equation for temperature loss is

$$\eta = \phi \mathrm{KT},$$

where η is temperature loss, ϕ is the thermal head, T is the length of the experimental period, and K is a multiplier of the thermal head or the thermal leakage modulus. At the

conclusion of the experiment proper the temperatures of the bath and calorimeter contents were arranged so that there was a thermal head of 0·124° C. between them. The rate of thermal leakage was found to be 0·000611° C. per minute.

$$0{\cdot}000611 = K \times 0{\cdot}124.$$

$$\therefore \qquad K = 0{\cdot}0049283.$$

Therefore a head of 0·400° C. for seven minutes will give a temperature loss of

$$\eta = 0{\cdot}0049283 \times 0{\cdot}400 \times 7$$
$$= 0{\cdot}014^{\circ}\ \text{C.}$$

The isothermal correction was 0·034° C. and the adiabatic correction was 0·014° C., *i. e.* total correction 0·048° C. The water equivalent of the calorimeter and its contents was 474·795 cals./deg., and the correction is thus

$$474{\cdot}795 \times 0{\cdot}048 = 22{\cdot}790 \text{ gram calories.}$$

The heat supplied to the calorimeter contents was 460·988, and therefore the corrected heat of reaction was

$$460{\cdot}988 - 22{\cdot}790 = -438{\cdot}198 \text{ gram calories.}$$

The intermediate heat of solution was thus

$$\frac{-438{\cdot}198 \times 74{\cdot}56}{8{\cdot}9318} \text{ gram cals./mol} = -3658 \text{ gram cals./mol.}$$

The Measurements of the Heats of Solution.

The salts used were "Analytical Reagents," recrystallized and tested qualitatively for likely impurities.

For the preparation of ethyl alcohol, 96 per cent. ethyl alcohol was poured on to a large quantity of freshly burnt lime and allowed to stand over it for some days with periodical shaking. It was then fractionated, the first and last runnings being rejected. It was then allowed to stand over freshly cleaned and turned metallic calcium and was refractionated, the first and last runnings being again rejected, and was found free from aldehyde and ammonia. It was stored in a vessel with a siphon attachment and a guard tube of phosphorus pentoxide.

The density of the alcohol was ${}^{25^{\circ}}_{5^{\circ}}\mathrm{D} = 0{\cdot}7849$.

1. Potassium Chloride in Water.

The pure salt was dried at 120° C. The weight of water used was 391·42 grams. The experimental results are given in Table III. W.E. denotes water equivalent.

TABLE III.*

Weight of a single portion of KCl.	W. E. (corr.), cals./deg.	Isothermal correction, ° C.	Heat of reaction, cals.	Molar concentration, $\frac{\text{mols KCl}}{100 \text{ mols } H_2O}$.	Integral heat of solution, cals./mol.	Mean molar concentration, $\frac{\text{mols/KCl}}{100 \text{ mols } H_2O}$.	Intermed. heat of solution, cals./mol.
8·9990	458·482	−0·022	−514·875	0·5555	−4266	0·2777	−4266
6·1740	455·287	−0·004	343·547	0·9345	4229	0·7450	4149
8·0160	455·502	−0·012	440·536	1·4315	4178	1·1830	4101
7·2502	459·670	−0·012	388·109	1·8791	4132	1·6553	3991
9·0768	468·751	−0·048	480·083	2·4394	4089	2·1592	3944
8·7958	470·222	−0·010	456·066	2·9824	4048	2·7109	3866
8·6616	459·922	−0·017	440·571	3·5171	4010	3·2497	3784
9·6128	462·302	−0·022	479·052	4·1100	3967	3·8135	3716
8·9318	474·795	−0·048	438·198	4·6619	3931	4·3859	3658
8·9984	447 927	−0·024	435·534	5·2170	3896	4·9394	3600
9·2673	451·848	−0·002	436·923	5·7890	3859	5·508	3516
9·8539	453·177	−0·029	459·580	6·3980	3824	6·093	3477
				7·082	3768	7·210	3399
			From heat of dilution	7·338	3752	7·692	3362
				8·045	3715	8·363	3312
				8·681	3687		

* In all the tables the sign at the top of a column, or in the column, refers to all values below, until a new sign is introduced.

The details necessary for the calculation of the water equivalent and the heat of reaction are given in Tables IV. and V.

TABLE IV.

Details for Determination of Water Equivalent.

Expt.	Drop in voltage across (*a*) heater,	(*b*) standard,[1] 1 ohm.	Time, secs.	Temp. diff. (corr.).	Water equivalent, cals./deg.
1	6·8380	0·4330	200·8	0·310	458·482
2	6·8770	0·4373	223·7	0·353	455·287
3	6·9120	0·4389	247·0	0·393	455·502
4	6·7719	0·4305	198·0	0·300	459·670
5	6·9780	0·4428	201·3	0·317	468·751
6	6·9480	0·4413	218·9	0·341	470·222
7	6·8790	0·4372	207·4	0·324	459·922
8	6·8800	0·4367	195·8	0·304	462·302
9	6·9660	0·4425	257·9	0·400	474·795
10	6·9050	0·4390	320·4	0·518	447·927
11	6·8280	0·4344	281·85	0·442	451·848
12	6·8720	0·4385	254·95	0·405	453·177
13	6·8790	0·4359	204·95	0·334	439·571
14	6·7039	0·4040	215·35	0·323	431·386
15	5·5652	0·3555	272·4	0·398	407·251
16	6·8770	0·4373	191·35	0·310	446·640

TABLE V.

Details for Determination of Heat of Reaction.

Expt.	Voltage drop across (*a*) heater,	(*b*) standard, 1 ohm.	Time, ecs.	Heat of reaction uncorrected, in cals.
1	6·6058	0·4207	760·3	−504·778
2	6·8880	0·4378	479·4	345·368
3	6·9370	0·4401	611·5	446·002
4	6·9020	0·4379	545·15	393·624
5	6·9830	0·4431	679·9	502·583
6	6·9530	0·4416	628·15	460·768
7	6·8820	0·4372	623·8	448·390
8	6·8670	0·4365	683·05	489·123
9	6·9320	0·4422	629·5	460·988
10	6·9120	0·4391	615·5	446·284
11	6·8360	0·4345	174·6	123·894
	6·8510	0·4352	438·2	312·126
12	6·8710	0·4390	392·7	282·983
	6·8640	0·4388	137·3	98·794
	6·8570	0·4387	126·55	90·945
13	3·0798	0·1948	128·95	18·482
14	3·0798	0·1977	255·15	37·114
15	3·0728	0·1952	203·9	29·218
16	4·5546	0·2873	253·65	79·294

For the determination of the total heat of solution L_s, the heat of dilution of 36·33 grams of potassium chloride solution saturated at 25° C. (containing 9·6062 grams KCl in 26·72 grams of water) with 400 grams of water was measured.

Heat of dilution $= -74{\cdot}471$ cals.

This forms a solution containing 9·6062 grams of potassium chloride in 426·72 grams of water. If we now imagine this solution to be prepared from salt and water, we can find the integral heat of this solution from the curve connecting the integral heats of solution already found. From these two values simple calculation gives the value for the total heat of solution $L_s = -3687$ cals. per mol of potassium chloride. By combining this value for the total heat of solution with the heats of dilution obtained in the region of saturation, we obtain three values for the integral heat of solution L_c and the differential heat of solution Λ_c, at these concentrations. 302·628 grams of a saturated solution of potassium chloride at 25° C. were diluted three times with a known weight of water. The results obtained are added to the heats of solution directly determined in Table III. The curves connecting the heats of solution with concentration have been drawn for potassium chloride with the values of Table III. The curve for the mean intermediate heat of solution is practically a straight line, and so may be used without correction for curvature to give the values of the differential heat of solution. Extrapolation to the saturation point gives a value for the *final heat of solution*, $\Lambda_s = -3291$ cals. per mol of potassium chloride. Further, the production of the curves for the integral heat of solution and the differential heat of solution give a value for the *first heat of solution*, $L_0 = -4315$ cals. per mol of potassium chloride. Also, by means of the formula $\phi_c = c(L_c - \Lambda_c)$, we may calculate from both curves the *differential heat of dilution* ϕ_c and also the *first heat of dilution*, $\phi_s = -34{\cdot}41$ cals. per mol of water. The final values are collected in Table VI.

Comparison with previous Results.

The agreement of these values with those of Wust and Lange (*l. c.*) is quite satisfactory, since the accuracy of the present results is probably not so great as in their case. The results are compared in Table VII. There is also fairly good agreement with some results of Brönsted (*Zeit. für physik. Chem.* lvi. p. 663, 1906), although in this lower concentration range the agreement is not so good as in the

Table VI.

The Heats of Solution and Dilution of Potassium Chloride in Water at 25° C.

Concentration, $\frac{\text{mols KCl}}{100 \text{ mols } H_2O}$.	Integral heat of solution, cals./mol KCl.	Differential heat of solution, cals./mol KCl.	Differential heat of dilution, cals./mol H_2O.
0·0	L_0 −4315	−4315	−0·00
0·5	4268	4214	0·30
1·0	4218	4100	1·22
1·5	4168	4020	2·295
2·0	4126	3942	3·680
2·5	4087	3877	5·250
3·0	4048	3811	7·110
3·5	4007	3744	9·205
4·0	3974	3672	12·06
4·5	3938	3628	13·95
5·0	3906	3585	16·05
5·5	3873	3540	18·315
6·0	3839	3495	20·64
6·5	3805	3448	23·205
7·0	3773	3415	25·08
7·5	3743	3377	27·45
8·0	3718	3338	30·40
8·5	3694	3302	33·32
8·691	3687	3291	34·41

$L_0 = -4315$; ; $L_s = -3687$; $\Lambda_s = -3291$; $\phi_s = -34{\cdot}41$.

Table VII.

Concentration, $\frac{\text{mols/KCl}}{100 \text{ mols } H_2O}$.	L_c, cals./mol KCl, present values.	L_c, cals./mol KCl, Wust and Lange.
0·0	−4315	−4285
0·5	4268	4245
1·0	4218	4205
1·5	4168	4165
2·0	4126	4123
2·5	4087	4082
3·0	4048	4043
3·5	4007	4004
4·0	3974	3966
4·5	3938	3930
5·0	3906	3894
5·5	3873	3860
6·0	3839	3828
6·5	3805	3798
7·0	3773	3770
7·5	3743	3743
8·0	3718	3720
8·5	3694	3700
8·691	3687	3692

higher concentrations. Brönsted's measurements were made at a temperature of 25·04° C. In Table VIII. the results are compared with those of Brönsted and with those of Wust and Lange for the same concentrations.

TABLE VIII.

Concentration, $\frac{\text{mols KCl}}{100 \text{ mols } H_2O}$	L_c, cals./mol KCl, present values.	L_c, cals./mol KCl, Brönsted.	L_c, cals./mol KCl, Wust and Lange.
0·167	−4302	−4266 .	−4273
0·333	4285	4255	4258
0·499	4268	4246	4245
0·667	4257	4235	4233
0·833	4235	4224	4218

These results probably show the limits of accuracy of the apparatus, since they were the first obtained, without any practice in manipulation. Among others, values have been obtained by Holluta and Werner (*Zeit. für physik. Chem.* cxxix. p. 262, 1927), who for a concentration of 1·107 mols KCl per 100 mols of water give 4216·1 cals., while the present curve gives 4210 cals.

Berthelot and Ilosvay (*Ann. de chim. et de phys.* xxix. p. 295, 1883), at a temperature of 18·5° C. and concentration 1 mol KCl per 100 mols water, give −4305 cals. By means of a formula for the temperature coefficient the value at 25° C. would be found to be −4136 cals. per mol of potassium chloride, while the present value is −4218. The difference is quite within the limits of accuracy attainable by these authors.

2. Potassium Thiocyanate in Water.

The pure salt was dried at 140° C. in an electric oven. The weight of water used was 349·36 grams. The results are given in Table IX.

The water equivalent and heat of reaction were calculated as before, and in this and all subsequent cases details will be found in the thesis of W. E. Soper, in the University of London, 1928.

The total heat of solution L_s was determined as before from dilution experiments. 34·18 grams of a saturated solution (at 25° C.) of potassium thiocyanate in water (containing 23·91 grams of potassium thiocyanate per

TABLE IX.

Weight of a single portion of KCNS.	W. E. (corr.), cals./deg.	Isothermal correction, °C.	Heat of reaction, cals.	Molar concentration, mols KCNS / 100 mols H_2O.	Integral heat of solution, cals./mol.	Moan molar concentration, mols KCNS / 100 mols H_2O.	Intermed. heat of solution, cals./mol.
8·5289	399·308	−0·031	−509·664	0·489	−5807	0·244	−5807
5·3256	394·925	−0·019	306·473	0·794	5724	0·642	5592
5·3254	394·875	−0·018	302·796	1·100	5669	0·947	5525
4·3218	397·321	−0·016	231·916	1·347	5585	1·223	5214
4·9438	398·577	−0·013	273·241	1·627	5561	1·487	5371
7·5628	387·271	−0·065	416·511	1·781	5557	1·558	5352
7·2498	386·130	−0·011	388·262	2·210	5478	1·995	5204
9·0490	381·488	−0·004	464·090	2·746	5382	2·478	4984
7·6404	395·051	−0·005	383·851	3·199	5311	2·972	4882
8·1138	379·051	−0·002	393·716	3·680	5233	3·439	4715
8·0698	381·525	−0·002	383·802	4·157	5163	3·918	4622
7·9192	384·206	−0·004	371·026	4·626	5101	4·392	4553
9·1110	384·761	−0·001	414·887	5·166	5031	4·896	4425
8·1463	386·094	−0·006	362·457	5·648	4970	5·407	4324
				28·18	3521		
						29·26	2818
				30·35	3463		
						31·99	2718
				33·63	3406		
						34·72	2713
				35·80	3355		
						37·50	2665
				39·21	3295		
						41·25	2647
				43·29	3235		

From dilution experiments .....

10·27 grams of water) was added to 370·1 grams of water, and the heat of dilution measured.

Heat of dilution	−597·890 cals.
Heat of solution from L_c curve.	−1393·875 cals.
Total heat of solution (calcd.).	−3235 cals./mol. KCNS.

Five intermediate heats of dilution have been combined with this value of the total heat of solution. They were obtained by diluting with five separate weighed quantities of water (about 12 grams) 407·210 grams of a saturated solution (containing 284·920 grams KCNS in 122·29 grams of water).

TABLE X.

Expt.	1.	2.	3.	4.	5.
Weight of water added, grms....	12·4317	12·8408	13·1762	13·3330	13·3556
Heat of dilution, cals.	−175·358	−175·991	−167·890	−167·885	−166·066

From these results and from the value of the total heat of solution L_s, values for the integral heats of solution L_c, and for the differential heats of solution Λ_c, may be calculated. The values are given in the table of experimental results (Table IX.).

The experimental values were plotted against concentration, and the differential heat of solution obtained from the curves, together with the extrapolated values for the first heat of solution. The first heat of dilution and the differential heat of dilution were obtained as before. The final values are given in Table XI.

No previous measurements have been found at this temperature, and, indeed, the only previous measurement is that given in Landolt-Börnstein's *Tabellen*, due to Joannis at 13° C., and concentration of 1 mol of potassium thiocyanate to 200 mols water, who gives −6·1 kilog. calories.

Discussion of the Results for Potassium Thiocyanate and Water.

The curves for potassium thiocyanate and water are quite regular and free from any characteristics. The heat of solution is negative.

It was not possible to obtain any values for potassium thiocyanate and ethyl alcohol, since the solubility is not very great and the process of solution is very slow. It was,

however, found that the heat of solution of potassium thiocyanate in ethyl alcohol is negative in sign as far as it could be observed.

TABLE XI.

Heats of Solution and Dilution of Potassium Thiocyanate in Water at 25° C.

Concentration, $\frac{\text{mols KCNS}}{100 \text{ mols } H_2O}$	Integral heat of solution L_c, cals./mol KCNS.	Differential heat of solution A_c, cals./mol KCNS.	Differential heat of dilution ϕc, cals./mol H_2O.
0·0	−5988	−5988	0·0
0·5	5795	5693	−0·51
1·0	5693	5494	1·99
1·5	5603	5325	4·17
2·0	5508	5157	7·02
2·5	5422	5003	10·475
3·0	5339	4859	14·40
3·5	5258	4727	15·585
4·0	5185	4614	22·84
4·5	5115	4492	28 035
5·0	5050	4380	33·50
5·5	4985	4270	39·325
.....	.....	.....	.....
30·0	−3470	−2792	−203·4
31·0	3447	2762	212·35
32·0	3426	2736	220·8
33·0	3406	2716	227·7
34·0	3387	2699	233·9
35·0	3368	2685	233·9
36·0	3350	2674	239·05
37·0	3332	2667	246·05
38·0	3314	2661	248·14
39·0	3298	2656	250·38
40·0	3281	2651	252·00
41·0	3267	2647	254·20
42·0	3252	2644	255·36
43·0	3239	2641	257·14
43·291	3235	2640	257·58

$L_0 = -5988$; $L_s = -3235$.

3. SODIUM THIOCYANATE IN WATER.

The pure salt was recrystallized and dried by heating to 140° C. The weight of water used was 348·00 grams. The results are given in Table XII.

TABLE XII.

Weight of a single portion of NaCNS.	W. E (corr.), cals./deg.	Isothermal correction, °C.	Heat of reaction, cals.	Molar concentration, $\frac{\text{mols NaCNS}}{100 \text{ mols } H_2O}$.	Integral heat of solution, cals./mol.	Mean molar concentration, $\frac{\text{mols NaCNS}}{100 \text{ mols } H_2O}$.	Intermed. heat solution, cals./mol.
4·7950	404·823	−0·027	−99·232	0·306	−1678	0·153	−1678
5·2886	405·782	−0·005	102·568	0·644	1622	0·475	1573
5·9389	403·858	−0·000	109·279	1·023	1574	0·833	1495
6·7007	407·977	−0·026	113·138	1·451	1514	1·237	1369
6·1119	399·609	−0·043	91·415	1·841	1450	1·646	1213
5·7219	401·737	−0·001	79·259	2·207	1396	2·024	1123
From dilution experiments				19·37	− 428	20·12	603
				20·93	445	21·87	609
				22·77	463	23·88	681
				25·00	486	26·55	873
				28·11	521		

The total heat of solution was determined, as before, from dilution experiments. 26·5556 grams of a saturated solution of sodium thiocyanate at 25° C. (containing 14·6649 grams of sodium thiocyanate in 11·8907 grams of water) was diluted with 329·65 grams of water.

Heat of dilution	−191·727 cals.
Heat of solution from L_c curve.	−285·979 cals.
Total heat of solution (calcd.) .	−521 cals./mol NaCNS

Four intermediate heats of dilution have been combined with this value of the total heat of solution. They were obtained by diluting with four separate weighed quantities of water (about 12 grams) 308·480 grams of a saturated solution of sodium thiocyanate at 25° C. (containing 164·605 grams of sodium thiocyanate in 133·805 grams of water).

Table XIII.

Expt.	1.	2.	3.	4.
Weight of water added, grams.	12·8760	14·3432	13·6866	14·5423
Heat of dilution, cals.	−97·225	−49·200	−35·663	−34·543

From these results and from the value of the total heat of solution the values of the integral heats of solution at these concentrations may be calculated. The values are added to Table XII.

The experimental values have been plotted against concentration, and the first heat of solution and values for the differential heats of solution obtained. The final values are added to Table XIV.

Table XIV.

[Heats of Solution and Dilution of Sodium Thiocyanate in Water at 25° C.

Concentration, $\frac{\text{mols NaCNS}}{100 \text{ mols } H_2O}$	Integral heat of solution L_c, cals./mol NaCNS.	Differential heat of solution, cals./mol NaCNS.	Differential heat of dilution, cals./mol H_2O.
0·0	−1677	−1677	0·0
0·5	1648	1571	−0·38
1·0	1574	1426	1·48
1·5	1500	1268	3·48
2·0	1425	1113	6·24

TABLE XIV. (*continued*).

Heats of Solution and Dilution of Sodium Thiocyanate in Water at 25° C.

Concentration, mols NaCNS / 100 mols H_2O	Integral heat of solution L_c, cals./mol NaCNS.	Differential Heat of solution, cals./mol NaCNS.	Differential heat of dilution, cals./mol H_2O.
20·0	434	These values are indefinite, since the curve goes through a maximum and there are not enough points to decide the course of the curve.	
20·5	439		
21·0	444		
21·5	450		
22·0	455	−612	+36·30
22·5	460	625	37·12
23·0	465	640	40·25
23·5	470	651	42·50
24·0	476	687	50·64
24·5	481	716	57·57
25·0	486	751	36·25
25·5	493	788	75·225
26·0	500	827	85·02
26·5	507	868	95·665
27·0	514	909	106·65
27·47	521	947	117·02

$L_0 = -1677$; $L_s = -521$; $A_s = -947$; $\varphi_s = +117{\cdot}02$.

There are no previous measurements to compare with the present values.

4. The Heat of Solution of Sodium Thiocyanate in Ethyl Alcohol.

The pure salt was carefully dried at 140° C. in an electric oven after being recrystallized several times from water. The weight of ethyl alcohol used was 258·08 grams. The experimental results are given in Table XV.

The total heat of solution was obtained, as before, from dilution experiments. A saturated solution of sodium thiocyanate in ethyl alcohol at 25° C. (containing 2·6832 grams of sodium thiocyanate in 12·7292 grams of ethyl alcohol) was diluted with 270·20 grams of ethyl alcohol.

Heat of dilution	70·122 cals.
Heat of solution from L_c curve.	36·803 cals.
Total heat of solution (calcd.)	−1007 cals./mol NaCNS

TABLE XV.

Heats of Solution of Sodium Thiocyanate in Ethyl Alcohol at 25° C.

Weight of a single portion of NaCNS.	W. E. (corr.), cals./deg.	Isothermal correction or temp. rise.	Heat of reaction, cals.	Molar concentration, mols $\frac{\text{NaCNS}}{100 \text{ mols EtOH}}$	Integral heat solution, cals./mol.	Mean molar concentration, mols $\frac{\text{NaCNS}}{100 \text{ mols EtOH}}$	Intermed. heat solution, cals./mol.
6·0357	226·500	0·335	+75·877	1·203	+1019	0·601	+1019
4·3938	226·155	0·159	35·959	2·074	871	1·638	648
4·0689	230·744	0·080	18·460	2·889	729	2·481	368
5·9800	238·124	0·050	11·906	4·081	563	3·985	161
5·9988	239·029	−0·032	−25·684	5·276	357	4·678	−330
5·3684	241·470	−0·005	−44·636	6·346	183	5·811	−674
5·8350	240·591	0·004	−68·833	7·509	6·5	6·927	−956
				8·814	−769	8·897	−1417
				9·164	−793	9·334	−1474
				9·505	−818	9·721	−1540
				9·938	−849	10·114	−1620
				10·391	−884	10·643	−1705
				10·896	−922	11·106	−1788
				11·416	−961	11·693	−1934
				11·970	L_s −1007		

From dilution experiments

The last three values in column 3 are isothermal corrections.

Seven successive intermediate heats of dilution were measured, starting from the saturated solution, and combined with this value for the total heat of solution. 253·64 grams of a saturated solution of sodium thiocyanate in ethyl alcohol at 25° C. (containing 44·156 grams of sodium thiocyanate in 209·484 grams of ethyl alcohol) were diluted successively with seven weighed quantities of ethyl alcohol.

From these results, and from the value of the total heat of solution, the values for the integral heats of solution may be calculated for these concentrations, as well as the mean intermediate heats of solution. The values obtained are added to the experimental results in Table XV.

TABLE XVI.

Expt.	Weight of alcohol added, grams.	Heat of dilution, cals.
1	10·2545	+24·792
2	10·4948	21·553
3	11·1688	20·741
4	11·0273	18·595
5	11·4903	17·149
6	9·8038	13·314
7	10·8691	13·563

The experimental values have been plotted against concentration, and the final values in Table XVII. have been

TABLE XVII.

Heats of Solution and Dilution of Sodium Thiocyanate in Ethyl Alcohol at 25° C.

Concentration, mols NaCNS 100 mols EtOH	Integral heat of solution L_c, cals./mol NaCNS.	Differential heat of solution Λ_c, cals./mol NaCNS.	Differential heat of dilution ϕ_c, cals./mol EtOH.
0·0	+1195	+1195	0·0
0·5	1117	1050	+0·33
1·0	1035	860	1·75
1·5	955	693	3·93
2·0	875	550	7·50
2·5	795	364	8·83
.....	.....	.....	.....
9·0	−790	−1427	+57·33
9·5	815	1514	66·40
10·0	848	1615	76·70
10·5	885	1705	86·10
11·0	920	1800	96·80
11·5	964	1896	107·18
11·970	1007	1992	117·90

$L_0 = +1195$; $L_s = -1007$; $\Lambda_s = -1992$; $\phi_s = +117{\cdot}90$.

obtained from these curves. By extrapolation we also obtain the final heat of solution, the first heat of solution, and the differential heat of solution.

Discussion of Results with Sodium Thiocyanate.

The curve drawn for the differential heat of solution of sodium thiocyanate in water passes through a maximum value. Similar curves were found for the chloride, bromide, and iodide of sodium by Wust and Lange.

An examination of the curves for sodium thiocyanate and ethyl alcohol shows that at lower concentrations the heat of solution is positive in sign, but with rising concentration the value becomes smaller, and finally becomes negative in sign. This might possibly point to the existence of an alcoholate at lower concentrations, but as yet it has not been isolated.

5. The Heat of Solution of Anhydrous Cupric Chloride in Water.

The pure salt was recrystallized from water, and dehydrated and dried by heating in an electric oven at 140° C. The weight of water used was 340·35 grams. The experimental results are given in Table XVIII.

The total heat of solution was obtained, as before, from dilution experiments. A saturated solution of cupric chloride in water (containing 10·7751 grams of $CuCl_2$ in 14·3643 grams of water) was diluted with 387·67 grams of water.

Heat of dilution	405·994 cals.
Heat of solution from L_c curve.	894·849 cals.
Total heat of solution (calcd.)...	6247 cals./mol $CuCl_2$

Four successive intermediate heats of dilution of the saturated solution have been made and combined with this value for the total heat of solution. 542·26 grams of a saturated solution of cupric chloride in water at 25° C. (containing 233·496 grams of cupric chloride ($CuCl_2$) in 308·764 grams of water) were diluted successively with four weighed quantities of water.

Table XVIII.

Heat of Solution of Anhydrous Cupric Chloride in Water at 25° C.

Weight of a single portion of $CuCl_2$.	W. E. (corr.), cals./deg.	Temperature rise, ° C.	Heat of reaction, cals.	Molar concentration, mols $CuCl_2$ / 100 mols H_2O.	Integral heat solution, cals./mol.	Mean molar concentration, mols $CuCl_2$ / 100 mols H_2O.	Intermed. heat solution, cals./mol.
3·0566	409·495	0·643	+263·305	0·120	+11724	0·060	+11724
3·8322	412·313	0·781	322·017	0·271	11590	0·195	11387
4·6039	417·830	0·908	379·390	0·452	11355	0·361	11082
3·5724	397·686	0·707	281·164	0·593	11193	0·522	10671
3·9836	406·092	0·760	303·630	0·750	11031	0·672	10420
3·9720	391·353	0·750	293·515	0·906	10865	0·828	10071
3·5679	396·564	0·650	257·767	1·046	10711	0·976	9716
From dilution experiments				8·712	6607	8·869	4218
				9·027	6515	9·185	4092
				9·344	6438	9·513	4033
				9·683	6349	9·866	3873
				10·049	6247		

TABLE XIX.

Expt.	Weight of water added, grams.	Heat of dilution.
1	13·5225	+177·370
2	12·4666	155·170
3	10·9380	133·064
4	13·3365	169·987

From these values and from the value of the total heat of solution the values for the integral heats of solution at these concentrations was obtained. The values obtained are added to the experimental values in Table XVIII. The experimental values have been plotted against concentration, and the final values were taken from these. The final values are given in Table XX. By extrapolation we obtain the final heat of solution, the first heat of solution, and the differential heats of dilution at saturation.

TABLE XX.

The Heats of Solution and Dilution of Anhydrous Cupric Chloride at 25° C.

Concentration, mols $CuCl_2$ / 100 mols H_2O	Integral heat of solution L_c, cals./mol $CuCl_2$.	Differential heat of solution A_c, cals./mol $CuCl_2$.	Differential heat of dilution ϕ_c, cals./mol H_2O.
0·0	+11850	+11850	0·0
0·5	11300	10754	+2·73
1·0	10763	9658	11·05
.....	.....	.....	.....
8·5	+6663	+4162	+212·58
9·0	6528	4110	217·58
9·5	8394	4020	225·53
10·0	6259	3802	245·70
10 049	6247	3778	248·11

$L_0 = +11850$; $L_s = +6247$; $A_s = +3778$; $\phi_s = +248{\cdot}11$.

Comparison with previous Values.

The only previous value is due to Thomsen at concentration 0·167 mol $CuCl_2$ per 100 mols of water, and is 11080 cals./mol., the value in the present work being 11625.

6. HEAT OF SOLUTION OF ANHYDROUS CUPRIC CHLORIDE IN ETHYL ALCOHOL.

The pure salt was recrystallized, dehydrated, and dried as before. It was carefully and quickly put into a dried and weighed pipette and weighed again. The weight of ethyl alcohol used was 251·870 grams. The experimental values are given in Table XXI.

TABLE XXI.

Weight of a single portion of $CuCl_2$.	W. E. (corr.), cals./deg.	Temperature rise, ° C.	Heat of reaction, cals.	Molar concentration, $\frac{\text{mols } CuCl_2}{100 \text{ mols EtOH}}$.	Integral heat solution, cals./mol.	Mean molar concentration, $\frac{\text{mols } CuCl_2}{100 \text{ mols EtOH}}$.	Intermed. heat solution, cals./mol.
5·8759	215·220	1·001	+215·436	0·799	+4931	0·400	+4931
4·6276	215·745	0·736	158·786	1·428	4792	1·113	4615
4·5658	213·305	0·705	150·380	2·049	4693	1·738	4430
5·0588	211·073	0·761	160·621	2·737	4578	2·393	4270
4·0896	211·959	0·593	125·692	3·293	4514	3·015	4133
4·3124	216·569	0·603	130·591	3·879	4438	3·586	4073
4·5458	217·671	0·613	133·432	4·497	4371	4·188	3948
From dilution experiments				11·91	3626	12·16	2915
				12·42	3597	12·68	2884
				12·95	3560	13·27	2634
				13·60	3516	13·90	2503
				14·20	3473	14·56	2430
				14·93	3422	15·32	2248
				15·71	3364	16·12	2188
				16·52	3307	17·02	2180
				17·52	3243		

The total heat of solution was obtained, as before, from dilution experiments. A saturated solution of anhydrous cupric chloride in ethyl alcohol at 25° C. (containing 4·8554 grams of $CuCl_2$ in 10·0146 grams of ethyl alcohol) was diluted by 258·73 grams of ethyl alcohol.

Heat of dilution	62·211 cals.
Heat of solution from L_c curve.	179·284 cals.
Total heat of solution (calcd.)...	3243 cals./mol $CuCl_2$

Eight successive intermediate heats of dilution of the saturated solution were made and combined with this value for the total heat of solution. 285·73 grams of a saturated solution of anhydrous cupric chloride in ethyl alcohol at 25° C. (containing 96·69 grams of $CuCl_2$ in 189·04 grams of ethyl alcohol) were diluted successively with eight weighed quantities of alcohol.

TABLE XXII.

Expt.	Weight of ethyl alcohol added, grams.	Heat of dilution, cals.
1	11·4598	+46·236
2	10·2208	40·994
3	11·0205	41·910
4	11·5225	37·087
5	10·1432	30·367
6	12·3432	32·172
7	10·7746	25·933
8	11·4326	21·114

From these results and from the total heat of solution the values for the integral and mean intermediate heats of solution are calculated for these concentrations. The values obtained are added to the values determined experimentally in Table XXI. The experimental values have been plotted against concentration, and the final values in Table XXIII. obtained. The first heat of solution and the final heat of solution are obtained by extrapolation, and the differential heat of dilution by the simple calculation used previously.

TABLE XXIII.

Heats of Solution and Dilution of Anhydrous Cupric Chloride in Ethyl Alcohol at 25° C.

Concentration, mols $CuCl_2$ / 100 mols EtOH	Integral heat of solution L_c, cals./mol CuCl.	Differential heat of solution, cals./mol $CuCl_2$.	Differential heat of dilution, cals./mol H_2O.
0·0	+5126	+5126	+0·0
0·5	4996	4875	0·6
1·0	4882	4665	2·17
1·5	4780	4490	4·35
2·0	4685	4360	6·50
2·5	4618	4245	9·32
3·0	4548	4134	12·42
3·5	4483	4075	14·28
14·0	3489	2975	71·96
15·0	3416	2551	129·75
16·0	3343	2296	167·52
17·0	3277	2182	186·12
17·5	3244	2175	186·87
17·52	3243	2176	186·94

$L_0 = +5126$; $L_s = +3243$; $A_s = +2176$; $\varphi_s = +186{\cdot}94$.

Discussion of the Results with Cupric Chloride.

In the case of water the first heat of solution is very high and positive in sign. With rising concentration the value for the heat of solution diminishes fairly rapidly, but it always remains comparatively high. With ethyl alcohol the heat of solution is positive in sign, but it does not vary so rapidly with rising concentration, although it does fall. Cupric chloride forms a stable hydrate, $CuCl_2 . 2H_2O$ with water, and a stable alcoholate with ethyl alcohol, $CuCl_2 . 2EtOH$ (see Lloyd, Brown, Bonnell, and Jones, J. Chem. Soc. p. 658, 1928). This would probably account for the high positive values for the heat of solution.

7. THE HEAT OF SOLUTION OF ANHYDROUS CALCIUM NITRATE IN WATER.

The pure salt was recrystallized several times from water, dehydrated by gentle heating in an electric oven, and finally heated for some hours in the electric oven at a temperature exceeding 180° C. The weight of water used was 355·47 grams. The experimental results are given in Table XXIV.

TABLE XXIV.

Weight of a single portion of $Ca(NO_3)_2$.	W. E. (corr.), cals./deg.	Temperature rise, ° C.	Heat of reaction, cals.	Molar concentration, $\frac{\text{mols } Ca(NO_3)_2}{100 \text{ mols } H_2O}$	Integral heat solution, cals./mol.	Molar concentration, $\frac{\text{mols } Ca(NO_3)_2}{100 \text{ mols } H_2O}$	Intermed. heat solution, cals./mol.
4·5948	388·337	·295	+114·559	0·142	+4129	0·071	+4129
4·1584	402·667	·269	108·318	0·271	4193	0·206	4264
7·0424	408·998	·460	188·138	0·489	4274	0·380	4373
6·1462	409·104	·412	168·551	0·679	4334	0·584	4489
6·8117	397·659	·480	190·878	0·890	4394	0·784	4587
6·2484	405·530	·452	183·300	1·084	4467	0·987	4802
				11·715	5480	12·006	4549
				12·297	5436	12·596	4418
From dilution experiments				12·896	5389	13·270	4230
				13·645	5326	14·084	4068
				14·523	5258		

The total heat of solution was determined, as before, from dilution experiments. A saturated solution of calcium nitrate in water at 25° C. (containing 16·1091 grams of $Ca(NO_3)_2$ in 12·2349 grams of water) was diluted by 336·65 grams of water.

Heat of dilution	−96·263 cals.
Heat of solution from L_c curve.	4280 cals./mol $Ca(NO_3)_2$
Total heat of solution (calcd.)	5258 cals./mol $Ca(NO_3)_2$

Four successive heats of dilution were measured and were combined with this value for the total heat of solution. 524·88 grams of a saturated solution of calcium nitrate in water at 25° C. (containing 297·625 grams of $Ca(NO_3)_2$ in 227·255 grams of water) were diluted successively with four weighed quantities of water.

TABLE XXV.

Expt.	1.	2.	3.	4.
Weight of water added in grams.	13·2236	13·5082	12·3702	13·2200
Heat of dilution in cals.	+126·524	+111·196	+85·944	+80·064

From these results and from the total heat of solution the values for the integral and mean intermediate heats of solution for these concentrations are easily calculated as before. The values are added to the experimentally determined values in Table XXIV. The experimental values have been plotted against concentration and the final values in Table XXVI. obtained from these curves. The first heat of solution and the final heat of solution are found by extrapolation, and the differential heat of dilution by calculation as before.

TABLE XXVI.

Heats of Solution and Dilution of Anhydrous Calcium Nitrate in Water at 25° C.

Concentration, mols $\frac{Ca(NO_3)_2}{100 \text{ mols } H_2O}$	Integral heat of solution L_c, cals./mol salt.	Differential heat of solution Δ_c, cals./mol salt.	Differential heat of dilution ϕ_c, cals./mol H_2O.
0·0	+4074	+4074	0·0
0·5	4277	4443	−0·78
1·0	4437	4666	2·29
.....	.....	.....	.....
11·5	5495	4590	+104·07
12·0	5458	4516	113·04
12·5	5420	4424	124·5

TABLE XXVI. (*continued*).

Heats of Solution and Dilution of Anhydrous Calcium Nitrate in Water at 25° C.

Concentration, mols $Ca(NO_3)_2$ / 100 mols H_2O	Integral heat of solution L_c, cals./mol salt.	Differential heat of solution A_c, cals./mol salt.	Differential heat of dilution ϕ_c cals./mol H_2O.
13·0	5380	4306	138·32
13·5	5339	4189	155·25
14·0	5299	4070	172·08
14·5	5260	3954	189·37
14·523	5258	3948	190·35

$L_0 = +4074$; $L_s = +5258$; $A_s = 3948$; $\phi_s = +190{\cdot}35$.

Comparison with previous Values.

Thomsen gives a value for 0·25 mol $Ca(NO_3)_2$ in 100 mols of water which is 3950 cals. per mol of salt. The value for this in the present work is 4184.

Pickering gives the two values for water :—

TABLE XXVII.

Concentration, mols $Ca(NO_3)_2$ / 100 mols H_2O	L_c (Pickering).	L_c (present work).
0·404	+3940	+4246
0·408	3945	4248

8. THE HEATS OF SOLUTION OF ANHYDROUS CALCIUM NITRATE IN ETHYL ALCOHOL AT 25° C.

The purified salt was recrystallized several times from water, dehydrated by general heating, and finally heated to a temperature exceeding 180° C. for some hours. The weight of ethyl alcohol used was 313·85 grams. The experimental results are given in Table XXVIII.

The total heat of solution was determined as before. The saturated solution of anhydrous calcium nitrate in ethyl alcohol at 25° C. (containing 6·2576 grams of $Ca(NO_3)_2$ in 13·1273 grams of ethyl alcohol) was diluted by 313·52 grams of ethyl alcohol.

Heat of dilution	76·296 cals.
Heat of solution from L_c curve.	282·934 cals./mol salt
Total heat of solution (calcd.).	5406 cals./mol $Ca(NO_3)_2$

TABLE XXVIII.

Weight of a single portion, $Ca(NO_3)_2$.	W. E. (corr.) cals./deg.	Temperature rise, ° C.	Heat of reaction, cals.	Molar concentration, $\frac{\text{mols } Ca(NO_3)_2}{100 \text{ mols EtOH}}$.	Integral heat solution, cals./mol.	Mean molar concentration, $\frac{\text{mols } Ca(NO_3)_2}{100 \text{ mols EtOH}}$.	Intermed. heat solution, cals./mol.
1·6617	—	—	—	0·152	—	—	—
4·5024	239·705	0·847	+203·030	0·552	+7402	0·352	+7382
5·2171	239·213	0·946	226·295	1·020	7264	0·786	7101
4·6550	235·347	0·843	198·397	1·434	7197	1·227	6977
4·1882	240·958	0·725	174·694	1·813	7108	1·624	6828
5·0582	243·425	0·864	210·319	2·266	7048	2·039	6807
3·6726	243·815	0·615	149·946	2·596	7001	2·432	6684
2·8787	247·637	0·473	117·287	2·854	6955	2·675	6670
From dilution experiments				11·157	5600	11·407	4763
				11·658	5564	11·913	4514
				12·168	5520	12·462	4369
				12·757	5467	13·084	4219
				13·411	5406		

Four successive heats of dilution of the saturated solution were made and combined with this value for the total heat of solution. 330·720 grams of a saturated solution of anhydrous calcium nitrate in ethyl alcohol at 25° C. (containing 106·759 grams $Ca(NO_3)_2$ in 223·961 grams of ethyl alcohol) were diluted by four weighed quantities of ethyl alcohol.

TABLE XXIX.

Expt.	1.	2.	3.	4.
Weight of water added in grams.	11·5429	11·3275	10·8146	11·5742
Heat of dilution in calories.....	39·909	34·381	28·738	23·623

From these results and the value of the total heat of solution the values for the integral heat of solution and the mean intermediate heat of solution may be obtained for these concentrations. The values obtained are added to Table XXVIII. The experimental values have been plotted against concentration, and the final values in Table XXX. obtained in the curves. The first and final heats of solution were obtained by extrapolation from these curves, and the differential heat of dilution by means of the simple calculation used before.

TABLE XXX.

The Heats of Solution and Dilution of Anhydrous Calcium Nitrate in Ethyl Alcohol at 25° C.

Concentration, $\frac{\text{mols } Ca(NO_3)_2}{100 \text{ mols EtOH}}$	Integral heat of Solution L_c, cals./mol salt.	Differential heat of solution A_c, cals./mol salt.	Differential heat of dilution ϕ_c, cals./mol EtOH.
0·0	+7584	+7584	0·0
0·5	7412	7244	+0·84
1·0	7280	7043	2·37
1·5	7170	6908	3·93
2·0	7084	6794	5·80
2·5	7018	6690	8·20
3·0	6935	6584	10·53
.....	.....	.....	.....
11·5	5579	4716	99·24
12·0	5533	4494	124·68
12·5	5489	4351	142·25
13·0	5443	4240	156·39
14·411	5406	4145	169·11

$L_0 = +7584$; $L_s = +5406$; $A_s = +4145$; $\phi_s = +169{\cdot}11$.

Comparison with previous values.

Pickering obtained the following values :—

TABLE XXXI.

Concentration, mols $Ca(NO_3)_2$ 100 mols EtOH	L_c (Pickering).	L_c (present work).
0·132	+7548	+7539
0·105	8708	7549
0·101	8711	7550

Discussion of the Results with Anhydrous Calcium Nitrate.

The heat of solution of anhydrous calcium nitrate in water is positive in sign. It rises with rising concentration to a maximum and then slowly falls. In the case of ethyl alcohol the value is positive, but greater than with water, and falls gradually with increasing concentration.

In this case, again, stable hydrates are known to exist. Graham (Phil. Mag. iv. pp. 265, 331, 1928) claimed to have isolated a crystalline alcoholate $2Ca(NO_3)_2$, 5EtOH. Lloyd, Brown, Bonnell, and Jones find $Ca(NO_3)_2 . 2EtOH$.

Chemical Department,
East London College,
University of London.

XXVII. *Liquid Drops on the same Liquid Surface.* *By* J. B. SETH, *M.A.* (*Cantab.*), CHETAN ANAND, *M.A.* (*Punjab*), *and* LACHMAN DAS MAHAJAN, *M.Sc.* (*Punjab*) *.

THE phenomenon of liquid drops formed and floating on the surface of the same liquid is of quite common occurrence. Thus, whenever a fine spray of water is falling on a surface of water, tiny drops of water can often be seen moving about on the water surface and finally coalescing with the general body of the liquid. The same effect is observed when a glass vessel containing some methylated spirit is bowed across its edge. A large number of drops, forming a regular pattern, are produced and remain floating on the surface for a short time, when they disappear in the body of the liquid. (A very familiar experiment described in text-books.) In the purification of aniline by distillation

* Communicated by the Authors.

one often finds that a condensed drop, falling from the delivery tube, remains floating on the aniline surface in the receiving vessel for one or two seconds and then suddenly mixes with the liquid. Last year Professor Kataline published a paper* in which he gave an account of a demonstration of this phenomenon. He used a solution of fluorescin in water containing some gelatine, and obtained drops with a diameter up to about 6 mm. and having velocities from 10 to 30 cm. per second, which kept swimming on the surface for a period up to 6 seconds. He conclusively demonstrated that these were drops of the liquid and not mere bubbles.

The object of the present investigation was to study in detail the conditions which make the formation of the floating drops easy, their size larger, and their lives longer. A large number of liquids have been tried and their properties studied, and a brief summary of the work is given below. By using suitable liquids under favourable conditions it has been possible to obtain floating drops as large as 12 mm. in diameter, and drops which kept floating on their liquid surface for nearly five minutes.

The easiest and most commonly applicable method of producing the drops is to fill the liquid in a burette and to allow it to flow down, drop by drop, on the surface of the same liquid kept in a suitable basin. The drops that float on the surface of the liquid can be classified under two headings: primary drops and secondary drops. The primary drops are obtained when the liquid is allowed to come down drop by drop from a rather small height, the minimum height being just a little greater than the diameter of the drop formed, and the maximum height for this primary drop formation going up to 2 or 3 cm., depending upon the liquid and its dilution. The drop as it comes down does not coalesce with the liquid immediately on its impact with the surface but remains floating for a short time. If now the height from which the drops fall is raised above the said maximum height, there is a cessation of the phenomenon until the height has reached a certain minimum value for a particular liquid, when the swimming drops on the liquid surface again make their appearance. These drops are formed by splashes (Worthington's splashes) which cause them to be detached from the main body of the liquid when they float on its surface. These we term secondary drops. For any particular liquid, thus, there is a certain range of height during which there is no formation of drops at all.

* *Zeits. f. Phys.* Jan. 1927.

The primary drops have, as a rule, larger sizes than the secondary, while the life of the secondary drops is generally longer than that of the primary ones. The primary drops are also less mobile compared with the secondary ones.

The phenomenon can be easily demonstrated with the help of Boys's soap solution, or a solution of phenyle in water. The curves in fig. 1 (*a*) show the maximum and minimum heights for primary and secondary drop formation respectively when the liquid employed is Boys's soap solution of different strengths. Fig. 1 (*b*) shows similar curves for phenyle. 25 per cent. soap solution and 30 per cent. phenyle solution had the smallest range of no drop formation.

Fig. 1.

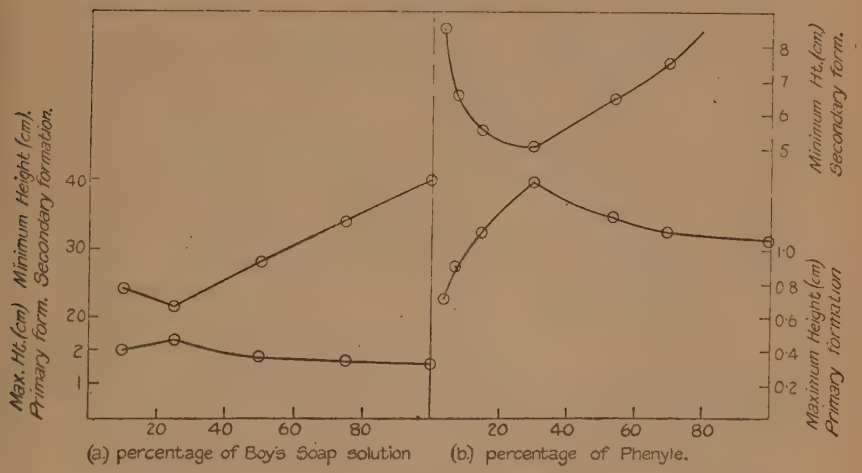

Among other methods of such drop formation may be mentioned : (1) dipping a piece of cotton cloth in the liquid and holding it above the surface, this method being most suitable for fats and oils at high temperatures ; (2) vibrating (by bowing) the sides of the vessel holding the liquid, this method is most suitable for liquids of low surface-tension like ether, petrol, methylated spirit, turpentine, etc., and gives rise to secondary drops ; (3) water-drops can be easily made to float by allowing a spray of water to fall, horizontally or vertically, on a basin full of water.

A large number of liquids were studied and the results as regards drop formation can be classified as follows :—

(1) Light liquids of low surface-tension and low viscosity show the formation of secondary drops. They are not easily

amenable to the formation of primary drops. If any such drops are formed their life is exceedingly small. Thus ether, alcohol, methylated spirit, kerosene oil, petrol, turpentine, etc., readily show the formation of secondary drops either by the burette or by the vibrating vessel method. Water gives no primary drops at all and gives rise to secondary drops by the burette or the spray method, but not by the vibrating vessel method.

(2) Inorganic substances and their solutions and thick syrupy liquids do not show this phenomenon at all. Thus mercury, solutions of inorganic salts in water, inorganic acids and their water solutions, glycerine, saturated sugar solution, etc., form neither the primary nor the secondary drops.

(3) Fats and oils at high temperatures show the phenomenon remarkably well. At comparatively low temperatures the primary formation is shown better, while at higher temperatures the secondary phenomenon is better shown. Thus paraffin-wax at 90° C. formed good primary drops which by coalescing with each other gave rise to some of the largest drops observed, having a diameter of about 12 mm. At this temperature it formed no secondary drops. At 150° C. it could not form primary drops, but tiny secondary drops were readily formed, some of which lasted for nearly five minutes. As a rule, the smaller the size of the drops the longer their life.

(4) Solutions of soap (Boys's soap solution or sodium oleate) in water, of phenyle in water, and of creosole in carbolic acid show both the primary and the secondary phenomena, and are perhaps best suited for such a study. Of these liquids phenyle is perhaps the most preferable on account of its cheapness, no difficulty or complications in preparing the solutions, and easy formation of drops of comparatively long life. A 30 per cent. solution of phenyle was found to be the best for the production of the primary drops and a 10 per cent. solution for the secondary drops. In the case of soap and creosole solutions as well, it was found that a smaller dilution is more suitable for primary drop formation and a greater dilution for the secondary phenomenon. The most suitable Boys's soap solution for the exhibition of these phenomena was a 15 per cent. one. With this solution drops as large as 12·4 mm. in diameter were obtained (by coalescence of several smaller drops and using a jet of 2·52 mm. diameter). It seems worth while mentioning that a 30 per cent. solution of phenyle was also found to be very suitable for easy production of bubbles and films of long life.

Several factors have to be borne in mind for easy production of the drops and prolonging their lives. Thus the surface of the liquid should be free from impurities like dust particles, etc. Impurities in the falling liquid itself make the formation of drops rather difficult and make them unstable. Impurities in the surrounding medium should also be avoided. Dusty air, for instance, does not favour the production of the phenomenon. This is very evident in the case of water drops, which are never formed until the surrounding air is free from dust and saturated with moisture. An electrically-charged rod brought near the drops makes them unstable, coalesce, and disappear quickly.

Temperature has different effects on different liquids. If the temperature of soap solution be raised, the formation of drops becomes almost impossible. In the case of water the formation of drops becomes easier at higher temperatures, but their size is decreased. With fats and oils a high temperature makes the formation of the drops very easy and also prolongs their life.

Movement of the drops on the surface prolongs their life. Thus the secondary drops, which are more mobile than the primary ones, have also the longer life of the two. Vibration or motion of the surface itself also tends to prolong the life of the drops. Thus the drops produced by the vibrating vessel method have a comparatively longer life. Also, if the drops are formed on the surface of a flowing stream of the liquid their life is prolonged.

The life of the drops also becomes longer when the drops are formed inside an immiscible liquid. Thus water drops formed on a water surface covered with petrol or kerosene oil or olive oil (Darling's drops) have a fairly long life. The effect of the surrounding medium is evidently due to the cushions of the medium formed in between the drop and the liquid surface. The more viscous the surrounding medium, the stronger the layer which prevents the drop from combining or mixing with the main body of the liquid. Thus the more viscous the surrounding medium, the stabler the drops and the longer their life.

Addition of a more viscous liquid to the mother liquid stabilizes the drops and prolongs their life. Thus, in case of soap solution, the life of the drops is considerably increased by addition of glycerine, and the greater the amount of glycerine added, the longer lived the drops. Similarly, in case of ether drops (by the vibrating vessel method), their life is considerably increased by the addition of a small quantity of mustard oil to the liquid.

The size of the drop is increased by increasing the radius of the jet from which the drops issue when this particular method of drop formation is employed.

It would appear that the properties which play an important part in the production of this phenomenon are surface-tension, viscosity, and density of liquid. A detailed investigation to find the values of all these quantities for the principal liquids experimented on was, therefore, undertaken. As a result of this, it appeared that viscosity is mainly responsible for the stability and the long life of the drops, and the surface-tension mainly for their size. It also appeared that the liquids most suitable for the formation of primary drops (having long life, easy formation, and large

Fig. 2.

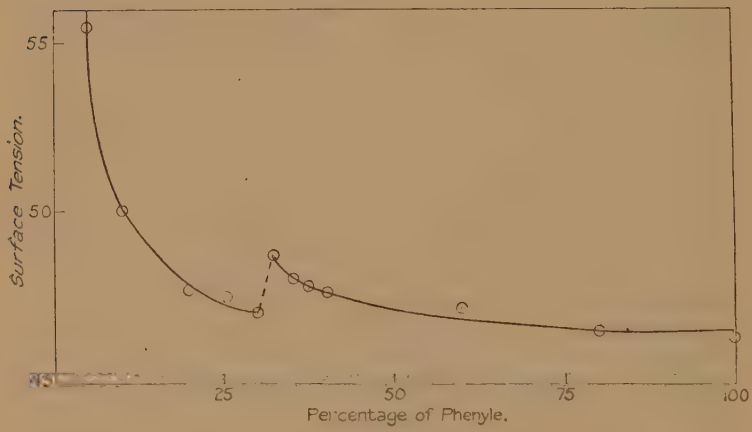

size) should have a surface-tension ranging between 20 and 80 dynes per cm., a viscosity up to about ·25 c.g.s. unit, and a density in the neighbourhood of unity. For the secondary formation by the burette method, the surface-tension should range between 15 and 80, the viscosity up to ·046, and the density about unity; and for the secondary formation by the vibrating vessel method, surface-tension 15 to 30, viscosity up to ·010, and density smaller than unity.

While studying the surface-tensions a very interesting observation was made. In the case of phenyle solution, for instance, it was found that the surface-tension decreased as the amount of phenyle in the solution increased till the 30 per cent. stage was reached. At this point there was a small sudden rise of the surface-tension, when again it

decreased but very slowly with the increase of phenyle in the solution. The surface-tension was determined by several methods, namely : by the rise in the capillary tube ; by weighing the drops ; by the method of ripples ; and by Warren's surface-tension balance method *. Fig. 2 exhibits the type of results obtained. It may be remembered that the best solution for exhibition of primary drops by phenyle was a 30 per cent. one, and that at this concentration the range of no drop formation is also a minimum for this substance. In the case of Boys's soap solution the concentration surface-tension curve shows a similar dip for a 15 per cent. solution, and a solution of this strength is also the most suitable for drop formation.

These coincidences indicate that the depression in the curve has an important bearing on the easy formation of floating drops. A detailed study of changes of surface-tension in these regions for these two liquids, and measurements of surface-tension and viscosity of oils at different temperatures, will perhaps be of help in elucidating the phenomenon and is proposed to be undertaken at a subsequent date.

Physics Laboratory,
Government College, Lahore.

XXVIII. *The Air-flow around a Circular Cylinder in the Region where the Boundary Layer separates from the surface. By* A. Fage, *A.R.C.Sc., of the Aerodynamics Department, The National Physics Laboratory* †.

Introduction.

(1) In some recent experiments on the measurement of the velocity distribution in the boundary layer along a smooth plane surface, J. M. Burgers ‡ and B. G. van der Hegge Zijnen have shown that the motion in the early part of the layer is laminar, and that a transition to the turbulent state begins at a critical value of $(V_0\delta/\nu)$, where δ is the thickness of the boundary layer, and V_0 and ν are the velocity and the coefficient of kinematic viscosity of the fluid. The

* Phil. Mag., Aug. 1927.

† Communicated by E. F. Relf, A.R.C.Sc.

‡ *Mededeeling*, Nos. 5 & 6. Laboratorium voor Aerodynamica en Hydrodynamica der Technische Hoogeschool te Delft.

critical value, which depends on the character of the turbulence initially existing in the fluid, was found to be about 3000 when the plate was mounted in a comparatively steady air-stream. It was also observed that the transition from the laminar to a turbulent state was accompanied by a marked opening-out of the boundary layer. There was, however, no apparent tendency for the layer to separate from the surface, which was aligned parallel to the direction of the undisturbed wind. To avoid ambiguity, it is necessary to mention here that the boundary layer is the narrow region in the immediate vicinity of the surface where the whole of the retarding influence due to the surface may be considered to operate; and that a flow is laminar when the speed and direction of motion at any point are independent of time, and turbulent when they change continually with time.

(2) It is a matter of common observation that when a surface is curved the boundary layer eventually separates from it; and this fact raises the interesting question as to whether the conditions in the layer around such a surface resemble those in the layer along a plane surface, and, if so, whether the phenomenon of separation is associated with the rapid opening-out of the boundary layer and the concomitant change from the laminar to a turbulent state of flow. To obtain information on this subject, a circular cylinder of large diameter was mounted in a wind tunnel and the boundary layer located from observations of total head taken close to the surface with an exceedingly small tube. The subsequent analysis will show that the distinctive traits of this curved boundary layer resemble those common to the layer along a plane surface; that there is a critical point on the cylinder; and that the separation of the layer from the curved surface occurs just beyond this critical point.

(3) There is a particular range of Reynolds's number— $VD/\nu = 10^5$ to $3{\cdot}5 \times 10^5$ approx., where D is the diameter— through which the character of the flow around a circular cylinder undergoes a marked change *. The drastic character of this change can be realized from the fact that the drag coefficient falls from 0·60 to 0·20 approx. over this range of (VD/ν). In view of the fact that the value of the investigation would be enhanced if these different types of flow (see fig. 9) were explored, it was decided to select a cylinder of large diameter, so that with the speed range available in the wind tunnel this particular range of (VD/ν) could be

* Relf & Simmons, Phil. Mag., February 1925.

covered. The diameter chosen was 8·9 inches. It will be realized that a further advantage of the large diameter is that it favours increased accuracy of observation, since the thickness of the boundary layer, which is small in any case, is directly proportional to the diameter at a constant value of (VD/ν).

Description of Experiments.

(4) The cylinder was mounted between the floor and roof of a 4-foot wind tunnel. The observations taken were confined to the plane passing through the median section

Fig. 1.

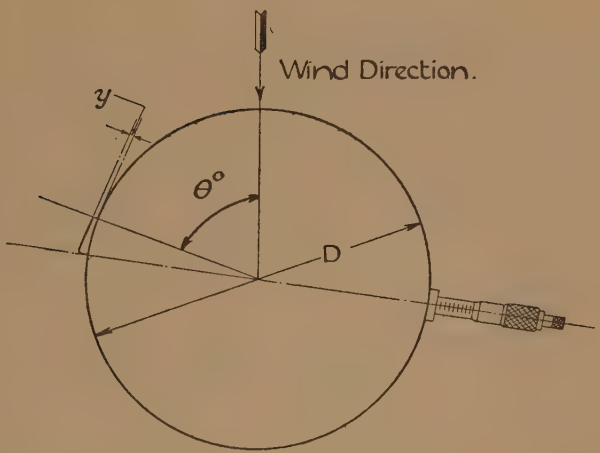

of the cylinder, where the flow can be regarded as two-dimensional. The experiments were designed to measure, at five wind speeds (22·0, 26·9, 39·2, 57·9, and 71·4 ft./sec.), radial distributions of total head near the surface. The method of experiment was to take, at each wind speed, with a very small tube (described later) observations of total head at known radial distances (y) from the surface as the cylinder was rotated by steps of 5° through an angular range extending from about 50° to 120°. The total-head distributions across radial lines were afterwards obtained by plotting these observations against y at a constant value of θ, where θ defines the position of the line measured from the direction of the undisturbed wind (see fig. 1). The minimum distance from the surface at which observations were taken was about

0·0037 inch, that is, when the tube touched the surface. The values of the total head at the surface (where the velocity is zero) were obtained directly from observations of pressure at a hole in the surface situated in front of, and some distance below, the small tube and beyond its influence. It was found at a later stage in the experiments that the observations (pressure and total head) taken near and beyond the region of maximum negative pressure were influenced by the presence of a micrometer head on the opposite side of the cylinder (see fig. 1). All the observations in the paper refer therefore to a cylinder with a micrometer head protruding from its surface. Further, the observations have not been corrected for the modification of the flow due to the constraint of the tunnel walls.

(5) *The Total-head Tube.*—Since the thickness of a boundary layer is, in general, very narrow, it was essential to use an exceedingly small total-head tube and to record its position relative to the surface with good accuracy. The tube was constructed from the finest hypodermic steel tube available (external diameter 0·0197 inch), pressed at the mouth into a rectangular form with the external dimensions 0·0074 inch by 0·021 inch approximately. The tube was mounted so that the longer side of the rectangular section was parallel to the axis of the cylinder. A microscopic examination showed that the opening in the mouth of the tube was irregular, but that the average width and height appeared to be about 0·0017 and 0·0053 inch respectively.

The small exploring total-head tube was soldered into a larger hypodermic steel tube, which passed through a small hole in the cylinder. This tube was moved radially by means of a micrometer screw mounted externally on the opposite side of the cylinder. The diagrammatic sketch of fig. 1 shows the method of mounting the total-head tube, and is self-explanatory. It should perhaps be mentioned that a suitable spring device was fitted within the cylinder to eliminate backlash between the sliding total-head tube and the rotating micrometer screw.

(6) It was at first intended that the position of the total-head tube should be measured directly on the micrometer scale. This method was, however, discarded because the datum reading involved contact of the tube with the surface and it was difficult to make sure that the tube, owing to its frailty, was not distorted. Moreover, the possibility of a deflexion of the supporting tube, due to a constraint at the

small hole in the cylinder through which this tube passed, could not be ignored.

The method of measurement finally adopted was to illuminate the generator of the cylinder, which was in the radial plane passing through the mouth of the total-head tube, by means of a band of light projected from behind and normal to this radial plane, that is, tangential to the surface at the generator. The distance between this generator and the centre of the mouth of the tube was then measured by means of a travelling microscope with cross wires, mounted in front of the cylinder and focussed on the mouth of the tube. This method proved both simple and accurate in operation, and it was possible to measure the radial distance of the tube from the surface to within four ten-thousandths of an inch.

(7) *The Accuracy of the Total-head Observations.*—Experiments were also devised to obtain information on the general accuracy of the observations taken with the small total-head tube, and more especially to determine whether these observations would allow a reliable estimate to be made of the thickness (δ) of the boundary layer. The principal doubt concerning the accuracy of observation arises from the fact that the width of the tube is in some cases a large fraction of the width of the region of total-head gradient near the surface, so that the pressure measured may not correspond to the total head in the filament of air impinging on the geometric centre of the mouth of the tube. These subsidiary experiments will now be described.

(8) It is well known that in the vicinity of the wall of a wind tunnel there is a layer of air, of appreciable width, across which there exists a gradient of total head. At the working section of the tunnel the width of this layer was about 5·5 inches, that is, 100 times greater than the thickness of the boundary layer near the point on the cylinder where the pressure has its maximum negative value (see later). To obtain some idea of the accuracy of observation in the boundary layer at this region of the cylinder (where the thickness of the layer was only about 7·5 times greater than the external width of the tube), it was decided to compare the total-head distribution in the "wall" layer measured with a large copy of the small exploring tube to a scale of 100 : 1, with the true distribution obtained with a small total-head tube. The two curves of total head are given in fig. 2; and it is seen that they are in very close agreement, except

within the inner 15 per cent. of the width of the layer at the wall. Included in fig. 2 is a curve (taken from fig. 6) which may be regarded as representative of the total-head distribution across a section of the boundary layer of the cylinder near the point of maximum negative pressure. There are marked differences in the two distributions of total head, but in general, the gradient of total head in the boundary layer of the cylinder does not appear to be more severe than that in the "wall" layer It follows, then, that the observations taken with the small exploring tube, although perhaps

Fig. 2.

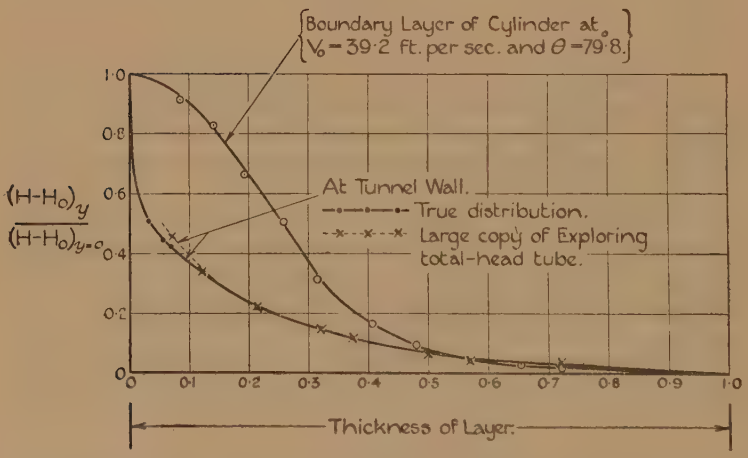

uncertain *very near* the surface (say within $0{\cdot}15\delta$), are reliable in the outer region of the boundary layer.

(9) To determine to what extent the smallness of the exploring tube would influence observations taken in a uniform stream, a comparison was made with observations taken with a much larger tube under corresponding conditions. It was found that over the speed range covered (15 to 80 ft./sec.) the scale effect was too small to be detected with any accuracy. It is of interest to mention that a confirmation of this result was obtained from the experiments with the cylinder, for it was found that the total head observed with the small tube just outside the boundary layer was equal, except occasionally at the lowest speed, to that measured with a much larger tube in the undisturbed stream.

Discussion of the Observations.

(10) *Pressure Observations.*—The distributions of pressure around the surface of the cylinder (with micrometer head), at the five wind speeds (V_0) of experiment, are given in fig. 3. The commonly accepted method of plotting, namely $(p-p_0)/\rho V_0^2$ against θ has been adopted, where p is the

Fig. 3.

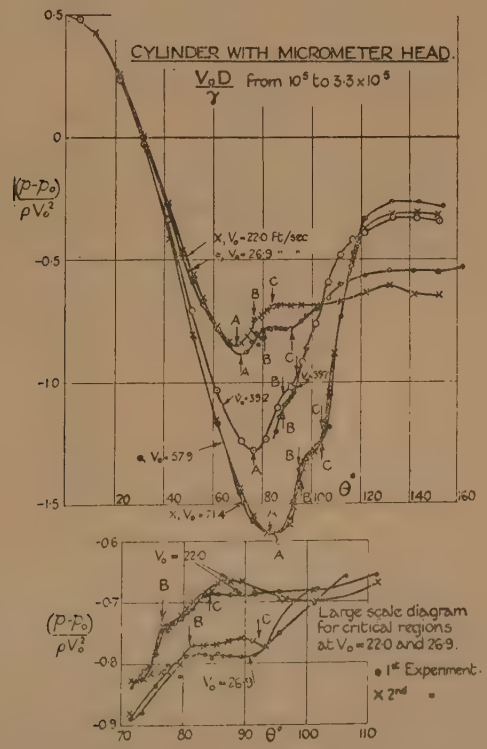

pressure at a point on the surface given by θ (see fig. 1), and p_0 and V_0 are the pressure and the velocity respectively in the undisturbed stream. These curves exhibit very clearly the marked changes in the pressure distribution which occur over the selected range of VD/ν (10^5 to $3{\cdot}3\times10^5$). The drastic character of these changes also manifests itself in the drag coefficient (k_D) which, as shown in Table I., falls from 0·63 to 0·22 over the same range of (VD/ν). It will be

observed that the coefficient of the maximum negative pressure increases with the wind speed, and also that there is a progressive displacement of the point at which this pressure occurs towards the back of the cylinder. The maximum negative pressure measured at the higher wind speeds 57·9 and 71·4 ft./sec. were $-1{\cdot}62\,\rho V_0^2$ and $-1{\cdot}63\,\rho V_0^2$ respectively. It should perhaps be mentioned that these values were greater numerically than the corresponding values for the naked cylinder, which were $-1{\cdot}43\,\rho V_0^2$ and $-1{\cdot}46\,\rho V_0^2$ respectively; and that these latter values are lower than the theoretical value ($-1{\cdot}62\,\rho V^2$) predicted for an 8·9-inch cylinder in an inviscid stream in a 4-foot tunnel.

TABLE I.

Cylinder in a 4-foot Tunnel. (With micrometer head removed.)

V_0 ft. per sec.	$\left(\frac{V_0 D}{\nu}\right)$.	Drag coefficient k_D.
22·0	102,600	0·634
26·9	125,400	0·511
39·2	182,800	0·227
57·9	270,000	0·192
71·4	333,000	0·218

(11) An important trait exhibited in each of the curves of fig. 3 is the pronounced inflexion (marked BC) between the point of maximum negative pressure (marked A) and the region where the pressure is almost constant. The principal purpose of the subsequent analysis will be to show that the change from the laminar to a turbulent state of flow in the boundary layer probably occurs in this region BC, and that the layer has completely separated from the surface at the point C.

(12) *Total-head Observations.*—The total head (H) at a point situated a radial distance (y) from the surface was measured with the small exploring tube against the datum total head (H_0) in the undisturbed stream. These observations, reduced to the non-dimensional form $(H-H_0)/\rho V_0^2$, are plotted against ($1000\,y/D$) in figs. 4–8 (a). The total

head at the surface ($y = 0$) was not measured directly, but was determined from the observations of pressure ($p - p_0$) by the relation $(H - H_0) = (p - p_0) - 0{\cdot}5\,\rho V_0^2$; these values are

Fig. 4.

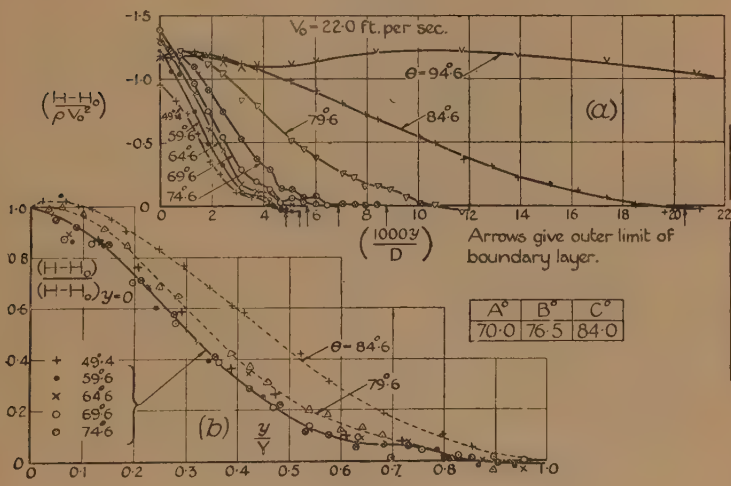

Fig. 5.

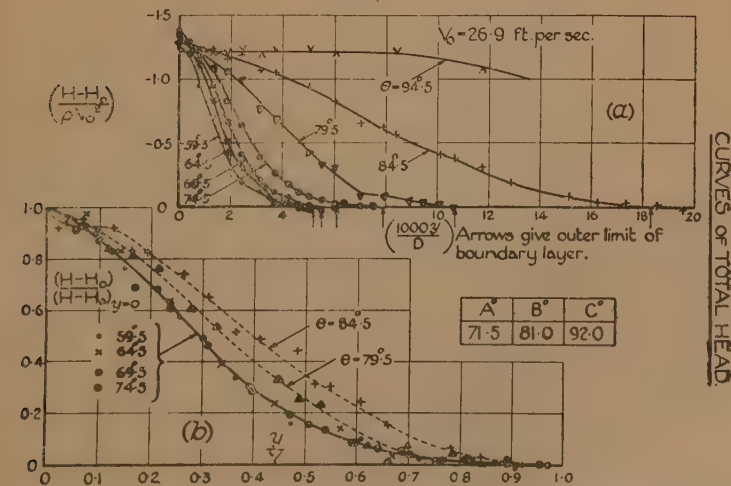

also plotted in figs. 4–8 (a). It is considered to be a matter of some importance that the estimated values of $(H - H_0)/\rho V_0^2$ at $y = 0$ support the tendencies indicated by the curves drawn through the observations taken with the tube.

In view of the fact that other workers may desire to use the experimental observations of total head given in figs. 4–8 (*a*), those taken at the extreme speeds of experiment

Fig. 6.

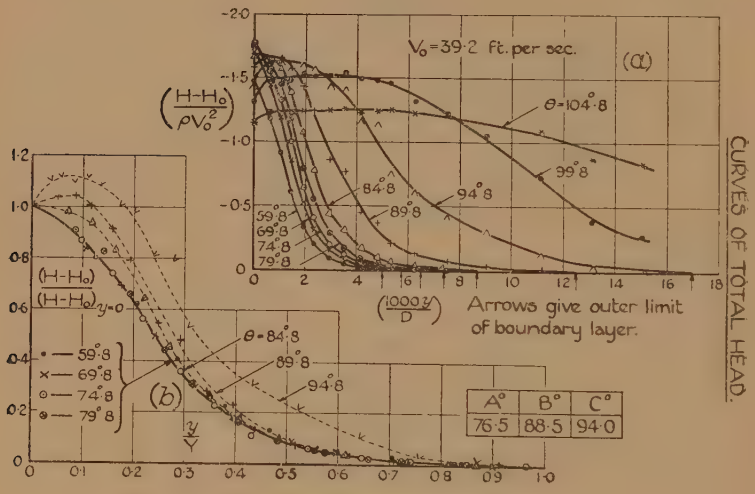

Fig. 7.

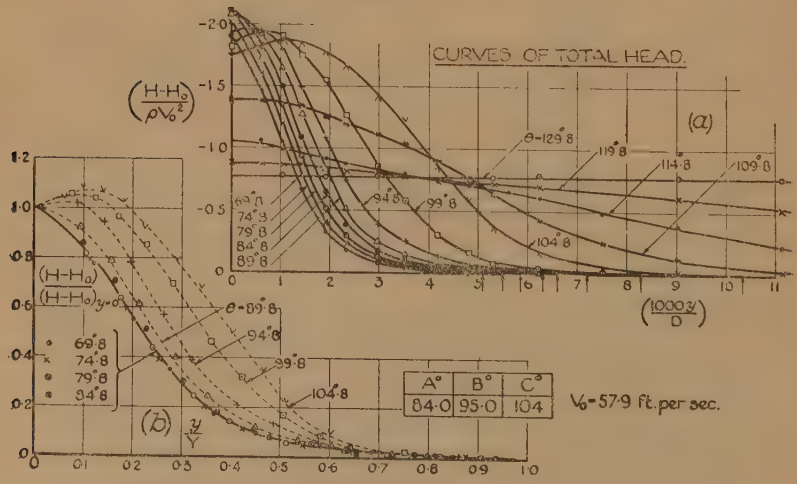

(22·0 and 71·4 ft. per sec.) are given in Tables II. and III., as well as in figs. 4 and 8 (*a*). The observations for the intermediate speeds are presented only in figs. 5–7.

Table II.

Values of $(H-H_0)/\rho V_0^2$ for $V_0 = 71{\cdot}4$ ft. per sec.
Value of $\theta°$ given at top of each column.

$\frac{1000y}{D}$.	49·8	59·8	69·8	74·8	79·8	84·8	89·8	94·8	99·8	104·8	109·8	114·8	119·8	129·8
0	−1·237	−1·595	−1·888	−2·010	−2·091	−2·121	−2·102	−1·973	−1·822	−1·732	−1·421	−1·096	−0·925	...
0·623	−0·816	−1·134	−1·430	−1·555	−1·670	−1·780	−1·860	−1·925	−1·930	−1·873	−1·330	−1·024	−0·919	−0·796
1·035	−0·462	−0·695	−0·940	−1·080	−1·225	−1·378	−1·531	−1·695	−1·830	−1·820	−1·254	−0·945	−0·859	−0·788
1·424	−0·225	−0·303	−0·550	−0·654	−0·794	−0·945	−1·120	−1·363	−1·655	−1·764	−1·175	−0·884	−0·834	−0·792
1·902	−0·097	−0·160	−0·258	−0·325	−0·408	−0·518	−0·683	−0·935	−1·345	−1·627	−1·058	−0·833	−0·813	−0·796
2·331	−0·048	−0·081	−0·137	−0·173	−0·222	−0·285	−0·400	−0·603	−1·030	−1·440	−0·995	−0·806	−0·802	−0·799
2·992	−0·022	−0·045	−0·060	−0·077	−0·102	−0·134	−0·187	−0·290	−0·585	−1·059	−0·849	−0·739	−0·764	−0·790
3·522	−0·014	−0·026	−0·039	−0·055	−0·067	−0·080	−0·110	−0·156	−0·367	−0·803	−0·759	−0·715	−0·759	−0·800
4·195	−0·001	−0·011	−0·018	−0·025	−0·031	−0·039	−0·056	−0·095	−0·181	−0·484	−0·608	−0·652	−0·732	−0·804
4·820	−0·001	−0·006	−0·011	−0·016	−0·021	−0·025	−0·030	−0·053	−0·102	−0·282	−0·483	−0·589	−0·695	−0·790
5·302	...	0	−0·010	−0·011	−0·011	−0·017	−0·023	−0·031	−0·061	−0·180	−0·379	−0·551	−0·680	−0·800
6·240	...	...	−0·006	−0·007	−0·006	−0·009	−0·014	−0·021	−0·061	−0·079	−0·241	−0·456	−0·630	−0·774
7·51	...	...	...	...	...	...	+0·014	+0·011	−0·006	−0·025	−0·134	−0·367	...	...
9·04	...	...	...	...	...	...	...	...	−0·006	−0·009	−0·065	−0·261	−0·512	−0·780
11·12	...	...	...	...	...	...	...	...	...	−0·008	−0·018	−0·131	−0·412	−0·775
13·13	...	...	...	...	..	...	..	...	...	...	−0·006	−0·070	−0·344	−0·775
15·05	...	...	...	...	...	...	...	...	...	...	0	−0·025	−0·229	−0·754

Fig. 8.

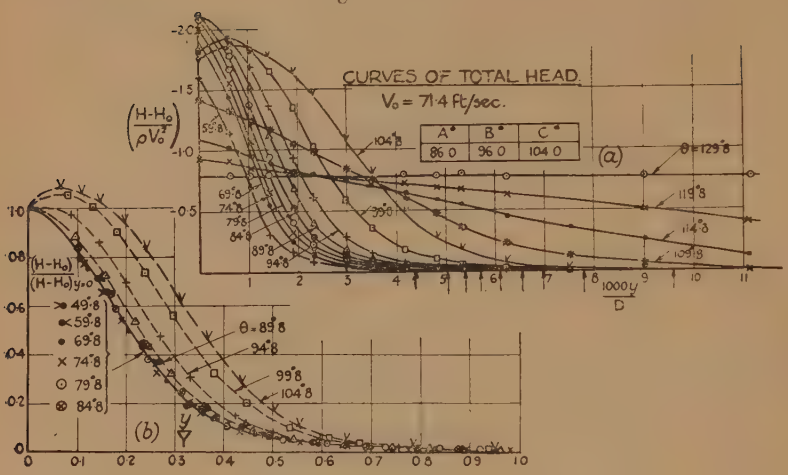

Table III.

Values of $(H-H_0)/\rho V_0^2$ for $V_0 = 22{\cdot}0$ ft. per sec.
Value of θ° given at top of each column.

$\frac{1000y}{D}$.	59·6	64·6	69·6	74·6	79·6	84·6	94·6	$\frac{1000y}{D}$.	49·4
0	−1·230	−1·300	−1·340	−1·290	−1·220	−1·180	−1·180	0	−0·953
0·429	−1·060	−1·165	−1·222	−1·223	1·209	−1·208	−1·175	0·623	−0·826
0·774	−1·041	−1·120	−1·194	−1·189	−1·220	−1·147	−1·083	1·035	−0·735
1·318	−0·743	−0·895	−0·978	−1·100	−1·195	−1·208	−1·183	1·424	−0·567
1·861	−0·487	−0·609	−0·750	−0·919	−1·119	−1·188	−1·160	1·902	−0·349
2·438	−0·324	−0·447	−0·545	−0·750	−1·042	−1·172	−1·142	2·331	−0·253
3·138	−0·108	−0·166	−0·294	−0·533	−0·839	−1·118	−1·107	2·992	−0·102
3·714	−0·090	−0·119	−0·195	−0·370	−0·796	−1·070	−1·100	3·522	−0·078
4·250	−0·055	−0·102	−0·137	−0·289	...	...	...	4·195	−0·012
4·672	+0·003	−0·005	−0·020	−0·131	...	...	...	4·820	+0·012
5·070	+0·003	−0·008	−0·061	−0·136	−0·516	−0·984	−1·100	5·302	+0·018
5·540	...	+0·050	−0·032	−0·067	−0·457	...	...	...	...
6·010	+0·003	+0·03	−0·020	−0·078	−0·382	−0·908	−1·130	.	...
6·42	...	+0·009	−0·008	−0·008	...	..	...	...	...
7·04	...	+0·012	+0·009	−0·014	−0·248	−0·804	...	...	...
7·51	...	...	−0·002	−0·014	−0·230	...	...	...	...
7·94	...	...	+0·009	+0·004	−0·154	−0·721	...	.	...
8·40	...	...	...	−0·002	−0·160	−0·692	−1·209	...	...
8·93	...	...	...	...	−0·125	...	...	...	...
9·51	...	...	...	...	−0·078	...	...	...	...
10·06	...	...	...	...	−0·020	−0·545	...	...	...
10·63	...	...	...	...	−0·008	−0·499	...	..	...
11·75	...	...	...	...	+0·050	−0·370	−1·200	...	...

(13) There are prominent features common to the total-head curves taken at each wind speed, V_0. A study of these features will now be made; and especially of those which are related to the flow around that part of the cylinder previously designated ABC, and characterized by a marked inflexion in the curve of the pressure distribution (see fig. 3). For convenience of reference, the values of θ at each of the points A, B, and C are given in figs. 4–8. Also, to indicate more readily the changes in the character of the total-head distribution at the several radial sections prior to the point C on the cylinder, a second series of curves (*b*) is included in each of the figs. 4–8. These curves (*b*) are obtained by plotting the ratio $(H-H_0)_y/(H-H_0)_{y=0}$ against (y/Y), where Y represents the value of y at the point where the total head just reaches the value (H_0) in the undisturbed stream. It will be noted that if the local air-stream has not separated from the surface, the value of Y is equal to the thickness (δ) of the boundary layer.

(14) The method of plotting adopted in figs. 4–8 (*b*) shows that the observations taken in a relatively large part of the boundary layer situated forward of the point (A), of maximum negative pressure,—the angular range covered varies from 25° for $V_0 = 22{\cdot}0$ to 35° for $V_0 = 71{\cdot}4$—lie on a common curve within the accuracy of experimental observation. In other words, the opening-out of the boundary layer and the fall of pressure around the surface do not influence (over this region) the character of the total-head distribution across a radial section. There is, however, a progressive change in the distribution, especially near the surface, as the position of the section is taken beyond the point A.

(15) It is to be expected that in the immediate vicinity of the point where the layer begins to separate from the surface the total head would change very slowly with the radial distance from the surface, that is, $\partial(H-H_0)/\partial y$ should tend to a zero value as y approaches its zero value; and also that when the "breakaway" was completed, the total head should remain constant over a relatively large radial distance from the surface. It should therefore be possible to obtain from the curves in figs. 4–8 (*a*) and (*b*) indications of the positions where the flow begins to leave the surface and where the separation is completed. This information is collected in Table IV. together with the values of θ defining the positions of the points B and C. The values of θ given in the columns 3 and 4 of the table are

only approximate, and refer to the curves which most closely fulfil a desired condition.

Table IV. reveals two important facts: firstly, that the boundary layer begins to leave the surface at the point B, since the value of $\partial(H-H_0)/\partial y$ is zero near this point; and secondly, that the separation appears to be completed at the point C. The flow in the region BC is therefore of a peculiar character, and that this is so is further indicated by the conspicuous "humps" in the total-head curves, exhibited near the surface at all speeds except 26·9 ft./sec. It is perhaps of interest to mention that since the tube was always pointing in the same tangential direction the "humps" in the total-head curve can be accounted for on the assumption of a reversal in the direction of flow.

TABLE IV.

V_0 ft./sec.	Value of $\theta°$ at point B. (Fig. 3.)	Value of $\theta°$ where $\frac{\partial(H-H_0)}{\partial y}=0$. (Figs. 4–8 (*b*).)	Value of $\theta°$ where the separation appears to be completed. (Figs. 4–8 (*a*) & (*b*).)	Value of $\theta°$ at point C. (Fig. 3.)
22·0	76·5	Near 79·6	Near 84·6	84·0
26·9	81·0	Not clear, say 84·5	94·5	92·0
39·2	88 5	Between 84·8 & 89·8	Near 94·8	94·0
57·9	95·0	Near 94·8	Near 104·8	105·0
71·4	96·0	Near 94·8	Near 104·8	105·0

(16) *Vortex Sheets.*—It should be possible to obtain an idea of the position of the region where the boundary layer separates from the surface from a pattern of the flow around the cylinder, or, better still, from the vortex sheets trailing behind the cylinder, since these sheets originate in the boundary layer. To locate the position of these sheets, observations of total head were taken across several lateral sections of the wake, with a tube which could be directed into the local stream. The nature of the total-head curves so obtained is illustrated in fig. 3 of an earlier paper dealing with the structure of vortex sheets *. The method of determining the position of points on the outer and inner

* Fage & Johansen, Phil. Mag. p. 421 (February 1928).

boundaries of a sheet is also described in the same paper. Briefly stated, a point on an outer boundary marks the position beyond which the total head is constant and equal to the value (H_0) in the undisturbed stream, and a point on an inner boundary where the total head has fallen to a minimum value. It should be added that the points on the outer and inner boundaries close behind a separation region were not taken from curves obtained from lateral explorations, but from the appropriate curves of figs. 4–8 (*a*), and also from some observations (not included in the paper) taken with a small exploring tube attached to the cylinder.

Fig. 9.

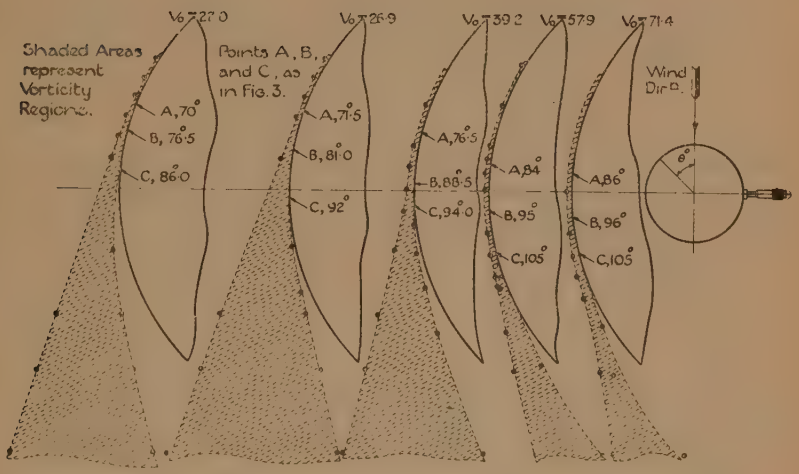

(17) The shape and position of the vorticity sheets trailing behind the cylinder, at each speed, are shown by the shaded areas in fig. 9. A retrograde movement of the separation region, and a more gradual separation of a vortex sheet from the surface, as the speed is progressively increased are clearly indicated; and the general impression created is that the flow is more comformable to the surface at the higher wind speeds. It is also seen that the formation of a marked dead-air region behind the cylinder commences almost immediately after the point C (BC is the separation region) at the lower speeds 22·0 and 26·9 ft./sec., but that this does not appear to be the case at the higher speeds 57·9 and 71·4 ft./sec. It does not, however, necessarily follow from the delay in the formation of a marked dead-air region at

these higher speeds that the separation of the boundary layer is not completed at the point C; for the layer after leaving the surface becomes a vortex sheet and opens out by the inflow of air across its boundaries, in a manner dependent on the general configuration of the neighbouring flow; and it may well be that the inner boundary of the sheet follows closely the contour of the surface, so that there is a very narrow band of "dead air" between the sheet and the surface. A study of the total-head curves taken at these higher speeds at the sections beyond the point C gives support to this point of view.

(18) *Velocity Distribution.*—If it be assumed that the pressure across a section of the boundary layer is uniform and equal to that measured at the surface, it follows that

$$\left[\frac{V_y}{V_{y=\delta}}\right]^2 = \left[1 - \frac{(H_0 - H)_y}{(H_0 - H)_{y=0}}\right]$$

within the layer. The value of the velocity (V_y) expressed as a fraction of the maximum velocity ($V_{y=\delta}$) can therefore be directly estimated when the corresponding value of $\left[\frac{(H_0 - H)_y}{(H_0 - H)_{y=0}}\right]$ is known. Further, figs. 4–8 (*b*) have shown that values of $\frac{(H_0 - H)_y}{(H_0 - H)_{y=0}}$ taken in the boundary layer extending some distance in front (the average range taken is about 20°) of the point A of maximum negative pressure fall very closely on a smooth curve when they are plotted against (y/δ). Values of ($V_y/V_{y=\delta}$) for this part of the boundary layer were therefore estimated from the above relation by the substitution of mean values of $\frac{(H_0 - H)_y}{(H_0 - H)_{y=0}}$ taken from the smooth curves of figs. 4–8 (*b*). The results are given by the full lines in fig. 10. No values of ($V_y/V_{y=\delta}$) for points very near the surface (that is, within $0{\cdot}15\delta$) are included because, as shown in § 8, the total-head observations in this region may be uncertain, and also because the predicted velocity is susceptible to small errors in $\frac{(H_0 - H)_y}{(H_0 - H)_{y=0}}$ as its value approaches unity. The curves in fig. 10 show that (over a range of θ° taken) the character of the velocity distribution across a section of the boundary layer taken at and prior to the point A changes consistently with the wind

speed. Included in fig. 10 are two dotted curves showing for the extreme speeds ($V_0 = 22$ and 71·4 ft. per sec.) the theoretical distributions of velocity across a section of the boundary layer at $\theta = 50°$ approx. These theoretical curves, which were obtained from Dr. Thom's solution* of the simplified boundary layer equations for the laminar flow around the front part of a circular cylinder, indicate a scale effect on the velocity distribution of the same character as that obtained from experiment. Further, the good agreement between the theoretical and experimental curves (the agreement is much closer when the comparison is made with the actual experimental curves at $\theta = 50°$ instead of the mean

Fig. 10.

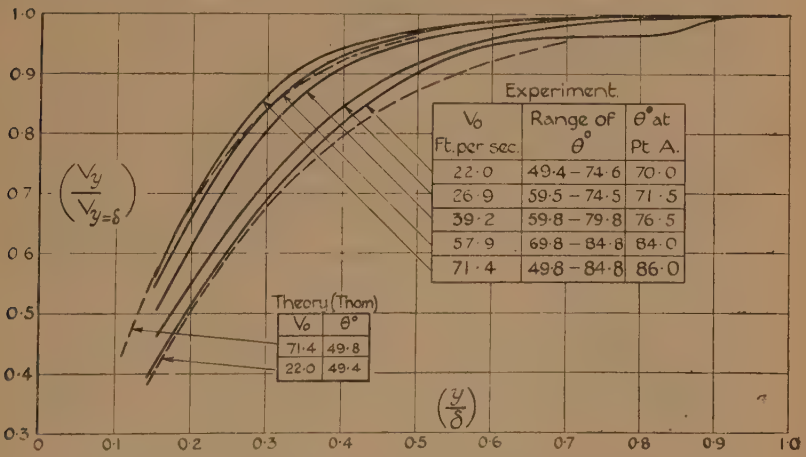

curves given in the figure) shows that the motion in the boundary layer at $\theta = 50°$ is laminar. Unfortunately, Dr. Thom's solution is not applicable in the region of maximum negative pressure, so that it is not possible to determine from a comparison with theory how far beyond $\theta = 50°$ the laminar motion persists. Further evidence on this subject can, however, be obtained from the work described in the following section.

Attention is directed to the peculiar shape of the outer part of the velocity curve taken at the lowest wind speed, 22 ft./sec., and it is tentatively suggested that this is

* Aeronautical Research Committee, R. & M. 1176.

connected with the relatively large disturbances in the general stream at this speed.

(19) *The Thickness of the Boundary Layer.*—B. G. van der Hegge Zijnen * has shown that the transition from the laminar to a turbulent state of flow in the boundary layer along a smooth plane surface manifests itself by a marked increase in the thickness of the layer. If this be an essential phenomenon accompanying a transition, an indication of the position of the transitional region on a cylinder (provided

Fig. 11.

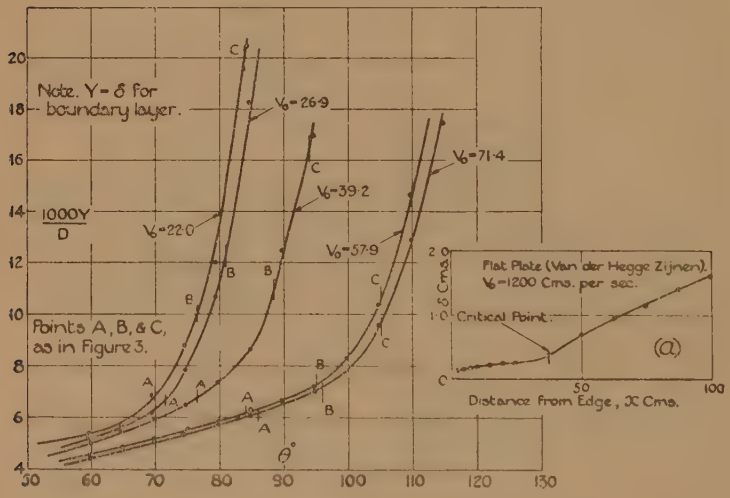

such a region exists) should be obtainable from a curve giving the variation of the thickness of the boundary layer with the angular distance around the cylinder. Also it is to be expected that the flow in the boundary layer around the cylinder does change, for it has been shown that the flow in the early stages is laminar and, it may be presumed, turbulent after the layer has separated from the surface (point C). The manner in which the boundary layer around the cylinder opens out is shown in the early part of the curves of fig. 11, where values of $(1000\,Y)/D$ are plotted against θ. The values of Y (Y is defined in § 13) were determined directly from curves similar to those given in figs. 4–8 (*a*), but plotted

* *Loc. cit.*

on a larger scale. Further, it follows from the definition of the term "boundary layer" that the value of Y gives the thickness (δ) of the layer prior to its separation from the surface.

The curves of fig. 11 show that up to the point A there is a steady increase in the value of Y (δ for the boundary layer) with the angular distance around the cylinder ; and also that the point B is situated near to the point where the rapid opening-out of the boundary layer begins. An inflexion similar to that at the point B was observed by van der Hegge Zijnen in the corresponding (δ, x) curves for the boundary layer along a plane surface (see fig. 11 (*a*)) ; and he established, on evidence derived from the distributions of velocity across suitably-chosen sections, that the transition from the laminar to a turbulent state of flow began at the critical point where the rapid opening-out of the boundary layer occurred. A similar transition appears to take place in the case of the cylinder, for it has been shown that the motion in the boundary layer at some distance anterior to the point A (maximum negative pressure) is laminar (this would, of course, be expected unless the initial disturbances in the general stream are exceptional) ; and it would appear justifiable to assume that the flow at the point C is turbulent, since at this point the separation from the surface is completed.

Critical Values.

(20) The evidence obtained from the pressure curves of fig. 3, the total-head curves of figs. 4–8, and the (δ, θ) curves of fig. 11 lead to the conclusion that the flow in the boundary layer around the cylinder is critical at (or near) the point B. A special significance is therefore attached to the values of Reynolds's numbers ($V_0\delta/\nu$) and ($V_{y=\delta}$) . δ/ν at this point. These values, computed for the five speeds, are collected in Table V. It should be added that an average value of the coefficient of kinematic viscosity (ν), namely that for the standard atmosphere of pressure 760 mm. and temperature 15·6° C., has been taken in the computation, and also that the value of $V_{y=\delta}$ at the outer limit of the boundary layer was determined on the assumption made in § 18 from the relation

$$\left[\frac{V_{y=\delta}}{V_0}\right]^2 = 1 + \frac{2(p_0 - p)}{\rho V_0^2},$$

where p is the pressure at the point B.

It will be observed in Table V. that the values of ($V_0\delta/\nu$) (there is a slight irregularity at $V_0 = 57{\cdot}9$ ft./sec.) and

$(V_{y=\delta}) \cdot \delta/\nu$ show a marked progressive increase with the mean speed, V_0.

It is necessary, if the correct interpretation of the results in Table V. is to be made, to bear in mind that they were obtained with the cylinder mounted in an artificial wind stream, so that an increase of the wind speed, V_0, probably involves a change in the "scale" of the turbulence initially in the stream. The importance of this initial turbulence has been demonstrated by van der Hegge Zijnen, who found that a change of turbulence in the general stream, due to the introduction of a screen, reduced the critical value of $(V_0\delta/\nu)$ for the plane surface from 3000 to 1600, even although the relative mean speed was unchanged. It is

TABLE V.

V_0 ft./sec.	At point B.					
	$\theta°$.	$\frac{\delta}{D}$.	$\frac{V_0\delta}{\nu}$.	$\frac{(p_0-p)}{\rho V_0^2}$.	$\left(\frac{V_{y=\delta}}{V_0}\right)$.	$\frac{\delta}{\nu}(V_{y=\delta})$.
22·0	76·5	0·0100	1030	0·74	1·57	1620
26·9	81·0	0·0122	1530	0·78	1·60	2450
39·2	88·5	0·0110	2010	1·05	1·76	3540
57·9	95·0	0·0073	1970	1·37	1·93	3800
71·4	96·0	0·0072	2400	1·38	1·94	4650

therefore not irrelevant to mention that an impression was formed as the experiments with the cylinder proceeded, that the general stream was relatively more disturbed at the lower speeds—see the appropriate curves of total head and velocity near $(y = \delta)$,—and this may *partially* account for the lower values of Reynolds's numbers measured at these speeds.

It is a noteworthy fact that the average values of $(V_0\delta/\nu)$ and $(V_{y=\delta}) \cdot \delta/\nu$ for the cylinder—they are 1790 and 3210 respectively—are of the same order of magnitude as the average value (3150) determined by van der Hegge Zijnen for the flat plate, and as the value (2300, lower critical) determined from the critical value for the flow in pipes, on the assumption that the radius of the pipe is equivalent to

the thickness of the boundary layer, and the velocity at the axis is equivalent to V_0.

Summary.

(21) An examination of the air-flow round a circular cylinder in the region where the boundary layer separates from the surface has been made from observations of total head taken with an exceedingly small tube. The diameter of the cylinder and the range of wind speed selected were such as to allow markedly different types of flow to be considered. The analysis indicates that there is a critical point on the cylinder where a transition from the laminar to a turbulent state of flow in the boundary layer begins. The transitional region is marked by a rapid opening-out of the boundary layer. The critical value of Reynolds's number for the boundary layer progressively increases with wind speed over the range taken in the experiments. The average of these critical values for the cylinder is of the same order of magnitude as the average value by van der Hegge Zijnen for a plane surface. The separation of the boundary layer from the surface occurs just beyond the critical point.

(22) In conclusion, the writer wishes to acknowledge his great indebtedness to Mr. J. H. Warsap, who took most of the experimental observations in the paper, and also to Mr. A. Monk, who made the small total-head tube.

XXIX. *Note on a Geometrical Radiation Problem.*

By E. A. Milne, *F.R.S.**

1. Dr. L. F. Richardson's recent interesting paper† on the radiation transmitted through a pair of parallel square apertures suggests that it may be worth while to publish the solution of the similar problem for a pair of circular apertures. Professor A. V. Hill two years ago required the solution of this problem for practical application to the case of a thermocouple receiver of circular section exposed to radiation through a parallel circular aperture, and asked me to investigate it. The problem happens to be one in which the necessary integrations can be effected in finite terms.

* Communicated by the Author.

† Phil. Mag. [7] vi. p. 1019 (Nov. 1928).

2. Let a, b be the radii of two circular apertures whose planes are perpendicular to the line joining their centres. Let l be their distance apart. Let P, P′ be any two points in the two apertures respectively, (r, θ), (r', θ') their plane-polar coordinates with reference to origins at the centres of the apertures.

Let I be the intensity of radiation, supposed uniform, at any point of one of the apertures. Then the amount R of radiant energy passing through the first aperture and reaching the other aperture is, per second,

$$\mathrm{I}\iiiint \frac{\cos^2\psi \, d\mathrm{S}\, d\mathrm{S}'}{\mathrm{PP}'^2},$$

where ψ is the angle between PP′ and the normal at P or P′, and $d\mathrm{S}$, $d\mathrm{S}'$ are elements of area.

Now
$$\cos\psi = l/\mathrm{PP}'$$
and
$$\mathrm{PP}'^2 = l^2 + r^2 + r'^2 - 2rr'\cos(\theta - \theta').$$

Hence

$$\mathrm{R} = \mathrm{I}l^2 \int_{r=0}^{r=a} \int_{r'=0}^{r'=b} \int_{\theta=0}^{\theta=2\pi} \int_{\theta'=0}^{\theta'=2\pi} \frac{rr'\, dr\, dr'\, d\theta\, d\theta'}{[l^2 + r^2 + r'^2 - 2rr'\cos(\theta - \theta')]^2}. \quad \ldots \quad (1)$$

But

$$\int_{\theta=0}^{\theta=2\pi} \int_{\theta'=0}^{\theta'=2\pi} \frac{d\theta\, d\theta'}{[\mathrm{A} - \mathrm{B}\cos(\theta - \theta')]^2} = \int_0^{2\pi} d\theta \int_0^{2\pi} \frac{d\phi}{[\mathrm{A} - \mathrm{B}\cos\phi]^2}$$
$$= 4\pi^2 \frac{\mathrm{A}}{(\mathrm{A}^2 - \mathrm{B}^2)^{3/2}}$$
if
$$|\,\mathrm{A}\,| > |\,\mathrm{B}\,|,$$

whence

$$\mathrm{R} = 4\pi^2 \mathrm{I}l^2 \int_{r=0}^{r=a} \int_{r'=0}^{r'=b} \frac{(l^2 + r^2 + r'^2)\, rr'\, dr\, dr'}{[(l^2 + r^2 + r'^2)^2 - 4r^2 r'^2]^{3/2}}.$$

In this put

$$r^2 = x, \qquad r'^2 = y.$$

Then

$$\mathrm{R} = \pi^2 l^2 \mathrm{I} \int_0^{a^2} \int_0^{b^2} \frac{(l^2 + x + y)\, dx\, dy}{[(l^2 + x + y)^2 - 4xy]^{3/2}}.$$

Next * put

$$l^2 + x - y = \xi.$$

Then

$$\mathrm{R} = \pi^2 l^2 \mathrm{I} \int_0^{b^2} dy \int_{l^2 - y}^{l^2 + a^2 - y} \frac{\xi + 2y}{[\xi^2 + 4l^2 y]^{3/2}} d\xi.$$

* I am indebted to Prof. L. J. Mordell for pointing out to me that the ensuing integrations are quite practicable.

The integration with respect to ξ is readily performed, and we obtain

$$R = \frac{\pi^2 I}{2} \int_0^{b^2} \left[\frac{a^2 - l^2 - y}{\{(l^2 + a^2 - y)^2 + 4l^2 y\}^{1/2}} + 1 \right] dy.$$

The last integration is effected by the substitution

$$a^2 - l^2 - y = \eta,$$

whence we find finally

$$R = \tfrac{1}{2}\pi^2 I \left[a^2 + b^2 + l^2 - \left[(a^2 + b^2 + l^2)^2 - 4a^2 b^2 \right]^{1/2} \right]. \quad (2)$$

This formula may be checked by noticing that, as $l \to 0$, R must tend to $\pi I . \pi c^2$, where c is the smaller of a and b;

Fig. 1.

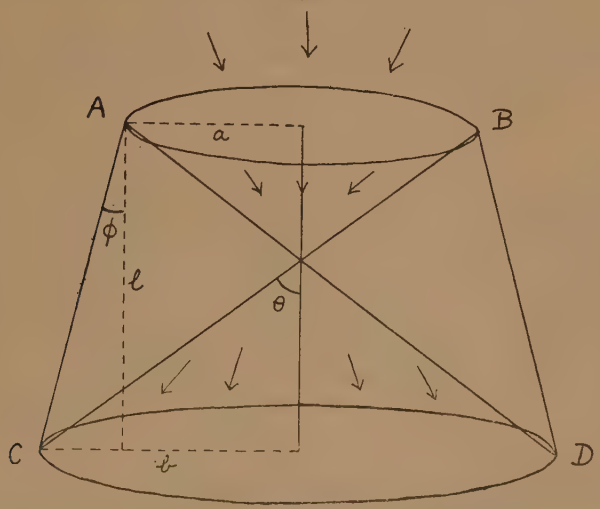

and that, as $l \to \infty$, $R \sim \pi^2 a^2 b^2 I / l^2 = I . \pi a^2 . \pi b^2 / l^2 =$ Intensity $\times$ area $\times$ small solid angle.

3. Professor A. V. Hill pointed out to me that, when $a = b$, the expression (2) can be given a simple trigonometrical form. The following is an extension of Hill's result to the general case.

Assume (without loss of generality) $b \geq a$, and put

$$\tan\theta = \frac{a+b}{l}, \qquad \tan\phi = \frac{b-a}{l}.$$

The angles θ and ϕ thus defined have the geometrical meanings indicated in fig. 1. All radiation incident on AB

at an angle of incidence less than ϕ reaches CD; no radiation incident on AB at an angle of incidence greater than θ reaches CD. Simple transformations then show that (2) reduces to

$$R = \tfrac{1}{4}\pi^2 l^2 I(\sec\theta - \sec\phi)^2. \quad . \quad . \quad . \quad . \quad (3)$$

If the screen containing the aperture AB were removed, the radiation falling on CD would be

$$\pi b^2 . \pi I = \tfrac{1}{4}\pi^2 l^2 I (\tan\theta + \tan\phi)^2.$$

Hence the fractional reduction caused by the aperture is

$$\left(\frac{\sec\theta - \sec\phi}{\tan\theta + \tan\phi}\right)^2 = \left[\frac{\sin\tfrac{1}{2}(\theta-\phi)}{\cos\tfrac{1}{2}(\theta+\phi)}\right]^2. \quad . \quad . \quad (4)$$

Similarly, if the radiation is incident on CD, the fractional reduction in the amount reaching AB caused by the screen containing CD is

$$\left[\frac{\sin\tfrac{1}{2}(\theta+\phi)}{\cos\tfrac{1}{2}(\theta-\phi)}\right]^2 . \quad . \quad . \quad . \quad . \quad . \quad . \quad (5)$$

When the apertures are equal, $\phi = 0$, and (4) and (5) reduce to $\tan^2\tfrac{1}{2}\theta$, which is Hill's result. This remarkably simple result for two equal circular apertures may be stated as follows. Let θ be the semi-vertical angle of the cone outside which no radiation incident on one aperture can reach the other. Then the radiation incident on the far face of the circular cylinder formed by the two apertures is reduced by the presence of the cylinder in the ratio $\tan^2\tfrac{1}{2}\theta : 1$.

No simple method of proof of the final result has suggested itself.

4. The result for a circular cylinder may be compared with Dr. Richardson's result for a cube. Dr. Richardson found that the radiation transmitted in series through two square apertures forming opposite faces of a cube is reduced as compared with what would pass through one aperture alone in the ratio $0{\cdot}6278/\pi = 0{\cdot}1998$.

The corresponding ratio for two circular apertures forming opposite ends of a cylinder of length equal to its diameter, by the above, is $\tan^2\pi/8 = 3 - 2\sqrt{2} = 0{\cdot}1716$. Thus a pair of square apertures separated by a distance equal to their side transmit slightly more radiation than a pair of circular apertures of the same area separated by a distance equal to their diameter.

Manchester,
November 26th, 1928.

XXX. *On the Attachment of Electrons to the Molecules HCl and NH_3.* *By* V. A. Bailey, *M.A., D.Phil.* (*Oxon*), *Associate Professor of Physics, University of Sydney, and* A. J. Higgs, *B.Sc.**

1. A METHOD for the study of the attachment of electrons to gas molecules, and the results of the application of this method to the case of dry air, were described in the issue of this Magazine for October 1925.

The intention there expressed of extending these studies to oxygen has been abandoned, for while the above communication was in the press, the results of an investigation on this gas was published by Dr. H. L. Brose †, which indicated that very few attachments occur when special precautions are taken to prevent the oxygen from becoming contaminated.

Fig. 1.

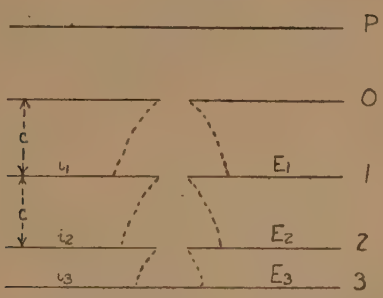

It was accordingly decided to investigate the gases hydrogen chloride and ammonia, and to leave for a possible future occasion the more difficult case which suggests itself, that, namely, of chlorine.

2. Before stating the results of these two gases, it is desirable to give a brief outline of the method, the detailed theory of which may be found in the original description ‡.

A uniform electric field of intensity Z is maintained throughout the space between the planes 3 and P in fig. 1 by suitable connexions to a battery of accumulators.

Electrons, emitted by the plate P under the influence of ultra-violet light, move downwards through the gas so that

* Communicated by Prof. J. S. Townsend, F.R.S.
† H. L. Brose, Phil. Mag. p. 536 (Sept. 1925).
‡ V. A. Bailey, Phil. Mag. p. 825 (Oct. 1925).

diverging streams of electrons and negative ions pass through the slits in the electrodes E_1, E_2, and E_3, as indicated by the dotted lines.

The number $\alpha n \,.\, dz$ negative ions are formed by attachment of electrons to molecules when n electrons move a distance dz in the direction of Z. It is easily shown that

$$\alpha = hu/l\mathrm{W}, \quad . \quad . \quad . \quad . \quad . \quad . \quad . \quad (1)$$

where h is the probability that an electron of velocity u should attach itself permanently to any molecule it may encounter, W is the mean velocity of drift of the electrons in the direction of Z, and l is the mean free path of an electron between successive collisions with molecules, the gas being at a pressure p. It follows that for a given gas α/p is a function of Z/p alone when Z and p are varied.

The divergence of electrons or ions is expressed by the same curve $y = \mathrm{R}(x)$, where y is the fraction of an approaching stream which passes through a slit, and x represents Z/k for electrons and Z for ions, k being the mean energy of an electron in terms of the mean energy of a molecule at 15° C. This curve, named the Normal Distribution Curve, may be calculated, or determined experimentally, for each diffusion chamber 01 and 12.

The two quantities k and α are separately unknown, but the function of them,

$$a = \mathrm{R}(\mathrm{Z}/k)e^{-ac}, \quad . \quad . \quad . \quad . \quad . \quad . \quad (2)$$

can be determined experimentally as follows :—

The ratios $\xi = i_2/i_1$ and $\eta = i_3/i_2$ of the currents to the electrodes are measured accurately, and the distribution ratios S_1 and S_2 calculated by means of the formulæ :

$$\mathrm{S}_1 = \frac{\xi(1+\eta)}{1+\xi(1+\eta)}, \qquad \mathrm{S}_2 = \frac{\eta}{1+\eta}.$$

The ratios R′ and R″ corresponding to the known value of Z for the chambers 01 and 12 respectively are obtained from the Normal Distribution Curves, and then a may be calculated by means of the formula :

$$a = \mathrm{S}_1(\mathrm{R}'' - \mathrm{S}_2)/(\mathrm{R}' - \mathrm{S}_1).$$

To obtain another relation between k and α, a_n is similarly determined from observations with the intensity Z/n and the pressure p/n, giving

$$a_n = \mathrm{K}(\mathrm{Z}/kn)e^{-an/c}.$$

The combination of this with (2) provides a pair of simultaneous equations in two unknown variables, which may then be solved by a graphical operation *.

3. The study of HCl and NH_3 was undertaken with the apparatus used in the examination of air, so an additional detailed account of it is unnecessary.

HCl gas was evaporated *in vacuo* from some of the middle fraction of a twice-distilled aqueous solution of pure HCl, and roughly dried over strong H_2SO_4. Then one part was stored over concentrated H_2SO_4 in a glass reservoir connected with the main apparatus through a mercury-sealed glass tap, and the other was similarly stored over anhydrous P_2O_5, both parts being at about 150 mm. pressure.

After the lapse of five months, samples of each were separately admitted to the mercury gauges and the diffusion instrument up to a pressure of $\frac{1}{2}$ mm., and with $Z = 20$ volts/cm. values of S_1 and S_2 were determined, as shown in the following table :—

Desiccator.	S_1.	S_2.
H_2SO_4	·529	·759
P_2O_5	·763	·801

The pair of values in the last line correspond closely to the distribution ratios determined for ions, namely

$$R' = ·754, \quad R = ·802;$$

so from these and other similar determinations it was concluded that the gas stored over H_2SO_4 was drier than that kept over P_2O_5. This was confirmed by the observation that within a few hours the latter formed a skin on the surfaces of mercury in the gauges which adhered to the glass walls in a troublesome manner, whereas the former left the gauges clean, even after many days. Consequently, only the gas dried over H_2SO_4 was investigated.

In the early experiments it was found that adsorption of gas by the internal surfaces of glass and metal reduced the pressure by several per cent. during the course of the observations. This effect was considerably diminished by saturating the surfaces overnight with gas at a pressure in the neighbourhood of those used on the following day. The practice adopted of removing this gas by pumping and

* *Loc. cit.* pp. 838–841.

washing out with hydrogen before introducing fresh gas, in no way reduced the efficacy of this procedure, as, even in a good vacuum, the surfaces take a long time to give up most of their adsorbed gas.

The surface exposed to the ultra-violet light was of copper, and gave an exceptionally good emission in the presence of HCl.

As illustrations some of the individual observations are shown in Table I., but the values of $-\log_{10}\alpha$ given in Table II. are the means of several observations.

The results for values of Z/p less than 10 or greater than 40 are not given, for the first indicated values of k are too low to allow of accurate deductions about α, and the second

TABLE I.

HCl.

p.	Z.	ξ.	η.	S_1.	S_2.	$-\log_{10}\alpha$.	Z/p.
mm.	volts/cm.						
1·0	10	·483	1·97	·589	·663	·542	10
·50	5	·378	·960	·426	·490	·524	10
·50	10	·357	2·35	·545	·702	1·18	20
·50	20	·258	3·23	·522	·763	1·09	40
.25	5	·253	1·17	·355	·539	·991	20
·25	10	·193	1·42	·319	·587	·954	40
·125	5	·170	·991	·253	·498	1·09	40

correspond to the occurrence of ionization by collisions of electrons with molecules which tends to falsify the calculations.

It may be seen from Table I. that, despite the low pressure used, the electrons attach themselves rapidly to molecules, for the ratios S_2 are notably greater than the corresponding ratios S_1, especially with the higher values of Z/p.

The values of k and α determined by the graphical method are shown in Table II., and the former are also represented by a curve in fig. 2 for comparison with the values of k in other gases.

It thus appears that for Z/p greater than 8 the energy of agitation of electrons in HCl is much lower than the energy of electrons in all the common gases examined to date*, namely H_2, N_2, O_2, CO_2, CO, NO, N_2O, and NH_3.

* J. S. Townsend, 'Motion of Electrons in Gases' (Clarendon Press, Oxford).

If the values of the velocity W were known, it would be possible to determine the values of λ, the fraction of their own energy lost by electrons in collisions with molecules, and of h, the probability of attachment. In the absence of such information, rough estimations may be made by assuming a value of the mean free path L (at 1 mm.

Fig. 2.

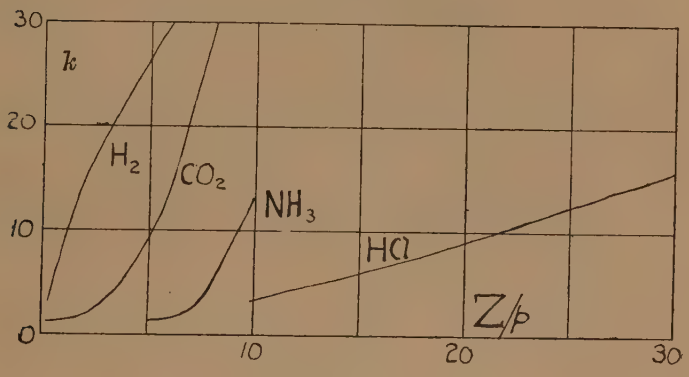

TABLE II.

Z/p.	p.	Z.	$-\log_{10} a$.	k.	a.	a/p.
	mm.	volts/cm.				
10	1·0	10	·541	3 2	·139	·133
	·50	5	·547		·063	
20	·50	10	1·15	8·9	·375	·750
	·25	5	·992		·187	
40	·50	20	1·06	25	·273	·543
	·25	10	·988		·135	
	·125	5	1·09			

pressure) deduced from measurements of the viscosity * of HCl, namely $L = 1{\cdot}96 \times 10^{-2}$ cm., and using the formulæ :

$$\lambda = 305\, L^2 (Z/p)^2/k^2,$$

$$h = 11{\cdot}1\, (a/p)\, L^2 (Z/p)/k.$$

Thus for $Z/p = 20$ it appears that $\lambda = 59$ per cent. and $h = 7 \times 10^{-13}$.

* Roth-Scheel, 'Konstanten der Atomphysik.'

4. Some preliminary experiments with NH_3 having shown that the gas reacted vigorously with the available P_2O_5, it was decided to adopt the desiccator recommended by C. Matignon * for the purpose of drying NH_3, namely the grey powder formed by pounding the metallic sodium with fused NaCl. This was considered to be simpler than purifying the P_2O_5 as recommended by Brereton Baker †.

One sample of gas was prepared by evaporation from an aqueous solution, stored first over KOH sticks for several months and finally over Matignon's desiccator. A second sample was prepared by heating *in vacuo* a mixture of pure ammonium chloride and calcium oxide, and passing the gas through a long tube containing KOH and Matignon's mixture into a flask containiug the latter alone.

After the lapse of several days these two samples were investigated in the diffusion instrument, and found to give snbstantially the same results, whose mean values are given in Table III.

As with HCl, it was necessary to reduce the large effects of adsorption by a preliminary saturation of the internal surfaces with the gas.

The values of S_1 and S_2 corresponding to $Z/p=8$ are remarkable in that S_1 is *greater* than S_2 at three pressures out of the five recorded. Another anomaly which shows itself with this value of Z/p is the notable *increase* with the pressure p of the apparent value of k estimated from the values of S_1 (or S_2). The latter anomaly also appears notably for $Z/p=9$.

In the face of these results it was clearly of no advantage to carry out the usual calculations, as these are based on considerations which seem to be violated.

It is probable, however, that the magnitudes of k determined from S_1 as if no ions existed are of some value, and these are accordingly given in the sixth column of Table III. under k_1.

For the values 6, 7, 8, and 9 of Z/p the close agreement between S_1 and S_2 indicates that few ions, if any, are formed by attachment.

For the values of Z/p greater than 9, S_2 is much larger than S_1, which indicates that a considerable amount of attachment is occurring at the higher velocities of the electrons.

The curve for NH_3 in fig. 2 represents the order of the

* C. Matignon, *Bull. de la Soc. Chim.* t. 3, no. 58, p. 353 (1908).
† Journal of the Chem. Soc. lxxiii. p. 422 (1898).

values of k given in the sixth column of Table III., and from this it will be noticed that k is the same low order for NH_3 and HCl when Z/p is less than 7, but for higher values k increases very rapidly with Z/p in NH_3.

TABLE III.

NH_3.

Z/p.	p.	Z.	S_1.	S_2.	k_1.	k_2.
5	4	20	·777	·801	1·19	
	2	10	·670	·699	1·31	
	1	5	·533	·575	1·38	
6	4	24	·779	·795	1·40	
	2	12	·667	·686	1·61	
	1	6	·541	·572	1·58	
	·5	3	·416	·442	1·53	
7	2	14	·614	·611	2·55	
	1	7	·519	·525	2·08	
	·5	3·5	·392	·407	2·02	
8	8	64	·745	·701	5·0	7·4
	4	32	·589	·594	6·60	6·83
	2	16	·520	·499	4·71	5·6
	1	8	·416	·409	4·08	4·6
	·5	4	·328	·331	3·75	3·2
9	2	18	·415	·439	9·23	8·78
	1	9	·312	·331	8·17	8·34
	·5	4·5	·262	·269	5·84	6·08
10	2	20	·377	·509	12·65	
	1	10	·268	·379	12·20	
	·5	5	·207	·270	9·43	
15	1	15	·376	·727	9·5	
	·5	7·5	·249	·552	12·3	
20	1	20	·512	·779	6·1	
	·5	10	·332	·645	8·9	

If some such rapid variation be the cause of the anomalies which appear with $Z/p = 8$, then to account through an instrumental error for the observations a much more rapid variation of k with Z/p must exist than is indicated by the above curve (fig. 2).

In the middle of the series of observations with NH_3 the instrument was thoroughly freed of this gas by means of a side-tube containing H_2SO_4 and re-tested with H_2 gas at pressures of 10 mm. and 32 mm. The measured values of S_1 and S_2 were in complete agreement with the standard distribution curves, for which S_1 is always about 40 per cent. less than S_2; so instrumental variations cannot be invoked in explanation.

A full discussion of the possible cause of the anomalies is better postponed to some future occasion, when the gas can be examined under more flexible conditions, to provide which a new instrument has been constructed.

For the present we may consider that the cause is possibly given by one of the following :—

(1) The electrons emitted by the plate issue with an energy of about 2 volts, and so may form some ions which subsequently change to electrons and neutral molecules.

(2) As indicated below, the gas contained a small quantity of H_2, and a small change in the concentration of this might well produce large effects, since k appears to vary rapidly with Z/p. Such a change in concentration would occur by the process of *effusion* through the tap admitting gas to the instrument.

Nearly a year after the above investigations were made, Mr. J. D. McGee examined with the new instrument the NH_3 gas left over by us, and obtained totally different results which more really resemble those for H_2. The containing flask was then opened with a flame, and the resulting small explosion and flash confirmed the supposition that the flask which formerly contained NH_3 now contained a considerable quantity of H_2.

There is no doubt that this is due to the slow decomposition of NH_3 by the sodium desiccator with formation of sodamide and hydrogen, and so it may be concluded that Matignon's method of drying is not fully satisfactory with this gas.

In the original experiments, repetitions of the observations after intervals of about a week had not shown any serious discrepancies, so the results given are probably of the right order for NH_3.

5. Nothing in these experiments supports the view that h is independent of the velocity of the electrons ; the contrary * is made to appear probable, especially in the case of NH_3.

* V. A. Bailey, Phil. Mag. xlvi. p. 218 (July 1923).

From these and earlier observations it may be provisionally concluded that with air, NO*, and H_2O * h diminishes as the velocity increases, and that h increases with the velocity in N_2O †, NH_3, and HCl over the range studied.

It is interesting to note that the gases H_2O, NH_3, and HCl, which appear to have relatively large values of h, also have relatively large values ‡ of $K-1$. So it may be of value to examine a possible association between h and the electric moment μ of a molecule. This quantity μ can be calculated from the variation of the dielectric constant K with temperature, by a theory due to Debye §, and its approximate values for a number of different molecules are given in the following table:—

Molecule.	H_2, N_2, O_2, C_2H_4, rare gases.	CO.	CO_2.	H_2O.	NH_3.	NCl.	Cl_2.
$\mu \times 10^{18}$.	Negligible.	1·2	1	18	15	15	1·3

For the molecules H_2, N_2, O_2, He, A, CO, CO_2, C_2H_4, which have low values of μ, h is known to be negligible, while for the molecules H_2O, NH_3, and HCl both μ and h are large.

The case of Cl_2 is of special interest, as its low value of μ suggests that this *molecule* has no great affinity for electrons, contrary to the conclusions of L. B. Loeb ‖ that h is greater than 5×10^{-4}. In view of the large affinity of HCl for electrons and the difficulty of preparing and keeping Cl_2 gas free from HCl through its great chemical activity, and the presence of sources of H_2 in the usual measuring apparatus, this is not surprising.

An analogous case is that of O_2, which was thought to have a considerable affinity for electrons, until the experiments of H. L. Brose ¶ showed that very few electronic attachments occur in the gas.

It is therefore highly desirable that experiments be conducted on very pure Cl_2 to examine this point.

* Skinker & White, Phil. Mag. xlvi. (October 1923).

† J. S. Townsend, 'Electricity in Gases,' p. 287. (Clarendon Press.)

‡ Schrödinger, 'Graetz Handbuch der Electrizität . . .' i. p. 192.

§ Victor Henri, 'Structure des Molecules,' pp. 16–26 (J. Herman, Paris). K. T. Compton, 'Science,' Jan. 15, 1926. O. Blüh, *Phys. Zeits.* xxvii. p 226 (1926).'

‖ L. B. Loeb, 'Kinetic Theory of Gases' (McGraw Hill).

¶ *Loc. cit.*

In conclusion we may notice that the experiments described here appear also to indicate that the adsorptive properties of a molecule are related to its h, which is in agreement with the known general correspondence between molecular polarity and adsorption.

Summary.

The method for the study of the attachment of electrons to molecules described in 1925 is applied to HCl and NH_3, and the results serve to indicate a certain correspondence between the probability of attachment to a given molecule and its electric moment as deduced from variations of dielectric constant with temperature.

XXXI. *On the Ionization Potentials of the Rare Earth Elements in relation to their position in the Periodic System.* *By* L. Rolla *and* G. Piccardi, *Instituto di Chimica generale della R. Università, Firenze (Italia)**.

THE binding forces with which the valency electrons are retained in an atom can best be measured by determining the ionizing potentials. In the case of the rare earths the spectroscopic data are insufficient to place the lines in series and so calculate the corresponding terms. Indirect means have been used in order to arrive at a classification of the elements between barium and hafnium. Thus measurements of atomic and molecular volumes of the elements and similar compounds have been used to give interesting figures. In this case the greater the binding strength the greater will be the contraction in isomorphous compounds.

Goldschmidt, Ulrich, and Barth [1] have determined the molecular volumes of the sesquioxides of the rare earths by the X-ray spectrographic method, and established the law that the molecular volume, in the crystalline compounds examined, diminishes with increasing atomic number. The work of V. Hevesy [2] on the series of the octo-hydro-sulphates and of Jantsch [3] on the double nitrates of magnesium confirm these results. The atomic volumes of the six elements (La, Ce, Pr, Nd, Sa, Yb) have also been measured, and, in spite of the large experimental errors, it seems as if one

* Communicated by the Authors.

ought to regard the contraction with increasing atomic number as demonstrated, in agreement with theory.

Astrophysical observations give to the rare earths a place of special importance in the constitution of the stars, and lead to conclusions of great value in the present problem.

In the solar spectrum (absorption spectrum) Rowland [4] recognized and catalogued in his tables 36 lines belonging to Ce, 17 to Nd, 32 to Y, 20 to Sc, and 69 to La.

Successive studies revealed an ever-increasing number of lines, and the elements Er, Eu, Gd, Pr, Sm, Dy were also recognized in the solar spectrum.

During the total eclipses of the Sun it is possible to photograph the spectrum of a very thin crescent of the solar chromosphere. In this case the crescent itself is used as the slit of the spectroscope, and is made up of many arcs of circles whose width varies with the height of the solar chromosphere from which the various elements radiate. Mitchell [5] and St. John [6], who studied this spectrum, came to the conclusion that all the rare earths present in the sun occur in the lower layer of the chromosphere from 0 to 500 km. high. Only La and Y reach a height of 600 km. From our knowledge of ionizing potentials we can account for these facts, and consequently a study of ionizing potentials is of great value in the interpretation of stellar spectra.

The validity of the mass-action law has been demonstrated for the case of atomic ionization into an electron and a positive ion. We can write, therefore,

$$\text{Neutral atom} \rightleftharpoons \text{positive ion} + \text{electron}. \quad . \quad . \quad (1)$$

By use of this equation notable progress has been made in astrophysics, especially by Megh Nad Saha [7]. It follows that the equilibrium constant K of equation (1), *i.e.* $[A^+]$, [electron], [neutral atom] is connected with the heat of reaction, *i. e.* the ionizing energy (U), and with the absolute temperature (T) by the equation expressing the law of mobile equilibrium:

$$U = -RT^2 \cdot \frac{d \log K}{dT} \cdot \quad . \quad . \quad . \quad . \quad . \quad . \quad (2)$$

In astrophysics the experimental determination of K is made by measuring the relation between the intensity of the arc lines (neutral atom) and of the spark lines (ionized atom) for the same element. Knowing U, we can calculate T, or, conversely, if T is known we can calculate U.

The distribution of the rare-earth elements in the solar chromosphere shows that their ionizing potentials vary very little with increasing atomic number. In work of a physico-chemical nature it is necessary to establish the validity of equation (1), and so arrive at a value of U by using (2).

We have solved this problem in a satisfactory manner with an experimental method of great simplicity [8].

A flame, which may be regarded as a stationary phenomenon, goes through a fine metallic gauze and hits a metal plate which is connected electrically to the gauze. By creating a difference of temperature between the gauze and the plate, a current flows continuously. No difference of potential is applied from outside. If, now, we introduce atoms (A) capable of being ionized under the said conditions into ions (A′) and electrons, the ions will discharge on one electrode and the electrons on the other (gauze or plate).

The difference in the current measured in the flame with and without atoms (A) gives us a measure of the number of electrons and ions which pass in one second between the electrodes.

Thus, when we know the number of neutral atoms passing per second from one electrode to the other, we have all the necessary data for calculating the rate of dissociation of (A) and the equilibrium constant of (1).

The current measured in this way is the result of movement of both positive and negative charges.

If the flame produced only positive or only negative charges, no current would flow. Thus, when an incandescent source of electrons such as platinum or iridium wire, bare or covered with a layer of non-volatile oxide, is placed below the gauze, we do not observe any variations of current.

This can be understood from the special form of cell that we used.

The final current can only be due to the simultaneous discharge of positive and negative charges in equal quantity.

In the first experiment we worked with an ordinary Bunsen flame. Into its upper part, which is homogeneous, we introduced two flat electrodes—the lower made of a net of platinum wire 0·1 mm. thick, with a 4-mm. mesh, the upper made also of platinum 15 × 20 mm. and 0·1 mm. thick.

The distance between net and plate was not less than 6 mm. nor more than 8 mm. A mirror galvanometer 160 ohms internal resistance and giving a deflexion of 1 cm. $= 2{\cdot}475 \times 10^{-7}$ amp. at 2 metres was inserted between the net and the plate. The galvanometer in this case acts

as an ammeter, since its resistance is negligible compared with the resistances of the flame between the electrodes. An experiment is carried out in the following manner :—After fixing the electrodes at a certain distance, we measure the current in the ordinary Bunsen flame (this gives a current of the order of 10^{-8} amp.). If the inrush of gas and of air

Table I.

Element.	Salt.	Atoms/sec.	Dissociation.	K.
Sodium.	Na_2SiO_3	$3{\cdot}44 \cdot 10^{15}$	$1{\cdot}41 \cdot 10^{-1}$	$6{\cdot}35 \cdot 10^{9}$
	$Na_2B_4O_7$	$4{\cdot}50 \cdot 10^{16}$	$3{\cdot}95 \cdot 10^{-2}$	$6{\cdot}40 \cdot 10^{9}$
	,,	$8{\cdot}66 \cdot 10^{16}$	$2{\cdot}66 \cdot 10^{-2}$	$6{\cdot}10 \cdot 10^{9}$
	Na_2CO_3	$4{\cdot}03 \cdot 10^{17}$	$3{\cdot}80 \cdot 10^{-3}$	$6{\cdot}03 \cdot 10^{9}$
	,,	$5{\cdot}14 \cdot 10^{17}$	$3{\cdot}33 \cdot 10^{-3}$	$5{\cdot}75 \cdot 10^{9}$
	Na_2SiO_3	$1{\cdot}23 \cdot 10^{15}$	$1{\cdot}25 \cdot 10^{-1}$	$1{\cdot}90 \cdot 10^{9}$
	$Na_4P_2O_7$	$1{\cdot}80 \cdot 10^{16}$	$1{\cdot}12 \cdot 10^{-2}$	$2{\cdot}20 \cdot 10^{9}$
	Na_2CO_3	$2{\cdot}69 \cdot 10^{17}$	$7{\cdot}35 \cdot 10^{-3}$	$1{\cdot}44 \cdot 10^{9}$
	,,	$4{\cdot}07 \cdot 10^{17}$	$6{\cdot}40 \cdot 10^{-3}$	$1{\cdot}68 \cdot 10^{9}$
	NaCl	$4{\cdot}36 \cdot 10^{18}$	$1{\cdot}85 \cdot 10^{-3}$	$1{\cdot}59 \cdot 10^{9}$
	$Na_2B_4O_7$	$4{\cdot}18 \cdot 10^{16}$	$4{\cdot}85 \cdot 10^{-2}$	$9{\cdot}85 \cdot 10^{9}$
	,,	$1{\cdot}34 \cdot 10^{17}$	$2{\cdot}67 \cdot 10^{-2}$	$9{\cdot}67 \cdot 10^{9}$
Barium.	$BaCl_2$	$2{\cdot}02 \cdot 10^{16}$	$1{\cdot}00 \cdot 10^{-1}$	$2{\cdot}00 \cdot 10^{10}$
	,,	$4{\cdot}62 \cdot 10^{16}$	$6{\cdot}60 \cdot 10^{-2}$	$2{\cdot}00 \cdot 10^{10}$
	$BaCl_2$	$8{\cdot}93 \cdot 10^{15}$	$1{\cdot}97 \cdot 10^{-1}$	$3{\cdot}40 \cdot 10^{10}$
	,,	$1{\cdot}20 \cdot 10^{16}$	$1{\cdot}55 \cdot 10^{-1}$	$2{\cdot}88 \cdot 10^{10}$
	,,	$3{\cdot}21 \cdot 10^{16}$	$1{\cdot}01 \cdot 10^{-1}$	$3{\cdot}30 \cdot 10^{10}$
	$BaCl_2$	$3{\cdot}46 \cdot 10^{16}$	$5{\cdot}67 \cdot 10^{-2}$	$1{\cdot}10 \cdot 10^{10}$
	,,	$5{\cdot}75 \cdot 10^{16}$	$4{\cdot}71 \cdot 10^{-2}$	$1{\cdot}10 \cdot 10^{10}$
Lithium.	Li_2SO_4	$1{\cdot}55 \cdot 10^{16}$	$4{\cdot}02 \cdot 10^{-3}$	$2{\cdot}52 \cdot 10^{7}$
	,,	$2{\cdot}33 \cdot 10^{16}$	$3{\cdot}55 \cdot 10^{-3}$	$2{\cdot}93 \cdot 10^{7}$
	,,	$5{\cdot}53 \cdot 10^{16}$	$2{\cdot}10 \cdot 10^{-3}$	$2{\cdot}47 \cdot 10^{7}$
	Li_2SO_4	$1{\cdot}85 \cdot 10^{16}$	$8{\cdot}48 \cdot 10^{-3}$	$1{\cdot}31 \cdot 10^{8}$
	,,	$2{\cdot}56 \cdot 10^{16}$	$7{\cdot}80 \cdot 10^{-3}$	$1{\cdot}57 \cdot 10^{8}$
	,,	$1{\cdot}21 \cdot 10^{17}$	$3{\cdot}27 \cdot 10^{-3}$	$1{\cdot}34 \cdot 10^{8}$
	Li_2SO_4	$6{\cdot}99 \cdot 10^{15}$	$8{\cdot}38 \cdot 10^{-3}$	$4{\cdot}91 \cdot 10^{7}$
	,,	$1{\cdot}34 \cdot 10^{17}$	$1{\cdot}86 \cdot 10^{-3}$	$4{\cdot}66 \cdot 10^{7}$

are well regulated, the current is absolutely constant. At a given instant we introduce under the net a bead containing a known quantity of salt, and measure the current and its variation with time. Then the bead is withdrawn, and it is observed that the current falls to its initial value.

Having plotted the values of current intensity against

time, we take the mean ordinate and subtract from it the value of the current produced in the pure flame. We then know the mean value of the ionization current, and from this follows immediately the concentration of the ions $[A^+]$ and of the electrons $[e]$, since we know the charge on an electron, and the two concentrations in (1) must be equal.

We also know, from the loss of weight of the bead and the duration of the experiment, the number of atoms introduced per second into the flame. Under the conditions of the Bunsen flame this number is practically the same as the number of neutral atoms.

We now have all the data necessary to calculate the equilibrium constant of (1).

By proper choice of the metallic salt we can obtain uniform evaporation, as shown by the constancy of the current during any experiment.

Thus for the first time we have been able to demonstrate experimentally the law of mass action for electronic equilibrium. The measurements always give the same value of K for the same atom and experimental conditions, though working at different concentrations.

Calculation of the Ionizing Potential.

We can, then, on a thermodynamic basis, apply equation (2) to obtain U the ionizing energy. The calculation is simplified if we regard U as independent of the temperature, so that if K_1 and K_2 are the equilibrium constants of (1) for temperatures T_1 and T_2, we have

$$\log K_2 - \log K_1 = \frac{U}{R}\left(\frac{1}{T_1} - \frac{1}{T_2}\right).$$

We have found that in the case of sodium the formula leads to results agreeing with those obtained spectroscopically.

We can simplify still further by integrating (2):

$$\log K = -\frac{U}{RT} + C, \quad . \quad . \quad . \quad . \quad . \quad (3)$$

where C is a constant of integration. Then, if we take two elements whose ionization potential is known, we can determine the constants of (3) for a standard flame. We can then determine U for every element by measuring $\log K$ under the given conditions. Our experiments have shown that the relation between V (ionizing potential) and $\log K$

is linear (see fig. 1 and Table II.)*. The three straight lines were obtained by varying the rate of flow and temperature of the flame.

Fig. 1.

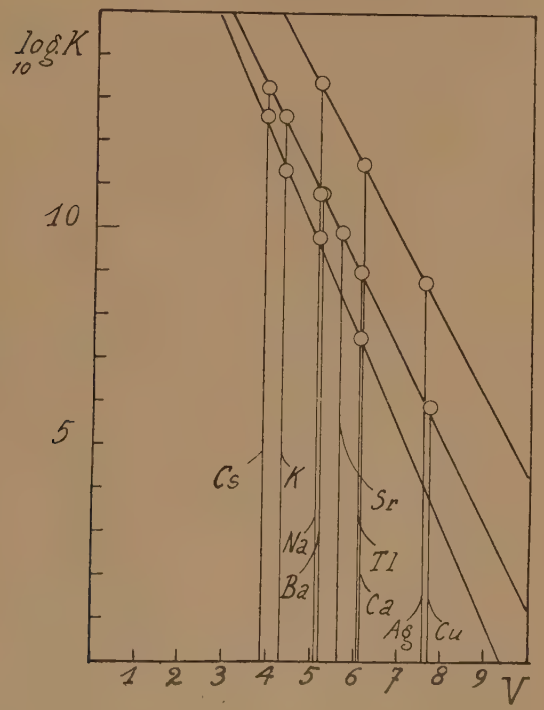

The slope of the line is

$$-\frac{1}{RT} = \tan\alpha,$$

and, expressing in volts,

$$\tan\alpha = -\frac{96500 \text{ coulombs}}{4{\cdot}186 \text{ joules} \times RT} = -\frac{23052}{RT},$$

or, in decimal logarithms,

$$\tan\alpha = -\frac{23052}{4{\cdot}571\,T}.$$

* This experimental fact agrees with the theory developed by Saha on the basis of Nernst's principle for ionization of the first kind: *the integration constant is the same for all atomic species* (chemical constant).

Table II.

Element.	V.	Log K.	Element.	V.	Log K.	Element.	V.	Log K.
Ca ...	3·89	12·628	Cs ...	3·89	13·270	Na ...	5·11	13·403
K ...	4·32	11·350	K ...	4·32	12·624	Ca ...	6·09	11·498
Na ...	5·13	9·793	Na ...	5·13	10·807	Ag ...	7·64	8·772
Tl ...	6·04	7·487	Ba ...	5·19	10·817			
			Sr ...	5·67	9·923			
			Tl ...	6·04	8·982			
			(Cu ...	7·69	5·905)			

The Influence of the Acid Radicles.

In the above method we have introduced a volatile salt into the flame in order to study equation (1) for the metal atoms. Generally we find that the volatile salts behave as if only the metallic atom would be present. The acid molecules and atoms resulting from the decomposition of the acid radicles have no influence on the ionization phenomenon, in spite of their known electron affinity.

This fact has already been observed by Arrhenius [9], Wilson, and others in some classic researches on the conductivities of salted flames. They showed that in the Bunsen flame the conductivity is independent of the acid radicle.

In our own experiment it is possible to vary the temperature conditions of the flame so that the influence of the anion of the volatilized salt becomes not only sensible but entirely preponderant.

Since the ionization potentials of the atoms I, Cl, S, O, etc., and of the molecules CO_2, SO_2, MoO_3, etc., are in general over 10 volts, we can understand how negligible will be the ionization of the acid radicle and its decomposition products at the temperature of the Bunsen flame.

Similarly, the electron affinity of these atoms and molecules is so small that the diminution in current between the net and plate can also be neglected in comparison with the increase produced by ionization of the metal atoms.

Frequently, however, this diminution is observable, and varies in magnitude with the nature of the anion. Thus, in the equilibrium :

$$\text{Neutral atoms} + \text{electron} \rightleftharpoons \text{negative ions}$$

the direction of the current will be reversed relatively to the current in the case of ionization :

$$A \rightleftharpoons \overset{+}{A} + \ominus.$$

So with flames of proper temperature we ought to observe a reverse current, due to

$$A \rightleftharpoons \bar{A} - \ominus \quad \text{or} \quad A \rightleftharpoons \bar{A} + \oplus.$$

Experiment confirms this [10].

We must make sure, however, that we are observing a reversed current and not simply a diminution, as it might seem at first sight. In the experiments on the conductivity of the salted flame, the electron affinity of an atom or a molecule manifests itself by diminishing the conductivity, *i. e.*, as a simple capture of negative charges ; in our case the phenomenon leads to an inversion of the current.

The method that we have described is applicable to the measurement of electron affinity, as one of us [11] has shown for Br, I, SO_2, SeO_2, and MoO_3.

Ionizing Potentials of the Rare Earth Elements.

The agreement of our results with those where comparison with spectroscopic results was available persuaded us to apply our method to the elements of the rare earths.

We replaced the Bunsen flame by a flame obtained by mixing coal-gas and oxygen so as to realize the temperatures necessary for volatilizing such refractory oxides. We were able to obtain steady gas-flows, so that the conditions may be considered constant.

An iridium net (wires of 0·6 mm. diameter) was used in place of the platinum one, and a thick piece of platinum with folded edges and supported on heavy brass rings formed the upper electrode. In this way there was considerable cooling by conduction, and whilst the iridium net got white-hot the platinum became light yellow.

The slope of the ionization curve was determined relative to sodium and calcium, using the data given in Table III.:—

Table III.

Atom.	Log K.	V.
Na	13·403	5·13
Ca	11·498	6·09

and therefore we have

$$\tan\alpha = \frac{13{\cdot}403 - 11{\cdot}498}{5{\cdot}13 - 6{\cdot}09} = -1{\cdot}98.$$

This value is in perfect agreement with that calculated from the temperature of the flame (about 2300° C.). Therefore, when in the formula

$$\tan\alpha = -\frac{23052}{4{\cdot}571\,T}$$

we put $T = 2300° + 273°$, we have

$$\tan\alpha = -1{\cdot}96,$$

and for $T = 2250° + 273°$,

$$\tan\alpha = -2{\cdot}00.$$

In order to volatilize such refractory oxides as those of the rare earths, we could, for example, use temperatures higher than those obtained in flames; but this is not always possible, as one sometimes melts the iridium net before the oxide is melted.

By exercising great care it has been possible to obtain results for nine oxides :—

TABLE IV.

Element.	Oxide.	Loss in weight, per sec.	Increase of current *.	Atoms, per sec.	Electr., per sec.	Log K.	V.
La ...	La_2O_3	$2{\cdot}06 \cdot 10^{-6}$	123°68	$8{\cdot}10 \cdot 10^{15}$	$1{\cdot}93 \cdot 10^{14}$	12·662	5·49
Ce ...	CeO_2	$5{\cdot}53 \cdot 10^{-6}$	7·61	$1{\cdot}92 \cdot 10^{16}$	$1{\cdot}18 \cdot 10^{13}$	9·866	6·91
Pr ...	Pr_4O_7	$2{\cdot}34 \cdot 10^{-6}$	72·25	$8{\cdot}38 \cdot 10^{15}$	$1{\cdot}12 \cdot 10^{14}$	12·168	5·76
Nd ...	Nd_2O_3	$1{\cdot}26 \cdot 10^{-6}$	15·88	$4{\cdot}50 \cdot 10^{15}$	$2{\cdot}48 \cdot 10^{13}$	11·133	6·31
Sa ...	Sa_2O_3	$1{\cdot}23 \cdot 10^{-6}$	8·07	$4{\cdot}23 \cdot 10^{15}$	$1{\cdot}26 \cdot 10^{13}$	10·576	6·55
Gd ...	Gd_2O_3	$1{\cdot}24 \cdot 10^{-6}$	6·16	$4{\cdot}12 \cdot 10^{15}$	$9{\cdot}61 \cdot 10^{12}$	10·406	6·65
Tb ...	Tb_4O_7	$2{\cdot}66 \cdot 10^{-7}$	2·40	$8{\cdot}53 \cdot 10^{14}$	$3{\cdot}75 \cdot 10^{12}$	10·212	6·74
Dy ...	Dy_2O_3	$1{\cdot}48 \cdot 10^{-7}$	1·50	$4{\cdot}76 \cdot 10^{14}$	$2{\cdot}34 \cdot 10^{12}$	10·060	6·82
Yb ...	Yb_2O_3	$1{\cdot}04 \cdot 10^{-6}$	2·16	$2{\cdot}79 \cdot 10^{15}$	$5{\cdot}35 \cdot 10^{12}$	9·582	7·06

* $1° = 2{\cdot}475 \cdot 10^{-7}$ amp.

The values in the fifth column have been obtained on the assumption that the oxide is dissociated into oxygen and metal, and that the metal is, at these temperatures, monatomic. This is legitimate owing to the extreme dilution.

Ionizing Potentials and the Periodic System.

If we plot the known ionization potentials obtained both spectroscopically and by the method described above against the atomic numbers of the elements, we obtain a curve showing the periodicity of Mendelejeff's system, which is in perfect agreement with the theory of atomic constitution (fig. 2). Here we notice the large abrupt falls of ionizing potential separating the short periods H–He, Li–Ne, Na–Ar; the two long periods of 18 elements each, K–Kr and Rb–Xe; and finally the longest period of 32 elements, Cs–Rd and in part of the period 87–U.

Fig. 2.

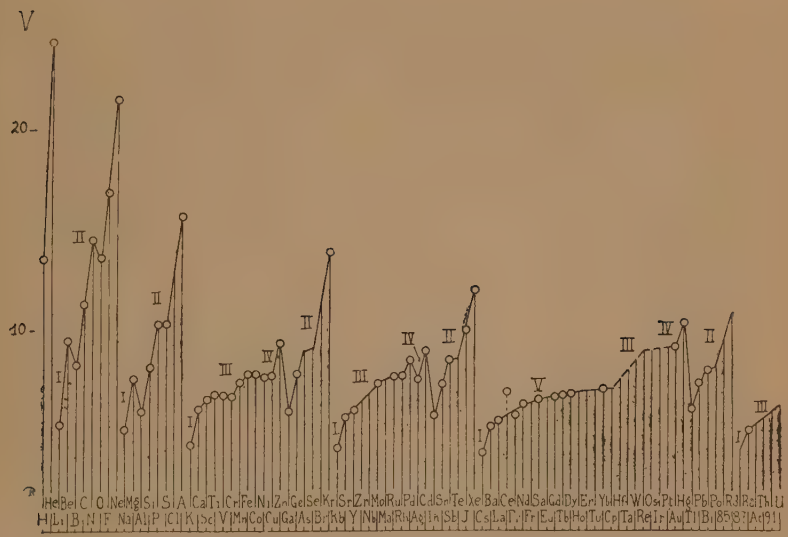
V
20
10
I
II
III
IV
V
He Be C O Ne Mg Si A Ca Ti Cr Fe Ni Zn Ge Se Kr Sr Zr Mo Ru Pd Cd Sn Te Xe Ba Ce Nd Sa Gd Dy Er Yt Hf W Os Pt Hg Pb Po Rd Ra Th U
H Li B N F Na Al P Cl K Sc V Mn Co Cu Ga As Br Rb Y Nb Ma Rh Ag In Sb J Cs La Fr Eu Tb Ho Tu Cp Ta Re Ir Au Tl Bi 85 87 Ac 91

The curve presents some characteristic marks which repeat themselves in the various periods. These marks are found to occur in the different periods at elements which bear a chemical resemblance to one another.

The marks I and II appear in all the periods; the mark III in the three long periods and in the portion of the period which completes the system; the mark IV in the long periods; whilst the mark V, which covers all the rare earth elements, occurs only in the longest period of 32 elements.

Hydrogen finds no homologous element in the system, and we can only relate it vaguely with the alkali metals; this fact is in perfect harmony with the peculiar nature of

this element; nor can we find homologues for the rare earths, and this agrees with the peculiarity of mark V. This preliminary examination shows clearly that the magnitudes of the ionizing potentials lend themselves beautifully to the representation of the periodic properties of the elements and to the grouping into periods and subperiods. This property is certainly due to the fact that the ionizing potential is characteristic of the free atom unaffected by valency or crystal bindings. The ionizing potential is measured when the elements are in the state of monatomic gases.

TABLE V.—Table of Ionization Potentials.

No.	Element.	V.	No.	Element.	V.	No.	Element.	V.
1 ...	H	13·53	32 ...	Ge	7·8	63 ...	Eu	—
2 ...	He	24·41	33 ...	As	—	64 ...	Gd	6·65
3 ...	Li	5·37	34 ...	Se	—	65 ...	Tb	6·74
4 ...	Be	9·5	35 ...	Br	—	66 ...	Dy	6·82
5 ...	B	8·34	36 ...	Kr	13·9	67 ...	He	—
6 ...	C	11·3	37 ...	Rb	4·16	68 ...	Er	—
7 ...	N	14·49	38 ...	Sr	5·67	69 ...	Tu	—
8 ...	O	13·56	39 ...	Y	6	70 ...	Yb	7·06
9 ...	F	16·9	40 ...	Zr	—	71 ...	Cp	—
10 ...	Ne	21·47	41 ...	Nb	—	72 ...	Hf	—
11 ...	Na	5·11	42 ...	Mo	7·35	73 ...	Ta	—
12 ...	Mg	7·61	43 ...	Ma	—	74 ...	W	—
13 ...	Al	5·96	44 ...	Ru	7·7	75 ...	Re	—
14 ...	Si	8·19	45 ...	Rh	7·7	76 ...	Os	—
15 ...	P	10·3	46 ...	Pd	8·5	77 ...	Ir	—
16 ...	S	10·31	47 ...	Ag	7·54	78 ...	Pt	—
17 ...	Cl	—	48 ...	Cd	8·95	79 ...	Au	9·25
18 ...	A	15·69	49 ...	In	5·76	80 ...	Hg	10·39
19 ...	K	4·32	50 ...	Sn	7·35	81 ...	Tl	6·08
20 ...	Ca	6·09	51 ...	Sb	8·5	82 ...	Pb	7·39
21 ...	Sc	6·57	52 ...	Te	—	83 ...	Bi	8
22 ...	Ti	6·81	53 ...	I	10	84 ...	Po	—
23 ...	V	6·76	54 ...	Xe	12	85 ...	—	—
24 ...	Cr	6·67	55 ...	Cs	3·89	86 ...	Rd	—
25 ...	Mn	7·41	56 ...	Ba	5·19	87 ...	—	—
26 ...	Fe	7·83	57 ...	La	5·49	88 ...	Ra	5?
27 ..	Co	7·81	58 ...	Ce	6·91	89 ...	Ac	—
28 ...	Ni	7·64	59 ...	Pr	5·76	90 ...	Th	—
29 ...	Cu	7·69	60 ...	Nd	6·31	91 ...	—	...
30 ...	Zn	9·35	61 ...	Fr	—	92 ...	U	—
31 ...	Ga	5·97	62 ...	Sa	6·55			

For H, He, Ne, A, Kr, Xe, O, S, Li, Na, K, Rb, Cs, Cu, Ag, Au, Mg, Ca, Sr, Ba, Ra, Zn, Cd, Hg, B, Al, Ga, In, Tl, Cr, Mn, Mo, Bi, Pb, Sb, I, see [13]; for Sc, Ti, V, Cr, Mn, Fe, Co, Ni, see [14], [15], and [16]; for Ru, Rh, Pd, see [17]; for Be, B, C, N, F, Ne, see [18]; for A, see [13] and [19]; for Kr and Xe, see [13] and [20]; for Sn, see [21]; for B, see [18] and [22]; for F, see [18] and [23]; for P, see [24].

TABLE VI.—Periods.

Marks.	I.	II.	III.	IV.	V.	VI.
I.	Li Be	Na Mg	K Ca	Rb Sr	Ce Ba	87 Ra
II.	B C N O F Ne	Al Si P S Cl Ar	Ga Ge As Se Br Kr	In Sn Sb Te I Xe	Tl Pb Bi Po 85 Rd	— — — — — —
III.	— — — — — — — —	— — — — — — — —	Sc Ti V Cr Mn Fe Co Ni	Y Zr Nb Mo Ma Ru Rh Pd	La Hf Ta W Re Os Ir Pt	Ac Th 91 U — — — —
IV.	— —	— —	Cu Zn	Ag Cd	Au Hg	— —
V.	— — — — — — — — — — — — —	— — — — — — — — — — — — —	— — — — — — — — — — — — —	— — — — — — — — — — — — —	Ce Pr Nd Fr Sa Eu Gd Tb Dy Ho Er Tu Yb Cp	— — — — — — — — — — — — — —

The curve presents some striking characteristics which are in agreement with our ideas of atomic structure, based upon the theories of Bohr and Hund[25]:—

(1) The addition of an electron in any orbit produces in general an increase * in the ionizing potential; this increase is greater for additions to external than to internal orbits.

The steepest portions of the diagram are the parts H–He, I, II, and IV, in which the added electron goes into an

* Except in the passage from nitrogen to oxygen, from phosphorus to sulphur etc., *i. e.*, from a 5-valent to a 6-valent element. This fact, which finds agreement with other facts, cannot as yet be explained precisely.

outer orbit (s or p); much less inclined are the portions III of the long periods, in which the added electron enters the orbit immediately within the outermost (orbit d). The portion V containing the rare earths is still less inclined. Here the electron enters orbits still nearer the nucleus (orbit $4f$, where the external orbit is $6s$).

Expressing these variations of the ionizing potentials by mean numbers, which must only be taken as illustrative, we observe that:

(*a*) For the addition of an electron to an s orbit the potential receives an increment included between 1·2 and 11 volts, while for the orbit p the increment is included between 0·82 and 2·25 volts.

(*b*) For the addition to a d orbit the potential increases by about 0·3 volt.

(*c*) For an addition to an f orbit, the case of the rare earths, the potential increases 0·14 volt.

This shows clearly that the potential responds much less for structural changes near the core than for changes in the outer orbits.

(2) When all the possible external orbits of a series are filled, the ionizing potential reaches a maximum. These maxima are represented by the rare gases. (One year after the publication [26] of our curve and its related properties, this fact was independently observed by Megh Nad Saha, who reported in his work [27] a curve of potentials constructed by R. N. Gosh and limited to the first three periods.)

(3) When the d orbits, internal to the s orbits, become saturated, the ionizing potential again reaches a maximum: these maxima are represented by the divalent metals Zn, Cd, Hg.

(4) The diagram shows two well-defined series of minima, both corresponding to the beginning of a new electronic ring. One series is represented by the alkali metals, and corresponds to the beginning of the s orbits; the other is represented by the trivalent metals B, Al, Ga, In, Tl, and corresponds to the beginning of the second ring of electronic orbits (p orbits).

(5) The influence of a change in atomic number over the ionizing potential is different for homologous elements belonging to marks I and II and those belonging to marks III and IV (mark V lies outside these considerations).

For the marks I and II an increase in the atomic number causes a decrease in the ionizing potential; this diminution

is more rapid for elements with high ionizing potentials than for those with low potentials. For example, we observe—

For the inert gases :

He.	Ne.	Ar.	Kr.	Xe.	Rd.
24·49	21·48	15·69	13·3	12·0	?

For the alkaline earth metals :

Be.	Ng.	Ca.	Sr.	Ba.	Ra.
9·50	7·61	6·09	5·67	5·19	5 ?

For the alkali metals :

Li.	Na.	K.	Rb.	Cs.	87.
5·37	5·11	4·32	4·16	3·89	?

In contrast to this we find in marks III and IV that the potentials fall slightly in passing from the third to fourth period, and then rise sharply in passing to the fifth. The rise is clearly due to the insertion of the rare earths, which pushes all the following elements as far as mercury to higher potentials. With the elements below mercury the addition of electrons takes place in internal orbits ; those coming after mercury add electrons to their outer ring (thallium and following), and the ionizing potential behaves normally.

This return to normal behaviour after such a perturbation is worth noticing as further evidence of the extent to which the ionization potential depends on the external structure, and of the importance, in theories of atomic constitution, of the very strange group of elements known as the rare earths.

The results found in the above experiments are in perfect agreement with the views of Bohr on general atomic structure and of Hund on the structure of particular elements. It is very interesting to study the marks III, as they should not show similarities too exact, because the triads Fe, Co, Ni ; Ru, Rh, Pd ; Os, Ir, Pt do not contain homologous elements ; in fact, the first two triads are notably different from one another.

(6) We can see also how the ionizing potentials can be taken—though not in an absolute sense—as an index of basicity agreeing with the chemical properties. Thus the elements with a distinct electropositive character—alkali metals, alkaline earth metals, and rare earth metals—have all rather small potentials ; while the elements with a distinct electronegative character—halogens and the nitrogen and oxygen groups—all have high potentials.

The inert gases, whose chemical stability is almost complete, possess in each period the maximum potential.

In the group of noble metals we find still further support for these general views. Thus the most electropositive is undoubtedly silver and the most electronegative is gold (it behaves, from the chemical point of view, as a real metalloid), whilst silver has the lowest ionizing potential, 7·54 volts, and gold the greatest, 9·25 volts.

We will not go further into the detailed examination of the peculiarities of the curve. At present it is enough to have constructed for the first time a sufficiently complete curve of potentials, to have shown how beautifully this represents the periodic system of the elements, and to have shown how to insert the rare earth group.

These values for the rare earths appear on a slightly-curved segment characterized by a small inclination and low values of the ionizing potential; cerium alone is exceptional, and this may be due partly to the fact that the oxide is only slightly dissociated, and partly to the less basic character of this element.

In general we observe that the ionizing potential increases regularly in an almost asymptotic curve with increasing atomic number. This regularity is found in other physical values, *e. g.* the atomic volumes and molecular volumes of similar compounds. No peculiarity appears for elements such as gadolinium, which are believed to possess particular properties; this shows that if these peculiarities exist, their origin must be sought in very deep zones of the atomic structure.

The behaviour of the ionizing potentials tells us that the external electronic shell is the same for all these elements, with the possible exception of cerium, in agreement with the results of long and tiresome studies of the chemical properties.

We have found the absolute values of the potentials for the rare earths to be rather small, varying from 5·49 to 7·06 volts, in good agreement with the strong basic character of these elements.

Bibliography.

(1) Goldschmidt, Ulrich, and Bahrt, *Osloer Akad. Ber.* no. 5 (1925). Goldschmidt, Barth, and Lunde, *Osloer Akad. Ber.* no. 6 (1925). Goldschmidt, *Osloer Akad. Ber.* no. 2 (1926).

(2) G. v. Hevesy, *Zeitschr. f. anorg. Chemie*, cxlvii. p. 217 (1925); cl. p. 68 (1925).

(3) G. Jantsch, *Zeitschr. f. anorg. Chemie*, lxxvi. p. 311 (1912).

(4) A. H. Rowland, Astrophysical Journ. i. pp. 29, 131, 222, 295, 377 (1895); ii. pp. 45, 109, 188, 306, 360 (1895); iii. pp. 141, 201, 356 (1895); iv. pp. 106, 227 (1896); v. pp. 11, 109, 181 (1897).
(5) S. A. Mitchell, Astrophysical Journ. xxxviii. pp. 407, 495 (1913).
(6) Ch. F. St. John, Astrophysical Journ. xl. p. 357 (1914).
(7) Megh Nad Saha, Phil. Mag. xl. pp. 472, 809 (1920); xli. p. 357 (1921).
(8) L. Rolla and G. Piccardi, *Rend. Reale Acc. Lincei*, (6) ii. pp. 29, 128, 173, 334 (1925).
(9) S. Arrhenius, *Ann. d. Physik*, xliii. p. 18 (1891).
(10) G. Piccardi, *Rend. Reale Acc. Lincei*, (6) iii. pp. 413, 566 (1926).
(11) G. Piccardi, *Zeitschr. f. Phys.* xliii. p. 899 (1927).
(12) L. Rolla and G. Piccardi, *Rend. Reale Acc. Lincei*, (6) iii. p. 410 (1926); (6) v. p. 818 (1927).
(13) K. T. Compton and F. L. Mohler, Bull. Nat. Res. Council, ix. pt. 1, no. 48 (1924).
(14) H. N. Russel, Astrophysical Journ. lxvi. p. 233 (1927).
(15) H. Gieseler and W. Grotrian, *Zeitschr. f. Phys.* xxv. p. 165 (1924).
O. Laporte, Proc. Nat. Acad. Sci. xii. p. 496 (1926).
K. Bechert, *Ann. d. Physik*, lxxvii. p. 537 (1925).
(16) N. K. Sur, Phil. Mag. (6) iv. p. 36 (1927).
(17) L. A. Sommer, *Zeitschr. f. Phys.* xlv. p. 147 (1927).
(18) R. A. Millikan and I. S. Bowen, Phil. Mag. (7) iv. p. 561 (1927).
(19) F. A. Saunders, Proc. Nat. Acad. Sci. xii. p. 556 (1926).
(20) J. H. Abbink and H. B. Dorgelo, *Zeitschr. f. Phys.* xlvii. p. 221 (1928).
G. Hertz and K. Kloppers, *Zeitchr. f. Phys.* xxxi. p. 463 (1925).
(21) J. C. McLennan, J. F. T. Jouug, and A. B. McLay, Proc. Roy. Soc. Canada, (3) xviii. p. 57 (1924).
J. B. Green and R. A. Loring, Proc. Nat. Acad. Sci. xiii. p. 347 (1927).
(22) Ralph A. Sawyer, *Naturwiss.* xv. p. 765 (1927).
(23) H. Dingler, Proc. Roy. Soc. Lond. A, cxiii. p. 223 (1926); cxvii. p. 407 (1927).
(24) O. S. Duffendach and H. Hutsteiner, Phys. Rev. (2) xxv. p. 501 (1924).
(25) F. Hund, 'Linienspektren und periodisches System der Elemente.' Berlin, 1927.
(26) L. Rolla and G. Piccardi, *Gazzetta chimica ital.* lvi. p. 512 (1926).
(27) Megh Nad Saha, *Phys. Zeitschr.* xxviii. p. 469 (1927).

XXXII. *The Crystal Structure of Nickel.* *By* L. Mazza *and* A. G. Nasini *.

[Plate IV.]

THE crystal lattice of nickel has been determined by different authors, but with somewhat divergent results.

According to Hull's (1) first determinations, nickel exists both in face-centred cubes and in body-centred faces, the lattice constant of the face-centred form being 3·54 Å. (2).

* Communicated by Prof. T. M. Lowry, F.R.S.

Other authors have observed only the face-centred form, and have given for the edge of the elementary cube values ranging from 3·499 to 3·54 Å., as set out in Table I.

The difference of 0·04 Å. between the recent values of Sacklowski and of Davey is not easy to explain, in view of the exactness of modern X-ray technique, which permits of readings to 0·001 Å. by the powder method. On the other hand, the lattice dimensions of pure nickel are not likely to vary to this extent, in view of the satisfactory agreement reached with other metals; nor can these discrepancies be attributed to deformation of the lattice, because in this case characteristic features ought to be developed in the spectrograms. Finally, a critical review of the data is rendered impossible by the absence in certain cases of experimental details as to the preparation and diameter of the sample, and also the distance between sample and anticathode.

TABLE I.

Lattice constant.	Authorities.
3·499±0·003 Å.	Davey, Phys. Rev. xxvii. p. 292 (1924).
3·51	F. Wever, *Mitt. Kaiser Wilhelm Inst. Eisenforsch*, iii. p. 17 (1922). McKeehan, Phys. Rev. xxi. p. 402 (1923).
3·518.....	H. Lange, *Ann. d. Phys.* lxxvi. pt. 4, p. 476 (1925).
3·52	S. Holgerson, *Ann. der Phys.* lxxix. pt. 1, p. 35 (1926).
3·53	H. Bohlin, *Ann. d. Phys.* lxi. p. 421 (1920).
3·536.....	G. L. Clark, W. G. Ashbury, and R. M. Wick, Journ. Am. Chem. Soc. p. 2661 (1925).
3·54	A. W. Hull, *loc. cit.* A. Sacklowski, *Diss. Greifswald* (1924).

The present experiments had their origin in an extended series of X-ray analyses by one of us (L. Mazza) of the nickel-copper alloys, in the course of which a number of samples of nickel were examined, with concordant results. We therefore thought it useful to make a complete series of exact experiments, with special precautions as to the purity of the samples, the possible influence of thermal and mechanical treatment, and the precision of the methods used to determine the lattice dimensions.

Experiments were also made to determine whether nickel can show at ordinary temperatures *, in addition to the face-centred form, the body-centred form recorded by Hull[1].

* In another paper we will report about the structure of nickel at high temperatures.

The following methods of preparation were used * :—

(1) *Electrolytic Deposition.*—The bath, already used successfully in other researches [3], had the following composition: $NiSO_4 . 7H_2O$, 40 g.; NH_4Cl, 20 g.; citric acid, 2 g.; water 1000 c.c. The nickel was deposited with a current-density of 0·003 amp. per cm.^{2} on a very thin wire (0·2 mm. diam.) of the same metal; in this way nickel wires of 1 mm. diam. were obtained.

With the radiations used by us the diffraction takes place in a very thin surface-layer; the internal core of drawn nickel wire has no influence on the results.

(2) *Reduction of the Oxide by heating in a Current of Hydrogen.*—The product was obtained as a light grey powder of metallic aspect. Nickel oxide was heated in a current of hydrogen at 600° C. during a period of 4 hours, when the reduction was practically complete.

(3) *Decomposition of Nickel Carbonyl.*—A thin plate of nickel formed by decomposition of $Ni(CO)_4$ on a hot metal plate was cut into strips about 3 mm. wide. These were bent very carefully (in order to avoid mechanical deformation) into hollow cylinders of 1 mm. diam.

Samples of pure commercial nickel were also examined which have been drawn by us in a steel wire-drawing machine to 1 mm. diameter. Some of them were further examined after rolling in a small rolling machine with steel cylinders, or after cold wire-drawing and also after prolonged annealing in a current of pure dry hydrogen in an electric furnace with a porcelain tube, followed in some instances by quenching in cold water. The annealing temperatures were controlled, and kept constant at 940° or 1200° C., by a thermocouple and a regulating resistance; the annealing and quenching temperatures are tabulated for each sample; time of annealing was usually 10 hours, but in one case it was extended to 30 hours.

The measurements were made by the method of Debye and Hull, with the following special features: the use of a new X-ray tube, regulated to give a very small surface of

* The method of preparation by cathodic deposition has not been used on account of the difficulty of obtaining the metal in a massive state. Recently Bredig and Allolio (*Zeitschr. f. phys. Ch.* cxxvi. p. 41, 1927) have examined some samples of nickel cathodically deposited in an atmosphere of hydrogen at a few tenths of a millimetre of pressure. These seemed to have a close-packed hexagonal structure.

the local point upon the anticathode [4]; maintaining a constant known distance between this focal point and the sample; the use of a precision spectrographic camera with diaphragms of accurately-calibrated dimensions. It was therefore possible to apply a correction for the divergence of the X-ray pencil, and to make use of the most accurate methods for determining the lattice constants from precision photograms [5].

A precision camera of great mechanical rigidity was used with a cylindrical film supporter of 57·3 mm. diam.

The film was attached closely to the film-supporter as to allow of comparable measurement with different samples.

The samples, in the form of cylindrical rods of about 1 mm. diam., were held in such a way that the axis of the rod always coincided with that of the film supporter.

The Röntgen tube, made in the laboratory workshop, was of the metallic type of Hadding, modified by the replacement of the afflux cathode by an electron cathode (Coolidge) and cooling devices [4]. The copper anticathode was excited with an alternating current of 60 k.v. max. and 15 m.a. intensity.

The distance between the centre of the spectrographic camera and the centre of the anticathode was 10 cm. In these conditions good photograms could be obtained with an exposure of 2½ hours.

The photogram obtained with electro-deposited nickel (without any further thermal or mechanical treatment) (Pl. IV. fig. 1) shows only nine diffraction lines, all derived from $K\alpha$ doublet of copper (mean value of $1 = 1{\cdot}539 \times 10^{-8}$ cm.). The lines are narrow and regular, from which we may infer that the electro-deposited nickel is not oriented, but consists of very small grains, though not of comparable size.

The results of the determination are recorded in Table II. In the first column, under "$\frac{\theta}{2}$," are recorded the values in degrees and minutes of the angles of each diffraction line, corrected in the usual way for the displacement due to the diameter of the preparation (1 mm.) and the divergence of the X-ray (diameter of diaphragm 1·2 mm., distance between sample and anticathode 10 cm.). In the second column are tabulated the corresponding sines; in the third, Miller's indices; in the fourth, the ratio

$$\frac{\sin^2\frac{\theta}{2}}{h_1^2+h_2^2+h_3^2};$$

in the fifth and sixth, those measured by a microphotometer and calculated by the formula:

$$I = N\left(\frac{d_{hkl}}{n}\right)^{2\cdot35}(A^2+B^2)$$

(where N represents the number of planes of the crystal considered as co-working to the formation of each line and (A^2+B^2) is the phase factor) for the following position of the atoms:

$$0\,0\,0\,;\ \tfrac{1}{2}\,\tfrac{1}{2}\,0\,;\ \tfrac{1}{2}\,0\,\tfrac{1}{2}\,;\ 0\,\tfrac{1}{2}\,\tfrac{1}{2}.$$

Finally, in the last column are tabulated the number N of planes co-operating in the formation of each line.

To calculate the lattice constant "a" we have taken into account [6], in deducing the mean value of the expression

$$X = \frac{\left(\sin^2\frac{\theta}{2}\right)}{h_1^2+h_2^2+h_3^2},$$

that each single measurement must be evaluated in relation to its certainty, according to Gauss's law of observation errors. Since, in the present instance, the "weight" is proportional to $\tan^2\frac{\theta}{2}$, the mean value X_0 is expressed by

$$X_0 = \frac{\Sigma X\tan^2\frac{\theta}{2}}{\Sigma\tan^2\frac{\theta}{2}}.$$

The limit of error for the length of the side of the elementary cube is then given by

$$\Delta a = \tfrac{1}{2}\,\frac{\sqrt{\dfrac{\left((X-X_0)\tan^2\frac{\theta}{2}\right)^2}{(n-1)\tan^2\frac{\theta}{2}}}}{X_0}\cdot a,$$

and the value of the lattice constant is then

$$a = a_0 \pm \Delta a,$$

where

$$a_0 = \frac{\lambda}{2\sqrt{X_0}}.$$

In calculating the values of the lattice constant and the limits of error, we have omitted the datum corresponding

approximately to the 78·5° line. This line, as is usually the case when the deviations are large, appears very shaded in all photograms, and is not suitable for an exact measurement on the comparator.

Since we could not rely upon getting values of a precision comparable with that obtainable with smaller angles, we thought it better not to use this line for the present calculations.

TABLE II.

Electrolytic Nickel Wire.

1 mm. diam. Diameter of the cylinder supporting the film, 57·3 mm. Copper radiations, Cu $K\alpha = 1{\cdot}539$ Å. Exposure, 2000 milliamp. minutes.

$\frac{\theta}{2}$ corrected.	$\sin\frac{\theta}{2}$.	$h_1\,h_2\,h_3$.	$\frac{\sin^2\frac{\theta}{2}}{h_1^2+h_2^2+h_3^2}$.	I. Obs.	I. Calc.	N.
22° 19′	0·3797	1 1 1	0·04806	ff.	100	8
26 0	0·4384	0 0 2	0·04806	f.	54	6
38 17	0·6196	2 0 2	0·04798	f.	47	12
46 32	0·7258	1 1 3	0·04790	f.	65	24
49 20	0·7585	2 2 2	0·04794	d.	19	8
61 14	0·8766	0 0 4	0·04802	d.	10	6
72 37	0·9543	3 1 3	0·04793	f.	33	24
78 5	0·9784	2 0 4	0·04787	f.	32	24

$a = 3{\cdot}514 \pm 0{\cdot}001$ A.
$d = 8{\cdot}925$.

From this value of "a" is calculated the density :

$$d = \frac{4 \times 58{\cdot}68 \times 1{\cdot}650 \times 10^{-24}}{(3{\cdot}514 \times 10^{-8})^3} = 8{\cdot}925.$$

The samples of nickel prepared by reduction from the oxide were tested by putting the powdered nickel in small tubes of paraffined paper of 1 mm. diam., using the same method as for electrolytic nickel. A photogram is shown in fig. 2 (Pl. IV.) and the relevant data are set out in Table III.

The length of the edge of the elementary cube is within 0·001 Å. of that of nickel obtained by electrolytical deposition.

TABLE III.

Nickel reduced from the Oxide.

Diameter of the sample, 1 mm. Diameter of the cylinder supporting the film, 57·3 mm. Copper radiations, Cu Kα = 1·539 Å. Exposure, 2000 milliamp. minutes.

$\frac{\theta}{2}$ corrected.	$\sin\frac{\theta}{2}$.	$h_1\,h_2\,h_3$.	$\frac{\sin^2\frac{\theta}{2}}{h_1^2+h_2^2+h_3^2}$.	I. Obs.	I. Calc.	N.
22° 17′	0·3792	1 1 1	0·04793	ff.	100	8
25 57	0·4376	0 0 2	0·04787	f.	54	6
38 15	0·6191	2 0 2	0·04791	f.	47	12
46 30	0·7254	1 1 3	0.04783	f.	65	24
49 19	0·7583	2 2 2	0·04792	m.	19	8
61 12	0·8763	0 0 4	0·04800	d.	10	6
72 36	0·9542	3 1 3	0·04793	f.	33	24
78 3	0·9783	2 0 4	0·04785	f.	32	24

$a = 3{\cdot}513 \pm 0{\cdot}001$ Å.
$d = 8{\cdot}918$.

TABLE IV.

Nickel from the Carbonyl.

Diameter of the sample, 1 mm. Diameter of the cylinder supporting the film, 57·3 mm. Copper radiations, Cu Kα = 1·539 Å. Exposure, 2000 milliamp. minutes.

$\frac{\theta}{2}$ corrected.	$\sin\frac{\theta}{2}$.	$h_1\,h_2\,h_3$.	$\frac{\sin^2\frac{\theta}{2}}{h_1^2+h_2^2+h_3^2}$.	I. Obs.	I. Calc.	N.
22° 19′	0·3797	1 1 1	0·04806	ff.	100	8
26 0	0·4384	0 0 2	0·04804	f.	54	6
38 17	0·6196	2 0 2	0·04798	f.	47	12
46 34	0·7262	1 1 3	0·04805	f.	65	24
49 21	0·7587	2 2 2	0·04797	d.	19	8
61 15	0·8767	0 0 4	0·04804	d.	10	6
72 38	0·9544	3 1 3	0·04794	f.	33	24
78 6	0·9785	2 0 4	0·04787	f.	32	24

$a = 3{\cdot}513 \pm 0{\cdot}001$ A.
$d = 8{\cdot}933$.

Nickel obtained from $Ni(CO)_4$ was examined in small hollow cylinders of 1 mm. external diameter prepared as already mentioned, avoiding all mechanical work capable of producing a deformation in the structure of the samples.

The reproduction of a photogram is given in fig. 3 (Pl. IV.), whilst the relevant data and the results of the mechanical calculations are set out in Table IV.

In this case again the length of the edge does not differ appreciably from the preceding values.

Table V.

Commercial nickel wire of 1 mm. diameter. Diameter of the cylinder supporting the film, 57·3 mm. Copper radiations, Cu Kα = 1·539 Å. Exposure, 2000 milliamp. minutes.

$\frac{\theta}{2}$ corrected.	$\sin\frac{\theta}{2}$.	$h_1 h_2 h_3$.	$\frac{\sin^2\frac{\theta}{2}}{h_1^2+h_2^2+h_3^2}$.	I. Obs.	I. Calc.	N.
22° 19′	0·3797	1 1 1	0·04806	ff.	100	8
26 0	0·4384	0 0 2	0·04804	f.	54	6
38 15	0·6191	2 0 2	0·04791	f.	47	12
46 35	0·7264	1 1 3	0·04797	f.	65	24
49 21	0·7587	2 2 2	0·04797	d.	19	8
61 16	0·8769	0 0 4	0·04805	d.	10	6
72 39	0·9545	3 1 3	0·04795	f.	33	24
78 7	0·9786	2 0 4	0·04788	f.	32	24

$a = 3{\cdot}510 \pm 0{\cdot}001$ Å.
$d = 8{\cdot}956$.

One of the spectrograms obtained with pure commercial nickel in cold-drawn wires of 1 mm. diam. is shown in fig. 4 (Pl. IV.) ; data and calculations are given in Table V.

It is remarkable that the photograms of this sample do not show the characteristics of a wire-drawing structure.

Table VI. shows the date for a similar sample after being annealed for 10 hours at 940° C.

The photogram does not differ appreciably from that of the same nickel when not annealed after cold drawing.

The diffraction lines are very narrow and do not show any trace of recrystallization.

The length of the edge of the elementary cell differs from that of the unannealed sample only by 0·004 Å.

Another sample of the same cold-drawn nickel was annealed during 30 hours at 1200° C. It showed under the microscope (with small magnification) the formation of large crystals.

A rough examination of the mechanical properties showed a remarkable diminution of ductility and a very low value for the tensile strength.

TABLE VI.

Diameter of the sample, 1 mm. Diameter of the cylinder supporting the film, 57·3 mm. Copper radiations, Cu Kα = 1·539 Å. Exposure, 2000 milliamp. minutes.

$\frac{\theta}{2}$ corrected.	$\sin\frac{\theta}{2}$	$h_1h_2h_3$.	$\frac{\sin^2\frac{\theta}{2}}{h_1^2+h_2^2+h_3^2}$.	I. Obs.	I. Calc.	N.
22° 19′	0·3797	1 1 1	0·04806	ff.	100	8
25 59	0·4381	0 0 2	0·04798	f.	54	6
38 17	0·6196	2 0 2	0·04798	f.	47	12
46 31	0·7256	1 1 3	0·04786	f.	65	24
49 21	0·7587	2 2 2	0·04797	d.	19	8
61 13	0·8765	0 0 4	0·04801	d.	10	6
72 38	0·9544	3 1 3	0·04794	f.	33	24
78 6	0·9785	2 0 4	0·04787	f.	32	24

$a = 3{\cdot}514 \pm 0{\cdot}001$ A.
$d = 8{\cdot}925$.

The photogram of this sample is given in fig. 5 (Pl. IV.). It shows clearly that annealing has given rise to a coarse-grained structure with a somewhat regular orientation.

There is also an almost complete absence of interference lines of the characteristic type which one gets from irregularly-oriented crystal particles having dimensions inferior to 1×10^{-2} mm., but larger than colloidal particles. The position of the single interference lines coincides accurately with the position of the lines of the previous photograms.

Some of the samples used in the three preceding experiments were subjected, after annealing, to a rapid cooling

(quenching). The photogram of a sample annealed for 10 hours at 940° C. and quenched from the same temperature is identical with the one of the unannealed sample.

A sample subjected to the same thermal treatment at 1000° C. gave a very different X-photogram (Pl. IV. fig. 6). One may easily detect the appearance of a recrystallization structure with irregular orientation, and this structure seems to be superposed on the pre-existing structure, whose type is that required for small crystal particles with completely irregular orientation. Notwithstanding the appearance of recrystallization the photogram shows some very narrow lines from which the lattice constant can be determined as in Table VII.

TABLE VII.

$\frac{\theta}{2}$ corrected.	$\sin\frac{\theta}{2}$.	$h_1 h_2 h_3$.	$\frac{\sin^2\frac{\theta}{2}}{h_1^2+h_2^2+h_3^2}$.
22° 18′	0·3794	1 1 1	0·04799
26 0	0·4384	0 0 2	0·04804
38 16	0·6193	2 0 2	0·04795
46 30	0·7254	1 1 3	0·04783
49 18	0·7581	2 2 2	0·04790
61 13	0·8765	0 0 4	0·04801
72 37	0·9543	3 1 3	0·04793
78 5	0·9905	2 0 4	0·04787

$a = 3{\cdot}514 \pm 0{\cdot}001$ Å.
$d = 8{\cdot}925$.

We thus find that samples of nickel which have been annealed for a long time and afterwards quenched show only a face-centred cubic structure, and that the dimensions of the elementary cell seem to have changed very little.

Conclusions.

(1) Nickel obtained (a) *by electrolytic deposition*, (b) *by separation from* $Ni(CO)_4$, (c) *by reduction of the oxide* crystallizes in face-centred cubes. The dimensions of the crystal particles range from 1×10^{-2} to 1×10^{-5} cm.

(2) The length of the edge of the elementary cell ranges from $3{\cdot}513 \pm 0{\cdot}001$ Å. to $3{\cdot}515 \pm 0{\cdot}001$ Å.

The mean value for samples of normal structure is $3{\cdot}514 \pm 0{\cdot}002$ Å., in close agreement with the values of Wever, of McKeehan, and of Lange (see Table I.).

(3) Pure cold-drawn nickel, after various thermal treatments, although sometimes showing peculiar recrystallization, always crystallizes in face-centered cubes. No confirmation has been found of Hull's observation of the existence of nickel crystallizing at ordinary temperature in body-centered cubes. The length of the edge of the elementary cube differs but little from that determined for the previous samples.

(4) Pure cold-drawn nickel subsequently annealed for a long time does not show recrystallization structures, detectable by X-ray analysis, for annealing temperatures up to 940° C. The appearance of characteristic recrystallization structures is only observed at temperatures of 1000° C. and above. Prolonged annealing (30 hours) at 1200° C. produces a recrystallization in coarse grains, irregularly oriented, giving rise to a marked reduction of properties such as ductility and tensile strengths.

(5) Quenching does not produce any change in the dimensions of the lattice of nickel.

(6) The relative intensity of the various lines is approximately the same in the photograms of all samples examined, and is in good agreement with the values deduced by means of the approximate formula adopted in the present calculations.

We wish to thank the Mond Nickel Co., Ltd., who presented us with some samples of pure nickel, and Dr. B. Nuterini for her help in the experimental work.

Literature.

(1) A. W. Hull, Phys. Rev. x. p. 691 (1917).
(2) A. W. Hull, Phys. Rev. xiv. p. 540 (1919); *ibid.* (1921).
(3) L. Mazza and E. Ciani, *Metall. Ital.* xviii. p. 1926.
(4) L. Mazza, *Nuovo Cimento* (1927).
(5) O. Pauli, *Zeitschr. f. Kryst.* lvi. p. 591 (1922). T. Barth u. G. Lunde, *Zeitschr. f. physik. Ch.* cxxi. p. 78 (1926).
(6) E. Broch, *Zeitschr. f. physik. Ch.* cxxvii. p. 446 (1927).

The Laboratory of Physical Chemistry.
The Royal University, Florence,

XXXIII. *On the Influence of a Hydrogen Atmosphere upon the Arc Spectra of Certain Metals.* *By* HENRY CREW *.

1. MORE than a quarter of a century ago, I described, in this Magazine †, some marked changes in the line spectra of magnesium, zinc, and iron when the air surrounding the electric arc which furnishes the light is replaced by an atmosphere of hydrogen. The arc employed at that time was produced by 100 volts acting between a fixed electrode made of the metal in question and a rapidly rotating electrode in the form of a disk made of the same metal. This arc was enclosed in an insulated brass case, so that a current of air flowing through the hood could be replaced by a stream of hydrogen gas without changing anything else about the entire apparatus. Corresponding to this change of atmosphere certain differences in the spectra were observed. The hydrogen introduced asymmetrical shading, changes in reversal, and marked alteration in intensity, sometimes greatly increasing the strength of a line, sometimes causing it almost to vanish. In general the spark lines were found to be most sensitive to hydrogen, and lines belonging to the principal and diffuse series were practically immune.

2. The explanation of most of this effect, which seemed to be entirely out of proportion to its cause, occurred to me only a few weeks ago. It is as follows. In using the arc, which has a rotating disk for one electrode, the image of the arc on the slit of the spectroscope is something like that

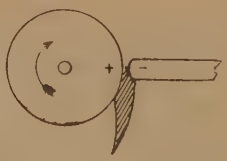

indicated by the shaded portion of the accompanying figure. Naturally one sets the brightest portion of this "flame" of luminous vapour on the slit; and, in air, this is the central portion. In hydrogen, however, one finds that the "flame" contracts to a mere fraction of its size in air, and recedes to a small luminous spot in the angle between the fixed and

* Communicated by the Author.
† Phil. Mag. l. p. 497 (1900).

moving electrodes. Under these circumstances again one naturally puts the brightest part of the spot on the slit, and this means that the source of light illuminating the slit is very near each of the poles. The result of the use of a hydrogen atmosphere is therefore to introduce what is known as "pole-effect." I was therefore mistaken in thinking that, on introducing hydrogen, I was changing only one independent variable. The principal pole-effect considered during the past twenty years has been a change of wave-length; but there are several other effects of this same cause which are easily seen by photographing the entire length of the arc in a spectrograph which is not astigmatic. Among these other effects the principal ones are the three mentioned above—namely, asymmetrical shading, reversal, and change of intensity.

It is generally believed, I suppose, that these effects are produced by the steep potential gradient (Stark effect), the change of temperature, and the change of vapour density which are met with in a close approach to either pole of the arc. In addition to these effects, one can predict also that an atmosphere of hydrogen will introduce certain chemical effects, such, for example, as the quenching of the cyanogen bands in the carbon arc, and the exclusion of the magnesium oxide bands when magnesium poles are used; also the introduction of bands due to metallic hydrides; and, what perhaps might *not* be expected in the arc, the appearance of the lines H_β, H_γ, H_δ.

3. In order to eliminate these pole-effects, and to discover the *bona fide* consequences of a hydrogen atmosphere, two methods were employed. The first consisted in using fixed electrodes in a water-jacketed chamber and *keeping the arc-length the same in air as in hydrogen*. This is not easy to do, since most arcs are maintained in hydrogen at ordinary barometric pressure only with difficulty; and this is true even when four or five hundred volts are employed. In this method the images of the two poles each lie on the slit.

The second and better method is the use of a vertical arc, projected upon the slit of the spectrograph by means of the ordinary quartz image-lens *and a reversing prism*, this latter being placed close in front of the slit. In this manner the image of the arc on the jaws of the slit lies at right angles to the slit; the image of neither pole lies on the slit; so that when the arc is maintained at constant length, the only effect, if any, which one gets, on surrounding the arc with hydrogen, is that due to hydrogen alone. Any pole-effect is

thus eliminated. The spectra of Zn, Cu, Cd, Mg, Al, and C, between λ 5000 and λ 3700 have recently been photographed in this manner ; and by use of the first method, where no glass is involved, the same spectra have been photographed between λ 5000 and λ 2200.

4. The purpose of this note is to describe a few typical spectral appearances which do *not* seem to be pole-effects.

The Spectrum of Magnesium.

Here the widening of the reversal does not always appear to be a pole-effect. This is notably true of the singlet λ 2852, where the width of reversal at the pole, in air, is approximately *one* Ångström unit, while in hydrogen it is more nearly *five* Ångströms in width. The singlet at λ 4571 is, on the contrary, quite unaffected by hydrogen.

The diffuse triplets at $\lambda\left\{\begin{matrix}2851{\cdot}6\\2848{\cdot}4\\2846{\cdot}7\end{matrix}\right\}$ and $\lambda\left\{\begin{matrix}2736{\cdot}5\\2733{\cdot}5\\2732{\cdot}0\end{matrix}\right\}$ are practically blotted out in hydrogen ; while the sharp triplet $\lambda\left\{\begin{matrix}2942{\cdot}1\\2938{\cdot}5\\2936{\cdot}8\end{matrix}\right\}$ is greatly weakened. The copper impurities at $\lambda\left\{\begin{matrix}3273{\cdot}964\\3247{\cdot}548\end{matrix}\right\}$ are relatively much weakened, but are still visible in hydrogen, in spite of the fact that each shows a distinct increase of intensity near the pole, in both the long and the short air arc. The calcium impurity at $\lambda\left\{\begin{matrix}3968{\cdot}475\\3953{\cdot}670\end{matrix}\right\}$ is weakened just as the copper ; but the aluminium pair $\lambda\left\{\begin{matrix}3961{\cdot}537\\3944{\cdot}670\end{matrix}\right\}$ is practically unchanged in passing from air to hydrogen.

The Spectrum of Zinc.

The singlet, λ 4298·4, is practically blotted out by hydrogen. The ubiquitous copper impurities $\lambda\left\{\begin{matrix}3273{\cdot}9\\3247{\cdot}5\end{matrix}\right\}$ are here also reduced to a mere trace of what they are in air. So also is the diffuse singlet, at λ 4629·8. But the triplet of the sharp series $\lambda\left\{\begin{matrix}4810{\cdot}5\\4722{\cdot}1\\4680{\cdot}2\end{matrix}\right\}$ is almost unaffected by hydrogen.

The Spectrum of Aluminium.

The outstanding difference between the aluminium arc in these two atmospheres is the appearance, in hydrogen, of a strong and open band with heads at λ 4241, λ 4259, λ 4353, of which no trace is found in air. This aluminium hydride band appears to have been first observed by Basquin *, studied by Eriksson and Hulthén †, and interpreted by Mulliken ‡.

As to impurities, the strong and almost omnipresent lead line at λ 4057·830 and the manganese lines at $\lambda\left\{\begin{matrix}4034{\cdot}489\\4033{\cdot}074\\4030{\cdot}760\end{matrix}\right\}$ come out very clearly in hydrogen, while they are barely visible in air. The diffuse zinc triplet, at $\lambda\left\{\begin{matrix}3345{\cdot}\\3302{\cdot}\\3282{\cdot}\end{matrix}\right\}$, is also brought out in hydrogen; while the merest trace of it appears in air. In contrast with this, the unfailing copper impurity at $\lambda\left\{\begin{matrix}3273{\cdot}964\\3247{\cdot}548\end{matrix}\right\}$ is equally strong in air and in hydrogen.

The Spectrum of Cadmium.

The only striking change in passing from air to hydrogen is the introduction of an enormous number of impurity lines between λ 5000 and λ 3200. Curiously enough, the lead line at λ 4057·8 comes out clearly in air while no identification of it is easily made among the multitude of foreign lines which record themselves in hydrogen. This behaviour of the lead line, it will be observed, is just the reverse of what happens in the aluminium arc.

The Spectrum of Carbon.

Here the only thing which one might not easily predict is the appearance of a fluting with a head at λ 4312, and extending towards the shorter wave-lengths. Other less pronounced bands are introduced in the neighbourhood of λ 3142 and λ 3155. Again, the hydrogen atmosphere blots

* Astrophys. Journ. xiv. p. 8 (1901).
† *Zeits. f. Physik*, xxxiv. p. 775 (1925).
‡ Phys. Rev. xxviii. p. 1207 (1926).

out many impurities, such as Fe $\left\{\begin{matrix}3440{\cdot}991\\3440{\cdot}612\end{matrix}\right\}$ and Si, 2881·587, while it intensifies the carbon spark line at λ 2478·6 and brings out strongly H_β and H_γ.

5. It is not unlikely that, if electrodes different from the few mentioned above were used, a hydrogen atmosphere would produce other spectral changes worthy of study. Just how a cause so gentle and feeble as a change of atmosphere around a storm-centre such as an electric arc carrying several amperes at ordinary barometric pressure can produce such marked alterations in the spectrum, is not easy to understand.

If one accepts the Bohr theory of radiation one is confronted with the problem of explaining how a hydrogen atmosphere can affect the ionization of the atom and how it can change the programme of an electron in falling back through various levels. Professor W. F. G. Swann has suggested that, since the molecule of hydrogen gas has a root-mean-square speed four times as great as that of oxygen or nitrogen, the number of collisions in a mixture of hydrogen and metallic vapour must be greater than in air; and hence the probability of certain electron-jumps may be increased, thus increasing the intensity of certain lines. It has also been suggested by Professor W. R. Ham that the reason copper impurities are weakened in hydrogen is that the "work function" for the positive copper ion is greater in an atmosphere of hydrogen than in an atmosphere of air; but just how this can come about is not clear. The striking temperature effects which Langmuir * obtained by directing a jet of hydrogen from a small tube into an electric arc leads one to think that a hydrogen atmosphere may not perhaps be such a mild agent as one may at first imagine it.

The conclusion of this note is, then, the description of certain phenomena which are introduced by an atmosphere of hydrogen, but which do not appear to be explicable as "pole-effects."

Northwestern University,
Evanston, Illinois.
September 3rd, 1928.

* 'Science,' lxii. pp. 463–464 (1925).

XXXIV. *On the Hydrolytic Adsorption by Humic Acid.* By Ashutosh Ganguli, *Lecturer in Chemistry, Serampore College, Bengal* *.

MICHAELIS and Rona †, in their classical work on the adsorption of electrolytes by blood charcoal, have estimated the adsorption of cations as well as anions, and found a regular order for these. During recent years Mukherjee and his co-workers ‡ have investigated a certain class of substances which liberate free acid when shaken with neutral solutions of electrolytes. This phenomenon is now known as hydrolytic adsorption.

According to Freundlich § the adsorbents which adsorb electrolytes polarly are probably amorphous solid electrolytes with one sluggish ion and one mobile ion. The more strongly adsorbed ion has a tendency to go to the interface and drags along with it the more weakly adsorbable ion in part to the interface, while the latter ion holds back the former in the solution ‖ ; thus an equilibrium is set up. In some cases, however, the ionic adsorption is accompanied by exchange-adsorption or hydrolytic decomposition.

Recently, in 1922, Mukherjee ¶ extended the electrical theory of adsorption of Freundlich, and explained the general nature of hydrolytic adsorption. According to him a particular ion penetrates the interface and enters within the double layer, forming a heavy "sluggish" ion, while the opposite ion is held by electrical attractive force in the mobile sheet of the double-layer. This mobile ion, if it happens to be an anion, can be exchanged for (OH) obtained from the dissociation of water, and pass into solution in the free state, thereby causing the liberation of acid. Thus the ionization of water into $H^{\cdot}$ and $(OH)'$ and the exchange of ions go on until equilibrium is attained, when all the ions in the mobile sheets have been replaced by H or $(OH)'$. Joseph and Hancock **, on the other hand, believe that the liberation of acids by shaking electrolytes with substances like silica is entirely chemical in nature, due to the formation

* Communicated by Prof. K. C. Kar.

† *Biochem. Zeitschrift*, xciv. p. 240 (1914).

‡ Journal of Ind. Chem. Soc. i. p. 191 (1925) ; *ibid.* iii. p. 371 (1926) ; *ibid.* iv. p. 458 (1827) ; J. C. S. cxxiii. pp. 2205, 3023 (1926) ; also Miller, Journ. Am. Chem. Soc. xlvi. p. 1150 (1924) ; Bartell & Miller, *ibid.* lxv. p. 1106 (1923).

§ 'Kapillarchemie' (Eng. Edn.), p. 207.

‖ *Ibid.* p. 212.

¶ Phil. Mag. xliv. (6) p. 330 (1922) ; *loc. cit.*

** J. C. S. cxxiii. p. 2022 (1923).

of insoluble silicates. In a recent paper * on the hydrolytic adsorption by chemically pure silica, Mukherjee and his co-worker have contradicted this view. Again, in a more recent paper Hahn † points out the existence of a relationship beween the adsorption of a radio element by a polar precipitate and the electric charge at the surface, and thus confirms the contention of Mukherjee.

"The adsorptive properties of humin for substances in solution is of great importance in agriculture" ‡. Russell § points out that neutral solutions of salts like KCl, if treated with samples of soils, give acid extract, though the extract with pure water is neutral. It has been suggested by Mukherjee || that the acidity of soils can be explained in the light of hydrolytic adsorption. Recently Kawamura ¶ performed some experiments with the synthetic humic acid. The present work has been undertaken in order to examine the nature of hydrolytic adsorption by humic acid, and thus explain the acidity of soils.

Experimental.

Kahlbaum's pure sample of humic acid was analysed, and was subsequently used in the following experiments:—1 gm of humic acid was taken in a Jena bottle and shaken in a mechanical shaker with 100 c.c. standard solutions of the electrolytes at different concentrations. This was allowed to stand for two or three days. The clear supernatant liquid was then transferred by means of a pipette in a well-cleaned dry hydrogen cell, and a very slow current of hydrogen was bubbled through it for more than two hours. The e.m.f. of this was determined against a normal calomel electrode by means of a K-type potentiometer (Leeds & Northrup). The concentration of hydrogen-ion C_H was calculated from the well-known equation

$$E = e_0 + \frac{RT}{nF} \log \frac{c_1}{c_2}$$

or

$$E - e_0 = \frac{RT}{nF} \log \frac{1}{C_H} = \cdot 059\ P_H.$$

e_0 is the absolute value of the electrolytic potential of

* *Loc. cit.*
† *Ber.* lix. p. 2014 (1926).
‡ 'A Manual of Agricultural Chemistry' (Ingle).
§ British Assoc. Report, p. 70 (1918).
|| *Loc. cit.*
¶ Journ. Phys. Chem. xxx. p. 1564 (1926).

hydrogen measured against "normal" calomel electrode, E is the observed e.m.f., and $P_H = \log \frac{1}{C_H}$, where C_H = concentration of H-ion.

TABLE I.

1 gm. of Humic acid 100 c.c. NaCl solution.

T = 28·5.

Concentration of NaCl gm.-equivalents per litre.	P_H.	$C_H 10^{-4}$.
1·00	3·35	4·467
0·5	3·42	3·802
0·25	3·51	3·090
0·1	3·62	2·399
0·000	4·56	0·2754

TABLE II.

1 gm. of Humic acid in c.c. KCl solution.

T = 35° C.

Concentration of KCl gm.-equivalents per litre.	P_H.	$C_H 10^{-4}$.
2·00	2·19	64·57
1·00	2·799	15·89
0·50	3·06	8·710
0·25	3·19	6·457
0·100	3·61	2·455
0·025	4·05	0·8913
0·005	4·48	0·3311
0·000	4·56	0·2754

TABLE III.

1 gm. of Humic acid in 100 c.c. $BaCl_2$ solution.

T = 35° C.

Concentration of $BaCl_2$ gm.-equivalent per litre.	P_H.	$C_H 10^{-4}$.
1·000	2·64	22·91
0·500	3·00	10·00
0·100	3·02	9·55
0·050	3·21	6·166
0·025	3·23	5·188
0·010	3·41	3·890
0·005	3·6	2·512
0·000	4·56	0·2754

TABLE IV.

1 gm. of Humic acid in 100 c.c. $AlCl_3$ solution.
T = 35° C.

Concentration of $AlCl_3$ gm.-equivalent per litre.	P_H.	$C_H 10^{-4}$.
1·000	2·28	52·48
0·500	2·28	52·48
0·250	2·33	46·77
0·100	2·66	21·88
0·050	2·66	21·88
0·025	2·77	16·98
0·010	2·95	11·22
0·000	4·56	0·2754

TABLE V.

1 gm. of Humic acid in 100 c.c. K_2SO_4.
T = 35° C.

Concentration of K_2SO_4 gm.-equivalent per litre.	P_H.	$C_H 10^{-4}$.
1·000	4·00	1·000
0·500	3·73	1·862
0·250	3·99	1·023
0·100	4·00	1·000
0·050	3·83	1·479
0·025	3·93	1·175
0·010	4·02	0·9550
0·000	4·56	0·2754

TABLE VI.

1 gm. of Humic acid in 100 c.c. of normal solutions of various electrolytes.

	Water.	NaCl.	KCl.	$BaCl_2$.	$AlCl_3$.	K_2SO_4
P_H	4·56	3·35	2·799	2·64	2·28	4·00
$C_H 10^{-4}$ ...	0·2754	4·467	15·89	22·91	52·48	1·00

Discussion of Results.

From the foregoing tables it will be observed that the concentration of hydrogen ion, and hence the amount of free acid liberated, varies directly with the concentration of the electrolyte. As has been observed in the introduction, the liberation of the free acid is due to the adsorption of cations by the humic acid particles to form a complex electrolyte. Thus the cation is fixed within the double layer, whereas the anion, which is held by electrical attraction in

the mobile sheet, is very readily exchanged by the more negative $(OH)'$. Hence the concentration of hydrogen ion is a measure of the primary adsorption of the cations. Now, as it is a function of the concentration of the electrolyte (the mass of humic acid taken being kept constant in each case), it obeys the adsorption law

$$a = \alpha C^{\frac{1}{n}},$$

where a is the amount adsorbed by unit mass of adsorbent, α and n are constant, and C is the concentration of the solution.

The effect of the valency is also marked, and we get a regular order for cations with common anion

$$Al > Ba > K > Na,$$

and again for anions

$$Cl < SO_4^2.$$

The above orders were also obtained by Michaelis and Rona *, and the same thing was postulated by Freundlich †. From theoretical considerations, Mukherjee ‡ indicated that the increase of charge of the adsorbent in contact with electrolytes also takes place according to the same orders.

Thus the liberation of acids from natural salts, when shaken with humic acid, can only be accounted for as due to hydrolytic adsorption, and not to the formation of any chemical compounds. The reaction can be represented thus:

$$\text{Humic acid} + KCl + nH_2O = [\text{Humic acid}, nH_2O \,.\, K]Cl,$$

$$[\text{Humic acid}, n(H_2O)K]Cl + H + OH' \rightleftharpoons [\text{Humic acid}\ nH_2O, K]OH' + HCl,$$

resembling somewhat Warner's complex compounds.

Summary.

(1) Experiments on adsorption of electrolytes by humic acid were performed, and concentration of hydrogen ion was determined, by electrometric method.

(2) It was observed that free acid was liberated in each case, the concentration of the H-ion being a function of the concentration of electrolyte and the nature of the electrolyte taken. A regular order was found.

(3) The acidity of soils has been explained as due to the hydrolytic adsorption of electrolytes by humic acid, which is an essential constituent of soils.

* *Loc. cit.* † *Loc. cit.* ‡ *Loc. cit.*

My best thanks are due to Dr. J. N. Mukherjee, D.Sc. (Lond.), for his kind help and keen interest in the work. My thanks are also due to Dr. K. C. Kar, D.Sc., for communicating this paper.

Physical Chemistry Laboratory,
University College of Science
and Technology, Calcutta.

XXXV. *The Spectral Phenomena of Spark Discharges.* *By* William Clarkson, *Ph.D., M.Sc., International Education Board Fellow, Physical Institute of the University of Utrecht* *.

SINCE the detailed phenomena and problems of spark discharges are so complicated, it is perhaps not generally known that their principal properties, both electrical and spectral, are quite simply derivable from a few known general principles. These are outlined in Part I. of this paper, where it is shown, by the close correlation between the derived and the observed data, that the scheme described accounts quite satisfactorily for the experimental facts.

The ideas put forward are then applied, in Part II., to the quantitative variations of the spectral intensities in the simplest spark discharge, the single-condenser discharge, and it is shown that the unexpected complexities here revealed are but accidental, and that the true form of these variations is as theoretical considerations would demand.

Part I. Oscillating Spark Discharge.

1. *Phenomena.*

The following is a summary of the characteristic phenomena of spark discharges as revealed by the work of Schuster [1], Hemsalech [2], Schenck [3], Milner [4], and Royd [5], an outline of which may be found in Baly's 'Spectroscopy,' vol. ii. pp. 153–157. Their analysis by rotating mirrors or films, for various inductances, proved that associated with the several distinct stages of the oscillating spark, viz. the initial flash, the oscillations and streamers, and the afterglow, were characteristic optical phenomena. Cataloguing these we have :—

A. *Initial Spark or Flash.*—1. Intense, narrow, instantaneous. 2. Followed by one or two weaker ones at half-

* Communicated by Professor Ornstein.

period intervals. 3. Weakened and finally eliminated by inductance (of course, here as later this latter may only mean, reduced below the threshold intensity for observation). 4. Exhibits air lines and, if intense, metal spark lines.

B. *Oscillations.*—1. Voltage initially at glow values (300–400 volts), falls rapidly to arc values (30–40 volts), and then changes but little for a much longer time, during which the current attains its maximum value [4], [5]; except when, 2. period of oscillation long, when voltage throughout near arc values [6]. 3. Exhibit streamers, puffs of space-charge (possibly from both poles) at each period. Velocity of particles in streamers diminishes rapidly from poles.

C. *Anomalies.*—Royd's [5] results for: A. 2. The flash followed directly by a weak one and a streamer. A. 3. The inductance has no influence. B 3. Several small puffs in each oscillation.

D. *Spectral Types.*—1. Continuous spectrum is brief. 2. In zinc and cadmium spark, hazy lines near poles seen, soon eliminated by inductance. 3. Spark lines. Strong in spark, appear in streamers, but progressively weaker and some only in first few. Generally confined to poles. If right over gap are weak in middle. 4. Arc lines. Throughout oscillations. Begin in middle of gap, spread, and persist through afterglow where very prominent.

E. *Effect of Inductance.*—1. Air lines disappearance. 2. Lines in general narrowed [2]. 3. When period great: *a.* arc lines extend over gap, and *b.* spark lines approach poles and some disappear, *i. e.* spectrum approaches arc type.

In the scheme now given, in which the electrical phenomena are derived in a form *a.* explaining the electrical and visual properties, and *b.* permitting the spectral properties to be inferred, the essential outlines will be attempted: details of many phenomena fall beyond the scope of such a treatment, and would demand separate investigation.

2. *Factors determining Optical Properties.*

To derive the spectral properties of a discharge, we require to know the intensity and the quality of the light throughout its course. The electrical factors determining these are well known; the chief are reviewed here.

The general intensity increases with the current. The metal spectra will replace those of the gas when much vapour is present. For this a certain heating of the electrodes is first necessary. There is a steady transition from spectra of lower to those of higher energetic states with increase of the

field, *e. g.*, increase of the potential fall, and hence the average velocity, per electronic mean free path, and of the relative ionization or increase of higher energetic states (this varies with the current density). These latter factors also tend to broaden the lines through Stark and temperature effects; these greatly transcend those of self-reversal.

3. *Dynamic Characteristics.* (See Ref. 7.)

From these it is possible to derive the electrical properties of the various phases of an oscillating spark; the development will be from the simplest to the most complex phenomena.

Fig. 1.

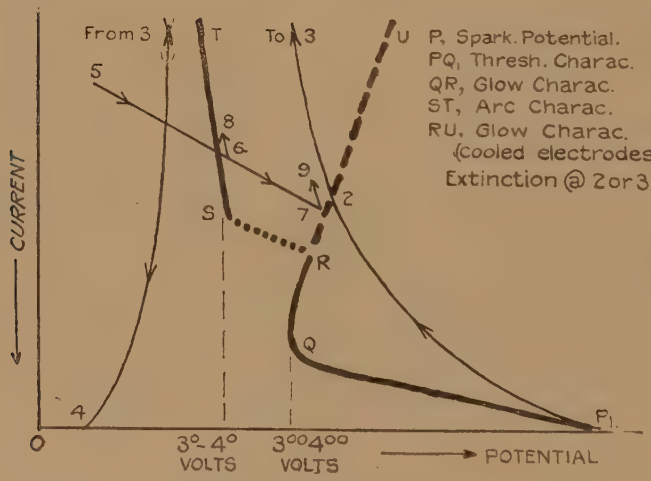

A. *Dynamic Critical Constants.*—Any stage in a discharge may be represented by a point on the appropriate voltage-current diagram (fig. 1). The significance of the static characteristic (PQRST) is that at any current it is the boundary between current-increase (build-up) for voltages higher and current-decrease (clear-up) for voltages lower than the one it exhibits. It determines when and where "striking" and "extinction" occur. OVERLOW

It should be noted in this connexion that, strictly speaking, energetic states and their distribution, not merely current, are the criteria, and that (though no change in principle is implied) the "characteristic" will be the virtual one these determine.

B. *Current Relations.*—The rate of multiplication of ions varies with the potential and thus the build-up and clear-up currents at any instant, which show a somewhat exponential variation with time, depend on the voltage-time relations. The current is a maximum at extinction.

These considerations are illustrated in the simple condenser discharge. *Simple Spark or Flash.* Striking at or beyond P. Voltage falling, roughly exponentially. Resultant characteristic 1, 2, 3 ; 2 may be anywhere on the static characteristic, but in sparks is generally on the arc stage. The duration of the flash depends on the tube constants and the size of the capacity.

Fig. 2.

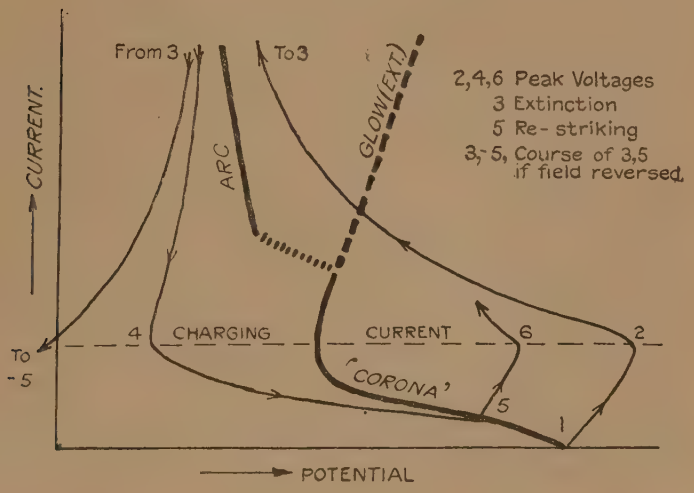

C. *With Charging Current.*—The greater the charging current the greater the period at the beginning and end of the discharge in which the charging current will exceed the discharging current, and the greater the voltages attained over the otherwise initial and final ones. Also there is a possibility of re-striking during clear-up. Thus, for example, we have *Modified Flash* (fig. 2). Track 1, 2, 3, 4, 5, 6. Peak voltages at 2, 4, 6. A final steady discharge at the value of the charging current may result (flash-steady discharge). Duration as in simple spark.

D. *Inductive Oscillations.*—Several complications are introduced through these.

(*a*) Reversal of Field.—A double characteristic must be

considered. Previous considerations will apply, however, so long as the electrodes are in a similar state.

(*b*) Unsymmetrical Characteristics.—The foregoing fails in the case of reversal for arc discharges, since, then, two characteristics are possible, depending on whether or not the electrodes will be vaporized, *i.e.* whether the electrodes are "hot" or "cold." The former gives the arc (30–40 volts), the later the glow (300–400 volts), characteristic despite the high current and metallic vapour. Even though only merely local heating, or a thermal layer, is necessary for vaporization, there seems no likelihood of this occurring during clear-up, where space-charge is dissipated, not created. The problem is illustrated in fig. 1. QRU is the glow characteristic for cooled electrodes, *i.e.* no metallic vaporization. Extinction may occur at 2 (electrode "cold"; this is the rule at low pressures) or at 3 (electrode vaporized; this is usual at high pressures with high current densities). 5, 6, 7 is a clear-up track from the arc stage in an oscillating field. Re-striking may take place at 6 (electrode "hot"), with resultant 6, 8, or at 7 (electrode "cold"), with resultant 7, 9.

(*c*) Damping.—The effect of introducing inductive windings is greatly to modify the discharge tracks through *a.* resistance—even a small resistance implies a considerable potential fall at high currents; and *b.* induction—the more rapid the build-up the greater the absorption of potential. Both sources will operate to accelerate the initial fall of potential in build-up. They also affect extinction.

Oscillating Spark.—As in fig. 2, but with successive strikings and extinctions on the positive and the negative voltage characteristics. For instance, after extinction, 3–5, not 3–4, occurs. Tracks much more angular than previously. Period of system the time-basis.

4. *Comparison of Results.*

In the running commentary here given, in which the observed and the inferred properties of the oscillating spark are compared and discussed, the fact that the dynamic discharges exhibit properties similar to those of related static discharges is tacitly assumed. Following the initial arrangement we have :—

A. *Initial Flash.*—1. At high pressure the glow-discharge is an intense narrow thread. The spark shows this form as its short duration is offset by its great intensity. Due to high voltages the build-up is very rapid and the duration

short. 2. Should succeeding re-striking occur on the threshold current characteristic, the first oscillations will be represented by progressively weaker flashes (or flash-steady discharges). 3. Increasing the inductance causes progressive damping-out of the flashes (to be seen in oscillograms)[6]. In the limit the condenser may become so choked that a flash is impossible. 4. The average voltage in the flash is high and the current densities (see A. 1) great; thus spark lines of the gas will be excited. Milner[4] suggests that in sparks, not the area but the current-density, to the limit of total ionization, increases with the current. The local heating, or thermal layer, may be intense enough to vaporize the metal (even pure sparks may show not only a strong metallic spectrum, but also an intense afterglow of metallic vapour)[7]. The vapour will first be noticeable at the poles. The fields and glows are strong there; hence strong local spark lines (see C. 3). The fields determine that the velocity of propagation of the zone of metallic vapour will fall off rapidly from the poles.

B. *Oscillations.*—1. This effect was discussed previously. It is impossible to say, however, whether the currents on re-striking actually do correspond to the extended glow characteristic, as the oscillograms are not detailed enough; certainly reversal and passing through zero of the voltage implies lower voltages and much more rapid clear-up than usual. The transition from extinction on the extended glow (as indicated by the currents attained), to extinction on the arc characteristic, is clearly seen in single-condenser discharges. It would appear, as we should expect, to be continuous. 2. With long periods the heating will be greater; thus the electrodes may remain "hot." 3. The puffs certainly represent dissipation of electrode glows. This is well seen in discharge-tubes[7]. It conceivably could occur any time after re-striking on the glow characteristic (as in fig. 1 : 6, 8), *i. e.*, even during the discharge, and represent distribution of ions and electrons by pressure, diffusion, or electrical effects.

C. *Anomalies.*—These are quite consistent with the foregoing on the supposition of the action of a small independent capacity (say that of the gap) and extreme damping of the main condenser. Thus within each main period would appear small capacity phenomena:—A 2. First period could be flash, flash, steady, as in fig. 2. A 3. The influence of the inductance on the flashes would be inappreciable. B 3. Secondary oscillations and puffs; this rather supports the above arguments on puffs during build-up.

D. *Spectral Types.*—1. The fields and activation are considerably greater than in the arc, where the continuous spectrum is not always obtrusive. 2 (see also A. 4). These almost certainly represent double ionization in the intense glows and fields at the electrodes, where also Stark and temperature effects will be extreme. These conditions will be removed by quite small damping. 3. The probability of high current densities and high fields, and thus the excitation of spectra of high order, decreases with the order of the oscillation. The most extreme conditions are at the poles. (Weak sparks often show conspicuous weakness in the middle.) 4. With the order of the oscillation the arc lines will show a progressive ascendency over the spark ones. The after-glow is low voltage.

E. *Effects of Inductance.*—The choking-out of the flash implies: 1. Weakening or even elimination of the gas spectrum, and 2. Corresponding reduction of Stark and temperature effects (Milner [4] records appreciable weakening of the core of the spark with inductance). 3. Limits, fields, and current densities also throughout the oscillations, so that, though this progressive limiting of "spark conditions" to the poles does not necessarily imply a weakening of the spark spectrum, the arc spectrum will be relatively as well as actually intensified.

5. *Conclusion.*

This excellent agreement here demonstrated justifies the opinion that the scheme developed embodies the essential principles for the appreciation of the properties of spark discharges, and that it is in a form convenient for practical purposes.

Further, it shows that the properties of oscillating spark discharges are too indefinite to permit of their spectral qualities having more than a somewhat uncertain qualitative significance. Where condensed sparks must be employed, they should take the form of a single-condenser discharge, in which alone the conditions are at all definable. In this connexion it would appear that probably a much more satisfactory and efficient source of spark spectra would be provided by the final stages of a flash. An intensified form of this could easily be reproduced by the discharge of a large condenser at as high a voltage as possible (say system of maximum energy) through an intense arc discharge, with exposure only at this instant. Gas and line-broadening effects should be small.

Part II. Intensity Relations in Single-Condenser Sparks.

1. *Introduction.*

As suggested, the flash presents interesting possibilities for quantitative work on the excitation of spectra and their variation with current and voltage. The paper of Prof. Ornstein and H. P. Bouwman [8] records the variation of the intensities of the arc and spark lines for the capillary of a helium Geissler tube, for single-condenser discharges, with initial voltage. The tube was in series with a spark-gap. Oscillations did not occur.

Fig. 3.

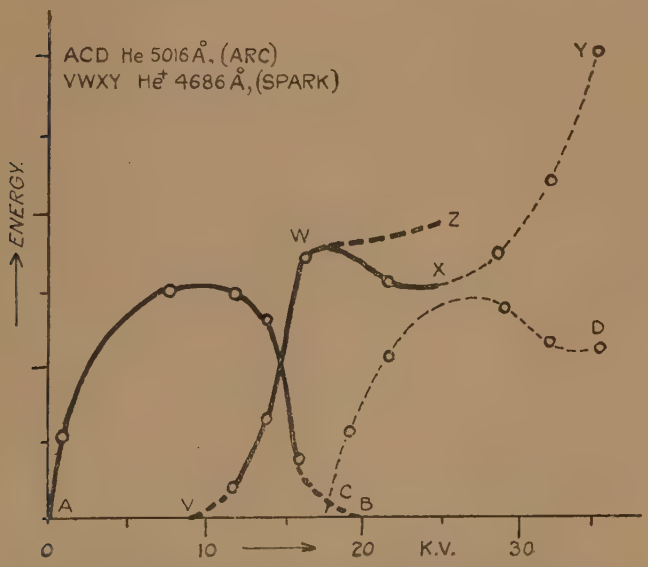

Fig. 3 expresses the results graphically : strong spark line VWXY, arc line ACD. Other lines showed exactly similar variations.

2. *Discussion.*

As far as AW the results are as we should expect, from the continuous increase in the energy of the spark and in the relative proportion of higher activation. (These latter will not be conspicuous at first, but later will bring about a rapid ascendency of spark over arc lines.) The steepness of XY after the kink in the spark curve at WX, and particularly the resurgence of the arc lines at CD, present

phenomena quite inexplicable theoretically. On seeking experimental grounds, duplication of flashes immediately suggests itself. We have :—

(*a*) The curve CD presents the same form as AC (the correspondence is remarkable).

(*b*) The spark curve can be resolved into similar components, and VW is to AB as XY is to CD (though the exact form of the curves at Y and D are uncertain) ; further, V and X correspond to their respective maxima.

(*c*) Though the energy which must be attributed to the secondary flash is too large to be derived from the charging current, it could come from this source, aided largely by the recovery of charge from the dielectric medium of the condenser.

Thus, so far, the explanation is most satisfactory, and we may proceed to examine the true experimental curves as far as valid, *i. e.* AB and VWX. CD and XY must be rejected. Due to the system employed in the estimation of the number of flashes, all points beyond C must be elevated by an amount proportional to the energy lost in the secondary flash. We may determine this roughly from a comparison of AB and CD. The corrected curve WZ results. No correction need be applied for the energy lost in soaking-in effects, as these will vary continuously with the initial voltage. At A, V, and B the curves are only probable ones, as the energy falls below the minimum for observation.

Two points call for comment : (*a*) the abrupt strengthening of the spark lines at V, and (*b*) the unexpected kink in the spark curve at W :—

(*a*) This is to be expected. It probably indicates a stage where the voltage-fall per electronic mean free path approaches a critical value for spark line excitation. On the other hand, a second cause may lie in the fact that the proportion of excited states increases explosively at the high current densities attained in sparks.

(*b*) This apparent anomaly really supports the explanation. Its occurrence is found to be associated with the first appearance of a many-lined spectrum, which would appear not to be due to metal from the glass on the electrodes. The excitation of the band spectrum of the gas would correspond to the striking of a discharge when the gas was in an active state : the very condition postulated in the foregoing treatment.

It is a pity, of course, that as yet we cannot sum the energies represented by the various spectra and check them with the total energy of the spark.

The writer has great pleasure in expressing his obligation to Prof. Ornstein in this work, and his indebtedness to the International Education Board.

Summary.

Part I.—1. A résumé is given of the electrical and optical properties of spark discharges.

2. The factors determining the optical properties of discharges are discussed.

3. The discharge phases and the current-time-voltage relations in an oscillating spark derived from general principles of discharges as schematized in dynamic characteristics.

4. It is shown that the observed phenomena and those derived from 2. and 3. are in excellent agreement. The scheme outlined, though simple, thus constitutes an adequate basis for the appreciation of spark phenomena. The production of spark spectra is discussed.

Part II.—1. The curves for the variation of the intensity of the arc and spark lines of helium (in a spark) with initial condenser voltage is given.

2. The double maximum in the arc intensities is explained by duplication of flashes. This implies some correction of the results.

3. The subsequent falling-off of spark intensities is attributed to diversion of energy into other spectra.

4. The true curve is established, and is shown to be in agreement with theoretical considerations.

References.

(1) Schuster and Hemsalech, Phil. Trans. cxciii. p. 189 (1900).
(2) Hemsalech, *Comptes Rendus*, cxii. p. 285 (1899); cxl. p. 1103 (1905); cxli. p. 1227 (1905).
(3) Schenck, Ap. J. xiv. p. 116 (1901).
(4) Milner, Phil. Trans. ccix. p. 71 (1908); Phil. Mag. xxiv. p. 713 (1912).
(5) Royd, Phil. Trans. ccviii. p. 333 (1908); Phil. Mag. xix. p. 285 (1910).
(6) Roschansky, *Ann. d. Phys.* xxxvii. p. 281 (1910).
(7) Clarkson, Phil. Mag. iv. pp. 849, 1102, and 1341 (1927).
(8) Ornstein and Bouwman, *Zeit. f. Phys.* xliii. p. 839 (1927).

XXXVI. *Note on the Method of Ritz for the Solution of Problems in Elasticity.* *By* Prof. G. R. Goldsbrough, *D.Sc., Armstrong College, Newcastle-on-Tyne* *.

§ 1. *Introduction.*

An analytical method was devised in 1909 by W. Ritz † for the solution of certain intractable problems in elasticity. In particular, he applied it to the problem of the deflexion of a thin, elastic, rectangular plate, clamped at the edges and bent by pressure applied to one of its faces ‡, and also to the problem of the flexural vibrations of a free rectangular plate §. Since that date the method has been applied to many similar problems ‖, while at the same time Ritz's original problem of the deflexion of the rectangular plate has been solved by other methods ¶.

A device used by the writer in solving certain tidal problems ** is also applicable in solving Ritz's elastic problems, and the purpose of this note is to show that the two processes produce exactly the same solution.

A difficulty that has always been felt with regard to Ritz's solution is that the final series deduced by him does not, term by term, satisfy the fundamental differential equation governing the problem, though he was able to prove that the function represented by the series would satisfy that equation. This point has some light thrown upon it by the comparison of the two methods in the present paper.

The original problem discussed by Ritz will now be examined. A very brief outline of Ritz's process will be given, and then the second method of solution will be worked out in full, and the results compared. It will be noted that Ritz's method is much longer and more complex than that of the writer.

* Communicated by the Author.

† *J. f. Math.* Bd. cxxxv. p. 1, and 'Gesammelte Werke,' p. 192.

‡ Ges. Werke, p. 223.

§ *Ibid.* p. 265.

‖ Timoschenko, Lond. Math. Proc. (ser. 2) xx. pp. 389 & 398 (1922).

¶ See Love, 'Elasticity,' 4th ed. p. 494, and Journ. Lond. Math. Soc. iii. pt. 2, p. 144.

** Proc. Roy. Soc. A, cxvii. p. 692 (1928).

§ 2. *Ritz's Method for the Deflexion of a Thin Rectangular Plate due to Normal Loading.*

Let the rectangular plate have dimensions a, b, and let p be the pressure-intensiy at the point (xy) referred to an origin at one corner of the plate. The equation to be satisfied * is

$$\frac{\partial^4 w}{\partial x^4} + 2\frac{\partial^4 w}{\partial x^2 \partial y^2} + \frac{\partial^4 w}{\partial y^4} = p/\mathrm{D}. \quad . \quad . \quad . \quad (1)$$

Further, since the plate is to be clamped at the edges, the additional conditions to be fulfilled by w are

$$\left.\begin{aligned} w &= 0 \\ \frac{\partial w}{\partial x} &= 0 \end{aligned}\right\} \text{ at } x=0,\ a\ ; \qquad \left.\begin{aligned} w &= 0 \\ \frac{\partial w}{\partial y} &= 0 \end{aligned}\right\} \text{ at } y=0,\ b. \quad (2)$$

In place of equation (1), Ritz considered the integral

$$\iint \left\{ \frac{1}{2}\left(\frac{\partial^2 w}{\partial x^2} + \frac{\partial^2 w}{\partial y^2}\right)^2 - pw/\mathrm{D} \right\} dx\, dy \quad . \quad . \quad (3)$$

taken over the rectangular plate.

The connexion between (3) and (1) lies in the fact that (1) is the condition that (3) shall have a stationary value.

Ritz now assumed for w a finite double series in the form

$$w = \sum_{m=1}^{\mathrm{M}} \sum_{n=1}^{\mathrm{N}} a_{mn} \xi_m(x/a) \xi_n(y/b). \quad . \quad . \quad . \quad (4)$$

The functions ξ are normal functions, and have the additional property that each, with its first observation, vanishes at 0 and a, b respectively. The form of the functions ξ is decided by the one-dimensional case of the problem, the thin rod clamped at each end. In the latter case the equation † to be solved is

$$\frac{d^4 u}{dx^4} = \left(\frac{\kappa}{a}\right)^4 u, \quad . \quad . \quad . \quad . \quad . \quad . \quad (5)$$

with the conditions $u=0$, $\dfrac{du}{dx} = 0$ at $x = 0, a$. Such a function ‡ is

$$\xi_n(x/a) = \cos \kappa_n x/a - \cosh \kappa_n x/a - (\sin \kappa_n x/a - \sinh \kappa_n x/a) \frac{\cos \kappa_n - \cosh \kappa_n}{\sin \kappa_n - \sinh \kappa_n}, \quad . \quad (6)$$

* Love, 'Elasticity,' p. 488.
† Rayleigh, 'Sound,' p. 261.
‡ *Ibid.* p. 273.

where κ_n is a root of the equation

$$\cos\kappa\cosh\kappa=1. \quad . \quad . \quad . \quad . \quad . \quad . \quad (7)$$

The functions $\xi_n(x/a)$ possess the properties

$$\int_0^a \xi_n\xi_n\,dx=0, \quad m\neq n,$$

and

$$\int_0^a (\xi_n)^2\,dx=a.$$

Ritz has further shown * that if $f(x)$ is any function of x, which, together with its first, second, and third derivatives, is finite and continuous in the interval $0 \leq x \leq a$; and which has its fourth derivative finite and possessing a finite number of maxima and minima in the interval; then $f(x)$ may be expanded in the convergent series

$$a_1\xi_1(x/a)+a_2\xi_2(x/a)+\ldots+a_n\xi_n(x/a)+\ldots, \quad . \quad (8)$$

where

$$a_n=\frac{1}{a}\int_0^a f(x)\xi_n(x/a)\,dx.$$

By an extension of the same reasoning, it may be shown that, under corresponding restrictions,

$$f(x,y)=\sum_m\sum_n a_{mn}\xi_m(x/a)\xi_n(y/b), \quad . \quad . \quad . \quad (9)$$

where

$$a_{mn}=\frac{1}{ab}\int_0^b \xi_n(y/b)\,dy\int_0^a f(x,y)\xi_m(x/a)\,dx.$$

In this way, for instance, whether p is constant over the plate or not †, we may write

$$p/\mathrm{D}=\sum_m\sum_n f_{mn}\xi_m(x/a)\xi_n(y/b), \quad . \quad . \quad . \quad (10)$$

where

$$f_{mn}=\frac{1}{ab}\int_0^b\int_0^a \frac{p}{\mathrm{D}}\xi_m(x/a)\xi_n(y/b)\,dx\,dy.$$

In place of the infinite series (9), Ritz took as an approximation the corresponding finite series already quoted in (4). On substituting in (3) and performing the integrations, using the properties of the functions ξ, we find

* Ges. Werke, p. 225.

† Provided the above conditions are fulfilled

$$\int_0^a\int_0^b \left\{\frac{1}{2}\left(\frac{\partial^2 w}{\partial x^2}+\frac{\partial^2 w}{\partial y^2}\right)^2 - pw/\mathrm{D}\right\} dx\,dy$$

$$= \int_0^a\int_0^b \Big[\frac{1}{2}\sum_m\sum_n\sum_r\sum_s a_{mn}a_{rs}\Big\{\frac{1}{a^4}\xi_m''(x/a)\xi_n(y/b)\xi_r''(x/a)\xi_s(y/b)$$

$$+\frac{1}{b^4}\xi_m(x/a)\xi_n''(y/b)\xi_r(x/a)\xi_s''(y/b)$$

$$+\frac{2}{a^2b^2}\xi_m''(x/a)\xi_n(y/b)\xi_r(x/a)\xi_s''(y/b)\Big\}$$

$$-\frac{1}{ab}\sum_m\sum_n f_{mn}\xi_m(x/a)\xi_n(y/b)\sum_r\sum_s a_{rs}\xi_r(x/a)\xi_s(y/b)\Big]\,dx\,dy$$

$$= \sum_m\sum_n\frac{1}{2}a_{mn}{}^2\left(\frac{\kappa_m{}^4}{a^4}+\frac{\kappa_n{}^4}{b^4}\right)+2\sum_m\sum_n\sum_r\sum_s a_{mn}a_{rs}\frac{\sigma_{mr}\sigma_{sn}}{a^2b^2}$$

$$-\sum_m\sum_n\frac{1}{ab}f_{mn}a_{mn}, \quad . \quad . \quad . \quad . \quad . \quad . \quad . \quad . \quad . \quad (11)$$

where we have written

$$\sigma_{mr}=\sigma_{rm}=\frac{1}{a}\int_0^a \xi_m''(x/a)\xi_r(x/a)\,dx. \quad . \quad . \quad (12)$$

The condition that (11) should be stationary is

$$a_{mn}\left(\frac{\kappa_m{}^4}{a^4}+\frac{\kappa_n{}^4}{b^4}\right)+2\sum_r\sum_s a_{rs}\frac{\sigma_{mr}\sigma_{ns}}{a^2b^2}=\frac{1}{ab}f_{mn}. \quad . \quad (13)$$

The summations in (13) are from $r=1$ to M and from $s=1$ to N, and the equation holds good for $m=1$ to M and $n=1$ to N. The series of equations so formed can be solved to give the values of the finite series of coefficients a_{mn}.

Ritz then proceeds to extend the values of M, N to infinity, and shows that a convergent series completely representing the function w under the required conditions is evolved. This completes his solution of the problem *. It remains to show that his algebraic relation (13) between the coefficients can be obtained directly from the equations (1) with the conditions (2).

§ 3. *Alternative Method of solving the same Problem.*

By virtue of the result (9) we may at the outset assume that w may be expanded in the doubly-infinite series

$$w=\sum_m\sum_n a_{mn}\xi_m(x/a)\xi_n(y/b). \quad . \quad . \quad . \quad . \quad (14)$$

* We have adhered closely to Ritz's notation, and equation (13) corresponds, term for term, to his equation (45), Ges. Werke, p. 229.

From the form of the functions it is clear that each term of (14) satisfies the conditions (2) independently. The series does not, however, satisfy the equation (1) term by term. The method * referred to enables us to surmount the difficulty. If we assume that the requisite conditions for uniformity of convergence are satisfied, we may substitute (14) in the left number of (1). We find then

$$\frac{\partial^4 w}{\partial x^4} + 2\frac{\partial^4 w}{\partial x^2 \partial y^2} + \frac{\partial^4 w}{\partial y^4} - p/\mathrm{D}$$

$$= \sum_m \sum_n a_{mn} \left[\left\{ \left(\frac{\kappa_m}{a}\right)^4 + \left(\frac{\kappa_m}{b}\right)^4 \right\} \xi_m(x/a)\xi_n(y/b) \right.$$

$$\left. + \frac{2}{a^2 b^2} \xi_m''(x/a)\xi_n''(y/b) \right]$$

$$- \sum_m \sum_n \frac{1}{ab} f_{mn} \xi_m(x/a)\xi_n(y/b) \quad . \quad . \quad . \quad . \quad . \quad . \quad . \quad . \quad (15)$$

The right member of (15) should vanish for all values of x, y in the range. The coefficients a_{mn} can be suitably chosen to secure this result. The functions $\xi_m''(x/a)$, $\xi_n''(y/a)$, as they satisfy the required conditions, can be expanded, by (8), in the form

$$\left.\begin{aligned} \xi_m''(x/a) &= \sum_r \sigma_{mr} \xi_r(x/a), \\ \xi_n''(y/b) &= \sum_s \sigma_{ns} \xi_s(y/b), \end{aligned}\right\} \quad . \quad . \quad . \quad (16)$$

where σ has the value (12).

On substituting these results in (15), and equating to zero the coefficient of $\xi_m(x/a)\xi_n(y/b)$, we find the equation

$$a_{mn}\left(\frac{\kappa_n^4}{a^4} + \frac{\kappa_n^4}{b^4}\right) + 2\sum_r \sum_s a_{rs} \frac{\sigma_{mr}\sigma_{ns}}{a^2 b^2} = \frac{1}{ab} f_{mn}, \quad . \quad (17)$$

This is exactly the limiting form of Ritz's equation (13), which is there arrived at by his own method.

The last few steps explain clearly how Ritz's solution, though it does not satisfy the equation (1) term by term, yet does so ultimately.

Each process is now only concerned with the solution of the system of linear algebraic equations (17). In regard to this, Ritz's paper is complete.

* Proc. Roy. Soc. A, cxvii. p. 692 (1928).

§ 4. *The Vibrations of a Rectangular Plate clamped at the Edges.*

The process mentioned in the last paragraph gives a ready solution of the problem of the flexural vibrations of a thin rectangular plate clamped at the edges. Assuming simple harmonic vibrations of period $2\pi/\sigma$, the equation * to be solved in place of (1) is

$$\frac{\partial^4 w}{\partial x^4}+2\frac{\partial^4 w}{\partial x^2 \partial y^2}+\frac{\partial^4 w}{\partial y^4}-\lambda w=0, \quad . \quad . \quad . \quad (18)$$

together with the conditions (2) as before.

Assuming the expansion for w, as in (14) substituting and reducing by means of (12), the resulting algebraic expression is

$$a_{mn}\{(\kappa_m/a)^4+(\kappa_n/b)^4-\lambda\}+2\sum_r\sum_s a_{rs}\sigma_{rm}\sigma_{sn}/a^2b^2=0. \quad (19)$$

The equation (19) holds for all values of m, n, and represents a doubly-infinite series of equations each containing a doubly-infinite number of terms. The eliminant of the set gives an equation in λ, the various roots of which correspond to the normal modes of vibration.

The equations (19) may be solved and the normal modes obtained exactly as was done by Ritz for the corresponding problem of the vibrations of a plate with free edges †.

XXXVII. *Temperature Coefficient of Gamma-Ray Absorption.* *By* L. Bastings, *M.Sc.*, *F.Inst.P.* ‡

OWING to recent improvements in the methods and technique of γ-ray measurements with a gold-leaf electrometer §, γ-ray absorption constants can now be determined with sufficient accuracy to make possible an investigation into the effect of temperature on the absorption. Preliminary experiments carried out and briefly reported some two years ago ‖ established the fact that the atomic absorption increases with temperature; and in the present account, experiments are described on a number of typical

* Love, 'Elasticity,' p. 496.
† Ges. Werke, p. 292.
‡ Communicated by Sir E. Rutherford, O.M., P.R.S.
§ Bastings, J. Scient. Instr. v. p. 113 (1928).
‖ Bastings, 'Nature,' cxix. p. 51 (1927).

metals, all of which show a definite increase in this constant with rise of temperature.

No previous attempt at this problem seems to have been made; but while the preliminary experiments were in progress, some similar results were published by Read*, dealing with the absorption of X-rays in the metals Al, Fe, Ni, Cu, Ag, and Pb. On raising the temperature, he found that, when due allowance had been made for the thermal expansion of the absorber, there remained in every case a small increase in the atomic absorption constant, amounting to about 0·2 per cent. per 100° C. up to temperatures near the melting-point of the absorber.

The Preliminary Experiments.

The first experiments were made with lead absorbers of about 17 cm. in diameter and 1·4 cm. in aggregate thickness. These could be inserted in a definite position in a tubular electric furnace 18 cm. in diameter and 50 cm. in length. The furnace was mounted between the source of γ-rays, a 10·37 mgm. tube of radium in equilibrium, and the gold-leaf electrometer, so that the absorber was 30 cm. from the source and 50 cm. from the centre of the electrometer. The temperature of the furnace was measured by a platinum resistance thermometer, inserted through a hole in the side, and the temperature was maintained constant to within 5° of 270° C. by hand regulation. Under these conditions the proportion of the rays absorbed by the screen decreased by about 0·4 per cent. per 100° C. rise in temperature; but when allowance was made for the expansion of the material, as explained below, the atomic absorption constant was found to increase by approximately 0·2 per cent. per 100° C. The measurements were sufficiently accurate to establish the existence of this increase; but no great reliance could be placed upon the magnitude deduced.

The New Experiments.

Accordingly a more suitable apparatus was designed. The furnace consisted of a quartz cylinder 38 cm. in length and 6·7 cm. in internal diameter, wound externally with nichrome strip and lagged in turn with alundum cement, kieselguhr, and asbestos wool. A temperature of about 1050° C. could be developed with 10 amps. at 100 volts. The temperature was measured by two chromel-alumel thermocouples inserted one in each end of the furnace, and

* Read, Phys. Rev. xxvii. p. 373 (1926).

resting almost in contact with the centre of the absorber when in its standard position. The junctions were read by a sensitive potentiometer, and were calibrated at four fixed points. Hand regulation was found adequate to maintain the temperature constant for several hours to within 1° at 500° and 2° at 1000°.

The escape of heat from the ends of the furnace was almost eliminated by a series of large asbestos screens, separated by air-gaps. And the electrometer was further thermally insulated by being enclosed almost completely in an asbestos box ; while heat from the source of illumination was eliminated by a cell containing a solution of ferrous ammonium sulphate. There was no evidence of the occurrence of any convection currents in the electrometer due to temperature gradients ; and, in fact, the temperature of the whole of the electrometer enclosure was almost independent of whether the furnace was on or off during an experiment.

The absorbers were cylindrical in shape and slightly smaller in diameter than the interior of the furnace. They could be accurately replaced in a standard position by the aid of a distance gauge. The radium was mounted on a geometrical stand, moving on an optical bench, and both this and the screen could be replaced with accuracy of two- or three-tenths of a millimetre. The solid angle subtended by the absorber at the source was a little more than adequate to include the whole of the electrometer within it.

Method of Measurement.

The general method of measurement was similar to that described in the previous paper *. The programme of observations consisted in taking ten timings of the leaf movement with each of the following dispositions :—

(*a*) furnace cold, absorber absent ;
(*b*) furnace cold, absorber present ;
(*c*) furnace hot, absorber present ;
(*d*) furnace hot, absorber absent.

The absorption constant at the lower temperature was deduced from (*a*) and (*b*), and at the higher temperature from (*c*) and (*d*). This procedure eliminates the effect of any extraneous change in absorption or scattering in

* Bastings, J. Scient. Instr. *loc. cit.*

and around the apparatus, as the result of the rise in temperature. The programme was repeated at least four times in each experiment; and ten experiments were performed with each absorber over every temperature range considered. The natural leak was measured before and after each series, and remained constant throughout the whole of the experiments at $0{\cdot}070 \mp {\cdot}002$ divisions per minute. Readings were of the order of from 14 to 35 divisions per minute, and it was seldom that the mean deviation from the average of ten readings was greater than 1 in 1000. The values of the absorption constants deduced could usually thus be relied on to 1 in 500, and the means to probably less than 1 in 1000.

Measurements were made with lead, iron, tin, and aluminium, and in addition, in the case of tin, the molten metal was employed in a cast-iron boat of special design. This boat, with its lid, was of cylindrical shape, and the rays were passed through it in a direction perpendicular to the parallel sides. The liquid enclosed subtended more than the requisite angle at the source. An exactly similar empty boat was used in a parallel set of control experiments.

Correction for Expansion.

A correction will have to be applied to the observations on account of the expansion of the absorber. This correction in the case of the liquid will be somewhat different from that in the case of the solid.

Consider the effect of raising the temperature of the absorber by t° C. Suppose E and I represent the electrometer readings with and without the absorber at the lower temperature, and E′, I′ the corresponding readings at the upper temperature.

Let n be the number of atoms per c.c. in the absorber, μ the atomic absorption constant, and d the thickness of the absorber, all at the lower temperature, while dashed letters refer to the corresponding quantities at the upper temperature. Then

$$\mathrm{R}=\mathrm{E}/\mathrm{I}=\exp(-n\mu d) \quad \text{and} \quad \mathrm{R}'=\mathrm{E}'/\mathrm{I}'=\exp(-n'\mu' d').$$

Now, if α be the mean coefficient of linear expansion of the material of the absorber over the temperature range t°,

$$n=n'(1+\alpha t)^3$$

and

$$d'=d(1+\alpha t).$$

So

$$n\mu' d=n'\mu' d'(1+\alpha t)^2=n'\mu' d'(1+2\alpha t),$$

approximately. Thus the increase in thickness of the absorber will have no direct effect on the absorption; but the increase in cross-sectional area removes from the path of the beam affecting the electrometer some of the atoms included in it at the lower temperature, and results in a decrease in the apparent absorption.

If, then, as we shall see, μ' is greater than μ, let us assume as a first approximation that the absorption constant has a linear temperature coefficient β over the range considered;

$$i.e., \qquad \mu' = (1+\beta t).$$

Then
$$n\mu d(1+\beta t) = n'\mu' d'(1+2\alpha t)$$

and
$$\beta = \frac{n'\mu' d'(1+2\alpha t) - n\mu d}{n\mu d \,.\, t}.$$

In the case of the liquid absorber, contained in a solid boat, the expansion of the liquid along the axis of the beam is determined by the coefficient of linear expansion (γ) of the boat In fact, now

$$d' = d(1+\gamma t)$$

and

$$n\mu d = \frac{n'\mu' d'(1+\alpha t)^3}{1+\gamma t}$$

$$= n'\mu' d'(1+3\alpha t-\gamma t) \qquad \text{approximately,}$$

and

$$\beta = \frac{n'\mu' d'(1+3\alpha t-\gamma t) - n\mu d}{n\mu d \,.\, t}.$$

A Typical Experiment.

The following represents a typical set of observations carried out according to the programme oulined above :—

Metal : iron. Thickness, $d = 2{\cdot}19_4$ cm.

Intensity. Divisions per minute.

	Cold. 14° C.			Hot. 365° C.		
			Means.			Means.
Screen present	17·61	17·63		17·54	17·55	
	17·61	17·62	17·62	17·56	17·55	17·55
Screen absent	34·59	34·56		34·37	34·32	
	34·57	34·60	34·58	34·34	34·35	$34{\cdot}34_5$

Ratio of intensities:

$$R = \cdot 5095, \qquad R' = \cdot 5110,$$

$$X = n\mu d = \cdot 6743, \quad X' = n'\mu' d' = \cdot 6714.$$

X′ corrected for expansion

$$= \cdot 6714\,(1 + 2 \times 14 \times 10^{-6} \times 351)$$

$$= \cdot 6780.$$

So
$$\beta = \frac{\cdot 6780 - \cdot 6743}{\cdot 6743 \times 351} = 16 \times 10^{-6}.$$

Results.

In Table I. are set out the results of the experiments, together with deductions therefrom.

TABLE I.

I.	II.	III.	IV.	V.	VI.	VII.	VIII.
Metal.	Thickness, cm.	R=I/E. Expl.	Temp. °C.	X $=\log_e 1/R$.	Mean $\alpha \times 10^6$.	$X(1+2\alpha t)$.	$\beta \times 10^6$.
Lead...	$1{\cdot}33_8$	·4485	15	·8018			
		·4519	273	·7942	31	·8069	25
Iron ...	$2{\cdot}19_4$	·5092	13	·6749			
		·5112	364	·6710	14	·6776	11
		·5134	722	·6666	16	·6742	13
		·5143	1041	·6650	6	·6675	4
Tin (solid).	$2{\cdot}50_0$	·5503	15	·5974			
		·5520	200	·5942	24	·5995	19
Tin (liquid).	,,	·5385	288	·6190			
		·5413	436	·6138	38	·6228*	41
Aluminium.	$3{\cdot}19_1$	·6696	15	·4011			
		·6713	243	·3985	25	·4030	21
		·6731	513	·3959	30	·3023	35

* $X(1+3\alpha t-\gamma t)$ with $\gamma = 15 \times 10^{-6}$.

Column III. contains the experimental values of the ratio I/E, and represents in every case the mean of at least ten values of this quantity. In these the mean error (mean difference from mean) exceeded 1 in 1000 in only one

instance (·0006 for tin at 436° C.). The resulting values of X (column V.) are of about the same reliability.

In column VI. are given the values adopted for the mean coefficient of linear expansion of the various metals over the temperature range employed. They have been deduced from the following published data :—

Lead :

0–100° : 29·3. Gruneisen, *Ann. d. Phys.* (4) xxxiii. pp. 33, 65 (1910).
0–320° : 33. Vicentini and Omodei, *Atti Tor.* xxiii. p. 38 (1887).

Iron :

0–700°. Formula in International Critical Tables, ii. p. 460.
700–1040°. { Le Chatelier, *C. R.* cxxix. p. 331 (1899). Guillaume, Proc. Phys. Soc. xxxii. p. 374 (1920).

Tin :

18–100° : 27. Gruneisen, *Ann. d. Phys.* loc. cit.
225° : 23. Vicentini and Omodei, *loc. cit.*
20–232° : 23 to 24. Cohen and Olie, *Zeit. f. phys. Chem.* lxxi. p. 385 (1910).
226–342° : 38. Vicentini and Omodei, *loc. cit.*

Aluminium :

0–300° : 25·6 } Scheel, *Ann. d. Phys.* (4) ix. p. 837 (1902).
0–500° : 27·4 }
600° : 31·5. Le Chatelier, *C. R.* cviii. p. 1096 (1889).
0–600°. Formula in International Critical Tables, ii. p. 459.

The value ascribed to iron above 700° is of doubtful significance, as the magnitude and location of the contraction that occurs above the Curie point does not seem to be accurately known; or, rather, it is probably considerably affected by the composition of the particular specimen. An error of as much as 40 per cent. may be involved in this particular value. The other values of α in Table I. are probably reliable to at least 5 per cent.

The values of β, the mean coefficient of atomic absorption over the range selected, are set out in column VIII. They are calculated for a selected range from the values in VII. for the upper limit of the range, and from those in V. for the lower limit. The accuracy of these results is determined chiefly by the accuracy of the experimental values of column III., and the corresponding exponentials of column V. If the two values in V., from which a result in VIII. is based, happened to be in error by half the maximum amount suggested above, and in the opposite

direction, the values of β would differ from those recorded by some six units. This may reasonably be fixed as the mean limit of uncertainty in the final results as a whole. Greater accuracy than this can hardly be hoped for until the reliability of ionization methods has been increased much further than seems at present possible. This uncertainty, in the case of iron above the Curie point, might convert β into a negative coefficient; but in view of the other results, this is unlikely. With this possible exception the atomic absorption undoubtedly increases with rise of temperature.

Bearing in mind this rather large experimental error, it will be seen that the value of β in each case falls very close to the corresponding value of α in column VI. And when the whole series is considered together—dealing as it does with four different metals having widely varying values for α, and being subjected to a considerable variety of temperature conditions,—the suggestion seems highly probable that there exists an intimate connexion, if not an agreement, between the two coefficients. In other words the atomic absorption is nearly, if not exactly, a function of the linear distance between the atoms of the absorber.

Discussion.

The existence of a temperature effect on γ-ray absorption is itself somewhat unexpected; and so every care has been taken to eliminate error in the experimental work. The measurements have in some cases been repeated under a variety of conditions (as by modifying the relative dispositions of the apparatus as far as possible) without producing any appreciable change in the results. In fact, the value for lead obtained in the later experiments differs by less than the experimental error from the much less reliable results in the earlier experiments, with an entirely different absorber, furnace, electrometer, and detailed disposition of the components. This alone makes it improbable that the effect is due to any extraneous influence.

The correlation between the two coefficients here suggested is still more unexpected. Any reasonable assumption of a similar nature that might be put forward seems likely to lead to a correlation between β and the coefficient of superficial expansion (2α), since the latter might be regarded as determining the target area of the atom exposed to the radiation. The experimental accuracy is quite sufficient, however, to exclude the possibility of this correlation.

No theory seems promising at the moment; and it is thought advisable to publish the conclusions so far arrived at, as the necessity has arisen for postponing further consideration of the problem for the present. A new method of attack is under consideration, and may be carried out later.

Acknowledgments.

Much of the apparatus used in these experiments was procured through a grant from the Royal Society; while the radium was loaned by Messrs. Watson & Sons (Electro-Medical), Ltd. I have much pleasure in acknowledging my indebtedness to these two sources.

The University, Durham.
Nov. 14th, 1928.

XXXVIII. *The Duration of Contact between the Pianoforte String and a Hard Hammer.* *By* D. Banerji, *M.Sc.* (*Lecturer, University College of Science, Calcutta*), *and* R. Ganguli, *M.Sc.* (*Lecturer, Serampore College*) *.

[Plate V.]

Introduction.

IN the acoustics of the pianoforte the duration of contact plays a most important part, and so its determination is of great interest.

Kaufmann's † solution of the case of the hammer striking a string of finite length at its centre is not of much practical value. In dealing with the more important case of a string struck near the end, he has assumed the shorter portion of the string to remain straight during the time of contact, and has derived an expression for the duration of contact given by the equation :

$$\frac{\tau}{\theta} = \frac{1}{\sqrt{\frac{M}{m_0}\left(4\frac{l}{a} - \frac{M}{m_0}\right)}} \tan^{-1}\left[\frac{\sqrt{\frac{M}{m_0}\left(4\frac{l}{a} - \frac{M}{m_0}\right)}}{-2\frac{l}{a} + \frac{M}{m_0}}\right],$$

* Communicated by the Authors.

† Kaufmann, Weid. *Ann.* liv. pp. 675–712 (1895).

where τ = duration of contact,

θ = period of the string,

l = total length of the string,

a = length of the shorter portion of the string,

M = mass of the string,

$m_0 = m + \rho a/3$, where m = mass of the hammer and

ρ = linear density of the string.

This equation is, however, restricted and does not hold when the shorter portion of the string is a good fraction of the total length. In a paper published in the 'Proceedings of the Royal Society,' Raman and Banerji * have therefore attempted a general solution, applicable to any point on the string. By assuming the case as similar to the problem of a loaded string, they have obtained a pressure-time equation for the struck point. Though this equation does not admit of easy analytical solution, they have nevertheless come to some very interesting conclusions, viz., that (1) the hammer gives discontinuous impulses to the string during the time of contact, and that (2) the time of contact changes discontinuously along the length of the string.

In the same paper they have also suggested another method of attacking the problem in the line of Kaufmann, which presumably has inspired Das † to extend Kaufmann's theory. On the assumption that the hammer gives discontinuous impulses at times in which the waves starting from the hammer come back to it after successive reflexions from the near end, Das has developed expressions for the pressures in successive epochs, F_1, F_2, etc., as given by the equations :

$$F_1 = 2\rho v_0 c e^{-kct},$$

$$F_2 = 2\rho v_0 c\left[e^{-kct} + e^{-k(ct-2a)}\{1-k(ct-2a)\}\right],$$

$$F_3 = 2\rho v_0 c\left[e^{-kct} + e^{-k(ct-2a)}\{1-k(ct-2a)\} + e^{-k(ct-4a)}\left\{1-2k(ct-4a)+\frac{k^2}{2!}(ct-4a)^2\right\}\right], \text{ etc.,}$$

where a = distance of the striking-point from the nearer end,

ρ = linear density of the string,

* Raman and Banerji, Proc. Roy. Soc. A, xcvii. p. 99 (1920).

† P. Das, Proc. Ind. Assoc. vii. pts. 1 & 2, pp. 13-20 (1921).

v_0 = initial velocity of the hammer,

c = velocity of propagation of transverse waves on the string,

$k = 2\rho/m$, where m = mass of the hammer,

t = variable time.

Das's solution is also of limited applicability, but it is worth while to see how much it can claim to be an advance on Kaufmann's. It may be noted in the meantime that the determination of duration of contact from Das's equations involves long and tedious calculations and laborious graphical methods.

The earliest experimental work on the pianoforte was made by Hipkins * and next by Kaufmann †. Observations on the nature in which the duration of contact changes with the struck point appear to have first been taken by Raman and Banerji ‡ by an electrical method. George § remarks that this method is open to objection, but he has never attempted to verify directly the conclusions arrived at by Raman and Banerji, neither has there been any attempt to test Das's pressure-time equations. All that George or R. N. Ghosh ‖ has done generally concerns Kaufmann's theory. Das ¶ has, however, in a later paper tried to show that his theory is indirectly supported by the results of an investigation on the energy of struck strings carried out by George and Backett **. But, very recently, Kar, Ganguli, and Laha †† found Das's theory to have no agreement with experimental evidence regarding the amplitudes of the different harmonics of struck strings. Furthermore, a careful study on the duration of contact—the most important element in the acoustics of struck strings—seems still to be wanting.

In the present paper attempts have been made to (1) determine accurately the duration of contact between the hammer and string when the latter is struck at various

* Hipkins, Proc. Roy. Soc. A, xxxvii. pp. 37–39, and xxxviii. p. 83 (1884).

† Kaufmann, *loc. cit.*

‡ Raman and Banerji, *loc. cit.*

§ George, Phil. Mag. xlvii. pp. 34 & 48 (1924), pp. 91–99 (1924); Proc. Roy. Soc. A, cviii. pp. 284–295 (1925).

‖ R. N. Ghosh, Phil. Mag. xlvii. p. 125 (1925); Proc. Ind. Assoc. ix. pp. 111 & 194 (1925); Phys. Rev. xxiv. p. 456 (1924), xxxvii. p. 135 (1926).

¶ Das, Ind. Journ. Phys. i. p. 437.

** George and Beckett, Proc. Roy. Soc. A, cxiv. (1927).

†† Kar, Ganguli, and Laha, Phil. Mag., March 1928.

points along its length, and the manner in which this duration changes with the struck point ; to (2) compare the experimental values with those calculated respectively from Das and Kaufmann's theories ; and further to (3) study the condition of the shorter portion of the string during the time of contact.

Experiment.

A string 240 cm. long and of mass 16·4 gm. was employed. One of its ends was tied to a firm support rigidly fixed on a table, and the other end, passing over an equally rigid fixed pulley, carried a heavy weight. Two vertical rafters, attached one to each end of the table, carried a horizontal rod at the top, from which a ball was freely suspended by fine threads, so that it just touched the string while at rest. This ball constituted the striking-hammer. The struck point was illuminated from above by an arc-lamp and focussed by a lens on a long and shallow wooden camera, with a slit in the middle of the cover and placed along the base of the table. The slide was pulled with a uniform high velocity from one end of the camera to its other end by a motor. The start of the motor was made simultaneous with the release of the striking-hammer by means of an electromagnetic arrangement. The cover of the slide was automatically closed on reaching the other end of the camera, and timing was so adjusted that the hammer impinged on the string just when the slide was carried across the slit.

Figs. 9 to 11 (Pl. V.) are specimen photographs of the time-displacement pictures that were obtained. Fig. 9 was obtained with a hammer of mass 46 gm. striking at 32 cm. from the end, and figs. 10 and 11 were obtained with a hammer of mass 13·4 gm. for 35 and 40 cm. respectively.

The speed of the motor could be regulated as desired. With a certain convenient speed the wave-form of the string vibrating under the tension of 10,903 kilograms was photographed. The distance from one crest to the next of the wave-picture is the distance traversed by the slide within the known period of the string. The velocity of the slide being thus accurately measured, the duration of contact was calculated from the time-displacement picture of the struck point by measurement along the time-axis of the distance intercepted between the point of first contact and the point where it left the string.

Results and Discussion.

In the time-displacement picture of the struck point it is not always possible to find exactly where the hammer leaves the string. In such cases, however, the vibration period of the shorter portion of the string is small compared with the duration of contact, and the correction to be applied for uncertainties in the measurement of the duration of contact is minimized by a comparison between the time-displacement picture of the struck point and that of a point on the shorter portion of the string very near to the struck point.

The duration of contact for different struck points in the case of a striking-hammer of mass 46 gm. is given in Table I. and graphically shown in fig. 1. Table II. gives

Table I.

$\frac{M}{m} = 0{\cdot}3565.$ $\theta = 0{\cdot}0356$ sec.

Velocity of the plate = 76·33 cm./sec.

a (cm.).	τ (sec.).
15	·0262
20	·0263
25	·0356
32	·0369
40	·0432
50	·0432
60	·0445
80	·0511
100	·0590

the case of a striking-hammer of mass 13·4 gm. A comparison between experimental values and those calculated respectively from Das and Kaufmann's theories is given therein and graphically shown in fig. 2. The experimental curve is found to be not quite smooth like the curve of Kaufmann, but is kinked. From fig. 2 it appears that the mean slope of the experimental curve (neglecting the kinks) changes in a manner similar to that of Das's. The kinks in our experimental curve owing to the discontinuous change are, however, far less prominent than those obtained in the theoretical curve of Das. Though the slope of the curve changes somewhat abruptly near the kinks, it never changes sign as predicted by Das. The table

Fig. 1.

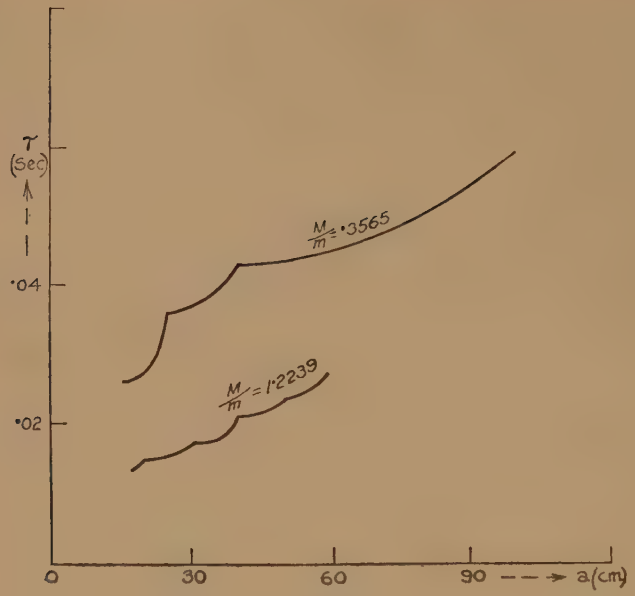

TABLE II.

$\frac{M}{m} = 1{\cdot}2239.$ $v_0 = 51{\cdot}39$ cm./sec.

$\theta = 0{\cdot}0356$ sec. $\rho = 0{\cdot}0569$ gm.

	τ (sec.).		
	Experimental.	From Das's theory.	From Kaufmann's theory.
15	·0123	·0114	·0117
20	·0142	·0131	·0113
25	·0151	·0153	·0150
30	·0170	·0179	·0164
35	·0179	·0173	·0176
40	·0205	·0198	·0189
45	·0211	·0210	·0200
50	·0233	·0241	·0209
55	·0248	·0268	·0217
60	·0266	·0292	·0222

shows clearly enough how much on the whole Das's theory can claim to be an advance on Kaufmann's.

Figs. 4 to 8 (Pl. V.) give the vibration pictures of the shorter portion of the string under different conditions. Only Kaufmann obtained similar pictures, but it is curious that he did not take much notice of them, apparently on the ground that his string was thin and hammer massive. The figures in the present paper, however, clearly show that the shorter portion of the string starts vibrating at the instant the hammer impinges on the string, and continues to

Fig. 2.

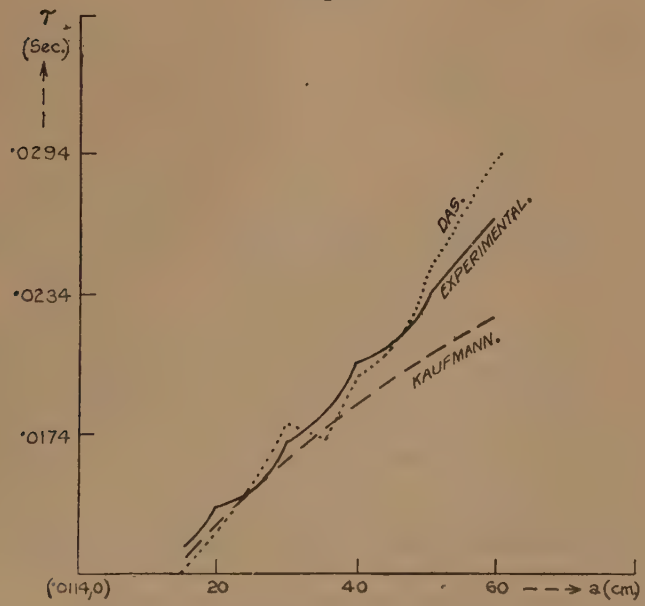

vibrate quite independently during the time of contact with nodes—one at the struck point and the other at the fixed end—and a loop at the middle, just as a string of the same length would vibrate under the same tension. It further shows that this vibratory character is maintained even for $\frac{M}{m} = 1{\cdot}2239$, and that its mean position at any instant is similar to that of a straight rod as contemplated by Kaufmann. Fig. 7 is the vibration picture of the middle point of the shorter portion of the string, and figs. 6 and 8 are those of points close to the struck point and the end respectively. It will be found that the displacement of any

of the above points is fairly proportional to its distance from the end. For illustration of the condition of the shorter portion of the string at any instant see fig. 3. Figs. 4 and 5 (Pl. V.) are vibration pictures of points 17 and 25 cm. respectively from the end for $m = 46$ gm., striking at 25 and 32 cm. respectively from the end. A proportional change in the period is clearly noticeable. After the separation of the hammer from the string, the whole string vibrates in a manner which appears to be largely dependent on the period of the shorter portion of the string.

Fig. 3.

Vibration pictures of the other side of the string have also been taken, but are not reproduced here. They will be the subject matter of a later communication.

Conclusions.

1. The curve showing the relation between the distance of the struck point and the duration of contact of the hammer with the string is not smooth like the theoretical curve of Kaufmann, but appears to be kinked. The mean slope of the kinked experimental curve agrees somewhat better with Das's theoretical curve. The actual kinks are, however, far less marked than those obtained in the theoretical curve due to the discontinuous changes predicted by Das. Though the slope of the curve changes somewhat abruptly near the kinks, it never changes sign as in Das's theoretical curve.

2. During the time of contact, while the struck point follows the movement of the hammer, the shorter portion of the string instead of remaining straight as contemplated by Kaufmann executes its fundamental mode of vibration.

Further work in this line is in progress and will form the subject of a future communication.

In conclusion we express our best thanks to Prof. S. K. Mitra for his interest in the work.

University College of Science,
92 Upper Circular Road,
Calcutta.
June 21, 1928.

XXXIX. *The Absorption of X-Rays from 0·63 to 2 Å.U.*

By Ivor Backhurst, *M.Sc., Physics Department, National Physical Laboratory* *.

Introduction.

MOST recorded measurements of monochromatic X-ray absorption have been for wave-lengths less than 1·0 Å.U., but the exact manner in which the true or fluorescent absorption depends on wave-length is to some extent obscured for most elements at short wave-lengths by the appreciable and uncertain relative magnitude of the scattering effect. The measurements of which an account is given here have been made for wave-lengths between 0·63 and 2 Å.U., for which the relation between absorption and wave-length may be obtained free from such uncertainty, the scattering being negligible. Included in this region of wave-length are the L discontinuities of platinum and gold, the K discontinuity of copper, and a possible multiple ionization discontinuity of silver. Departures from the cube law of absorption have been found that are sufficiently well marked to be well beyond suspicion of coming within the margin of experimental error. It is desired to emphasize this point, as well-known writers [1] have from time to time expressed the opinion that no real departure from the cube law had been definitely established. Direct methods of measurement have been used throughout to determine the absolute value of the mass absorption coefficient; balance methods furnishing the absorption relative to aluminium have been used as well, but only to provide check measurements.

The principal difficulty in the direct measurement of absorption, as frequently mentioned in the literature of the subject, is the maintenance of constant X-ray intensity, involving as it does the constancy of both potential and current of the X-ray tube, and the constancy of position of focal spot and similar factors. This difficulty is greater for longer than for shorter wave-lengths, as larger currents are needed in the former case to compensate for the lower potential and consequent reduction in intensity. Special care was on this account taken in the arrangement and design of the apparatus to secure a constant and intense X-ray beam, and the experimental arrangement will therefore

* Communicated by Dr. G. W. C. Kaye.

be described in some detail. It is thought that the principal error in the present research has probably occurred in the measurement of the effective mass per unit area of the very thin sheets of absorbing material, as with an X-ray beam of necessarily small cross-sectional area the mass of absorbing element in its path was always very small, and often less than 0·05 milligramme. This error was, however, reduced as far as possible by the use of a number of sheets, and results obtained with different sheets rarely differed by more than 2 per cent.

Apparatus and Method of Experiment.

The X-ray tube, of which a horizontal section is shown to scale in fig. 1, had a tungsten filament cathode and was a modification of one described by Siegbahn. It was designed to utilize the full power of the high-tension supply over the

Fig. 1.

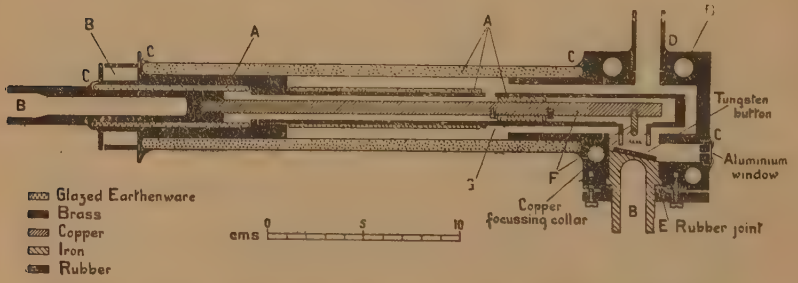

voltage range required and to allow easy changing of the anticathode. The insulating tubes A were of glazed earthenware and were unpuncturable at the voltages used. The anticathode end of the X-ray tube was made by drilling a rectangular brass block. This method of construction avoided the use of soldered joints in any position where a leak would introduce vapour from the water-cooling system and be troublesome to locate. Both upper and lower faces of the brass block were water-cooled, and water-channels B were drilled through the block. The tungsten anticathode consisted of a tungsten button welded to an iron base which was water-cooled. Copper and iron anticathodes were also used. This end of the X-ray tube was earth connected and vigorously cooled from the main supply; the other end was at high potential and cooled from a thermo-syphon. The vacuum joints were the four wax joints C, the soldered one D, and the rubber one E. The latter was held by a

clamping ring with steel screws, removal of which enabled the anticathode to be changed, the tungsten filament renewed, or the focussing collar adjusted. The window was aluminium foil. The rods F were copper, the remaining parts of the X-ray tube not mentioned above were brass. The vacuum was maintained by two mercury-diffusion pumps in series supported by a rotary oil pump, and ice traps prevented condensation of mercury in the X-ray tube. Liquid air or other mercury-vapour traps were found unnecessary, as a tungsten filament would last for several months if not placed too near the axis of the focussing collar, and the tube would not pass a measurable current unless the filament was heated. The glazed earthenware tube immediately surrounding the brass tube G prevented the latter from sputtering on to the main insulating tube, as it otherwise would have done in the presence of mercury vapour. Periodical dismantling was thereby avoided, and it was unnecessary to undo any joint except the rubber one.

The tube current ranged from 35 milliamps. at 25 kilovolts to 80 milliamps. at 11 kilovolts, and a sufficiently strong X-ray beam was furnished to enable the general radiation to be used as well as the characteristic. This facilitated the close investigation of certain regions of wave-length such as those of the L-absorption edges. The general radiation, even with a tungsten anticathode, was weaker than the characteristic under the conditions of experiment, but it was particularly desirable with the general radiation to employ a small angular width of reflected beam in order that the latter might be nearly enough homogeneous. It was consequently very important that the intensity of the primary beam should be as high as possible.

The high-tension supply was not a constant potential one, but a satisfactory constant effective potential was obtained by supplying a high-tension transformer with current from a rotary converter driven by a battery. The transformer was of the "power" type, with ample iron core, and rheostats were excluded from the supply circuit, so that the voltage applied to the X-ray tube was inappreciably affected by small fluctuations in tube current. Alteration of voltage was effected by means of an auto-transformer and by connecting in series or parallel the two windings of the high-tension transformer. The filament temperature and the focussing collar determined the amount of the tube current, and slight variations in the latter during an experiment were corrected by means of a rheostat controlling the filament current. This was supplied from a battery, and

the tube current could be maintained constant to within 1 per cent. It was found possible to adjust the focussing collar so that an increase of tube current above a chosen value C made comparatively little difference to the intensity of the X-ray beam. By making the value of C somewhat less than the amount of current available the tube could be operated at a maximum current, while small variations in the latter produced little effect on X-ray intensity. The distance between the focussing collar containing the tungsten filament and the anticathode being very short (between 3 and 6 mm. along the axis), there was little movement of focal spot, and the primary X-ray beam made an angle of about 10° with the face of the anticathode.

In consequence of the above arrangements, the steadiness of the beam obtained after reflexion from a calcite crystal was quite satisfactory, and errors produced by fluctuations in X-ray intensity were less than those introduced in the observation of electrometer deflexions. About 1 per cent. fluctuation occurred amongst individual readings of these, but the mean of at least five readings was invariably taken.

As one slit was included in the window of the X-ray tube, only one lead slit was required on the spectrometer between the tube and the crystal. The reflected beam passed through two lead slits A and B before entering the ionization chamber, one of the slits B being close to the latter. The absorbing screen was held by a spring clamp flat against the face of slit A on the side next the crystal. The maximum angular width of the reflected beam passing into the ionization chamber was determined by slits A and B, and varied from 4·5′ of arc for the shorter wave-lengths to 45′ for the longer. The corresponding range of wave-length included in the width of the beam was therefore between 4 and 6 per cent. Narrower slits were used for characteristic radiation, although this width was necessary to obtain satisfactory intensity with general radiation; but it will be shown that negligible error was thereby occasioned.

At potentials between 10 and 25 kilovolts, as was found by Wagner and Kulenkampff[2], the wave-length ($\lambda_m/2$) is somewhat shorter than the shortest wave-length excited by the voltage on the tube, if λ_m is the wave-length of maximum intensity of the general radiation, intensity being measured by the ionization method. In the present investigation the tube voltage was always adjusted to a value somewhat less than that required to excite $\lambda/2$, where λ was the wave-length selected by the crystal, so that λ was always nearly equal to λ_m, and the rate of variation of intensity with λ was

practically zero over the width of the beam. Under these conditions we have for the experimental value "μ_a" of the absorption coefficient "μ" at a wave-length $\lambda_a=(\lambda_1+\lambda_2)/2$,

$$\mu_a = (1/t)\log\left[(\lambda_2-\lambda_1)\Big/\int_{\lambda_1}^{\lambda_2} e^{-\mu t}\,d\lambda\right], \quad \text{where } I=I_0e^{-\mu t}.$$

The thickness "t" of the absorbing screen was chosen so that the wave-length investigated was in the neighbourhood of the value "λ_0" for which $\mu t=(n-1)/n$, where $\mu=k\lambda^n$, k being constant. This is a point of inflexion on the curve $I=f(\lambda)$, which is very nearly a straight line in this region if n is approximately 3. A sufficient number of absorbing screens were used to keep the ratio I_0/I between the limits 1·8 and 2·5, so that the errors due to inhomogeneity of beam were as follows :—

For the case $n=3$, the first limit corresponds to

$$\lambda_1 = 0{\cdot}93\lambda_0, \qquad \lambda_2 = 0{\cdot}99\lambda_0$$

for the maximum width of beam, and the difference between the experimental value μ_a and the true value $k\lambda_a^n$ is less than 0·08 per cent., while for the second limit

$$\lambda_1 = 1{\cdot}09\lambda_0, \qquad \lambda_2 = 1{\cdot}15\lambda_0,$$

and $k\lambda_a^n-\mu_a$ is less than 0·3 per cent. For intermediate values of I_0/I the error is less and travels through a zero value. The upper limit of I_0/I was taken further from the value, for which $\mu t=(n-1)/n$, than the lower limit, on account of the fact that the percentage error in the value found for μ is $(1/\mu t)\times$ percentage error in I_0/I, so that it was desirable to have μt not much less than unity.

Two crystals and two ionization chambers were mounted on the spectrometer, so that the balance method could be used to check values found with a single chamber by the direct method. The latter was the method mostly used as it afforded greater sensitivity. The ionization current was measured with a Compton electrometer, the time for a given deflexion (approximately the last two-thirds of the deflexion from zero) being observed with and without the absorbing screen in position. The rate of deflexion over the observed range was very nearly constant, and the correction for "natural leak" varied from $\frac{1}{2}$ to 1 per cent. Sulphur insulation was used throughout. The ionization chambers were filled with methyl bromide.

The slit B, close to an ionization chamber, subtended at no point in the absorbing screen a solid angle greater than

0·00003 of a complete solid angle, so that the fraction entering the ionization chamber of the total scattered radiation from the absorbing screen was quite inappreciable. With the ionization chamber set just out of position for reception of the reflected beam, no ionization current could be observed, the amount of scattered radiation from other sources being therefore also negligible. This was further checked by exposure for several hours of a photographic film between the slits A and B, with the ionization chamber set to receive the reflected beam.

In the case of aluminium, the absorbing screens were made from rolled sheets of the metal, but the screens of other elements were built up from carefully-selected sheets of beaten leaf. The mass per unit area was found by weighing, so that determination of the mass absorption coefficient "μ/ρ" did not involve a knowledge of the density ρ. In measuring the absorption, the screen was moved for each observation in such a manner that the narrow strip areas effecting the absorption were approximately evenly spaced over the weighed area. At least ten readings were included in a set and were taken alternately with and without the absorption screen in position. Usually not more than 3 per cent. difference existed between the greatest and least values found for the absorption coefficient, when the latter was calculated separately from each of the five pairs of readings. This was considered to indicate a reasonable degree of uniformity in the thickness of the screens, in view of the fact that the total thickness mostly lay between 0·001 and 0·01 mm. All the screens were made from metal of a high degree of purity.

Results.

Since the mass-scattering coefficient σ/ρ is not known at all accurately, and is in these experiments only a very small fraction of μ/ρ, the results are given in terms of the latter rather than of the mass fluorescent absorption coefficient τ/ρ, which is obtained from μ/ρ by subtracting σ/ρ. With the logarithm of μ/ρ plotted against the logarithm of the wave-length λ, the experimental points were found to lie on straight lines within the limits of observational error, but with μ/ρ plotted against λ^3 straight lines within the limits of error were not generally obtained. The results are therefore best represented by equations of the form $\mu/\rho = a\lambda^n$. In the graphical representation $\log \mu/\rho$ has been plotted against $\log \lambda$ rather than μ/ρ against λ^n, as in the former method circles having the same radii and drawn with the experi-

mental points as centres can be used to denote the same percentage error in μ/ρ and λ for all points of the graph.

Silver.

For silver, using the method of least squares and a log graph (fig. 2), the equation calculated is

$$\log \mu/\rho = 1{\cdot}844 + 2{\cdot}79 \log \lambda, \quad \text{or} \quad \mu/\rho = 69{\cdot}9\,\lambda^{2{\cdot}79}. \quad (1)$$

Fig. 2.

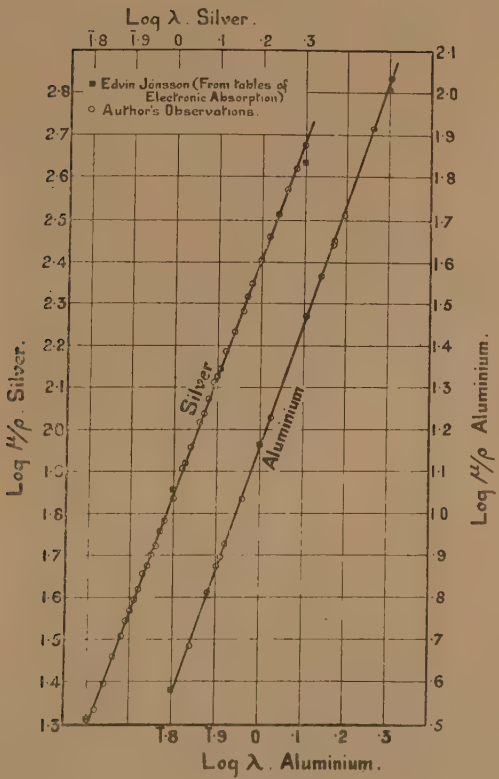

The experimental points are given in Table I.; circles with 1 per cent. radii drawn on them on the log graph are all cut by the straight line represented by (1). On a $(\mu/\rho, \lambda^3)$ graph, equation (1) represents an appreciably curved line. The straight line approximating to it with the condition that

the maximum percentage difference in μ/ρ should be less than for any other has the equation

$$\mu/\rho = 62{\cdot}4\lambda^3 + 4{\cdot}47. \quad . \quad . \quad . \quad . \quad . \quad (2)$$

Its maximum difference is 4·25 per cent., well beyond the limits of experimental error, and the term 4·47 is too high to represent σ/ρ. The experimental data cannot therefore be expressed properly by one equation of the form

$$\mu/\rho = a\lambda^3 + b.$$

Alexander [3] has suggested that in the neighbourhood of $\lambda = 1{\cdot}0$ Å.U. there is a break in the absorption curve, and that two equations,

$$\mu/\rho = a\lambda^3 + b \quad . \quad . \quad . \quad . \quad . \quad . \quad (3)$$

and

$$\mu/\rho = a'\lambda^3 + b', \quad . \quad . \quad . \quad . \quad . \quad (4)$$

TABLE I.

	Log μ/ρ.			Log μ/ρ.	
Log λ.	Silver.	Gold.	Log λ.	Silver.	Gold.
$\bar{1}{\cdot}82$	1·335	1·969	0·024	—	1·909
$\bar{1}{\cdot}84$	1·395	2·024	0·027	1·920	—
$\bar{1}{\cdot}86$	1·459	2·087	0·04	1·958	1·956
$\bar{1}{\cdot}88$	1·510	2·140	0·06	2·018	2·009
$\bar{1}{\cdot}89$	1·545	—	0·07	2·038	2·031
$\bar{1}{\cdot}90$	1·568	2·202	0·08	2·072	2·062
$\bar{1}{\cdot}91$	1·594	—	0·094	2·112	—
$\bar{1}{\cdot}92$	1·620	—	0·10	2·126	2·104
$\bar{1}{\cdot}928$	—	2·265	0·107	2·145	—
$\bar{1}{\cdot}93$	1·656	—	0·12	2·186	2·168
$\bar{1}{\cdot}94$	1·672	2·219	0·14	2·234	2·217
$\bar{1}{\cdot}948$	—	2·245	0·16	2·283	2·267
$\bar{1}{\cdot}95$	1·702	—	0·17	2·315	2·291
$\bar{1}{\cdot}96$	1·723	2·159	0·18	2·348	2·319
$\bar{1}{\cdot}97$	1·757	2·168	0·20	2·403	2·372
$\bar{1}{\cdot}98$	1·784	2·198	0·22	2·460	2·423
$\bar{1}{\cdot}99$	—	2·225	0·24	2·513	2·469
0·00	1·835	2·252	0·26	2·572	2·528
0·01	—	2·267	0·28	2·623	2·577
0·02	1·906	—	0·30	2·679	2·630

will accurately represent the data in this region of wavelength. If the values in Table I. are plotted on a $(\mu/\rho, \lambda^3)$ graph, it at once appears that two straight lines will provide a good fit, but it is difficult to select the exact point for the break, as the eye is influenced by the spacing of the points, and is apt to make insufficient allowance for the disparity in the percentage errors represented by equal distances at different parts of the graph. A change of scale of the graph may produce a change in the apparent position of the break. It seems as well, therefore, to use some method of fixing the latter other than simple inspection of the graph, and a method that appears to be as good as any is to assume that equation (1) is accurate and determine equations (3) and (4) so that the maximum percentage difference between corresponding values of μ/ρ calculated from (1) and from (3) and (4) should be less than for any other pair of equations similar to (3) and (4). This particular condition is chosen since the experimental error is approximately a constant percentage of μ/ρ, while the value of μ/ρ varies from 20 to 500. The position found for the break in this way is at $\sqrt{\lambda_1\lambda_2}$, where λ_1 and λ_2 are the limits of the wavelength range over which the approximation is made. This follows from the fact that, if $\mu/\rho = k\lambda^n$ is approximated to with the above condition by one equation $\mu/\rho = a\lambda^3 + b$, the maximum percentage error E in μ/ρ is dependent only on n and λ_1/λ_2, being given by

$$\mathrm{E} = \frac{100\,\mathrm{N}}{2+\mathrm{N}},$$

where

$$\mathrm{N} = m^m\left(\frac{1-p}{1-p^m}\right)\left\{\frac{\dfrac{1-p}{1-p^m}-1}{1-m}\right\}^{m-1} - 1,$$

and

$$m = n/3, \quad p = \lambda_1^3/\lambda_2^3, \quad m<1, \quad \text{and} \quad p<1.$$

The further p departs from unity the greater the value of E, so that with two equations of the form $\mu/\rho = a\lambda^3 + b$, for the minimum value of E, $\lambda_1/\lambda_B = \lambda_B/\lambda_3$ or $\sqrt{\lambda_1\lambda_2} = \lambda_B$, the wavelength of the break.

In this way the position of the break in the L-absorption curve for silver is fixed at 1·122 A.U., and the two equations are

$$\mu/\rho = 67{\cdot}0\,\lambda^3 + 2{\cdot}71 \quad . \quad . \quad . \quad . \quad . \quad (5)$$

and

$$\mu/\rho = 59{\cdot}4\,\lambda^3 + 13{\cdot}5, \quad . \quad . \quad . \quad . \quad . \quad (6)$$

the maximum percentage difference in μ/ρ between (1) and (3) (4) calculated on μ/ρ from (1) being less than 1·2. Using Allen's [4] results, Alexander has given the equations

$$\mu/\rho = 74{\cdot}1\lambda^3 + 2{\cdot}0 \quad \text{and} \quad \mu/\rho = 55{\cdot}8\lambda^3 + 27{\cdot}0,$$

which put the break at 1·110 Å.U. Allen represented his experimental data by two equations of the form

$$\mu/\rho = a\lambda^n + \sigma/\rho,$$

and found 1·10 Å.U. as the wave-length at which there occurred a change in the index n from 2·92 to 2·6, the constant "a" changing from 73 to 76 or 78, and the true mass-scattering coefficient σ/ρ being regarded as negligible.

It seems very questionable as to what extent any special physical significance should be attached to such a break, in the absence of other than absorption data, since it is also possible to represent μ/ρ by a continuous function of λ. Alexander has deduced a theory of multiple ionization from the possible positions of breaks in K-absorption curves, and found that $\lambda_{KK'}$, the wave-length of a break, was inversely proportional to A^2, A being atomic number. It should be noted, however, that a law something of this nature seems to be a necessary consequence of considerations such as the following. The data upon which the law depends are thirteen values of $\lambda_{KK'}$, six of which are for elements Fe, Ni, Cu, and Zn (A from 26 to 30), and on a graph of $\sqrt{1/\lambda}$ against A are clustered in a group and serve only to fix rather approximately one point of the curve. Two values, *i. e.* for Mo and Ag, are based on Richtmyer's [5] results; but the remaining five, which are deduced from Allen's results for Ag, Sn, W, Pt, and Au (A from 47 to 79), mainly determine the nature of the curve. For these five elements Allen found that $\mu/\rho = a\lambda^n + \sigma/\rho$, in each case n having the same value, 2·92, and the data extending from 0·08 Å.U. to λ_K, the wave-length of the K-absorption edge. If the data for each element are represented by two equations of the form $\mu/\rho = a\lambda^3 + b$, with the condition that for any value of λ the maximum percentage difference in the values of μ/ρ, calculated from the appropriate one of these equations and from Allen's equation, should be less than for any other pair of equations of the form $\mu/\rho = a\lambda^3 + b$, then, as shown above, it follows that

$$\lambda_{KK'} = \sqrt{\lambda_1\lambda_2} = \sqrt{0{\cdot}08\lambda_K}$$

for each element. Since λ_K is inversely proportional to A^2, the law, $\lambda_{KK'}$ inversely proportional to A, is a necessary consequence, and would give a somewhat better fit to the data than the law, λ_{KK} inversely proportional to A^2, deduced by Alexander. It may further be remarked that, while in the case of these elements two equations of the form $\mu/\rho = a\lambda^3 + b$ are being used to approximate to an equation of the form $\mu/\rho = c\lambda^{2\cdot92} + d$ between limits of wave-length $\lambda_1 = 0{\cdot}08$ Å.U. and $\lambda_2 = 0{\cdot}153$ Å.U. to 0·485 Å.U., only one equation of the form $\mu/\rho = a\lambda^3 + b$ is used for Al, for which the same index $n = 2{\cdot}92$ was found by Allen to hold over a range $\lambda_1 = 0{\cdot}08$ Å.U. to $\lambda_2 = 2$ Å.U. Yet, as shown above, the degree of approximation depends only on n and λ_1/λ_2, so that in the case of each of the elements Ag, Sn, W, Pt and Au, the data could be better represented by one equation of the form $\mu/\rho = a\lambda^3 + b$, with no break at all, than could the data for Al, for which one equation is made to serve since no multiple ionization effect would be expected for Al in this region of wave-length.

On the whole it would appear that, as far as the experimental results go, there is nothing to indicate discontinuities of a type attributable to multiple ionization phenomena. On the theoretical side it is not at all clear why multiple ionization should be expected to produce discontinuities of the above type. This question has been investigated by Richtmyer [6], who, with the help of recent data, has extended Turner's [7] calculation of the energy necessary for double K ionization on the basis of Wentzel's [8] theory, and finds that for elements of atomic number up to 51 it should be greater than twice that required for single ionization. The wave-lengths of the breaks considered above correspond to considerably smaller energy values. On account of this and other reasons, Richtmyer deduces that there is no theoretical justification for the conclusion that any obvious relation should exist between such discontinuities and multiple ionization. Recently Edvin Jonsson [9] has obtained results which show that when allowance is made for the K, L, M, etc. absorption jumps, the average electronic absorption μ_e is for all elements the same function of $N\lambda$, or very nearly so, N being atomic number. The function of $N\lambda$ is such that for any element the absorption curve on a $(\log \mu/\rho, \log \lambda)$ graph is quite continuous apart from the K, L, M, etc. absorption jumps. Values taken from Jonsson's tables are plotted in fig. 2, and show quite good agreement, except between 1·5 and 2 Å.U.

Aluminium.

Experimental values for aluminium are shown in Table II.,

Table II.

	Log μ/ρ.			Log μ/ρ.	
Log λ.	Aluminium.	Copper.	Log λ.	Aluminium.	Copper.
$\bar{1}\cdot84$	0·685	1·680	0·12	—	2·440
$\bar{1}\cdot88$	0·811	1·791	0·141	1·568	—
$\bar{1}\cdot90$	0·875	—	0·17	1·642	1·670
$\bar{1}\cdot91$	0·896	—	0·172	1·651	—
$\bar{1}\cdot92$	0·928	1·900	0·186	—	1·726
$\bar{1}\cdot96$	1·035	2·000	0·195	1·711	—
0·00	—	2·128	0·24	—	1·865
0·027	1·230	2·179	0·26	1·920	1·946
0·04	—	2·230	0·28	—	1·997
0·107	1·472	2·416	0·30	2·040	2·064

and applying the method of least squares to obtain the best straight line on a log graph (fig. 2), the equation found is

$$\log \mu/\rho = 1\cdot156 + 2\cdot91 \log \lambda \quad \text{or} \quad \mu/\rho = 14\cdot3\,\lambda^{2\cdot91}. \quad (7)$$

This straight line cuts every circle drawn with an experimental point as centre and radius representing 1 per cent. The curve that equation (7) represents on a (μ/ρ, λ^3) graph can, however, be closely approximated to by a straight line. The maximum percentage difference between corresponding values of μ/ρ calculated from (7) and from

$$\mu/\rho = 13\cdot67\,\lambda^3 + 0\cdot388 \quad . \quad . \quad . \quad . \quad . \quad (8)$$

for any value of λ between the limits $\log\lambda = \bar{1}\cdot8$ and $\log\lambda = 0\cdot3$ is 1·9, and is less than for any other straight line on the (μ/ρ, λ^3) graph, percentage being reckoned on the value of μ/ρ from (7). If on this graph an ellipse is drawn, with each experimental point as centre, having semiaxes representing 1 per cent. change in μ/ρ and λ respectively, the straight line (8) will just cut most of these ellipses, but the fit is certainly not so good as with (7). The value 0·388 so obtained for σ/ρ, although the latter is not known at all accurately, must certainly be too high, but the agreement between (7) and (8) becomes appreciably poorer if a value as low as, say, 0·15 is put for the constant term of (8).

Allen's equation $\tau/\rho = 14{\cdot}0\lambda^{2{\cdot}92}$ is in good agreement with (7). Martin [10] found $\mu/\rho = 13{\cdot}9\lambda^{2{\cdot}98}$, but considered that the cube law also represented his results within experimental error. Values from Jonsson's table (fig. 2) are in good agreement with (7), but show an index rather less than 2·91 between 1 and 2 A.U. On the whole it would appear fairly certain that the fluorescent absorption in aluminium between 0·5 and 2·0 A.U. is very nearly proportional to

Fig. 3.

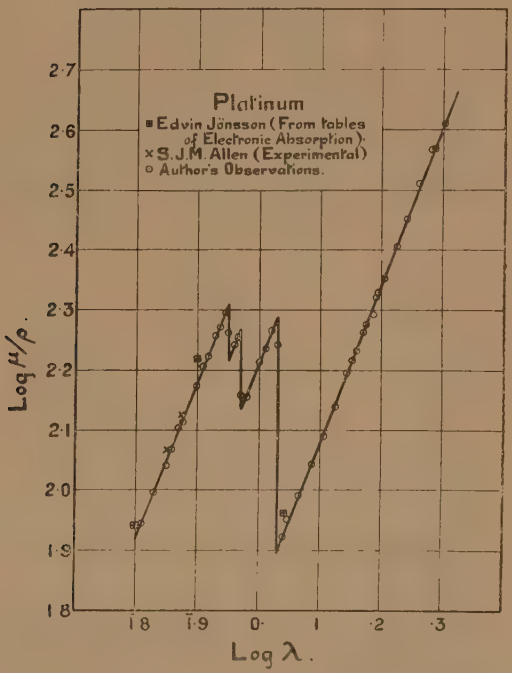

λ^3, but not accurately so, the value of the index being definitely somewhat less than three.

Platinum and Gold.

For platinum and gold the region of wave-length around the L-absorption edges was investigated closely with the object of measuring the magnitudes of the L-absorption jumps as accurately as possible. As shown in fig. 3 and Table III. for platinum, and fig. 4 and Table I. for gold, the the values of $\log \mu/\rho$ plotted against $\log \lambda$ were in each case

TABLE III.

Platinum.

Log λ.	Log μ/ρ.	Log λ.	Log μ/ρ.	Log λ.	Log μ/ρ.
$\bar{1}$·809	1·946	$\bar{1}$·965	2·255	0·1516	2·216
$\bar{1}$·829	1·997	$\bar{1}$·97	2·159	0·16	2·232
$\bar{1}$·849	2·041	$\bar{1}$·98	2·156	0·17	2·263
$\bar{1}$·859	2·068	0·00	2·214	0·175	2·277
1·869	2·104	0·01	2·237	0·187	2·293
1·877	2·115	0·02	2·266	0·191	2·322
$\bar{1}$·899	2·173	0·03	2·242	0·195	2·331
$\bar{1}$·909	2·206	0·04	1·923	0·204	2·354
1·918	2·223	0·047	1·952	0·224	2·407
$\bar{1}$·929	2·257	0·065	1·992	0·24	2·452
$\bar{1}$·937	2·272	0·086	2·044	0·26	2·512
1·947	2·296	0·106	2·091	0·28	2·568
1·950	2·262	0·124	2·140	0·30	2·610
$\bar{1}$·96	2·242	0·143	2·196	—	—

Fig. 4.

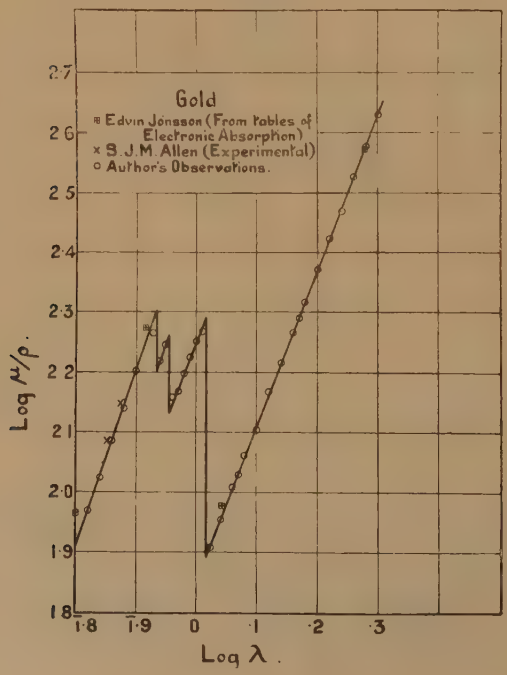

found to fall on four straight lines within the limits of experimental error. The equations for platinum are:

$$\log \mu/\rho = 2{\cdot}443 + 2{\cdot}60 \log \lambda, \quad . \quad . \quad . \quad (9)$$

$$\log \mu/\rho = 2{\cdot}347 + 2{\cdot}60 \log \lambda, \quad . \quad . \quad . \quad (10)$$

$$\log \mu/\rho = 2{\cdot}210 + 2{\cdot}60 \log \lambda, \quad . \quad . \quad . \quad (11)$$

$$\log \mu/\rho = 1{\cdot}816 + 2{\cdot}64 \log \lambda; \quad . \quad . \quad . \quad (12)$$

and for gold:

$$\log \mu/\rho = 2{\cdot}495 + 2{\cdot}91 \log \lambda, \quad . \quad . \quad . \quad (13)$$

$$\log \mu/\rho = 2{\cdot}395 + 2{\cdot}91 \log \lambda, \quad . \quad . \quad . \quad (14)$$

$$\log \mu/\rho = 2{\cdot}251 + 2{\cdot}64 \log \lambda, \quad . \quad . \quad . \quad (15)$$

$$\log \mu/\rho = 1{\cdot}848 + 2{\cdot}61 \log \lambda. \quad . \quad . \quad , \quad (16)$$

If $\log \mu/\rho$ at the absorption edge L_1 (the edge having the shortest wave-length of L_1, L_2, L_3) is calculated from each of these equations and differences are taken, the values given in column S of Table IV. are obtained.

TABLE IV.

	Levels compared.	R= Log of ratio of energy levels.	S= Log of ratio of absorption co-efficients.	R−S.
Platinum.	L_1/M_1	0·625	0·629	−0·004
	L_2/M_1	0·604	0·533	0·071
	L_3/M_1	0·544	0·396	0·148
Gold.....	L_1/M_1	0·623	0·628	−0·005
	L_2/M_1	0·603	0·528	0·075
	L_3/M_1	0·541	0·401	0·140

It has been found by E. Jonsson that the total L-absorption jump is equal to the ratio of the energy levels L_1 and M_1, and the figures in Table IV. agree with this to about 1 per cent. The same rule evidently does not hold for the partial L jumps, but in the case of platinum and gold the following equalities may be noted:

$$J(L_1/M_1) = (E_{L_1}/E_{M_1}), \quad . \quad . \quad . \quad . \quad . \quad (17)$$

$$J(L_2/M_1) = \frac{1}{k}(E_{L_2}/E_{M_1}), \quad . \quad . \quad . \quad . \quad (18)$$

$$J(L_3/M_1) = \frac{1}{k^2}(E_{L_3}/E_{M_1}), \quad . \quad . \quad . \quad . \quad (19)$$

where $k^2 = \sqrt{2}$. The numerical values are given in Table V.

TABLE V.

	Platinum.	Per cent. difference.	Gold.	Per cent. difference.
$J(L_1/M_1)$.....	4·26	0·9	4·25	1·2
(E_{L_1}/E_{M_1}).....	4·22		4·20	
$J(L_2/M_1)$.....	3·41	0·9	3·37	0·0
$\frac{1}{k}(E_{L_2}/E_{M_1})$.....	3·38		3·37	
$J(L_3/M_1)$.....	2·49	0·4	2·52	2·9
$\frac{1}{k^2}(E_{L_3}/E_{M_1})$.....	2·48		2·45	

These equalities may have no theoretical significance whatever, but as (17) appears to be true for all cases so far examined, any simple relations holding for one or two cases between the L_2 and L_3 jumps and the corresponding energy-level ratios seem worthy of notice.

No theory of absorption so far available appears capable of furnishing the magnitudes of either the K or L jumps with a reasonable degree of accuracy, but as pointed out recently by Richtmyer [11], the actual increase in absorption coefficient at the K-absorption edge is given to a fair degree of approximation by the theory of L. de Broglie [12]. The theory is equally successful in this respect for the L discontinuities of platinum and gold, although it gives values considerably too large for the ratios that constitute the absorption jumps. L. de Broglie's expression for the part of the atomic fluorescent absorption coefficient due to the electrons of the energy level E_x, where x stands for K, L, or M, etc., is

$$\tau_{ax} = (\pi e^2/mh^2c^4) \,.\, n_x \,.\, E_x^2 \,.\, \lambda^3, \quad \text{where } \lambda \not> \lambda_x. \quad . \quad (20)$$

The ratios of the absorption coefficients at the L-absorption edges should be, when scattering is negligible,

$$J_{L_3} = \frac{n_{L_3}E_{L_3}^2 + n_{M_1}E_{M_1}^2 + n_{M_2}E_{M_2}^2 + \ldots}{n_{M_1}E_{M_1}^2 + n_{M_2}E_{M_2}^2 + \ldots},$$

$$J_{L_2} = \frac{n_{L_2}E_{L_2}^2 + n_{L_3}E_{L_3}^2 + n_{M_1}E_{M_1}^2 + n_{M_2}E_{M_2}^2 + \ldots}{n_{L_3}E_{L_3}^2 + n_{M_1}E_{M_1}^2 + n_{M_2}E_{M_2}^2 + \ldots},$$

$$J_{L_1} = \frac{n_{L_1}E_{L_1}^2 + n_{L_2}E_{L_2}^2 + n_{L_3}E_{L_3}^2 + n_{M_1}E_{M_1}^2 + n_{M_2}E_{M_2}^2 + \ldots}{n_{L_2}E_{L_2}^2 + n_{L_3}E_{L_3}^2 + n_{M_1}E_{M_1}^2 + n_{M_2}E_{M_2}^2 + \ldots},$$

The calculated values in Table VI. are obtained with the aid of the table of energy levels in Siegbahn's book and by assuming Stoner's [13] distribution of electrons among the energy levels.

TABLE VI.

		J_{L_1}.	J_{L_2}.	J_{L_3}.
Platinum...	Experimental	1·25	1·37	2·47
	Calculated...	1·39	1·54	5·43
Gold	Experimental	1·26	1·36	2·53
	Calculated	1·38	1·54	5·40

Few other experimental values of the L-absorption jumps are available for comparison. In the paper in which he gave his absorption theory, L. de Broglie quoted without details the following as experimental values for platinum: $J_{L_1}=1·4$, $J_{L_2}=1·63$, $J_{L_3}=2·7$. A. Dauvillier [14] has made measurements on gold, using both ionization and photographic methods. Assuming a λ^3 law, he has apportioned the mass absorption coefficient at L_1 among the different electron groups as in Table VII.

TABLE VII.

Electron group.	M+N+O etc.	L_3.	L_2.	L_1.
Portion of μ/ρ.....	42	62	41	35

No other experimental figures are given, but the corresponding values of the absorption jumps would be $J_{L_1}=1·24$, $J_{L_2}=1·39$, $J_{L_3}=2·48$.

The increase in absorption coefficient at the absorption edge should be given directly by expression (20), which may be simplified to

$$\tau a_x=(\pi e^2/mc^2)n_x\lambda_x. \quad . \quad . \quad . \quad . \quad . \quad (21)$$

Calculated and experimental values are compared in Table VIII., and in view of the simplicity of expression (21), the agreement seems undoubtedly good, and lends support to Stoner's scheme of electron distribution.

L. de Broglie's theory undoubtedly gives with fair approximation the absorption produced by an electron at the critical wave-length at which it begins to absorb. It can give only very approximately the ratios of the absorption coefficients at the K and L edges, as it supposes absorption to fall off with decreasing wave-length according to the cube law, and for the L and M electrons the absorption does not fall off as fast as this. The values of the ratios

determined from the theory are in consequence all larger than those found experimentally.

The absorption of platinum and gold on both sides of the L discontinuities was measured by Allen, who obtained for platinum the equation $\tau/\rho = 345\,\lambda^{2\cdot92}$ corresponding to (9), and $\tau/\rho = 65\,\lambda^{2\cdot92}$ and $\tau/\rho = 66\,\lambda^{2\cdot6}$ corresponding to (12). and for gold, $\tau/\rho = 360\,\lambda^{2\cdot92}$ corresponding to (13), and $\tau/\rho = 69\,\lambda^{2\cdot92}$ and $\tau/\rho = 70\,\lambda^{2\cdot6}$ corresponding to (16). Allen has thus assumed a break in the absorption curve at 1·1 Å.U. for both platinum and gold. In view, however, of the author's results for the absorption between the two L edges nearest $\lambda = 1\cdot1$ Å.U. (equations (11) and (15)), where for both platinum and gold the index is much more nearly 2·6 than 2·9, it would appear improbable that any break at 1·1 Å.U. really occurs. Allen's equations with index

Table VIII.

Element.	Absorption edge.	Wave-length.	Assumed number of electrons.	Increase in absorption coefficient.	
				L. de Broglie's theory.	Experimental.
Platinum	L_1	0·892	2	50·3	41
	L_2	0·932	2	52·5	50
	L_3	1·070	4	120·4	115
Gold ...	L_1	0·861	2	48	41·6
	L_2	0·901	2	50	48·2
	L_3	1·038	4	116	118·7

2·6 for the M absorption agree well with equations (12) and (16), but his equations for the L absorption depart very considerably from (9) and (13) giving higher values of μ/ρ. The experimental values (figs. 3 and 4) found by Allen for the L absorption in this region are, however, for both platinum and gold in much nearer agreement with (9) and and (13). Values from Jonsson's Tables (figs. 3 and 4) are everywhere considerably higher for both platinum and gold than those given by equations (9), (12), (13), and (16), except between 1·5 and 2 Å.U.

Copper.

Results for copper are shown in Table II. and fig. 5. The wave-length range includes the K-absorption edge, and the equations found are

$$\log \mu/\rho = 2\cdot116 + 2\cdot72 \log \lambda, \quad . \quad . \quad . \quad (22)$$

$$\log \mu/o = 1\cdot173 + 2\cdot95 \log \lambda. \quad . \quad . \quad . \quad (23)$$

The ratio J_K of the absorption coefficients at the K edge is 8·15, and the increase in μ/ρ is 276. On the theory of L. de Broglie the ratio should be about 20 and the increase in μ/ρ 239. Jonsson has calculated E_K/E_{L_1} to be 8·23, and found 8·2 experimentally for J_K. It is particularly noteworthy that the slope of the K-absorption curve in the neighbourhood of the K edge on a ($\log \mu/\rho$, $\log \lambda$) graph is considerably less than the slope of the L curve near the K edge. Richtmyer and Warburton[15] found that copper accurately followed

Fig. 5.

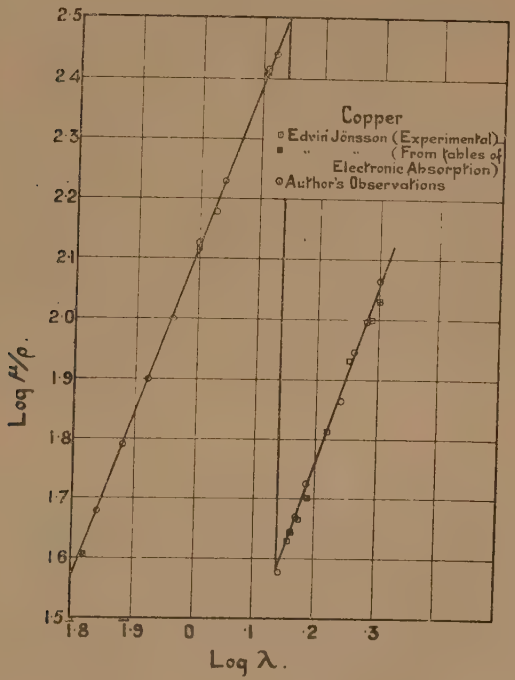

the cube law between 0·12 Å.U. and 0·30 Å.U., but concluded that the law did not hold near the K edge. Allen obtained the equation $\tau/\rho = 132\lambda^{2·70}$ for wave-lengths between 0·85 Å.U. and the K edge, and L. H Martin found 2·8 as the index. Alexander, who attributed the departure from the simple cube law to multiple ionization, found experimentally the equation $\mu/\rho = 128·8\lambda^3 + 6·0$ near the K edge.

Values for copper calculated from Jonsson's tables are in

good agreement with equation (22) above, and are shown in fig. 5. Most of the available data for copper agree in giving a relation between μ/ρ and λ for the K absorption near the K edge which cannot be expressed accurately by an equation of the form $\mu/\rho = a\lambda^3 + \sigma/\rho$, where by σ/ρ is meant the actual mass scattering coefficient.

On the other hand, the part of the L-absorption curve near the K edge shows a very near approach to the cube law and, in fact, between the K edge and 2 Å.U. could just be represented by it within experimental error, although the best fit to the data in Table X. is provided by equation (23). For this region of wave-length, Allen found the equation $\tau/\rho = 14{\cdot}5\,\lambda^{2{\cdot}92}$ and Martin $\mu/\rho = 14{\cdot}1\,\lambda^3$, both in near agreement with above. Jonsson's tables give for any element on a ($\log \mu/\rho$, $\log \lambda$) graph an absorption curve the slope of which decreases everywhere with increase of λ, and the curve for copper, although coinciding very closely with that given by equation (22) from $\log \lambda = \bar{1}{\cdot}8$ up to the K edge, shows no increase in slope between the K edge and $\log \lambda = 0{\cdot}3$ to correspond to equation (23). Jonsson's experimental points (fig. 5) show, however, quite good agreement with equation (23), and the best straight line through them would have a slope slightly greater than 2·95. On the whole it seems, therefore, that the average electronic absorption cannot be accurately the same function of $N\lambda$ for all elements, although it would appear to be very nearly so.

Summary.

A description is given of a form of X-ray tube convenient for absorption measurements with homogeneous radiation in the neighbourhood of 1 Å.U., and the results are given of measurements with silver, aluminium, platinum, gold, and copper for wave-lengths between 0·63 and 2 Å.U. The relation between absorption and wave-length was nowhere found to conform exactly to the cube law, the departure from this law often being very considerable. The question is considered as to the possible existence of discontinuities due to multiple ionization. No general law has been found that would fit accurately the data obtained for all the elements examined, although that found recently by Edvin Jonsson appears to furnish a good approximation. The K-absorption jump of copper and the L-absorption jumps of platinum and gold were measured, and the results are compared with theory.

In conclusion the author wishes to thank Dr. Kaye, the Superintendent of the Physics Department, for the provision of facilities for this research, and especially for his continued interest.

References.

(1) *E.g.*, A. H. Compton, 'X-Rays and Electrons,' p. 530 (Macmillan & Co., London, 1927), and Maurice de Broglie, 'X-Rays,' p. 57 (Methuen & Co., London, 1925).
(2) E. Wagner and H. Kulenkampff, *Ann. der Phys.* (4) lxviii. p. 369 (1922).
(3) Lowell M. Alexander, Phil. Mag. xxiii. p. 670 (1927).
(4) S. J. M. Allen, Phys. Rev. xxvii. p. 266 (1926), and xxviii. p. 907 (1926).
(5) F. K. Richtmyer, Phys. Rev. xviii. p. 13 (1921).
(6) F. K. Richtmyer, Phil. Mag. vi. p. 64 (1928).
(7) L. A. Turner, Phys. Rev. xxvi. p. 143 (1925).
(8) G. Wentzel, *Ann. der Phys.* lxvi. p. 437 (1921); *Zeits. f. Phys.* xxxi. p. 445 (1925).
(9) E. Jonsson, "Absorptionsmessungen im langwelligen Rontgenbiet und Gesetze der Absorption," *Uppsala Universitets Årsskrift*, 1928, *Matematik och Naturvetenskap* 1.
(10) L. H. Martin, Proc. Camb. Phil. Soc. xxiii. p. 783 (1927).
(11) F. K. Richtmyer, Phys. Rev. xxx. p. 755 (1927).
(12) L. de Broglie, *Journ. de Phys. et le Radium*, iii. p. 33 (1922).
(13) E. C. Stoner, Phil. Mag. xlviii. p. 719 (1924).
(14) A. Dauvillier, *Comptes Rendus*, clxxviii. p. 476 (1924).
(15) F. K. Richtmyer and F. W. Warburton, Phys. Rev. xxii. p. 539 (1923).

XL. *On the Interpretation of X-Ray Crystal Photographs.*—Part I. *Use of Photographic Grids.* *By* Wm. H. George, *M.Sc., Ph.D., F.Inst.P., Assistant Lecturer in Physics in the University of Leeds* *.

[Plate VI.]

Summary.

The paper describes a *photographic grid method*, applicable to any X-ray spectrometer, of measuring X-ray photographs. The photographic plate or film is supported in the X-ray camera (*e.g.*, fig. 1) *entirely* by geometric constraints. A flash of light, together with a printing frame (fig. 2), also fitted with geometric constraints, is used to impress upon the X-ray photograph an image of some network suitable for the interpretation of the particular type of X-ray photograph. A single calibration photograph is taken, and used to fix accurately the geometric

---

* Communicated by Prof. R. Whiddington, F.R.S.

constraints of the printing frame. Any subsequent photograph then shows on development both the X-ray photograph and a correctly aligned interpretative grid (*e. g.*, fig. 3, Pl. VI.).

Various modified applications of the method in X-ray crystallography are discussed, and also the application of grid methods to research in subjects other than X-ray crystallography.

IN all research work much time has to be spent upon tasks which do not demand creative thought, and it is usually best to carry out these tasks by almost any adequate method which occurs to the worker rather than to spend long periods seeking elegant methods. In the subject of X-ray crystallography the conditions would appear to be different, for here many workers in all parts of the world have to carry out again and again the same type of task.

The first stage in present-day crystal analysis consists in an attempt to determine the space-group of the crystal. A careful analysis of this process shows that whilst the X-ray crystallographic part of the work involves considerable skill and experience, it does not, in general, demand creative thought. We are therefore justified in regarding the worker, whilst he is carrying out this part of the analysis, as an operating machine. The methods here described are the result of a critical examination of the efficiency of this machine.

Measurement of X-Ray Photographs.

An essential part of the interpretation of any crystal X-ray photograph consists in a determination of the position upon the plate or film of the spots or lines which record X-ray diffraction effects produced by planes in the crystal. It is the purpose of the present paper to show how this measurement of photographs can be made by what may be called a *photographic grid method*. A flash of light is used to impress upon the plate or film a correctly-placed latent image of any set of lines or points which may be useful in interpreting the particular type of photograph. On development the sensitive film shows both the X-ray picture and a suitably-placed interpretative grid. A full application of the principle of *geometric constraints* is essential to the method. After an initial calibrating photograph has been taken, the precision required in all subsequent photographs is achieved automatically.

Before describing the essential details, we may note the alternative methods available for the measurement of X-ray crystal photographs.

Direct Measurement.

The photograph may be directly measured by use of dividers, transparent or opaque scales, or a measuring microscope. When these methods are applied to any but the simplest X-ray photograph, they are exceedingly long and tedious. Moreover, the measuring microscope gives an accuracy much greater than is normally required in X-ray crystallography as distinct from that required in X-ray spectroscopy. Its use is needed only for very accurate determination of the size of the unit cell, for which photographs having sharply-defined lines are necessary.

Bernal Method for Rotation Photographs.

The second method, due to Bernal *, is applicable to single crystal rotation photographs when reciprocal lattice theory is to be used for interpreting the results of the measurements. The method as described consists in using an enlarging lantern to project an image of the X-ray photograph on to a chart from which two of the reciprocal lattice cylindrical coordinates of the spot may be directly read. In actual practice the images of many of the spots projected on to the chart cannot be seen. Moreover, if the chart were intended for use in this way, it would have been printed on white opaque paper instead of on tracing paper. The publication of the method in this impracticable form was an oversight, and on the suggestion of Mr. Bernal the best method devised by him is here described.

Four operations are necessary for each photograph :— (i.) An opaque spot of ink is put as near as possible to the centre of each X-ray spot (on the glass side of the negative if a plane plate is used). (ii.) Some optical enlarging device is adjusted to give a magnification of $10/r$ for a plane plate or $5/r$ for a cylindrical film, where r is the distance of the plate or film from the crystal. (iii.) An image of the plate or film is then projected on to a sheet of paper, and again an ink spot is placed as near as possible to the centre of each projected spot. (iv.) The appropriate chart (I. for a plane plate or II. for a cylindrical film), printed on tracing-paper, is then fitted over this projection so that, for as many as possible of the sets of four points (or pairs on the equatorial layer-line), each of the points in a set gives the same reading on the chart.

In actual practice the fitting of the chart is difficult, for even if the plate is truly perpendicular to the X-ray

* Proc. Roy. Soc. A, cxiii. p. 130 (1926).

beam and parallel to the axis of rotation of the crystal, the "spotting in" both on the original negative and on its projection, together with the defects of the optical system, introduces errors. These errors are such that the four-fold (or twofold on the zero layer-line) symmetry of the rotation photograph is destroyed. Still greater difficulty is experienced with oscillation photographs, for these have at most only two quadrants alike, whilst the most general type (little used at present) have all four quadrants different.

In the methods now to be described all these operations, and the consequent errors introduced by them, are eliminated. The accuracy attained is equal to that of any of the other methods, with the exception of the use of the travelling microscope in the measurement of sharply defined lines, such as are obtained in spectroscopy.

Fig. 1.

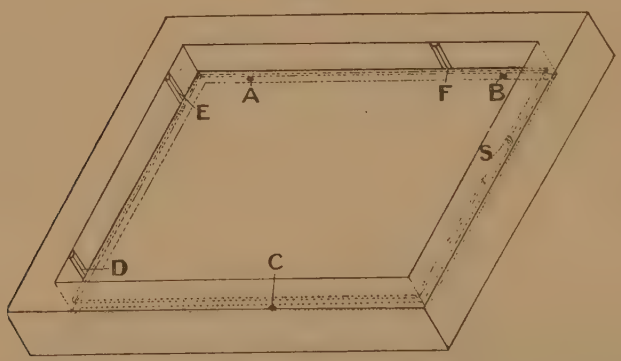

Typical plane-plate X-ray camera fitted with six geometric constraints.

Photographic Grid Method.

In adopting the photographic grid method, two modifications of the X-ray apparatus are normally required. The first is an addition to the X-ray camera of three geometric constraints or their equivalent. The second is the preparation of a printing-frame.

Modification of X-Ray Camera.

(i.) *Plane Plate.*

In all types of photographic spectrometer the plate-holder of the X-ray camera is provided with three geometric constraints (*e. g.*, three spherical-ended screws, ABC of fig. 1) or their equivalent, on to which the sensitive film

of the photographic plate is pressed by a spring or by gravity. By this means the distance of the sensitive film from the crystal is known from an initial calibration of the instrument. However, with this arrangement the plate still has three degrees of freedom. If the grid method is to be used, these three remaining degrees of freedom must be removed by the addition to the camera of three more constraints acting upon two edges of the plate. For example, three steel rods or agate knife-edges may be fixed inside the camera at DEF of fig. 1. The spring (S) serves to keep the plate pressed against the constraints (DE). A spring opposite to F has not been found necessary. So long as the principle of removing the remaining three degrees of freedom of the plate is obeyed, the constraints may be added in any convenient way, and it is usually quite unnecessary to have a new camera made. Care must be taken that the constraints stand out far enough to prevent any irregularity in the edge of the plate from touching the interior of the camera. That is, even the most roughly cut photographic plate must be supported *solely* by the six constraints, ABCDEF.

Calibration Photograph.—When these additions have been made to whatever type of plate-holder is used, the camera is loaded with a plate pressed against the six constraints, and a complete rotation photograph is taken by rotating about the needle axis any fine needle-shaped crystal which gives good body reflexions of X-rays. The crystal should be carefully *centred* so as to give some sharply-defined narrow black spots on the photograph, which is required as a calibration photograph determining once and for all the relative positions of the three constraints DEF and the axis of rotation or support of the crystal on the spectrometer. A Laue photograph might also be used as a calibration photograph.

(ii.) *Cylindrical Camera.*

The modification necessary to the ordinary cylindrical camera will be clear if the following details are noted. It will be found that the edges of commercial films are straight to a high order of accuracy. To the bottom of the X-ray cylindrical camera is added a narrow horizontal rim perpendicular to the sides of the cylinder, and in loading the camera the X-ray film is always pushed down so that its bottom edge rests on this ledge (1 mm. wide or so). The film is then rotated round inside the cylinder until one

of the vertical edges touches a stop. This stop may be a cylindrical metal pin pushed radially through the side of the cylindrical camera wall at a height (*d*) above the bottom of the film, of about half the width of the film. An opaque black paper envelope having three sides sealed should be prepared for permanent use. One of its dimensions should be about 1 mm. less than the height of the particular size of film used, and at one edge a small hole should be cut at height (*d*) above the bottom of the film. This ensures that the bottom edge of the film and the point of a vertical edge actually touch the constraints provided. As a minor point, it may be noted that errors due to distortion of the film caused by a wrinkled black paper envelope may be avoided

Fig. 2.

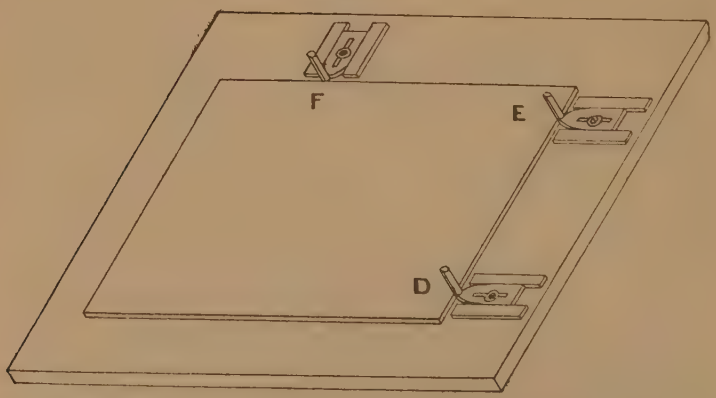

Printing-frame fitted with three geometric constraints.

by preparing the envelope upon a cylinder and allowing the gum or paste to dry whilst the envelope is still on the cylinder. This envelope is, of course, necessary whether or no the grid method is used.

As before, a calibration photograph must be taken for use in setting the constraints of the printing-frame.

We come now to the second modification necessary when the grid method is to be adopted.

Initial Preparation of the Printing-frame.

Fig. 2 shows a convenient form of printing-frame. This consists of a brass frame into which is sealed permanently a glass plate, the *grid*, the preparation of which is dealt with in the following section. Three constraints, DEF, consisting

again of steel cylinders or agate knife edges perpendicular to the plane of the grid, are initially adjustable in a direction perpendicular to the edge of the plate. Since the edges of commercial plates and films are *not* straight edges *mutually perpendicular*, it is essential that the *constraints in the printing-frame touch the same points of the X-ray plate or film as do those in the X-ray camera.*

The final stage in the initial preparation of the printing-frame consists in brightly illuminating the grid from below and carefully adjusting, relative to it, the calibrating X-ray photograph. When this has been done, the constraints of the frame are moved up to touch the edges of the plate or film, and are there screwed down firmly. Spring washers under the screw-heads facilitate the adjustment. The X-ray photograph having been removed, the printing-frame is then ready for use.

Preparation of Grid.—The grid consists of a glass plate having a relatively opaque background and transparent lines or spots. Its method of preparation depends mainly upon the nature of the lines or spots, and this in turn depends upon the theoretical method to be adopted for interpreting the measurements made upon the photograph. We will assume that the choice of network has been made. Simple networks such as sets of straight lines or circles can be machine-ruled.

A more widely applicable method consists in using a good camera, such as is used for preparing lantern-slides, to prepare the grid photographically. The network should be drawn on a large scale with Indian ink upon white Bristol board or good tracing-cloth, the width of the lines used being such that fine lines are obtained upon the grid with the particular scale of reduction used. The drawing should be brightly illuminated with as uniform a distribution of intensity as possible so as to give uniform opacity to the background of the grid. Drawings upon tracing-cloth may be illuminated from behind through an opal glass screen, and any drawing should be so aligned relative to the camera that the centre of the network is about 1 mm. off the centre of the photographic plate. This ensures that when the grid has been sealed in the routine brass printing-frame the X-ray plate will overhang the edges of the grid by about 1 mm., and so permit contact with the three geometric constraints.

In photographic preparation of grids, slow-process plates should be used and development should be carried out slowly in a hydroquinine developer. In brief, the technique of the antern-slide maker should be used. As these photographic

grids are required for permanent use, great care should be taken to fix and wash them thoroughly. It would probably be convenient to protect the film side with a coat of suitable varnish, although the writer has used an unprotected grid for one year without producing in it any appreciable signs of wear.

If reciprocal lattice theory is to be used for the interpretation of rotation or oscillation X-ray photographs, one or other of the Bernal (*ibid.*) charts should be used in preparing a suitable grid. For a plane plate, Chart I. should be photographed with a reduction of $10/r$, and for a cylindrical film, Chart II. with a reduction of $5/r$, where r is the distance in cm. from the crystal to the sensitive film. An example of the use of a grid, prepared from Chart II., is shown in Pl. VI. (fig. 3).

If measurements upon an X-ray photograph are required in cms., quite good grids can be prepared by the use of the old-fashioned engraved graph paper. Examples of the use of such grids are reproduced elsewhere *. They were there used for research in acoustics.

Routine Use of Printing-frame.—When the grid has been prepared and sealed into the printing-frame and the three constraints, DEF, have been permanently screwed down by aid of the calibration photograph, the printing-frame is ready for routine use. It is convenient to fix it horizontally over a hole in the bench in the photographic dark-room, and at about 1 metre below it a pocket flash-lamp bulb and battery should be fixed and connected to a tapper- or morse-key on the bench.

When the X-ray camera is to be loaded with a *plane plate*, the photographic plate is first placed film side downwards on to the grid, and is pushed up to the constraints, DEF of fig. 2. The key is then tapped for a fraction of a second, and the plate is placed against the constraints of the camera (fig. 1), the image of the grid remaining latent during the X-ray exposure. If preferred, this printing of the grid may, of course, be done after the X-ray exposure, just before the plate is put in the developing-dish. The complete operation does not occupy more than 2–5 seconds. The tapping of a key does not provide a fine adjustment of the exposure to light, but in practice it is quite as accurate as is necessary. Each worker gets used to tapping so as to give, on development, lines of the intensity which suits him best. For example, if he anticipates giving an over

* George, Phil. Mag. (6) xlvii. p. 591 (1924), xlviii. p. 34 (1924); 'Nature,' cxiii. p. 387 (1924).

exposure to X-rays the flash of light should be longer, since the plate will not be developed for so long. The flash-lamp can be covered with one or more layers of white tissue paper if it is too bright. The plates used by the writer seem to need a shorter exposure to light in the grid printing than the films used.

When the X-ray camera is to be loaded with a *cylindrical film*, the operations are almost the same as for a plate, except that after the film has been placed on the grid, it should be pressed in contact with the grid before the morse-key is tapped. An old photographic plate covered with black paper is suitable for this purpose. The final pushing of the film on to the constraints of the printing frame should be done *after* the film has been pressed flat. A corner may be cut of the film to identify the edge which has been pressed against the single constraint (*i. e.*, the constraint which is at height d above the bottom edge of the film). The film is then put in the envelope, and the camera is loaded as previously described (p. 377). The modifications necessary with the type of cylindrical camera in which the cylindrical form is imposed upon the film by pressing it on to the *outside* of a cylinder will be obvious.

No matter what type of camera be used, it is of the utmost importance to the success of the grid method that the plate or film be supported *solely* by geometric constraints which actually touch the plate or film. The particular type of constraints used is unimportant. The plate or film may be rigidly fixed in some other frame, the edges of which may be used to make contact with the constraints if this is found more convenient.

When the grid method as here described is used, every photograph shows on development both the X-ray photograph and the *correctly-placed* interpretative grid. The coordinates of the spots are read off directly by eye with or without the aid of a low-power large-field lens, whilst the X-ray plate is illuminated from behind by diffused light (*e. g.*, a large sheet of brightly illuminated white blotting-paper having a matt surface, or opal glass illuminated from behind). An example is shown in Pl. VI. (fig. 3). The grid used was prepared from the Bernal Chart II., and the X-ray photograph was prepared by rotating about a cubic axis a diamond (slightly mis-set). In the figure the axis of rotation is horizontal. None of the slight fogging of the film is due to the light used in the grid process, as can be seen by examining the parts of the original film which were protected by metal clips during the X-ray exposure.

The irregular fogging was introduced by the photographic processes used to get a reproduction of black spots on white background so as show the appearance of the original film.

Partial Applications of the Methods.—Various partial applications of the methods here described are of value in special cases.

If it is not desired to have any markings on the X-ray plate except those produced by the X-rays, then a print on to another photographic plate can be made from the grid plate. This print is placed and fitted over each X-ray plate or film in turn so that the sensitive sides are in contact. Several research workers are now using, in this way, grids prepared from the Bernal charts. The objections to this method are that (i.) the fog of the grid plate is added to that of the X-ray plate, (ii.) each X-ray negative needs a new fitting of the chart and is liable to be displaced during use, and (iii.) a layer of glass is always interposed between the observer and the X-ray spots and lines.

For purposes of reproduction an ordinary X-ray negative can be clamped on to one of these glass prints from a grid, and the two together used in the ordinary photographic enlarging lantern *.

The principle of the geometric constraints could be very conveniently applied to work with the measuring microscope, for, by providing three more constraints than usual, every plate to be measured would merely need to be pushed on to the constraints in order to be correctly aligned for the measuring process.

Advantages of the Complete Grid Method.—The grid method, by the use of a single skilled operation (the setting of the three constraints, DEF of fig. 2), entirely replaces the many hundreds of skilled operations carried out by the X-ray crystallographer in one year alone. It therefore saves an appreciable amount of his time and energy. It is not usual to discuss this "efficiency" of the worker in research, but its consideration is forced upon the X-ray crystallographer by the excessive amounts of time he finds himself spending in operations which are neither creative thinking nor operations directly required as the result of such thought.

The negative obtained when the complete grid method is used is, of course, a fuller record than is an ordinary X-ray negative, and it can be interpreted away from laboratories. For example, if a suitable Bernal chart be used to prepare

* Moseley Student's Report to the Royal Society, 1927.

the grid, then a single crystal rotation or oscillation photograph can be interpreted without the interpreter knowing the plate distance or the wave-length of the monochromatic X-rays used to prepare the photograph. In a precision cylindrical camera used for taking a complete rotation photograph, only one-quarter of the usual sized film need be used. For most oscillation photographs (all except the most general, where all four quadrants of the photograph are different), only half the usual size of film is required. In all photographs the "centre" is permanently determined and recorded for the given spectrometer. The writer would suggest that the reproduction in a scientific journal of one-quarter of a single crystal rotation photograph taken with the use of the grid method, would record more information concerning the actual results of the experimental part of the research work relevant to crystal structure determination, than would a table showing the results of very accurate measurements made with a measuring microscope upon the X-ray negative. This statement may appear controversial when one examines some of the papers on crystal structure now published, but it can best be discussed later when the methods of determining indices are treated.

A curious feature is observed when the grid method is used with films. These are coated on both sides with sensitive material, and the X-rays, of course, penetrate through the film, producing a blackening on both sides of the developed record. The light used to print the grid, however, does not penetrate through the first layer of sensitive gelatine. Hence a film taken by the grid method shows in transmitted light both the network and the X-ray photograph, but when it is examined by light reflected from one side only, it shows only the X-ray photograph if the side examined is the one which was not in contact with the grid plate in the printing frame.

Use of Grid Method in other Types of Research.—The grid method could usefully be applied to many types of experimental research work where the same kind of photograph is taken many times. For example, in instantaneous photography, if the film or plate be supported by geometric constraints, then its position relative to the phenomenon being photographed is always the same to a high degree of accuracy. One modification which the writer (*ibid.*) found useful in optical photography consists in incorporating the grid into the apparatus so that a separate printing-frame is unnecessary. This simplification is not possible in X-ray photography nor in optical photography with radiation

which would be heavily absorbed by the grid plate. Care must be taken, when this simplified process is used, that the focussing is correct *after* the radiation has passed through the grid plate.

Acknowledgments.

The methods here described were devised whilst I was working as the Moseley Student of the Royal Society at the Davy Faraday Laboratory of the Royal Institution, London. I therefore wish to thank the Royal Society for financial aid and Sir Wm. Bragg and the Managers of the Davy Faraday Laboratory for their generous hospitality there.

It is hoped to deal in Part II. with certain types of rotation photographs taken with the grid method, and in Part III. with moving-film photographs.

XLI. *Note on the Platinum Thermometer Temperature Scale.* *By* F. E. Hoare, *B.Sc., A.R.C.S., Assistant Lecturer in Physics, University College of the South-West of England, Exeter* *.

AT the Seventh General Conference (1927) of the International Bureau on the International Temperature Scale it was recommended that platinum thermometers should be used for the realization of the absolute scale from the ice point to 660° C., the temperature to be deduced from the formula

$$R_t = R_0(1 + at + bt^2).$$

The constants R_0, a, and b should be determined from the ice, steam, and sulphur points respectively, the purity and physical condition of the platinum being such that the ratio $\frac{R_t}{R_0}$ shall not be less than 1·390 for $t = 100°$ C., and 2·645 for $t = 444·6°$ C. Hence the fixed value of the difference coefficient d, usually taken as $1·5 \times 10^{-4}$, in the equation

$$X = t - pt = d(t - 100)t,$$

where pt is the temperature on the platinum scale, has not been adopted, but must be separately determined for each thermometer.

* Communicated by Prof. F. H. Newman.

In order that the solution of a large quadratic equation for each temperature may be avoided, it is very convenient in practice to calculate the value of the correction X to be applied to the platinum thermometer temperature, as defined by the equation

$$pt = \frac{R_t - R_0}{R_{100} - R_0} \times 100$$

for any value of the difference coefficient, from tables which give the value of the correction for a certain value of d. This may be done in the following manner.

Consider two platinum thermometers which are at the same temperature as calculated on the platinum scale. Let the difference coefficients for the two thermometers be d and d', and the centigrade temperatures to which the platinum temperature corresponds be t and t' respectively. Then

$$X = t - pt = d\,(t-100)t$$

and

$$X' = t' - pt = d'(t-100)t',$$

where X and X′ represent the corrections to be applied to the first and second thermometers respectively.

Also let

$$t' = t + x \quad \text{and} \quad d' = d + y.$$

Then

$$t + x - pt = (d+y)\,(t-100+x)\,(t+x);$$

and on expanding and substituting $t - pt = d(t-100)t$,

$$x = \frac{yt(t-100)}{1 - d'(2t-100+x)}$$

$$= \frac{yt(t-100)}{1 - d'(2t-100)},$$

if, as is usually the case in practice, x is small in comparison with $2t-100$.

Therefore

$$x = \frac{y\mathrm{X}}{d\{1 - d'(2t-100)\}}. \quad \ldots\ldots \quad (1)$$

The value of t is directly obtainable from the tables already mentioned, as is also the value of X. Solving this equation for x is a much simpler operation than determining t' from the ordinary quadratic equation.

The temperature t' is given by the equation

$$t' = pt + \mathrm{X} + x:$$

and if $d'(2t-100)$ is small in comparison with unity, the correction reduces to

$$X' = X + x = \frac{d'}{d} \cdot X,$$

which is the form proposed by Griffiths *. This correction is not accurate, and can be used only for the most approximate work.

The relative accuracy of the method given above for finding the correction for any value of d is illustrated in the following table. The second and third columns are the values of the temperature on the centigrade scale, obtained by solving the equations for X and X′, for certain values of *pt*, using different values for d. The fourth column gives the temperature obtained by using equation (1), assuming $d = 1{\cdot}5 \times 10^{-4}$ and $d' = 1{\cdot}6 \times 10^{-4}$.

	t° C.		
pt.	$d=1{\cdot}5\times10^{-4}$.	$d=1{\cdot}6\times10^{-4}$.	Using equation (1).
197°	200	200·2101	200·2101
470°	500	502·3375	502·3364
1002°	1200	1220·9977	1220·8861

Thus, even at such a high temperature as 1200° C., and using a value of d' which is outside that generally obtained in practice, the correction gives temperatures correct to a tenth of a degree centigrade. The calculations can usually be made with sufficient accuracy on an ordinary slide-rule.

XLII. *On the Thermal Efficiency of Standard Cycles for Internal Combustion Engines.* *By* H. H. Jeffcott †.

Introductory.

1. THE principal object of the present paper is to give an account of a simple method for the calculation of the thermal efficiency of certain standard cycles for internal combustion engines using as the working fluid air or other real gas of which the specific heats vary with the temperature.

Sir Dugald Clerk, in his recent ‡ paper on Standards of

* 'Nature,' liii. p. 45 (1895).

† Communicated by the Author.

‡ Sir Dugald Clerk, "Standards of Thermal Efficiency for Internal Combustion Motors," Min. Proc. Inst. C.E. ccxxv. p. 279 (1928).

Thermal Efficiency, states that "the time has come for the application of accumulated knowledge to the substitution of real working fluids for the ideal properties which were necessary because of ignorance of the real." In the following pages the working fluid will ordinarily be supposed to be air, but the method will be developed so as to be of general application.

2. The symbols used are as follows :—

The suffixes 1, 2, 3, 4 refer to the four corners of the indicator diagram, and correspond respectively to the commencement of compression of the charge, the end of compression, the end of ignition or commencement of expansion, and the end of expansion or commencement of discharge.

p represents the pressure of the working fluid.
v ,, ,, volume of the working fluid.
t ,, ,, temperature of the working fluid, ° C.
T, T′ ,, ,, temperature of the working fluid, ° C. absolute.
C_p ,, ,, specific heat of the working fluid at constant pressure in heat units.
C_v, ,, ,, specific heat of the working fluid at constant volume in heat units.
R ,, ,, gas constant.
γ ,, ,, ratio $\frac{C_p}{C_v}$ for the working fluid.
H ,, ,, total heat of the working fluid at T, p, and v.
η ,, ,, thermal efficiency of the cycle.
r ,, ,, ratio of compression $\frac{v_1}{v_2}$.
r' ,, ,, ratio of expansion $\frac{v_4}{v_3}$.
ρ ,, ,, ratio $\frac{v_3}{v_2}$.
ρ' ,, ,, ratio $\frac{v_4}{v_1}$.
σ ,, ,, ratio $\frac{p_3}{p_2}$ in cycle V.
ϕ(T) and ψ(T) represent functions of T defined in paragraphs 6 and 7.
$a', a, b, c \ldots k, l, m$ represent various numerical constants.

3. We shall consider five different ideal cycles on the pressure-volume diagram. The principal features are indicated in figs. 1–5.

All these cycles are made up of adiabatics, and of straight lines on the diagrams. For all cycles the thermal efficiency is measured by

$$\frac{\text{Heat input} - \text{Heat rejected}}{\text{Heat input}}.$$

4. The specific heats of gases at constant pressure and at constant volume vary with the temperature, and the extent of this variation can exercise an important influence on the thermal efficiencies of ideal cycles of the kind here considered. For the working fluids met with in practice, the specific heat may be represented with close approximation by an algebraical expression in ascending powers of T, where T represents the absolute temperature. Thus we can find appropriate values of the coefficients a, b, c ..., so that

$$C_v = a + bT + cT^2 + \ldots$$

is a close approximation. The difference of the specific heats $C_p - C_v$ is approximately constant, and accordingly

$$C_p = a' + bT + cT^2 + \ldots$$

so that

$$a' - a = C_p - C_v = R.$$

We are justified in using an algebraical expression of this kind, for the coefficients can be chosen so that the values of the specific heats calculated therefrom will lie within the probable errors of the experimental values corresponding to the various values of the temperature that fall within the range to be considered. Moreover, we propose to apply to such approximate representation the process of integration only, and not differentiation, so that mathematically we are on safe ground.

5. It is necessary to employ the fundamental relation for gases connecting pressure, volume, and temperature. In this investigation the simple approximate relation

$$pv = RT \quad . \quad . \quad . \quad . \quad . \quad . \quad . \quad (1)$$

will be sufficiently exact for our purpose, having regard to the ranges of temperature and pressure involved.

Other equations have been proposed by various workers more accurately representing the relation of pressure, volume,

and temperature for various gases, notably those suggested by van der Waals, Clausius, Boltzmann, Berthelot, Kamerlingh Onnes, Dieterici, and Wohl. Thus van der Waals's equation is of the form

$$\left(p+\frac{\alpha}{v^2}\right)(v-\beta)=\mathrm{RT},$$

where α refers to the cohesive forces between the molecules, and β refers to the volume occupied by them.

Figs. 1–5.

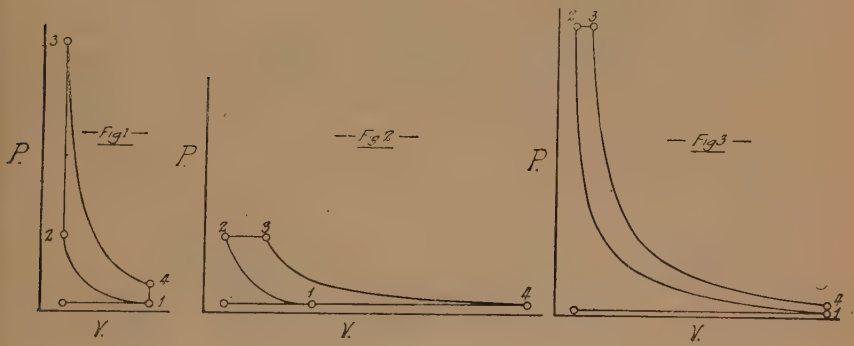

Figs. 4 & 5.

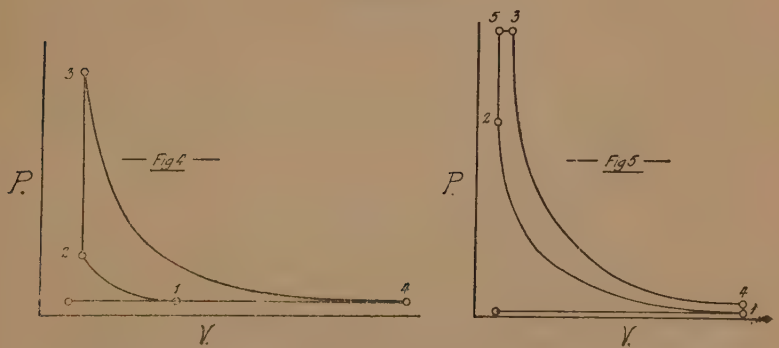

When the pressure is measured in atmospheres, and the volume is unity at 0° C. and one atmosphere pressure, then for air $\alpha=\cdot00257$ and $\beta=\cdot00209$, or, according to some observers, $\beta=\cdot00156$.

Having regard to the degree of accuracy required for our present purpose, and to the values of p and T involved, it will be seen that the simpler equation $pv=\mathrm{RT}$ is a sufficiently close approximation for the behaviour of the gas.

6. *Equation to Adiabatic.*—The adiabatic on the pressure-volume diagram is conditioned by the fact that no external heat is transmitted to or taken from the working fluid in passing from one point to another on the adiabatic curve. In particular we consider two adjacent points on the curve of which the coordinates are p, v and $p+dp$, $v+dv$, the corresponding temperatures being T and T$+d$T. The increment of heat dH added to or taken away from the working fluid is measured by $C_v d\mathrm{T}+p\,dv$, since $C_v d\mathrm{T}$ represents the change of internal energy of the gas, and $p\,dv$ is the work done in its expansion.

For every consecutive pair of points on the adiabatic this increment must be zero. Accordingly we have

$$d\mathrm{H} = \mathrm{C}_v dt + p\,dv = 0. \quad . \quad . \quad . \quad . \quad . \quad (2)$$

Also $$pv = \mathrm{RT}.$$

Hence $$\mathrm{C}_v \frac{d\mathrm{T}}{\mathrm{T}} + \mathrm{R}\frac{dv}{v} = 0.$$

Therefore

$$\int \mathrm{C}_v \frac{d\mathrm{T}}{\mathrm{T}} + \mathrm{R}\log_e v = k,$$

where k is a constant of integration.

Now

$$\mathrm{C}_v = a + b\mathrm{T} + c\mathrm{T}^2 + \ldots.$$

Hence, on integrating,

$$a\log_e \mathrm{T} + b\mathrm{T} + \frac{c}{2}\mathrm{T}^2 + \ldots + \mathrm{R}\log_e v = k.$$

Let $\phi(\mathrm{T})$ represent

$$a\log_e \mathrm{T} + b\mathrm{T} + \frac{c}{2}\mathrm{T}^2 + \ldots.$$

Hence, for an adiabatic,

$$\phi(\mathrm{T}) + \mathrm{R}\log_e v = k.$$

If v_1, T_1 and v_2, T_2 be the volumes and temperatures at two points on the same adiabatic,

$$\phi(\mathrm{T}_2) - \phi(\mathrm{T}_1) + \mathrm{R}\log_e v_2 - \mathrm{R}\log_e v_1 = 0.$$

Representing $\frac{v_1}{v_2}$ by r, this becomes

$$\phi(\mathrm{T}_2) - \phi(\mathrm{T}_1) = \mathrm{R}\log_e r. \quad . \quad . \quad . \quad . \quad (3)$$

In like manner we obtain for the adiabatic, through v_3, T_3 and v_4, T_4,

$$\phi(T_3)-\phi(T_4)=R\log_e r', \quad . \quad . \quad . \quad . \quad (4)$$

where

$$r'=\frac{v_4}{v_3}.$$

In passing, we observe that, if $b=c=\ldots=0$,

$$\log_e T_2-\log_e T_1=\frac{R}{a}\log_e\frac{v_1}{v_2},$$

and as $\frac{R}{a}=\gamma-1$, this reduces to

$$p_2v_2^{\gamma}=p_1v_1^{\gamma},$$

which is the equation to the adiabatic when C_p' and C_v' are constant.

7. We next consider the heat put in or abstracted along one of the straight lines of the pressure-volume diagram. For the sake of generality we shall take a line oblique and having as its equation

$$p=lv+m. \quad . \quad . \quad . \quad . \quad . \quad . \quad (5)$$

As in paragraph 6, the increment of heat dH added in passing from p, v to $p+dp$, $v+dv$ is

$$dH=C_v dT+p\,dv, \quad . \quad . \quad . \quad . \quad . \quad (6)$$

and the total heat added in raising the temperature from T_2 to T_3 and the volume from v_2 to v_3 is

$$H_3-H_2=\int_{T_2}^{T_3}C_v'dT+\int_{v_2}^{v_3}p\,dv.$$

Now
$$\int C_v dT=\int(a+bT+cT^2+\ldots)\,dT$$
$$=aT+\frac{b}{2}T^2+\frac{c}{3}T^3+\ldots$$
$$=\psi(T) \quad \text{say.}$$

Also
$$\int_{v_2}^{v_3}p\,dv=\int_{v_2}^{v_3}(lv+m)\,dv$$
$$=\frac{l}{2}(v_3^2-v_2^2)+m(v_3-v_2).$$

Since $pv = RT$, we have $v(lv+m) = RT$, and as this is true for the points v_2, T_2 and v_3, T_3, we find

$$\frac{l}{2}(v_3^2 - v_2^2) + m(v_3 - v_2) = \tfrac{1}{2}R(T_3 - T_2) + \tfrac{1}{2}R\left(T_2\frac{v_3}{v_2} - T_3\frac{v_2}{v_3}\right).$$

Put $\frac{v_3}{v_2} = \rho$, and we have

$$\int_{v_2}^{v_3} p\,dv = \tfrac{1}{2}R(T_3 - T_2) + \tfrac{1}{2}R\left(T_2\rho - \frac{T_3}{\rho}\right).$$

Hence, finally,

$$H_3 - H_2 = \psi(T_3) - \psi(T_2) + \tfrac{1}{2}RT_3\left(1 - \frac{1}{\rho}\right) - \tfrac{1}{2}RT_2(1-\rho). \quad (7)$$

The heat rejected $H_4 - H_1$ between the temperatures T_4 and T_1 is found in like manner to be represented by the expression

$$H_4 - H_1 = \psi(T_4) - \psi(T_3) + \tfrac{1}{2}RT_4\left(1 - \frac{1}{\rho'}\right) - \tfrac{1}{2}RT_1(1-\rho'). \quad (8)$$

The thermal efficiency η is then

$$\eta = \frac{(H_3 - H_2) - (H_4 - H_1)}{H_3 - H_2}. \quad (9)$$

8. The values of r, r' ; ρ, ρ' may now be written down for the various types of cycle :—

I.	$\rho = \rho' = 1$,		$r = r'$;
II.	$\rho = \frac{T_3}{T_2}$,	$\rho' = \frac{T_4}{T_1}$,	$\frac{r}{r'} = \frac{\rho}{\rho'}$;
III.	$\rho = \frac{T_3}{T_2}$,	$\rho' = 1$,	$\frac{r}{r'} = \rho$;
IV.	$\rho = 1$,	$\rho' = \frac{T_4}{T_1}$,	$\frac{r'}{r} = \rho'$;
V.	$\rho\sigma = \frac{T_3}{T_2}$,	$\rho' = 1$,	$\frac{r}{r'} = \rho$.

9. Substituting these values in $H_3 - H_2$ and $H_4 - H_1$, we have

I. Constant volume admission, constant volume rejection :

$$H_3 - H_2 = \psi(T_3) - \psi(T_2),$$
$$H_4 - H_1 = \psi(T_4) - \psi(T_1) ;$$

II. Constant pressure admission, constant pressure rejection :

$$H_3 - H_2 = \psi(T_3) + RT_3 - \psi(T_2) - RT_2,$$

$$H_4 - H_1 = \psi(T_4) + RT_4 - \psi(T_1) - RT_1.$$

III. Diesel—constant pressure admission, constant volume rejection :

$$H_3 - H_2 = \psi(T_3) + RT_3 - \psi(T_2) - RT_2,$$

$$H_4 - H_1 = \psi(T_4) - \psi(T_1).$$

IV. Atkinson — constant volume admission, constant pressure rejection :

$$H_3 - H_2 = \psi(T_3) - \psi(T_2),$$

$$H_4 - H_1 = \psi(T_4) + RT_4 - \psi(T_1) - RT_1.$$

V. Dual—constant volume admission followed by constant pressure admission, constant volume rejection. Here we include in $H_3 - H_2$ the heat input up to the corner (5) of the diagram. Then

$$H_3 - H_2 = \psi(T_3) + RT_3\left(1 - \frac{1}{\rho}\right) - \psi(T_2),$$

$$H_4 - H_1 = \psi(T_4) - \psi(T_1).$$

10. The thermal efficiency of any of the cycles considered may be obtained with the aid of equations (3), (4), (7), (8), (9), and the appropriate relations in paragraph 8.

Usually the efficiency can be expressed in terms of three of the quantities involved, such as T_2, T_3, r ; but in cycle V the value of σ is also required.

The solution of these equations is not very troublesome, but the graphical process now to be described leads with great rapidity to the desired result.

Two diagrams are required, preferably drawn on squared paper. On the first (fig. 6) are plotted values of $\phi(T)$ as ordinates against corresponding values of T as abscissæ. Also on this diagram a curve is plotted giving as ordinates $R \log_e r$ against r as abscissæ.

On the second diagram (fig. 7) are plotted values of $\psi(T)$ as ordinates against corresponding values of T as abscissæ. Also a second curve is plotted to represent $\psi(T) + RT$. To save space, both these curves are shown on the second diagram, instead of having a separate figure for each type of

cycle. Accordingly we label these curves respectively I_1, I_2, III_2, IV_1, V_2 and II_1, II_2, III_1, IV_2.

These diagrams may be used in the following manner, and to fix the ideas we shall illustrate their application to cycle I. It is, however, still more convenient to employ fig. 9, as described in paragraph 12.

Suppose T_2, T_3, r to be given. We must find r' by aid of the relations of paragraph 8 for the appropriate cycle. Fig. 6 gives the value of T_1 in terms of T_2 and r in accordance with the adiabatic relation of equation (3). Thus on the axis of abscissæ choose $r=r$, and the ordinate to the appropriate curve represents $R\log_e r$. Choose the value T_2 on the axis of abscissæ, and the corresponding ordinate of

Fig. 6.

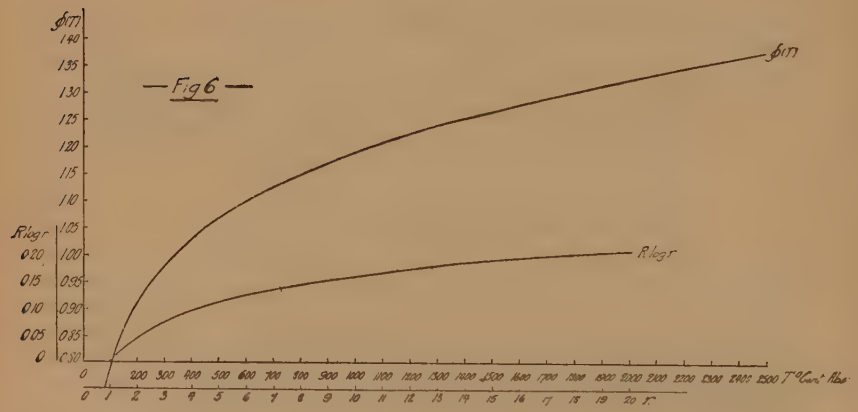

the $\phi(T)$ curve gives $\phi(T_2)$. Subtract the ordinate $R\log_e r$ from the ordinate $\phi(T_2)$, and, with this difference as ordinate, proceed horizontally to intersect the $\phi(T)$ curve. This intersection corresponds to T_1. In like manner T_4 is obtained in terms of T_3 and r'.

Next we use fig. 7 to give H_3-H_2 and H_4-H_1. Erect ordinates at the positions corresponding to T_2 and T_3 to meet the $\psi(T)$ curve. The difference between the ordinates represents H_3-H_2 to scale.

In like manner the difference between the ordinates at T_4 and T_1 to the $\psi(T)$ curve represents H_4-H_1. Thus H_3-H_2 and H_4-H_1 are immediately obtained, and the value

$$\eta = \frac{(H_3-H_2)-(H_4-H_1)}{H_3-H_2} \quad \text{follows.}$$

For cycle II. a few trials may be necessary in finding T_4 from fig. 6. There

$$r' = \frac{r T_2}{T_1 T_3} T_4,$$

Fig. 9 (combining figs. 7 and 8).

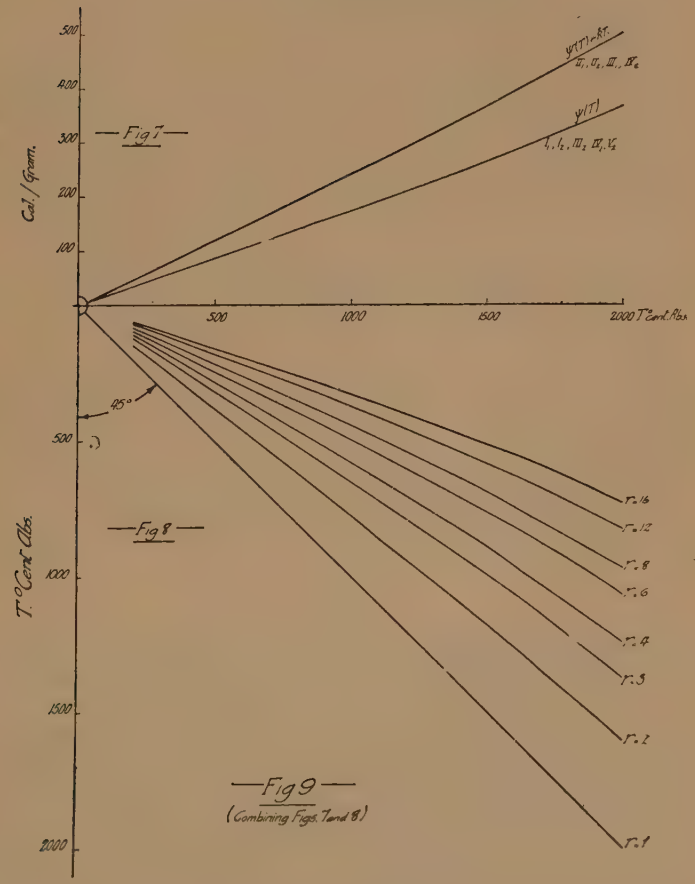

and we know T_2, T_3, r, and have just determined T_1. Assume a probable value of T_4, and with the resulting value of r' use fig. 6 to find T_4. This will give an indication of the value of T_4, and a further trial value can be chosen and the process repeated until the value of T_4 resulting from fig. 6 agrees with the trial value.

No other difficulties are encountered except with cycle V, where, in finding $H_3 - H_2$, the value of ρ is involved. The appropriate curve may be added to fig. 7, and be labelled V_1 to correspond with the particular value of ρ. Or, instead of obtaining the value of $H_3 - H_2$ wholly from the curve, the part $RT_3\left(1-\frac{1}{\rho}\right)$ may be calculated directly in the expression given in paragraph 9.

11. Where the curves of specific heats cannot well be represented by algebraic formulæ, we may construct ϕ and ψ by a graphical (or tabular) process, thus:—

Plot (or tabulate) the values of C_v against the corresponding values of T. Then at a large number of values of T plot (or tabulate) $\frac{C_v}{T}$. The area between this curve and the axis of abscissæ, and bounded by ordinates at T_1 and T_2, represents approximately the value of

$$\int_{T_1}^{T_2} \frac{C_v}{T}\, dT.$$

Plot a curve representing at each point T upon it the area measured from $T=0$ to $T=T$. This is the curve $\phi(T)$ of paragraph 6.

In like manner the area contained between the curve C_v and axis of abscissæ, and bounded by the ordinates T_1 and T_2, represents approximately the value of

$$\int_{T_1}^{T_2} C_v\, dT.$$

Plot a curve representing the area measured from $T=0$ to $T=T$. This is the $\psi(T)$ curve of paragraph 7.

12. The construction of fig. 6, by which the adiabatic relation of T and v is determined, may be more conveniently arranged in the form shown in fig. 8. In that figure T' and T are the coordinates, and the curves marked 1, 2, 3, ... are drawn to correspond with values of $r=1$, $r=2$, etc. Thus to find T_2, corresponding to the value of $r=r$ and $T=T_1$, it is merely necessary to follow the ordinate through T_1 to its intersection with the curve r, and the intercept gives the value of T_2, which is on the same adiabatic with T_1, corresponding to the value r.

Fig. 8 may be prepared with the aid of fig. 6, or may be constructed directly from the equations.

It is convenient to arrange fig. 8 on the same sheet with

fig. 7, and the efficiencies may then be obtained very readily (see fig. 9).

In this form the diagram may be most conveniently drawn and employed for calculating the thermal efficiencies of various ideal cycles.

13. The diagram may, however, also be used as a convenient means for determining the values of T, v that lie on the same adiabatic, and also the values that correspond to the same total heat put into the gas. When several sets of values are obtained in this way, they may be plotted on a pressure-volume diagram with the aid of the relation $pv = RT$.

In this manner we can draw on the pressure-volume chart the isothermal lines $pv = RT = \text{constant}$, the adiabatic lines for p, v (since those for T, v have been obtained), and the lines of constant total heat H.

Thus the calculations involved in the preparation of such a chart are facilitated, and information similar to that given in a Mollier chart is obtained.

Such chart may be employed to give the thermal efficiency by plotting on it the given values of T_2, T_3, v_1, v_2 that define the cycle, and completing the diagram with the aid of the adiabatics. When this is done, the total heats put in or taken out may be got from the total heat lines on the chart. Thus H_1, H_2, H_3, and H_4 are obtained, and

$$\eta = \frac{(H_3 - H_2) - (H_4 - H_1)}{H_3 - H_2}$$

is deduced.

14. So far the method has been described in general terms. We have now to obtain suitable numerical values for the constants. For air the values of C_p and C_v are given in tables by Partington and Shilling in calories per gram or C.H.U. per lb.

Examination of these figures indicates that their second differences are small. Accordingly it is found that they can be represented to an accuracy within the probable errors of experiment by the equations

$$C_v = 0{\cdot}1717 + 5{\cdot}4 \times 10^{-6} t + 1{\cdot}09 \times 10^{-8} \times t^2 \text{ calories per gram,} \quad . \quad . \quad . \quad (10)$$

$$C_p = 0{\cdot}2403 + 5{\cdot}4 \times 10^{-6} t + 1{\cdot}09 \times 10^{-8} \times t^2 \text{ calories per gram,} \quad . \quad . \quad . \quad (11)$$

$$R = C_p - C_v = {\cdot}0686 \text{ calories per gram,} \quad . \quad . \quad . \quad . \quad . \quad (12)$$

where t represents degrees centigrade.

The values of C_v and C_p calculated from these formulæ are compared in the following table with those tabulated by Partington and Shilling :—

Temp. ° C.	C_v.		C_p.	
	P. & S.	Calcd.	P. & S.	Calcd.
0	·1715	·17170	·2404	·24030
500	·1771	·17712	·2457	·24572
1000	·1881	·18800	·2566	·25660
1500	·2043	·20432	·2729	·27292
2000	·2260	·22610	·2946	·29470

Converting to degrees centigrade absolute, we put

$$T = 273{\cdot}1 + t,$$

and obtain approximately

$$C_v = 0{\cdot}1710 - 5{\cdot}54 \times 10^{-7} T + 1{\cdot}09 \times 10^{-8} T^2 \text{ calories per gram.}$$

Accordingly for air we have

$$a = 0{\cdot}1710, \qquad b = -5{\cdot}54 \times 10^{-7},$$
$$c = 1{\cdot}09 \times 10^{-8}, \qquad R = 0{\cdot}0686.$$

The diagrams of figs. 6 and 7 have been plotted from these figures.

15. As an example of the use of the digrams, we shall find the thermal efficiency of a Diesel cycle using real air, in which it is given that the compression ratio is 14, the ratio of volumes at end and beginning of ignition is 1·75, and the temperature at end of compression is 850° C. abs.

In our notation $T_2 = 850$, $r = 14$, $\rho = 1{\cdot}75$.

From paragraph 8, $T_3 = 1487$, $r' = 8$.

With the aid of the diagram (fig. 9) we commence at the point $T_3 = 1487$ on the axis of abscissæ, and proceed vertically to intersect the $\psi + RT$ curve in the point of which the ordinate is $H_3 = 362$.

On the other side of the axis of abscissæ proceed vertically from $T_3 = 1487$ to the curve $r' = 8$ (from which we note that $T_4 = 690$), then horizontally to the 45° line, then vertically to intersect the ψ curve in the point whose ordinate is $H_4 = 120$.

In like manner proceed vertically from $T_2 = 850$ to intersect the $\psi + RT$ curve in $H_2 = 208$, and then to intersect the curve $r = 14$ (which intersection gives $T_1 = 290$). Then proceed horizontally to the 45° line, then vertically to intersect the ψ curve in the point whose ordinate is $H_1 = 50$.

Then $H_3 - H_2$ is proportional to

$$362 - 208 = 154,$$

and $H_4 - H_1$ is proportional to

$$120 - 50 = 70,$$

so that

$$\eta = \frac{(H_3 - H_2) - (H_4 - H_1)}{H_3 - H_2} = \frac{84}{154} = 0{\cdot}545.$$

16. When the gas used as working fluid suffers dissociation, the determination of the thermal efficiency becomes considerably more complex.

An approximate solution may be obtained by following the methods already described.

When, as is sometimes the case, the energy of dissociation may be regarded approximately as varying with the temperature for a particular cycle, the effect may be represented by assuming an apparent specific heat which varies with the temperature and which includes the true specific heat with an addition representing the dissociation energy.

The calculation of the thermal efficiency then proceeds exactly as before, but with the apparent substituted for the true specific heat.

This hypothesis is often justifiable when it is remembered that the figures for dissociation in many cases are not well ascertained and the effect on engine efficiency is often not considerable.

XLIII. *Two Simple Methods of purifying Radium Emanation.* *By* William G. Moran, *B.Sc., Dalhousie University, Halifax, Canada* *.

THE many advantages of using radium in the form of emanation for therapeutic purposes are well known. The types of apparatus hitherto used for purifying and tubing the emanation have been usually so complicated that their use has been restricted to a few large institutions where the

* Communicated by Prof. G. W. Henderson.

amount of radium was great enough to justify the cost of the necessary apparatus and highly trained personnel *. There is undoubted need of an apparatus of low cost and simple operation to permit the wider adoption of the emanation method. In addition, such simplification would be of advantage in physical laboratories where radon is used for research purposes.

The emanation, as pumped off from an aqueous solution of radium salt, is mixed with relatively large amounts of hydrogen and oxygen. If the emanation comes in contact with stopcock grease, some CO_2 is also generated. Oxygen is readily removed by ignition with hydrogen, while the CO_2 is taken up by KOH. There always remains, however, an excess of hydrogen, the removal of which constitutes the main difficulty in the purification of the emanation.

In the development of the apparatus described below, many of the usual details and complications have been found to be unnecessary. It is felt that its low cost and ease of operation by relatively unskilled technicians justifies this addition to the already rather long list of published descriptions.

In this apparatus the use of liquid air has been avoided, and the purification is by purely chemical means. Furthermore, it was found unnecessary to remove the water-vapour, so that the usual phosphorus pentoxide is dispensed with. This feature has permitted great simplification of the apparatus. The emanation is pumped from the solution into the simple purifying tube, and from there pushed directly into the fine capillary tube.

Two different methods of purification will be described. In the first a hot filament coated with copper oxide ignites the oxygen with part of the hydrogen and oxidizes the excess hydrogen. The second method employs a spark to ignite the oxygen, while the excess hydrogen passes through the walls of a heated palladium tube into the outside air. In both methods crystalline KOH is used to remove the CO_2.

The apparatus figured on p. 401 has been in use for two years at Victoria General Hospital, Halifax, Canada, with 200 mg. of radium. The concentration attained in routine operation is from 75 millicuries to 125 millicuries per cubic millimetre at a pressure of 25 cm. of mercury. This is ample

* References to various types of purifying apparatus are given by Hess, Phil. Mag. xlvii. p. 713 (1924). Another type of apparatus has been described by Curtis, J. O. R. S. & R. S. I. xvii. p. 77 (1928).

for all therapeutic and most physical purposes, and is quite comparable with the purification obtained with much more complicated apparatus *.

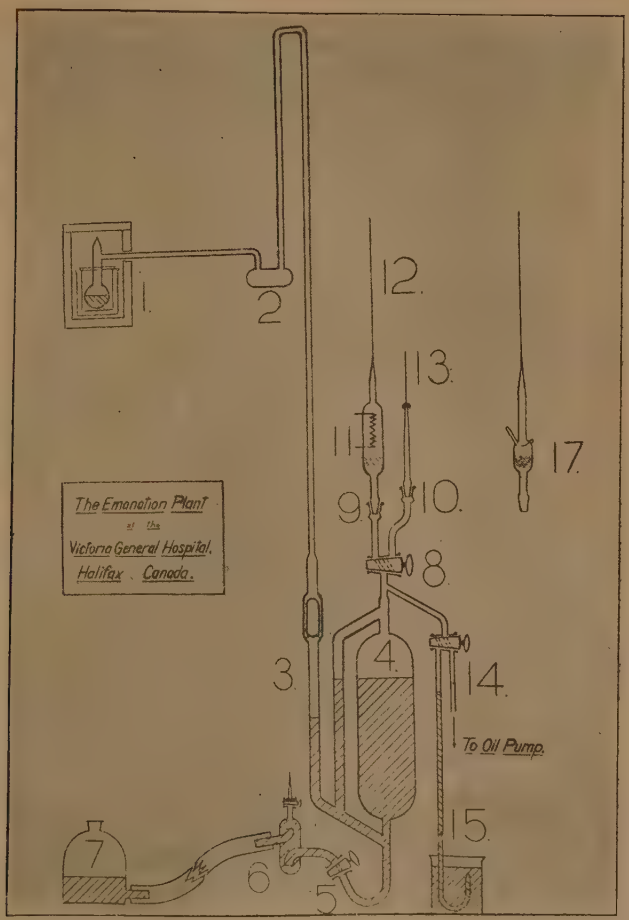

Method 1.

The radium salt is dissolved in 75 c.c. of water in the flask labelled 1 in the diagram. The emanation and associated

* An earlier emanation plant from which this apparatus was evolved is described by Dr. G. H. Henderson, Trans. N. S. Inst. of Sci. xvii. pt. 1, p. 44 (1926).

gases are withdrawn by the Toepler pump 4, and introduced into the purifying unit 11. The spiral filament shown is of platinum, copper plated and oxidized. When heated electrically to a bright red heat, it readily ignites the oxygen with part of the hydrogen and oxidizes the excess hydrogen. About 10 gms. of KOH fused in a thin layer around the inside wall of the purifying tube removes the CO_2 formed from the lubricant of stopcock 8 and union 9. The purified emanation is then forced up into the thin-walled capillary 12 by lifting the mercury reservoir 7, and is sealed off with a small flame and removed. Most of the water-vapour apparently condenses on the walls as the emanation is forced up into this tube. In the short section containing the purified emanation under a pressure of roughly 25 cm. of mercury, not more than 10 per cent. of the volume can be water-vapour.

When desired, a portion of the purified emanation may be allowed to diffuse back into the half-emptied pump cylinder 4 and introduced through the other arm of stopcock 8 into the capillary 13. A number of different-sized capillaries mounted on interchangeable male sections of the ground-glass union 10 may be attached, evacuated and filled from a single purification.

The details of the purifying tube are as follows:—The body of the tube is 10 cm. long, 2 cm. diameter. The filament is of platinum wire 20 cm. long, 0·20 mm. diameter, electroplated with copper to 0·35 mm. diameter, and wound into a spiral 5 cm. long. The platinum leads are 0·60 mm. diameter. The filament is heated by a current up to 4 amps. at 8 volts from a small laboratory transformer. The mercury film which adheres to the filament when the mercury is raised up around it is distilled off by a few seconds' heating when the mercury is lowered. The platinum core makes the filament rigid at red heat, so that the usual quartz supporting rod is omitted, while its high melting-point prevents easy burning-out of the filament. Little trouble has been met with from alloying of the platinum and copper. Two such units in constant use for six months are still serviceable. The oxide coating is readily renewed by simply heating in air for a minute. One coating of oxide is sufficient for several hundred millicuries purification. One coating of KOH is sufficient for several thousand millicuries. Quantities as low as 25 m.c. of emanation have been handled, yielding concentrations as mentioned above. Greater concentration is obtained with larger quantities of emanation.

Method 2.

In this method the excess hydrogen passes through the walls of a heated palladium tube into the outside air.

The purifying unit 17 is attached at the interchangeable union 9, in place of unit 11. A palladium tube is sealed through the shoulder of the glass tube as shown. To heat this palladium tube, a current through a few turns of platinum wire 0·20 mm. diameter, wound on a mica sleeve which slips over the tube, is used. The mixture of gases from the solution is introduced into the purifying tube in the same manner as in the previous method. A spark is passed between the inside end of the metal tube, and a platinum wire sealed through the opposite shoulder. This unites the oxygen with the hydrogen. The palladium tube is heated, and the excess hydrogen passes through it into the outside air. Fifteen minutes' heating reduces the inside partial pressure from 1·0 cm. to 10^{-3} mm. of mercury. A layer of KOH removes the CO_2 as in the former method.

The purified emanation is then pushed up into the thin-walled capillary, sealed off under a pressure of about 25 cm. of mercury, and removed; or it may be distributed among various-sized capillaries attached in turn at the interchangeable union 10, and filled as before mentioned. Concentrations as high as 200 millicuries per $mm.^3$ have been attained, though 125 millicuries per $mm.^3$ is the usual concentration in routine operation. This type of unit is somewhat smaller than the copper-oxide filament type, has nothing to burn out, and gives a slightly higher degree of purification. Five months of steady use has not noticeably lessened the rate of passage of the hydrogen through the palladium.

The details of this unit are as follows:—The body of the tube is 2 cm. long, 2 cm. diameter. The palladium tube is 1·2 cm. long, 2·5 mm. diameter, closed at one end and welded at the other end to a platinum tube of the same diameter, 2·0 cm. long. This welded tube was taken from an old type X-ray tube. The platinum end of the tube is sealed through the glass as shown. A current up to 4 amps. at 8 volts through the wire on the mica sleeve heats the palladium to around 250° C. About 10 gms. of KOH are fused around the inside wall as in the type just described.

The purifying unit is designed so that less than 1 per cent. of the purified emanation is trapped in the palladium tube when the emanation is forced up in the capillary. The

mercury film on the inside of the palladium tube is distilled off by a few seconds' heating after the mercury is lowered. No trouble has been met with due to erosion of the metal by the mercury.

It may be mentioned that at any stage in the procedure the emanation may be withdrawn from the purifying tube, pushed out from the delivery tube 15, and collected over mercury in the trough. The use of rubber pressure tubing between the levelling bulb 7 and the Toepler pump 4 has been intentional. It is felt that the use of heavy air-pressures to move mercury in fixed apparatus is attended with very great risks. Attention may also be drawn to the three stopcocks. With the pump cylinder 4 full of mercury and the stopcock turned off, the keys of each in turn may be removed for cleaning, without spilling any mercury or letting air into the apparatus. The last is of some little importance when small quantities of emanation are to be purified. Routine practice has been to clean stopcocks 5 and 14 every six months and 8 every month.

Summary.

A simple apparatus for the purification of radium emanation is described which is low in cost and easy in operation. The use of liquid air is avoided and the removal of water-vapour has been found unnecessary. Two different methods of purification are given. One method ignites the oxygen and hydrogen with a hot copper-oxide filament, which also oxidizes the excess hydrogen. The other method uses a spark to unite the oxygen and hydrogen, while the excess hydrogen passes through the walls of a heated palladium tube into the outside air. The emanation is pumped from the solution into the single small purifying tube, and from there pushed directly up into the thin-walled capillary. The emanation may be withdrawn and collected over mercury at any stage in the purification. The concentration attained compares favourably with the results obtained with the complicated installations.

The author's grateful thanks are due to Dr. G. H. Henderson, Dr. D. MacIntosh, and Dr. H. L. Bronson, of Dalhousie University, for helpful suggestions and appreciated criticism. His thanks are also due to Dr. S. R. Johnston, Radium Therapist, and Mr. W. W. Kenney, Superintendent of the Victoria General Hospital, Halifax, Canada, for their kind and generous support in this research.

XLIV. *On the Waves associated with β-Rays, and the Relation between Free Electrons and their Waves.* *By* G. P. Thomson, *M.A., Professor of Natural Philosophy in the University of Aberdeen* *.

THE following paper is a development of an idea contained in a letter to 'Nature,' published April 21st, 1928, which arose from the work of Ellis and Wooster and others on primary β-rays.

It is now generally accepted that the β-rays of the continuous spectrum are primary products of the disintegration of those radioactive substances which emit them, and that each atom in disintegrating gives one β-ray. This has been shown by Gurney † for RaB, RaC, ThB and ThC, and by Emeléus ‡ for RaE. These β-rays cover a wide range of energy (40,000 volts to 1,050,000 volts for RaE), and Ellis and Wooster § have shown that the total heating effect of the RaE is represented by the kinetic energy of the β-rays determined from their magnetic spectrum. It follows that this represents the original energy distribution, and that no considerable part of the energy is dissipated either before the ray leaves the atom or in internal changes in the atom after the ray has left it. We are thus reduced to suppose either that the conservation of energy does not apply to each individual process, or that among the atoms either of the RaE or of its product RaF (or both) there are some individuals with a million volts more energy than others, or that there is some way at present unknown by which the atoms can equalize their energies.

It seems difficult to believe that this large amount of energy would not affect previous or subsequent rates of transformation. One might expect, for example, that some atoms of RaF which contained an unusually large amount of energy would break up faster than the rest, so that the curve of decay would not be exponential. Actually, of course, RaF (polonium) was one of the cases from which the exponential law was originally deduced.

The difficulty of supposing that the atoms of RaF as they are formed can arrive at a state of equipartition with one another is greatly increased by the fact that the individual atoms may be widely spaced with non-radioactive atoms in

* Communicated by the Author.

† Proc. Roy. Soc. cix. p. 540 (1925), and cxii. p. 380 (1926).

‡ Proc. Camb. Phil. Soc. xxii. p. 400 (1924).

§ Proc. Roy. Soc. A, cxvii. p. 109 (1927).

between. Radiation by quanta in the ordinary way would in many cases be absorbed by these neutral atoms, which presumably could not store it in their nuclei, but would absorb it photo-electrically and ultimately turn it into heat, contrary to the experiment.

The remaining alternative, that the energy is not conserved in each individual act of emission, does not sound so wild to-day as it would have done before the introduction of quantum mechanics ; but one would still feel great diffidence in urging its consideration if it were not that, as I hope to show, it appears as a natural consequence of the wave theory of matter in a way which also explains why β-rays should be exceptional in this respect.

On de Broglie's theory a freely-moving particle is accompanied by waves of length $\lambda = h/p$, where p is the momentum of the particle, and, as is well known, this idea has been fully confirmed by diffraction experiments. In most cases so far considered we are concerned with a large number of particles ; for example, a beam of cathode rays. In such a case we represent the beam either, if it is regarded as ideally homogeneous, by a simple sine-wave, or, if it is complex, by some sort of Fourier integral. For example, in the simple case of one dimension under no force, we have, as Darwin * has shown,

$$\psi(x, t) = \int e^{i\frac{2\pi}{h}\left(px - \frac{p^2}{2m} + mc^2 t\right)} \phi(p)\, dp, \quad . \quad . \quad (1)$$

where $\phi(p)$ represents the amplitude of waves at a given value of p. In such a case the wave as a whole represents the whole beam, and there is no assignment of any particular wave to a particular particle.

The initial distribution of particles is translated into a wave function at the beginning of the calculation, and the wave "interpreted" at the end by assuming that the square of the amplitude at any point gives the chance of an electron being found there.

In the case of radioactive emission it is necessary to consider a separate wave for each atom, for the equality of particles emitted and atoms transformed is exact and not statistical. This is shown in the case of α-ray transformations by the simultaneous occurrence of α-ray and recoil tracks in a Wilson chamber, and for all transformations by

* Darwin, Proc. Roy. Soc. cxvii. p. 258 (1927). (I have included the intrinsic energy, mc^2, throughout, and the expressions therefore differ slightly from his.)

the change in atomic number according to the Fajans-Soddy law. The form of this wave thus becomes a subject for investigation.

In the case of the primary β-rays the number of particles as a function of their momentum has been measured for RaE by Ellis, and for RaB and ThB by Gurney. In each case the form in the region investigated is not far from an error function. If we write

$$N\,\delta p = N_0\, e^{-\frac{(p-p_0)^2}{d^2}}\,\delta p$$

for the number of particles in a range of momentum p to $p+\delta p$, the following table shows p_0 and d; the other columns we shall need later :—

	$p_0\times10^{17}$.	$d\times10^{17}$.	$\bar{\lambda}\times10^{10}$.	$\sigma\times10^{10}$.	$\bar{\lambda}/\sigma$.	$e^{-\bar{\lambda}/4\sigma^2}$.	$\lambda_0'\times10^{10}$.	$\pi\sigma\times10^{10}$.
Ra B	2·5	1·3	2·6	·80	3·3	·07	2·1	2·5
Th B	1·6	1·0	4·1	1·04	4·0	·02	3·2	3·3
Ra E	3·4	1·8	1·9	·58	3·3	·07	1·6	1·8

Darwin has shown that for one dimension in force-free space an error distribution in momentum corresponds to a wave whose initial intensity is represented also by a (different) error function. The method can be extended to the case of spherical symmetry which presumably applies here. The wave equation is

$$\frac{1}{2m}\left(\frac{h}{2\pi i}\right)^2\nabla^2\psi = -\frac{h}{2\pi i}\frac{\partial\psi}{\partial t} - mc^2\psi,$$

including the intrinsic energy of the electron. For spherical symmetry

$$\nabla^2\psi = \frac{\partial^2\psi}{\partial r^2} + \frac{2}{r}\frac{\partial\psi}{\partial r}.$$

Write $u=\psi\,.\,r$, the wave equation becomes

$$\frac{h}{2\pi i}\frac{\partial u}{\partial t} + mc^2\,.\,u = \frac{h^2}{8\pi^2 m}\frac{\partial^2 u}{\partial r^2}.$$

Following Darwin's method, we take

$$u = \int_{-\infty}^{+\infty} e^{i\frac{2\pi}{h}(pr-bt)}\,\phi(p)\,dp,$$

and the equation gives

$$b = p^2/2m + mc^2 \quad \text{and} \quad \psi = u/r.$$

Assume for the initial value of ψ when $t=0$,

$$\psi(r,0) = \frac{1}{r}\exp\left[-\frac{1}{2\sigma^2}(r-r_0)^2+\frac{i2\pi}{h}mv(r-r_0)\right].$$

This gives a finite value for $\int_0^r \psi\psi^* \, dr$, and so is permissible.

Then

$$\frac{1}{r}\int_{-\infty}^{\infty} e^{i\frac{2\pi}{h}pr}\phi(p)\,dp = \frac{1}{r}\exp\left[-\frac{1}{2\sigma^2}(r-r_0)^2+i\frac{2\pi}{h}mv(r-r_0)\right],$$

when, by inversion of the Fourier integral, we find

$$\phi(p) = \frac{\sigma\sqrt{2\pi}}{h}\exp\left[-\frac{1}{2}\left(\frac{2\pi\sigma}{h}\right)^2(p-mv)^2-i\frac{2\pi}{h}pr_0\right]$$

and

$$\psi(r,t) = \frac{1}{r}\frac{\sigma}{\sqrt{\sigma^2+i\,ht/2\pi m}} \exp\left[-\frac{1}{2}\frac{(r-r_0-vt)^2}{\sigma^2+i\,ht/2\pi m}+i\frac{2\pi}{h}mv\left(r-r_0-\tfrac{1}{2}vt-\frac{c^2t}{v}\right)\right]. \quad . \quad . \quad . \quad (2)$$

Thus, corresponding to an initial density

$$\rho = \frac{1}{r^2}e^{-\frac{(r-r_0)^2}{\sigma^2}},$$

the distribution in momentum is given by $\phi(p)$ as

$$N = N_0\exp\left[-\left(\frac{2\pi\sigma}{h}\right)^2(p-mv)^2\right].$$

Thus

$$p_0 = mv, \quad d = h/2\pi\sigma.$$

The mean wave-length $\bar{\lambda}$ is

$$h/p_0 = h/mv.$$

If σ is regarded as the "uncertainty of position" and d as the "uncertainty of momentum,"

$$d\sigma = h/2\pi,$$

which is Heissenberg's relation

It will be seen from the figures in the table that the uncertainty of position is of the order of the wave-length, and much greater than the size of the nucleus, which might at first sight have been supposed to determine it.

The above investigation neglects the effect of the attraction of the nucleus. Darwin has shown that for constant acceleration in a straight line the solution can still be written in the form (1) if ϕ is taken as a function ϕ' of p and t such that $|\phi'(p.t)| = |\chi(p-mgt)|$ and $\chi(p)$ is the original $\phi(p)$. Thus the same error law of distribution in momentum holds, but about a new mean value. The same would presumably hold for slowly-varying fields. Now, the whole potential drop outside the radius of the L-orbit (say about $2{\cdot}5\times10^{-10}$) is only about 20,000 volts, and it would seem that outside this distance, which is of the order of the mean wave-length, the chief effect of the field would be to produce a small change in the mean momentum; it will therefore be neglected in what follows.

It seems to be more than a coincidence that the ratio of $\bar{\lambda}/\sigma$ only varies over a range of from 3 to 4. The values of $\exp-\bar{\lambda}^2/4\sigma^2$, given in the last column of the table, show that the amplitude at a distance from the centre of the original group of half a wave-length is always less than a tenth of that in the centre. In the above analysis the amplitude and (imaginary) phase of the wave function correspond to quite separate initial conditions, roughly position and velocity. As Schrödinger * has remarked, the complex character of the wave equation is more than a mathematical device, and we are not entitled to separate the solution into real and imaginary parts; a graph, for example, of the real part of the wave would have no significance. He has suggested that we are really dealing with an equation involving fourth-order differential coefficients with respect to the space coordinates, which has been factorized into two complex equations of the second order.

Now, in the case of a disturbance in a physical medium, the displacement is a real function of the coordinates, and can be analysed by Fourier series. If the form of the disturbance is known, we can find an expression for the wave-length for which the Fourier coefficient is a maximum. In our case the natural expression to take for the disturbance is the initial "density"

$$\rho=\frac{1}{r^2}e^{-\frac{(r-r_1)^2}{\sigma^2}}.$$

Unfortunately this involves the unknown r_0; but if r_0/σ is large, the expression approximates to (constant) $e^{-n^2\sigma}$, and the calculation can be made.

* Schrödinger, *Ann. der Phys.* lxxxi. p. 109 (1926).

The result is that the wave-length λ_0, for which the Fourier coefficient is a maximum, is equal to $\pi\sigma$. This λ_0 is not directly comparable with $\bar{\lambda}$, because $\bar{\lambda}$ was found by plotting the number of particles against the *momentum* as abscissa instead of against the *wave-length*. It can easily be shown that if we had plotted against wave-length, the maximum ordinate would have come at

$$\lambda_0' = \frac{2\bar{\lambda}}{1+\sqrt{1+4d^2/p_0^2}}.$$

The table shows the agreement between λ_0' and $\pi\sigma$ or λ_0. In view of the neglect of σ/r_0, it is as good as can be expected, and is strong support for the view that the β-ray is governed by a concentrated disturbance in something that behaves like a physical medium.

It should be noticed that the exponential form for the initial disturbance was chosen largely for mathematical convenience. It is true that it gives the observed distribution in velocity of the rays, but probably any disturbance approximately symmetrical and limited to a region of appropriate size would give a distribution of something like the observed Gaussian form. Thus a short portion of a sine curve abruptly terminated at each end gives a function of the form $\frac{\sin^2 k(\lambda-\lambda_0)}{k^2(\lambda-\lambda_0)^2}$. It is doubtful if the experiments could distinguish between a function of this form and one of Gaussian type if the constants were suitably adjusted.

There is, in fact, some reason to suppose that the actual disturbance is like a heavily-damped sine curve having displacements of both signs. One is tempted to regard the wave of the β-ray as the sound produced by the firing of an atomic gun whose bullet is the electron. Just as the existence in a sound-wave of a compression without a rarefaction is impossible, so it seems possible that here also the disturbance should be of both signs. Of course the analogy must not be pressed too far, for the atomic case differs from the real one in that the atomic bullet is controlled by waves after emission, and travels with them. However, it seemed worth while to test whether waves propagated according to an equation of the type suggested by Schrödinger would behave like sound-waves, where a compression automatically produces a rarefaction, or like waves on a stretched string where a displacement, in one direction only, can be propagated unchanged.

Waves in a Lath.

The equation of waves in a thin lath is

$$\frac{\partial^4\psi}{\partial x^4} = -a^2\frac{\partial^2\psi}{\partial t^2},$$

and so is of the type proposed. I used a strip of veneer 7 metres long, 5 cm. wide, and 1·175 mm. thick. This was hung from the roof by long cords spaced 30 cm. apart and loaded with pieces of lead bent over it at intervals of 10 cm. It gave waves slow enough to be easily followed by the eye. There was considerable dispersion, the shorter waves going faster. However the lath was distorted, the disturbance after a short distance consisted of a complete wave with displacements in both directions. This was true whether the lath was bent by the hands and suddenly released, or disturbed by a blow, either concentrated or spread over a considerable length. The ends of the lath were attached to flexible cotton ropes hanging in loose festoons to diminish the reflexion of the shorter waves, which otherwise, on account of their greater speed, might interfere with the formation of the main wave.

It therefore seems most likely that a primary β-ray at the moment of emission is associated with a short heavily-damped wave like the sound-wave caused by an explosion, and that the spreading of this wave by dispersion causes the variation of speed observed in the rays.

Evidence for Particles.

As stated above, it is possible to find a wave function to represent a stream of particles whose existence is only considered at the end of the experiment when it is necessary to account for the effect actually observed, such as the activation of a grain on a photographic plate, a throw on a Geiger counter, or even, if many electrons are present, the deflexion of an electrometer. The question arises as to how far it is desirable or possible to ascribe an individual existence to the particles before their detection. This point comes up especially in the case of radioactivity, where the particles have sufficient energy to be detectable singly and not merely statistically. Gamow * has recently put forward a theory of α-ray emission which regards the α-ray outside the atom as a continuous, approximately monochromatic, wave whose intensity diminishes exponentially with the time, according to the same law as the radioactive decay of the radioactive substance in bulk. There is a corresponding

* *Zeit. für Phys.* li. p. 204 (1928).

function for the inside of the nucleus, the two satisfying suitable boundary conditions to ensure continuity. Now, a treatment of this kind meets with two difficulties. The wave from a single atom, or even from a very small speck of radioactive matter, must be supposed extremely feeble, especially for a substance of long life, and the chance of a particle occurring simultaneously at two places outside the atom is extremely remote. But actually such a speck gives rise to Wilson tracks, each of which contains a very large number of drops. This difficulty can theoretically be avoided by regarding the formation of each drop as a separate "experiment." Thus there is a very small chance of the formation of the first drop, which can be calculated from the original wave function. When this is formed, a new wave function must be taken, much greater in amplitude and approximately directed on the line from the radioactive speck, because the formation of the drop shows that a particle was there within certain narrow limits of time and space, and presumably came from the speck. The same thing must be done for each drop of the track. While this view is logically possible, it seems very cumbrous, and even greater difficulties arise in the explanation of Geiger and Bothe's experiments, where the "particles" are quanta.

The second type of difficulty, which is especially noticeable in radioactivity, is a one-sidedness in the "interpretation." Consider, for example, an atom of radium in a small enclosure. It is possible, at least in theory, to make it emit light and examine the spectrum. This will not affect the radioactivity in any way. Suppose such an examination is made, say, once a second. Then there will come a time when the spectrum will change to that of emanation, and simultaneously, or approximately so, an α-ray will appear which could be detected by its scintillation.

Now, each observation involves making an "interpretation," *i. e.*, a decision as to the position of the α-particle. When the spectrum is that of radium, the α-particle is supposed in the nucleus; when it is that of emanation, the particle is not in the nucleus, and presumably is outside. But the difficulty is this: as long as the particle is judged *in* the nucleus, there is a constant chance of its being found inside or outside at the next observation; but once it has been found outside, we know from experience that there is no chance of its being afterwards found inside again. What was a question of probability has become a matter of certainty. Something of an irreversible nature has occurred, and the only natural explanation is to suppose a particle actually *moving outwards*,

at any rate after it has left the nucleus. Such a particle would be supposed to carry the charge, but not to modify the propagation of the wave.

It may be mentioned in passing that concentration of energy in one direction cannot be expressed by representing the wave as a "pocket" concentrated round a point; such a pocket, at least if finite, will spread and lose its shape.

But there is a difficulty in the above view which comes out particularly strongly in the case of the β-ray, and is another reason why it is necessary to abandon conservation of energy in this case. The conception of a particle in motion is almost meaningless unless it can be supposed to have a definite velocity at a definite time. But a short wave-train is not monochromatic, and each wave-length has its own velocity. Which is the velocity of the particle? In a long train there is a corresponding uncertainty in the position of the particle which may be anywhere in the train. This is, of course, an instance of the Heissenberg uncertainty relation for a free particle expressed in terms of wave mechanics, from which it follows as an immediate consequence. In fact, the speed of a particle can only be found accurately if its waves are nearly monochromatic, and this is only possible if the train is a long one, *i. e*, if the particle's position is very uncertain. The product of the "uncertainties," suitably measured, is $h/2\pi$.

We can, however, keep both the conception of moving particles and the whole analytical machinery of the wave mechanics (at least for free electrons) if we are prepared to allow the possibility of an electron changing speed in force-free space. This can be seen as follows:—Take the wave equation in the form

$$-\frac{h}{2\pi i}\frac{\partial\psi}{\partial t} = \frac{1}{2m}\left(\frac{h}{2\pi i}\right)^2 \Delta\psi + \mathrm{U}\psi,$$

where U is the potential energy and Δ is

$$\sum_s\left(\frac{\partial^2}{\partial x_s^2} + \frac{\partial^2}{\partial y_s^2} + \frac{\partial^2}{\partial z_s^2}\right),$$

where x_s, y_s, z_s are coordinates relating each to one of the s electrons in the system, and U is expressed in terms of these coordinates. Then $\rho = \psi\psi^* = |\psi|^2$ is the density of electricity, *i. e.*, the chance of an electron being at the point in question in the $3s$ dimensional space. Schrödinger (*l. c.*) has shown that the quantity

$$j = -\frac{h}{4\pi i m}(\psi\,\mathrm{grad}\,\psi^* - \psi^*\,\mathrm{grad}\,\psi)$$

obeys the continuity equation

$$\frac{\partial \rho}{\partial t} + \operatorname{div} j = 0.$$

Thus the motion is statistically the same as if the electrons moved with velocity $V = j/\rho$; *i.e.*, if a swarm of electrons had actually the density $\psi\psi^*$ at some initial time, and if they moved with the above velocity, $\psi\psi^*$ would represent the density at any subsequent time. When only a few, or one, electrons are present if $\psi\psi^*$ represents the initial chance of one being at a point, if it be supposed to move with the above velocity, $\psi\psi^*$ will always represent the chance of its presence, as can easily be seen by considering a large number of similar systems with the electrons initially in all possible positions.

For $s > 1$ the above "velocity" is not in three-dimensional space, and so is of little physical significance. We will return to this case later, and consider now the case of one electron as directly applicable to the β-ray problem. Then

$$V = \frac{h}{2\pi m} Im . \{\operatorname{grad} \log \psi\},$$

where ψ is given in our case by (2).

This gives $$V = \frac{t(r - r_0 - vt)}{t^2 + (\sigma^2 2\pi m/h)^2} + v,$$

and it is thus a function of the time ; it is obviously radial. If r is the coordinate of the particle, $V = \frac{dr}{dt}$. Let

$$y = r - vt \quad \text{and} \quad \sigma^2 2\pi m/h = T,$$

then $$\frac{dy}{dt} = \frac{t(y - r_0)}{t^2 + T^2},$$

which gives $$r = vt + c\sqrt{t^2 + T^2} + r_0.$$

The constant of integration C is determined by the initial conditions. If the value of r for the particle at $t = 0$ is $r = r_0 + \xi$, then the value at any later time is

$$r = r_0 + vt + \xi\sqrt{1 + (t/T)^2}.$$

Initially the velocity is v in all cases ; it then changes, and when t is large

$$r = r_0 + vt + \frac{\xi t}{T},$$

giving a velocity $v + \frac{\xi}{T}$.

T measures the length of the wave-train ; if T/ξ is large, the velocity is nearly v at all times.

Looked at from the wave point of view, the initial short group will break up as it goes along, owing to dispersion; and after it has gone a distance very large compared with a wave-length, it will consist of an approximately monochromatic wave of slowly-changing wave-length and amplitude. Any portion forms a nearly monochromatic group ; and if the whole wave passes into a magnetic field, as in a β-ray spectrum experiment, each such group will undergo a change of direction appropriate to its wave-length. Such a group approximates to the monochromatic wave

$$\psi = a \exp\left[\frac{2\pi i}{h}\{vx - t(mc^2 + \tfrac{1}{2}mv^2)\}\right],$$

which gives $V = p/m$ as on ordinary mechanics. As is well known, the group velocity in such a case is also p/m, so that the particle keeps with the group.

Conservation of Energy.

The energy given out by the act of emission may regarded as associated either with the wave or the particle, or both. If we suppose that the ordinary expression $\frac{1}{2}mV^2$, which is known to be true for an ordinary electron (*i.e.* one with a long train of waves), holds in our case also, the energy of the particle will in general change after emission, since V changes. The initial velocity v is, however, the same in all cases, and since the wave is also the same, any energy associated with it will be the same. Thus the total energy of emission is a constant, and the energy left in the atom is constant. On this view, the departure from conservation occurs outside the nucleus, and is *essentially associated with the shortness of the wave-train*, as the above expression for v shows clearly ; it is therefore only likely to be noticeable when an electron has been very suddenly accelerated, as in the emission of a β-ray from the nucleus.

Since a particle in a group like this is equally likely to gain or lose a given amount of *velocity*, there will be a statistical gain of kinetic energy in the subsequent motion if second-order terms are considered. If we suppose that the wave possesses energy when highly concentrated which it loses on spreading out, the conservation of energy can be kept as a statistical law.

The variable part of the velocity cannot be directly observed because of the uncertainty principle, but it is

necessary to assume it to make the scheme logically self-consistent. To some this may seem an objection to the introduction of particles at all, but it seems impossible to work long with any theory without unobservable quantities coming in; for example, in optics—phase and even frequency come under this head. It is, of course, only the *variation* in velocity which is inaccessible to observation; the average speed can be measured by the most direct method imaginable, namely actual timing, as in des Coudres experiment.

Problems involving more than One Electron.

There are two classes of "many-electron" problems. One which can be treated by representing a stream of electrons as a solution of a wave equation with only three variables; the other in which the wave equation itself must involve $3n$ independent variables, as in the case of a complicated atom. The former method is equivalent to ignoring the mutual action between the electrons, or, at most, to representing it by its average effect on the potential. There is no essential difference from the case of one electron. If, indeed, as is commonly done, the initial beam of electrons is represented by a monochromatic wave, this is an idealization even for a single electron; but however the electron was originally produced, and whatever its original wave-train, by the time it has gone even a fraction of a millimetre, there will be a train of an immense number of waves over which the change in wave-length is quite negligible. The assumption of a monochromatic wave is thus justified for all practical purposes; and if there are many electrons, the only difference is an increase in the effective amplitude of the wave, as long as the Coulomb and Ampère forces between the electrons are negligible. Each electron has its own wave system which determines the chance of its being at any assigned place. The assumption of a single wave for the whole beam is merely a convenient way of superposing the essentially independent effects of the separate electrons.

When, however, the importance of the mutual interactions makes it necessary to use a many-dimensioned wave equation, the definition of velocity which we have used so far breaks down. This case occurs especially with the electrons which form part of an atom. In these cases the conception of velocity loses most of its value as there is no practical means of measuring it, even approximately. Schrödinger has shown, however, that it is possible, even in this case, to

devise a consistent definition. Thus, if the density associated with electron σ is defined by

$$\rho_\sigma = \int\ldots\int . \psi . \psi^* \tau_1\tau_2\ldots\tau_{\sigma-1} . \tau_{\sigma+1}\ldots\tau_N,$$

where the quantities τ_1 etc. are the elements of space associated with the various electrons, and we define a quantity,

$$\iota_s = \int\ldots\int \frac{h}{4\pi i m}(\psi \operatorname{grad}\psi^* - \psi^* \operatorname{grad}\psi)\tau_1\tau_2\ldots\tau_{\sigma-1}\tau_{\sigma+1}\ldots\tau_N,$$

then

$$\frac{\partial\rho_\sigma}{\partial t} + \operatorname{div}\iota_s = 0.$$

Thus, if ρ_s is regarded as measuring the probability of the presence of the electron, ι_s/ρ may be taken for its velocity. I understand from a conversation with Prince L. de Broglie that, in a paper at the last Solvay Conference, he has considered the results of applying his expression for the velocity of a particle (which is practically the same as that used above) to the case of a non-monochromatic wave. See also 'Wave Mechanics,' de Broglie and Brillouin, p. 136 (note in English edition).

Summary.

(1) The variation of the speed of the electrons in the continuous β-ray spectrum can be regarded as due to the dispersion of a short wave-group associated with each ray.

(2) The mean velocity is about that to be expected if the group had the form of an error function of sufficient spread to give the observed range of velocity.

(3) The possibility of a group in the form of a heavily-damped wave is considered, and an experiment described concerning the propagation of waves along a thin lath.

(4) An expression is considered for the velocity of an electron associated with a given wave, and it is shown to give consistent results in this problem. It leads to the consequence that the velocity of an electron may vary even in force-free space, which explains Ellis and Wooster's experiment on the heat generated in the disintegration of RaE. This variation of velocity is essentially associated with a short wave-train.

Aberdeen,
Jan. 7th, 1929.

XLV. *On the Superficial Properties of Mercury.*

To the Editors of the Philosophical Magazine.

Gentlemen,—

M. L. Oliphant and L. L. Bircumshaw have published in the September issue of the Philosophical Magazine the results of some researches on the superficial properties of mercury.

M. L. Oliphant states a selective absorption of carbon dioxide by a fresh surface of mercury; L. L. Bircumshaw re-examines the long-debated question of the true value of the surface tension of mercury in vacuum and in various gases. Both the authors come to the conclusion that the variations of surface tension observed in mercury by Stöckle, but not always observed by other physicists, have an effective existence.

Both the authors suggest the hypothesis of a superficial molecular or atomic orientation or arrangement in liquid mercury.

Now, as a matter of fact, some researches I have accomplished in 1921–22 * give a direct and strong support to the idea of a superficial atomic or molecular arrangement in mercury. I concluded that "*la surface fraîche du mercure change avec le temps, pour atteindre un arrangement (atomique ou moléculaire) ayant la plus grande stabilité; c'est à dire ..... la plus petite énergie potentielle de la couche double superficielle, donc la plus petite tension superficielle.*

"Cet arrangement s'achève dans un temps très court (celui dit de *relaxation* ?) dans le vide, mais il est fortement ralenti par les chocs moléculaires du gaz, si la surface de mercure y est préparée. Si la surface est préparée dans le vide, puis qu'on introduise le gaz, les chocs ne sont désormais plus capables de détruire l'arrangement déjà accompli.

"Tout le mond remarquera la relation entre ces idées et les récentes théories de M. Langmuir sur la constitution de la couche superficielle des liquides. Peut-être, dans ce cas, est-on conduit plus directement à l'hypothèse d'un arrangement superficiel d'un liquide."

The experiments were carried on by the large-drop method in different gases (air, CO_2, N_2, H_2) at various pressures (0·1 mm. to 100 mm. Hg): an asymptotical value of the surface tension is reached the more quickly the more rarefied is the surrounding gas.

* *Atti Acc. Torino*, lvii. p. 81 (1921); *id.*, *ib.* lvii. p. 541 (1922). *C. R.* clxxv. p. 519 (1922).

The statement of such a molecular surface rearrangement throws light upon Stöckle's results, and does not disprove the experimental conclusions of M. L. Oliphant. It is likely that molecular arrangement of fresh liquid surfaces can be paralyzed as well by molecular bombardment from the surrounding gas, as by selective absorption.

The very object and the fundamental result of my researches was the close connexion between surface tension and voltaic character *.

Perhaps that is the reason why Mr. Oliphant and Mr. Bircumshaw have passed over the experimental arguments I have pointed out in favour of molecular rearrangement in a fresh surface of mercury.

Believe me,

Yours faithfully,

Torino.
16 September, 1928.

Prof. Eligio Perucca

XLVI. *Uniformly-diffused Light through Two Apertures.*

To the Editors of the Philosophical Magazine.

Gentlemen,—

In the Philosophical Magazine for November 1928, No. 39 (p. 1019), there is a paper by Mr. L. F. Richardson on "The Amount of Uniformly-diffused Light that will go in Series through Two Apertures forming Opposite Faces of a Cube."

In that paper the author gives an approximate solution of the question by the method of finite differences. He finds that "the amount of light, uniformly diffused with brightness I, that will go in series through two apertures forming opposite faces of a cube of edge l" is

$$\Phi = (0{\cdot}6278 \pm 0{\cdot}0001) l^2 \mathrm{I}.$$

This case has an accurate solution in the following form †:

$$\Phi = \left(4\sqrt{2}\,\mathrm{arc\,tg}\frac{1}{\sqrt{2}} - \pi + \lg\frac{4}{3}\right) l^2 \mathrm{I}.$$

The Photometr. Laboratory,
State Optic. Institute,
Leningrad.
November 19th, 1928.

Yours truly,

A. Gerschun.

* Intended as the place of the metal in the voltaic series.

† The above-mentioned question can be regarded as a particular case of an example given in R. A. Herman's book, 'A Treatise on Geometrical Optics' (Cambridge, 1900), Chapter ix. Example 16, p. 218.

XLVII. *Notices respecting New Books.*

Collected Physical Papers of Sir Jagadis Chunder Bose. With 123 illustrations. (Longmans, Green & Co., 1927. Price 10*s.* net.)

THIS volume contains a collection of the papers on Physics written by Sir Jagadis Bose. Many of them were written a considerable number of years ago, some of them dating back thirty years or more, to the time when the study of the properties of electric waves, stimulated by Hertz's important experiments, was engaging the attention of a large number of experimental physicists. In these researches Bose played a part by his introduction of a method of generating electrical waves of shorter length than those in general use at that time. He obtained in this way results concerned with polarization, double refraction, and cognate topics which are of importance. It is therefore of value to have available in one volume a reprint of these papers of Sir Jagadis Bose.

The volume contains a number of other papers which are also of interest to the physicist, which trace the gradual building up of his methods for dealing with the properties of living matter. We may therefore recommend the volume, not only to the attention of physicists, but also to all those who are interested in the new aspects of biology which have been studied by Sir Jagadis Bose,—aspects which cannot well fail to be of very considerable importance when the biological sciences come to be further developed in those domains where the recent findings of physics, chemistry, and bio-chemistry are relevant.

Thermodynamics applied to Engineering. By Arthur F. Macconochie, B.Sc. [Pp. xv+260, with 65 figures and two folding charts.] (London: Longmans, Green & Co., Ltd., 1927. Price 12*s.* 6*d.* net.)

The author has divided his treatment of engineering thermodynamics into three sections. The first section contains an elementary treatment of thermodynamical principles with a discussion of various simple cycles, followed by a brief account of the properties of fluids in motion. Section II. deals with the application of these principles to boilers; steam-engines, including the uniflow engine; steam and impulse-reaction turbines. Section III. deals with the application to internal combustion engines, including Diesel engines and gas turbines, and to refrigerating plant. The treatment is elementary throughout, and the volume is intended to meet University degree requirements.

A useful series of tables of thermodynamic properties of saturated steam, superheated steam, saturated ammonia vapour, saturated mercury vapour, and of carbon dioxide, as well as a table of the mean specific heat of superheated steam and tables of

trigonometric functions and of logarithms, are added. In a pocket at the end are given Mollier diagrams of total heat and Entropy for steam and of total heat and pressure for ammonia.

A valuable feature for the student is the addition at the end of each section of a list of topics for discussion, a selection of worked numerical examples, and a number of examples for the student. A large proportion of these examples are taken from the examination papers for B.Sc.(Eng.) London.

Vorlesungen über Theoretische Physik an der Universität Leiden. Von Prof. H. A. Lorentz. Band I. *Theorie der Strahlung.* Bearbeitet von Prof. A. D. Fokker. [Pp. x+81, mit 17 Figuren.] (Leipzig: Akademische Verlagsgesellschaft m.b.H., 1927. Price, geb. M.7.80.)

The publication of the lectures on theoretical physics, delivered by the late Prof. Lorentz at the University of Leiden, is proceeding contemporaneously in England and Germany. The first volume of the German edition is devoted to the lectures on the theory of radiation; these are included in the second volume of the English edition. Both are translations from the second Dutch edition, edited by Prof. Fokker.

The lectures, which were delivered in the years 1910–11, are concerned with the classical researches of Kirchhoff, Boltzmann, Wien, and Planck; the last section of the volume deals with the radiation formula of Planck. They are written with the clearness of thought and lucidity of expression which were characteristic of Prof. Lorentz. No attempt has been made to include more recent developments of the theory, but the volume can be recommended as giving one of the best accounts of the classical bases of the theory of radiation. As an elementary introduction to more advanced study it cannot be improved upon.

Wien-Harms, Handbuch der Experimentalphysik: Band XV. "*Radioaktivität*," von K. W. F. Kohlrausch. [Pp. xii+885 mit 285 Abbildungen.] (Leipzig: Akademische Verlagsgesellschaft m.b.H., 1928. Preis geh. M.79; geb. M.81.)

A brief introduction is followed by three long chapters, devoted respectively to the γ-, β-, and α-rays (treated in this order). These chapters occupy nearly three-fourths of the whole book. Shorter chapters follow, on recoil atoms, miscellaneous effects of the radiations, transformation theory, the experimental technique of Radioactivity, a general account of the radioactive families and their members, and the nucleus of the atom, respectively.

This arrangement of the subject-matter—æsthetically less satisfying than the historical-inductive development of radioactive theory—is, no doubt, in part dictated by the obvious difficulties in the way of any attempt to present a contemporary and comprehensive account of a rapidly expanding experimental science.

The arrangement adopted by Professor Kohlrausch has the merits of facilitating reference to specific problems, and of providing a framework on which newer work can be grafted, in succeeding editions, with a minimum of interference with the existing plan of the book.

The treatment is throughout comprehensive rather than specialized, encyclopædic (generally in the best sense of the term) rather than critical. It is a difficult task for a single writer to cover the whole field of modern radioactivity; it is, therefore, no matter for surprise that Professor Kohlrausch should have been most conspicuously successful in his chapter on γ-ray problems, where he is a recognized authority. Other parts of the field are less completely covered, but the extensive bibliography of original papers, and the excellent Author Index, make the work very useful for reference.

The book is an outstanding example of fine—even luxurious—standards in production. The diagrams are beautifully drawn and very clearly reproduced (although Pettersson's condensation apparatus presents an unfamiliar aspect when printed upside down, with the mercury and liquid air apparently levitating in their respective tubes!). There can be no doubt that the book calls for a genuine tribute to the enterprise of the publishers and to the industry and scholarship of the author. Although its appeal will necessarily be most cogent in Middle European countries, the volume should also find a welcome here.

XLVIII. *Proceedings of Learned Societies.*

GEOLOGICAL SOCIETY.

[Continued from vol. vi. p. 1072.]

November 7th, 1928.—Prof. J. W. Gregory, LL.D., D.Sc., F.R.S., President, in the Chair.

Dr. L. F. Spath gave an account of the recent landslide at 'Windy Corner,' above Rocken End, in the Isle of Wight, and referred to some alarming reports that had appeared in the Press. He showed a series of lantern-slides, which, as he suggested, told their own story.

The structure of the Undercliff was simple; it was not unimportant to remember that there was a slight seaward dip, and that porous rocks rested on impervious clays. Landslips were thus bound to recur at more or less frequent intervals. The resisting and curiously weathered chert-beds that form so conspicuous a feature near the top of the cliff, occasionally overhang, but, in spite of being extensively fissured, they do not break away so readily as might be imagined. In July, however, there was a considerable fall; and some views taken while this fall was actually in progress

were most impressive. After this fall the débris of Chalk, Chloritic Marl, and 'Upper Greensand' were banked up against the cliff, reaching almost to the top and covering the road below.

After two months the unstable foundation on which this enormous weight had fallen (that is, remains of previous falls and landslips) gave way. On September 21st there was a vast subsidence of the pile of rocks at the top, and a slipping of the whole Undercliff in front of it out to sea. The slide was doubtless helped by the lubricating action of the water thrown out at the junction of the porous rocks above and the Gault clay below (locally known as 'Blue Slipper'). Moreover, the Gault not only formed the foundation (resting on a more solid base of the Sandrock Series), but was present in various isolated masses brought down in former landslips, and all this confused mass was constantly being eroded at the seaward end. The upper portion of the sunken mass with its chasms, leaving a fine, slickensided, cliff-section down almost to the base of the Gault (250 to 300 feet from the top), was particularly impressive. Lower down, there were seen remains of the ashphalt-surface of the destroyed Undercliff road (about 900 feet altogether), pushed down by the rock avalanche, a pond in course of formation, and the heavily fissured ground below as far as Rocken End. This quaking ground of confused material, being forced forward, even pushed up the floor of the sea, and formed a ridge, a little way out, which, however, was rapidly worn away again.

The whole mass was still moving, and small fresh falls occurred during the speaker's visit a few days after the slide; but he appealed to the Fellows to look for ammonites in the Passage-Beds between the Gault and the 'Upper Greensand' as soon as the cliff-section was approachable, perhaps in the spring.

November 21st, 1928.—Prof. J. W. Gregory, LL.D., D.Sc., F.R.S., President, in the Chair.

The following communications were read:—

1. 'The Geology of the Country around Kenilworth (Warwickshire).' By Frederick William Shotton, B.A., F.G.S.

The paper deals with an area of 59 square miles, of which Kenilworth forms the centre, and completes the mapping of the so-called 'Permian' rocks at the southern termination of the Warwickshire Coalfield. The strata are shown to be conformable with the Carboniferous deposits on the north, and must therefore be regarded as belonging to that system. The total thickness of post-Keele Carboniferous beds is estimated at about 3500 feet, with the top of the sequence overlapped unconformably by Keuper sandstone. Various subdivisions are made, the most important being a well-developed conglomerate (Gibbet Hill Conglomerate) above the Tile Hill Marl Group, and two breccia-bands at Kenil-

worth. The pebbles of these coarse beds have been examined petrographically, and compared with possible parent-sources (Nuneaton, the Lickey Hills, the Welsh borderland), and from this evidence, and several other lines of inquiry, views have been formulated concerning the geography and earth-movements of the period. The possible relationship of the Kenilworth breccias to those of Clent is also discussed.

The superficial deposits of the area have been mapped for the first time. They are divisible into an eastern and a western type, and subdivisions have been made in each. The eastern deposits show considerable regularity of disposition. A small mammalian fauna is recorded from interglacial gravels, believed to be older than the Chalky Boulder Clay.

Fluvio-glacial gravels and a series of five terraces along the course of the Avon are also dealt with.

2. 'The Carboniferous Section at Cattybrook, near Bristol.' By Stanley Smith, M.A., D.Sc., F.G.S., and Sidney Hugh Reynolds, M.A., Sc.D., F.G.S., Professor of Geology in the University of Bristol.

About 5 miles north of Bristol the Carboniferous Limestone rim of the Bristol Coalfield is traversed by the South Wales branch of the Great Western Railway, by means of the Patchway Tunnel. In the railway-cuttings west of that tunnel, and in the adjacent brickworks, the rocks which are the subject of this paper are exposed. The rocks represented are the uppermost part of the Carboniferous Limestone (D_2 and probably D_1) and the Coal Measures. The D_2 beds, which are mainly calcareous, are finely exposed in the cutting for the down-line, which affords (with the possible exception of the Avon Section) the finest exposure of this horizon in the Bristol district. Red, coarsely oolitic and current-bedded limestones, which often pass rapidly into grits, are the most characteristic rocks. The limestones contain much iron, which often gives to them a characteristically streaky appearance.

At the western end of the main cutting the D_1 beds and Coal Measures are brought into contact by the Cattybrook Fault, and on both sides of this for some 200 yards the rocks show an astonishing amount of disturbance. East of the fault the D_1 beds are traversed by a powerful line of thrust, and every surface hard enough to show this feature is slickensided. West of the fault the ironstone-bands in the Coal Measures may be crumpled up, or torn apart so as to resemble a series of isolated nodules; while the bands of anthracite may be shattered into little bits about a quarter of an inch or half an inch long, or reduced to lenticular pieces 2 to 4 inches long, each bordered by slickensided surfaces.

[*The Editors do not hold themselves responsible for the views expressed by their correspondents.*]

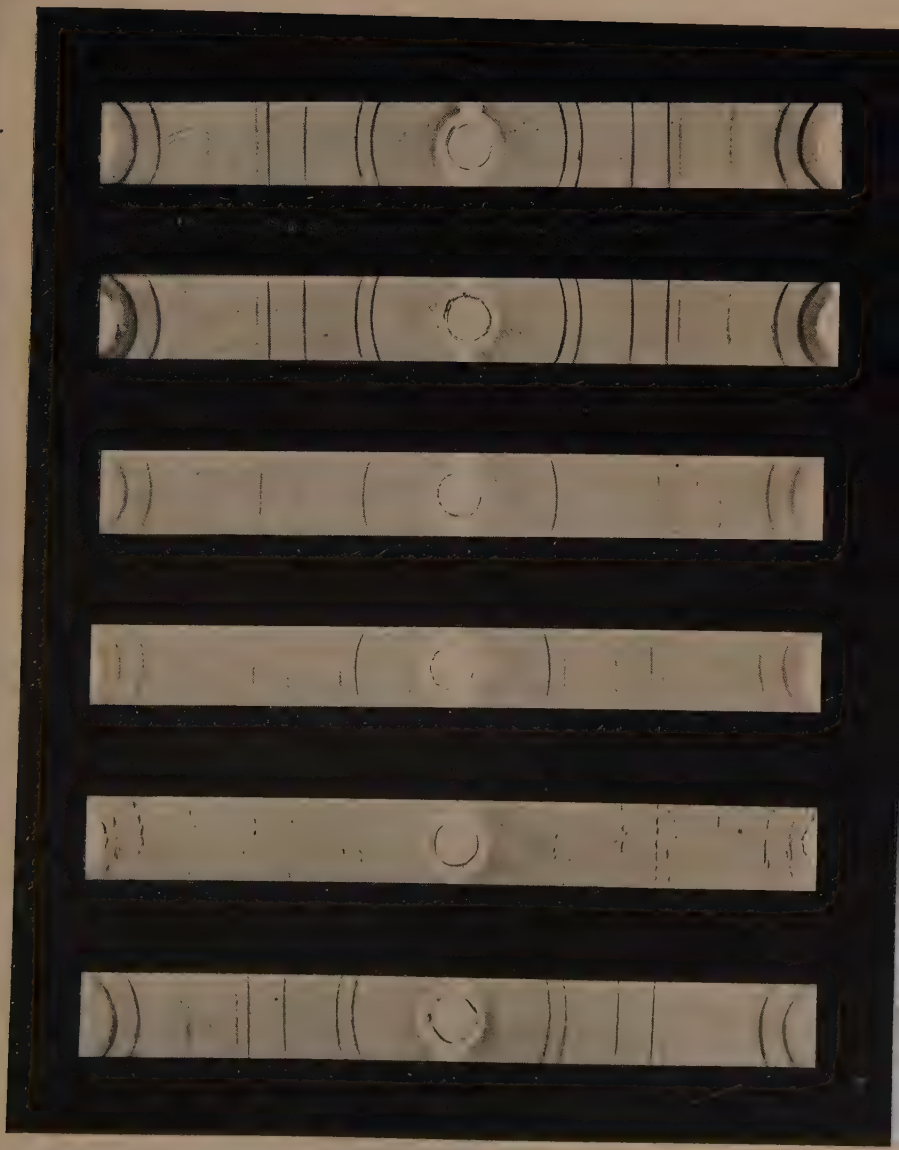
1.
2.
3.
4.

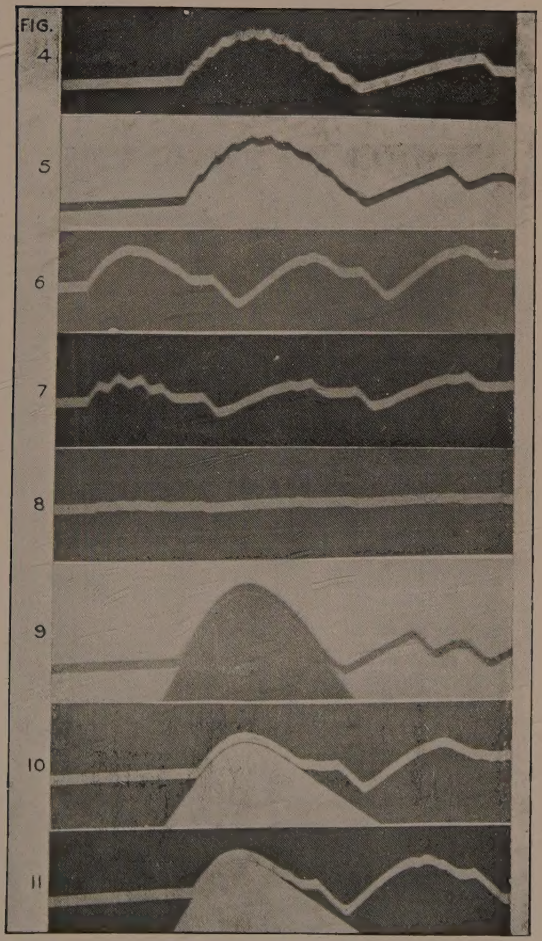
FIG.
4
5
6
7
8
9
10
11

FIG. 3.

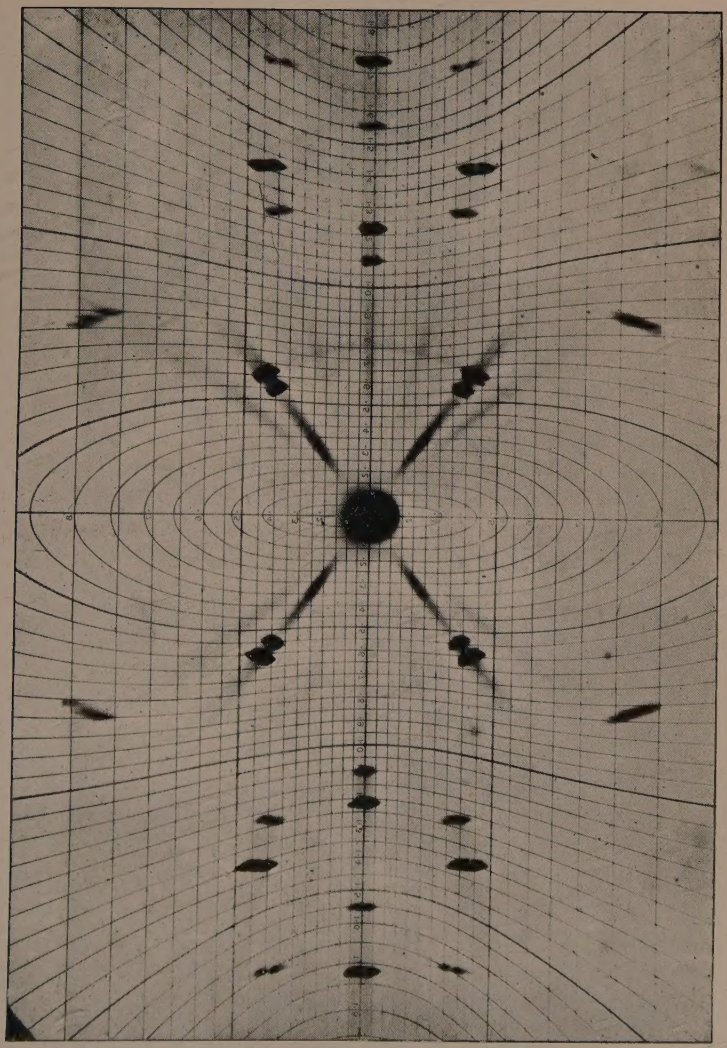

Example of appearance of actual X-ray film when the grid method is used in taking a single crystal rotation photograph.